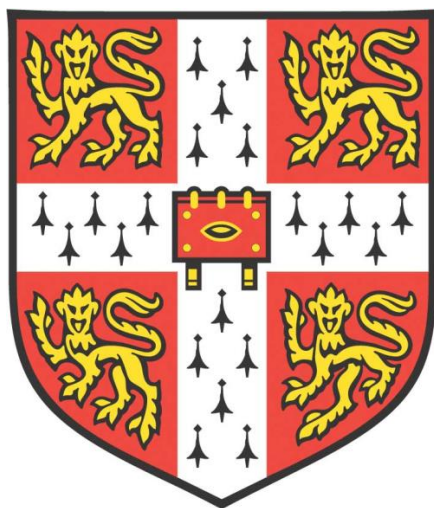# Unlocking the genetic potential of the root system, rhizosheath mucilage and microbiome of wheat (*Triticum aestivum* L.)

**Emily Cathy Marr**

**Christ's College, Cambridge**

**NIAB and the Department of Plant Sciences**

# University of Cambridge

This dissertation is submitted for the degree of Doctor of Philosophy

December 2020

# DECLARATION

This dissertation is my original work and a product of my own research endeavours and includes nothing that is the outcome of work done in collaboration except where specified in the text. It has not been previously submitted, in part or whole, to any university or institution for any degree, diploma, or other qualification.

In accordance with the Graduate School of Life Sciences guidelines, this thesis is does not exceed 60,000 words, and it contains fewer than 150 figures.

Signed:_____

Date:_____18th December 2020_____

Emily Cathy Marr *BA (Hons) Cantab., MA (Hons) Cantab., MRSB*

# Abstract

Emily Cathy Marr
Unlocking the Genetic Potential of the Root System, Rhizosheath Mucilage and
Microbiome of Wheat (*Triticum Aestivum* L.)

An increasing global population, projections of climates that will challenge sufficient crop production, and a detrimental use of fertiliser and pesticides mean that we need to increase the productivity of land currently under cultivation with minimal impact on the environment. Wheat is the second largest contributor to global crop production and is cultivated across a range of latitudes across both hemispheres. The wheat root system is a crucial determinant of plant performance, yet roots are overlooked in breeding due to the challenge of studying organs below ground. Evidence from the literature indicate that water and nutrient uptake are often suboptimal in high yielding and stressed environments. Facilitating the incorporation of root system characteristics into breeding programmes and developing crop management strategies that enhance root function could be key to increasing yield potential and stability, while minimising inputs. To fill the knowledge gap on root-rhizosphere-yield interactions the research presented here falls into three strategic areas: root system architecture (RSA), root secretions and the rhizosphere microbiome.

1) Genetic mapping of RSA in the Avalon x Cadenza Doubled Haploid (AxC) mapping population identified quantitative trait loci (QTL) for seedling seminal root angle, length and growth rate. Replicable QTLs were associated with root angle and mapped to chromosomes 3A and 4D, explaining 7% of phenotypic variation. After extensive root phenotyping, the tails displaying phenotypes at the extremes of the population distribution were taken forward for field trials. Correlations between seedling root phenotypes and the root and canopy phenotypes of mature plants grown in the field were calculated.

2) Root secretions represent a significant loss of fixed carbon from the plant, yet they are thought to confer benefits in relation to plant water status, nutrition, salinity stress, microbial interactions and the development of the rhizosheath. Enzyme-linked immunosorbent assays (ELISAs) were used to quantify the amount of high molecular weight polysaccharides in the

rhizosheath of AxC tails, determine the influence of genotype on secretion and investigate potential interactions with RSA.

3) A metagenomics study of the microbial population within the rhizosheath of AxC tails uncovered differences in microbial community composition between lines of the same species. Lines grouped according to phenotype (level of secretion, RSA, yield) showed that the microbiome of high-yielding lines differed from that of low-yielding lines. The level of secreted polysaccharides was associated with differences in the microbiome.

Overall, this research presents a novel, multi-faceted study of the root system, from seedling to mature plant in the field, as a holistic approach to crop improvement is more robust than the unlikely discovery of a "silver bullet".

# ACKNOWLEDGEMENTS

# CONTENTS

# LIST OF FIGURES

# LIST OF TABLES

# LIST OF ABBREVIATIONS

| | |
|---|---|
| 2,4-D | 2,4-dichlorophenoxyacetic acid |
| AGP | Arabinogalactan protein |
| AIC | Akaike information coefficient |
| ANOVA | Analysis of variance |
| ARE | Auxin response element |
| ARF | Auxin response factor |
| AX | Neutral arabinoxylan |
| AxC population | Avalon x Cadenza doubled haploid mapping population |
| BLUP | Best linear unbiased prediction |
| bp | Base pairs |
| BWA | Burrows-Wheeler Aligner |
| CP | Construction phase |
| cv. | Cultivar (plural cvs.) |
| Defra | Department for environment and rural affairs |
| DH | Doubled haploid |
| DMSO | Dimethyl sulphoxide |
| DNA | Deoxyribonucleic acid |
| DRO1 | *DEEPER ROOOTING 1* |
| ELISA | Enzyme-linked immunosorbent assay |
| EST | Expressed sequence tag |
| FL | Fraction length |
| FP | Foundation phase |
| Gal | Galactose |

| | |
|---|---|
| GAX | Glucuronoarabinoxylan |
| Gb | Gigabase |
| GRU | Germplasm Resources Unit |
| GS | Growth stage |
| GX | Glucuronoxylan |
| GxE | Gene x environment |
| HRGP | Hydroxyproline-rich glycoprotein |
| HRP | Horseradish peroxidase |
| HS | High sensitivity |
| ICIM | Integrated composite interval mapping |
| ITS | Internal transcriber spacer |
| IWGSC | International Wheat Genome Sequencing Consortium |
| JIC | John Innes Centre |
| K | Potassium |
| KASP | Kompetitive Allele-Specific Polymerase chain reaction |
| KP | Kinandang Patong rice cultivar |
| KSU | Kansas State University |
| LSU | Large subunit |
| MAGIC | Multiparent Advanced Generation Intercross |
| Mbp | Megabase pairs |
| MP | Milk powder |
| N | Nitrogen |
| NDRE | Normalised Difference Red Edge |
| NDVI | Normalised Difference Vegetation Index |

| | |
|---|---|
| NIR | Near-infrared |
| NIL | Near-isogenic line |
| OH | Hydroxyl |
| OTU | Operational taxonomic units |
| P | Phosphorous |
| PBS | Phosphate buffered solution |
| PCA | Principal component analysis |
| PCoA | Principal coordinate analysis |
| PCR | Polymerase chain reaction |
| PERMANOVA | Permutational multivariate analysis of variance |
| PGPB | Plant growth-promoting bacteria |
| PGPR | Plant growth-promoting rhizobacteria |
| PP | Production phase |
| QTL | Quantitative trait locus |
| RCA | Root cortical aerenchyma |
| REML | Restricted maximum likelihood |
| RIL | Recombinant inbred line |
| *RHT* | *Reduced height* gene |
| RNA | Ribonucleic acid |
| rRNA | Ribosomal ribonucleic acid |
| RSA | Root system architecture |
| SNP | Single-nucleotide polymorphism |
| spp. | Species (plural) |
| SSU | Small subunit |

| | |
|---|---|
| t/ha | Tonne per hectare |
| VIS | Visible light |
| VRN1 | VERNALISATION1 gene |
| VST | Variance stabilisation transformation |
| WGIN | Wheat Genetic Improvement Network |
| WGRC | Wheat Genetics Resource Centre |
| WT | Wild type |
| XLLG | Xyloglucan nonasaccharide |
| XXLG | Xyloglucan octasaccharide |
| XXXG | Xyloglucan heptasaccharide |
| XY | Xylan |

# 1
# Introduction

Wheat (genus *Triticum* L.)  is the second greatest contributor after *Zea mays* (maize) to global crop production at 765 million metric tonnes per annum (USDA, 2020). The genus *Triticum* consists of over 40 diploid, tetraploid and hexaploid species (Huang *et al.*, 2002). The most commonly cultivated wheat species are hexaploid bread wheat (*T. aestivum*, 95% of global production, (genus *Triticum* L., 2n = 6x = 42, AABBDD) and tetraploid durum wheat (*T. turgidum* ssps *durum*, 2n = 4x = 28, AABB, 5% of global production). *T. aestivum* originated in the Fertile Crescent around 10,000 years ago from a spontaneous hybridisation event between domesticated emmer wheat, *T. turgidum* ssp. *dicoccum* (2n = 4x = 28, AABB), and the wild goat grass *Aegilops tauschii* (2n = 2x = 14, DD) (El Baidouri *et al.*, 2017). Emmer wheat originated from a natural hybridisation between two diploid wheat species, einkorn wheat (*T. urartu*, 2n = 2x = 14, AA) and spelt (*Ae. speltoides*, 2n = 2x = 14, BB). Durum wheat was developed by artificial selection of domesticated emmer wheat (Dubcovsky and Dvorak, 2007). Bread wheat can be categorised into winter, facultative and spring wheat, based on their requirement for exposure to vernalisation (low temperature, 0 – 5 ⁰C, for 30 – 60 days) in order for the apical meristem to transition from vegetative to reproductive phase. The vernalisation requirement of winter types prevents cold damage to the reproductive structures that would occur in winter months if transition initiated soon after autumn sowing. Facultative wheat has less stringent vernalisation requirements and spring wheat does not require a period of vernalisation (Tranquilli and Dubcovsky, 2000). Bread wheat is currently grown across the globe in a variety of climates with a range of precipitation, temperature and radiation patterns, although the most intensive wheat cultivation occurs in the temperate latitudes of both hemispheres (Leff *et al.*, 2004).

## 1.1 Contribution of crop root structure to food security

The projected increase in drought incidence and unpredictable weather events require the development of crops that are capable of yielding enough to meet demand in a changing climate. For example, the UK faces challenges of hotter, drier summers and warmer, wetter winters, as projected by UKCP18 in probabilistic, global, regional and local projections (Met Office, 2019). Furthermore, nutrient use inefficiency can result in environmental and economic losses. According to estimates from 2005, 2007 and 2008, global fertiliser production releases 575 megatonnes of greenhouse gases each year (Gilbert, 2012). Phosphorous fertilisers are made from non-renewable reserves which are predicted to be exhausted in the next 50-100 years (Cordell *et al.*, 2009). Nitrogen fertilisers represent one third of the cost of cereal production (Le Gouis *et al.*, 2000; Fageria and Baligar, 2005). In the UK and parts of Europe, there is a growing movement towards converting land that is currently cultivated to land dedicated to wildlife (Navarro and Pereira, 2015; Ceauşu *et al.*, 2015). This calls for sustainable intensification: increasing food production per hectare while minimising inputs (Araus *et al.*, 2008; Garnett *et al.*, 2013). By producing more food on the same or smaller area of cultivated land, other land can be set aside for wildlife and 'ecosystem services' without a negative impact on food security (Ewers *et al.*, 2009; Balmford *et al.*, 2018). Environmental and economic production costs can be reduced by developing more efficient crop cultivars.

Although root system architecture (RSA), the spatial configuration of roots in the soil, is important for nutrient and water uptake, selection for RSA is generally not directly incorporated into breeding programmes due to the challenge of phenotyping organs below ground (Waines and Ehdaie, 2007). However, RSA has a direct impact on crop grain yield (Lynch, 2007; Smith and Smet, 2012) and improved root systems can ensure that a higher proportion of applied fertiliser is taken up by the crop. The Green Revolution dramatically increased wheat yields thanks to the *Reduced Height* (*Rht*) genes which shortened plant stature, reduced lodging (the displacement of the plant from its vertical position) and reduced the amount of energy directed towards shoot growth. However, the *Rht* genes have pleiotropic effects including altered disease resistance and potentially reduced root growth (Saville *et al.*, 2012; Bai *et al.*, 2013).

Over twenty dwarfing and semi-dwarfing genes have been identified in wheat (Börner *et al.*, 1996; Rebetzke *et al.*, 2012). The most widely used dwarfing genes are the homoeologous semi-dwarfing alleles, *Rht-B1b* and *Rht-D1b* (previously known as *Rht1* and *Rht2*), located on the short arms of chromosomes 4B and 4D respectively (Börner *et al.*, 1996). The wild-type *Rht-B1a* and *Rht-D1a* alleles at these loci are found in tall plants and encode DELLA genes, which repress gibberellin-responsive growth (Pearce *et al.*, 2011). A gain of function mutation in *Rht-B1b* and *Rht-D1b* resulted in constitutive repression of the GA response (Gale and Marshall, 1973).

There are varying reports on the effect of *Rht* genes on the wheat root system. A study undertaken at the seedling stage suggested that *Rht-B1b* has the pleiotropic effect of increasing primary root length and total root length (Li *et al.*, 2011). On the other hand, Mac Key (1973) noted that "a tall wheat plant tends to have a deep, and a short wheat plant a shallow root system", and Fradgley *et al.* (2020) documented that modern varieties had fewer nodal roots with a greater spread compared with landraces, which displayed greater root number and narrow growth angle. Other studies have reported that cultivars of the Green Revolution have smaller root systems than landraces (locally adapted wheat that pre-dates the start of industrial breeding practices), resulting in sub-optimal nutrient and water uptake (Virmani, 1971; Gupta and Virmani, 1973; Waines and Ehdaie, 2007). A study of two tall and three semi-dwarf winter wheat varieties found no significant relationship between plant height and rooting depth (Cholick *et al.*, 1977). However the small sample size makes it difficult to draw inferences about the wider population of wheat cultivars.

Inconsistent results highlight the plasticity of the root system and support the findings that RSA is very responsive to the environment (Manschadi *et al.*, 2008; Walter *et al.*, 2009). Phenotypic plasticity is the ability of an organism to alter its phenotype in response to the environment and may involve changes in physiology, morphology, anatomy, development, or resource allocation (Sultan, 2000; Schneider and Lynch, 2020). It is likely that RSA has indirectly been selected for through breeding for yield potential (McGrail, 2020) and that in high input agricultural conditions, smaller root systems are capable of sufficient nutrient uptake with a relatively low metabolic burden that allows more biomass to be directed to the grain. However, breeding under high input conditions may not have selected for RSA that promotes high yields in an ever-increasing unpredictable climate, including periods of drought. For example, the varieties Gaines and Nugaines, two of the first varieties of semi-dwarf wheat, had low yields when grown outside

of the high rainfall of Washington State, where they were developed (McGrail, 2020). It has been suggested that direct selection for an efficient root system tailored to specific agricultural environments may lead to a second Green Revolution, where increased resource capture could enhance yields and reduce fertiliser requirement by capturing more nutrients before they leach out of the root zone (Lynch, 2007).

Classification of cereal root types are rarely standardised and certain terms may be used to describe the same root type or different root types (Zobel and Waisel, 2010). Throughout this text, root classification will respect the following description. The root system of cereals is composed of two types: seed-borne and shoot-borne roots. Seed-borne roots, also known as embryonic, primary or seminal roots, emerge from the scutellar and epiblast nodes of the hypocotyl and are between three and six in number (Manschadi *et al.*, 2013). Shoot-borne roots, also known as crown, nodal or adventitious roots, emerge four to twelve weeks after germination from the basal nodes of the main shoot and tillers (Klepper *et al.*, 1984). The first embryonic root will hereon be referred to as the primary root, and subsequent embryonic roots as seminal roots (Figure 1.1).
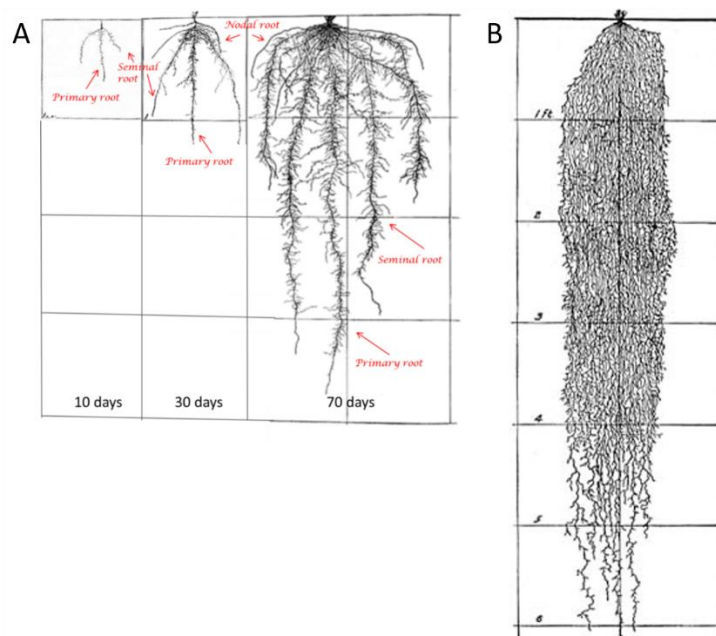


**Figure 1.1 The wheat root system.** Diagram showing traces of the wheat root system 10, 30 and 70 days after germination (A) and at maturity (B) (Adapted from Weaver and Bruner, 1926). Depth scale is marked in increments of feet (30.5 cm). The ten day-old plant only displays seed-borne roots, comprising the primary root and seminal roots. After 4-12 weeks, the plant develops shoot-borne roots, which may be referred to as crown, nodal or adventitious roots.

Lateral roots branching off the main root axes contribute to anchoring, and nutrient and water uptake (Lucas *et al.*, 2000). Seminal roots are functionally active for the entire life of the plant and tend to grow deeper than crown roots, therefore contributing more to water and nutrient uptake (Watt *et al.*, 2008; McGrail, 2020). Although deep roots provide some anchorage, spreading roots play a vital role in lodging resistance as anchorage strength increases to the third power with increasing root spread (Berry *et al.*, 2007). Therefore, crown roots can be important for lodging resistance. Root systems are dynamic and changes in the soil water and nutrient profile trigger changes in root distribution within the soil strata. For example, localised nitrate and phosphate application enhances root proliferation in *Triticum aestivum* L. (wheat), maize and *Vicia faba* (faba bean) (Tang *et al.*, 2008; Gao *et al.*, 2019). However, root responses can vary between varieties. For example in response to drought, Ehdaie *et al.* (2012) reported an increase, a decrease and no change in root biomass in three different wheat genotypes.

Soil factors which have the largest effect on RSA are penetration resistance, pore distribution, and water and nutrient availability (Hoad *et al.*, 2001). The greatest phenotypic determinants of resource capture are root length, rooting depth and degree of root-soil contact (Hoad *et al.*, 2001). The identification of an effective RSA must take into consideration the role of the different root types, their interaction with the environment and the dynamics of the water cycle throughout the year. A root ideotype (the idealised appearance of a plant variety) called "steep, cheap and deep" has been proposed in maize for rapid exploitation of deep soil strata (Lynch *et al.*, 2013). It is based on the fact that water and nitrate move to deeper soil strata over time and are depleted in surface soil. Thus, root systems with rapid exploration of deep soil would optimize water and nitrogen capture (Lynch *et al.*, 2013). The similarity of the root systems of different monocots means that the model can also be applied to wheat. It is characterised by seminal roots with steep growth angles and early root vigour. The steeper the root angle, the deeper the roots are predicted to grow (Lynch *et al.*, 2013). Roots that grow faster than the mobility of nitrate within the soil could prevent nitrates leaching deeper than the root zone. Plants that establish a deep root system in regions of drought have a higher chance of survival (Bruce *et al.*, 2002). On a soil with an available water-holding capacity of 15% (water that can be extracted by roots), an increase in rooting depth of 14 cm should provide an extra 20 mm of water, which should support one extra tonne per hectare (t/ha) of biomass growth (AHDB, 2018). The advantages of a steep root system have been demonstrated experimentally in multiple crop species. In maize (Gao and Lynch,

2016) and bean (Ho *et al.*, 2005), genotypes with a steeper angle of root growth have an increased rooting depth for a given elongation rate and perform better in terminal drought conditions (progressively depleting soil moisture) than genotypes with wider angles of root growth. An optimal root system achieves a balance between metabolic cost and effective foraging. Root density should be high enough to ensure exhaustive soil exploration. However, too high a root density results in increased respiration and competition between roots of the same plant (Ge *et al.*, 2000; Rubio *et al.*, 2001; Postma and Lynch, 2012). An anatomical feature, root cortical aerenchyma (RCA), reduces respiratory requirement. RCA comprises tissue with air-filled cavities in the root cortex due to programmed cell death of some cortical cells. It normally forms in response to hypoxia or drought and nutrient deficiencies as it provides a low resistance pathway for gas exchange (Drew *et al.*, 1979; Fan *et al.*, 2003; Bouranis *et al.*, 2006; Zhu *et al.*, 2010). Ensuring its constitutive expression could allow greater root growth and resource capture for a given metabolic investment.

Subsoil water is a reliable water reserve as it is not prone to evaporative losses. Therefore, deep-rooting crops benefit from access to subsoil water, particularly when terminal drought occurs during grain-filling (Kirkegaard *et al.*, 2007). Deep water is replenished during seasons of heavier rainfall, the timing of which varies according to geography (Ahmed *et al.*, 2018). Depending on the timing of rainfall, farmers may need to manage the land in ways that conserve soil moisture to tide the crop through their growing season (Hunt, 2017). RSA traits are important for optimising water uptake. However, the configuration of the roots in the soil is not the only limiting factor: even when root length density is adequate, maximum water uptake is still not achieved (Ahmed *et al.*, 2018). This is likely to be due to hydraulic resistances at the soil-root interface or within the root (Vadez, 2014).

In instances of severe drought, a small but deep root system tends to provide the best yields. However, greater root biomass results in better yields when plant-available water is enough to support grain production (Ehdaie *et al.*, 2012). Furthermore, plants that extract water at too great a rate may exhaust available water before grain filling and suffer the consequent water deficit (Figueroa-Bustos *et al.*, 2020), again highlighting the advantage of a moderate root system density. Optimising timing of water extraction can be achieved by capitalising on a shallow root system early in the season to capture rainfall and a deeper one later in the season when drought is more dominant (Manschadi *et al.*, 2006; Gao and Lynch, 2016).

The projected changes in crop growth environments means that root plasticity could be an appropriate target for breeding programmes (Schneider and Lynch, 2020). Phenotypic plasticity is the ability of an organism to alter its phenotype in response to the environment and may involve changes in physiology, morphology, anatomy, development, or resource allocation (Sultan, 2000; Schneider and Lynch, 2020). A crop that is able to adapt its RSA to environmental conditions in a way that maintains productivity could be advantageous. Plasticity may be adaptive, maladaptive, or neutral in regard to fitness, and adaptive plasticity, which is positively associated with fitness may be undesirable in crop production (Schneider and Lynch, 2020). For example, a stress response that reduces plant growth may be evolutionarily adaptive but it would not be beneficial for crop production. Some may argue that we should not select for genes regulating RSA because plastic root responses to local environmental conditions override the default genetic programme. Selecting genes that regulate plasticity (i.e. the response of RSA to the environment) may be more effective for breeding resilient crops than selecting RSA genes. On the other hand, plasticity may not be desirable if an adaptive response leads to a reduction in grain yield. The selection of an RSA trait that remains constant in a range of environments could stabilise yield. Effective breeding requires an understanding of the physiological effect of phenotypes and groups of phenotypes. In the end, it is likely that stacking a suite of adaptive genes could allow us to harness the power of plasticity in crop development (Schneider and Lynch, 2020).

## 1.2 Contribution of the root secretions to food security

The rhizosphere (narrow region of soil or substrate that is directly influenced by root secretions) is a carbon-rich, diversity-rich microenvironment largely engineered by the root system through the secretion and absorption of compounds. Root secretions – the ensemble of compounds released by roots to the rhizosphere – has significant implications for the fitness of a plant. Secreted compounds comprise mucilage, root exudates and up to 6% proteins (Nguyen, 2003). Mucilage comprises the complex of large, highly-branched plant polysaccharides (Badri and Vivanco, 2009). Exudates comprise low-molecular weight sugars, amino acids, organic and inorganic acids, secondary metabolites, phenolics and phytosiderophores (Jones *et al.*, 2005; Fischer *et al.*, 2010; Dippold *et al.*, 2014; Gunina and Kuzyakov, 2015). Mucilage contributes to the formation of the rhizosheath. The rhizosheath is the soil-polysaccharide complex that adheres

to roots and established thanks to mucilage secretion and the presence of root hairs, which enmesh soil particles (Watt *et al.*, 1994; Moreno-Espíndola *et al.*, 2007; Haling *et al.*, 2010, 2014; Brown *et al.*, 2012; Delhaize *et al.*, 2012; George *et al.*, 2014). First documented in 1887 by Volkens, who observed it on the roots of xerophytic grasses (Price, 1911), the rhizosheath has since been recorded in other plant families (Brown *et al.*, 2017).

Compounds released by the roots account for 5-70% of total carbon fixed by the plant during photosynthesis, depending on species and study (Whipps and Lynch,1983; Whipps, 1984; Newman, 1985; Whipps, 1987; Badri and Vivanco, 2009). This significant energetic cost presumably provides justifiable benefit to the plant. As a target for crop breeding, there is a case for determining the minimum energy cost necessary to achieve the benefits associated with mucilage. The roles of the rhizosheath include maintaining hydraulic conductivity during soil drying (Read *et al.*, 2003; Zickenrott *et al.*, 2016), promoting and inhibiting microorganisms (Pausch *et al.*, 2016), nutrient acquisition (Read *et al.*, 2003), and protection from metal toxicity (Morel *et al.*, 1986; Archambault *et al.*, 1996).

Because of its role in water and nutrient uptake, the rhizosheath is an important agronomic trait (Badri and Vivanco, 2009). It is likely to be linked to RSA as the configuration of roots in the soil determines the capacity of a plant to forage for water and nutrients. The spatial distribution of different root classes determines the location of mucilage secretion in the soil, particularly given the differential release of polysaccharides along the length of the same root (Rovira, 1969). For example, the root cap and the zone immediately behind the root tip is generally considered to be a site of major exudation, yet older parts of the roots have been seen to exude organic compounds (Pearson and Parkinson, 1961; McDougall, 1970; Rovira, 1969). It is possible that root hairs are also key contributors to mucilage secretion as Werker and Kislev (1978) reported small drops of mucilage on the root hairs of *Sorghum bicolor* L. (sorghum). This implies a dual role of root hairs in the formation of the rhizosheath: mucilage secretion and the trapping of soil particles. There is extensive evidence that the rhizosheath does not form in the absence of root hairs (Moreno-Espinola *et al.*, 2007; Shane *et al.*, 2011; Delhaize *et al.*, 2012; George *et al.*, 2014 Brown *et al.*, 2017). Root hairs have significant impact on the uptake of water and nutrients, and can comprise up to 77% of the total root surface area of cultivated crops (Parker *et al.*, 2000; Fan *et al.* 2001; Grierson *et al.*, 2001; Michael, 2001).

Historical data on the rhizosheath has often been anecdotal and subjective, and quantitative records have only begun gaining traction in recent years (Brown *et al.*, 2017). This means that the rhizosheath could represent an important, underexplored agronomical trait. Root hair density, root hair length, rhizosheath size, mucilage abundance and composition all represent targets for the development of cultivars with mucilage that fosters an agronomically beneficial microbiome, facilitates nutrient uptake and buffers against changes in soil moisture. In order to deliver high levels of food security while reducing environmental impacts, a rhizosphere that contains optimal proportions of polysaccharides could encourage the proliferation of a microbiome that increases plant growth, nutrient uptake, and suppresses pathogens. The scope for this is further reviewed in Chapter 3.

## 1.3 Contribution of the crop root microbiome to food security

In light of the tight relationship between plants and the microbes inhabiting them, the plant microbiome has been referred to as the "second genome" of the plant (Turner *et al.*, 2013). Distinct communities of microorganisms (fungi, bacteria, protozoa, archaea) inhabit different parts of a plant. For example, in the phyllosphere (plant aerial surfaces), the leaves and flower, and potentially even the different parts of the flower, are thought to harbour distinct microbiomes (Vorholt, 2012; Aleklett *et al.*, 2014). Below ground, the rhizosphere teems with microbial life, with one report of up to 1011 microbial cells per gram root in the wheat rhizosphere (Egamberdieva *et al.*, 2008).

Indeed, multiple studies report an enrichment of microorganisms in the rhizosphere relative to the bulk soil (Donn *et al.*, 2014; Fan *et al.*, 2017). Thanks to root secretions, the rhizosphere represents a nutrient-rich habitat compared with the generally carbon-limited bulk soil (Wardle, 1992; Semenov *et al.*, 1999). Furthermore, the composition of the body of compounds secreted by roots differentially favours (or inhibits) microbial species, resulting in a selection of certain communities. Plants do not only provide a service: they also receive benefits from microbial activity through the production of compounds including phytohormones, exopolysaccharides, osmolytes, antioxidants, hydrogen cyanide, antibiotics and hydrolytic enzymes (Fatima *et al.*, 2019). Evidence indicates that microorganisms facilitate the uptake of minerals that are often present in forms inaccessible to plants (Bais *et al.*, 2006); they can provide drought tolerance

(Kim *et al.*, 2012), heat tolerance (Castiglioni *et al.*, 2008), salt tolerance (Zhang *et al.*, 2008; Fatima *et al.*, 2019) and protection from pathogens (Berendsen *et al.*, 2012); they can enhance plant growth and photosynthesis through the production of phytohormones (Ali *et al.*, 2009; Ulrich *et al.*, 2019). Evidently, the substantial cost to the plant of secreting organic compounds from the roots must have a payoff.

In an agricultural context, the three-way interaction of crops, microbes and abiotic factors contribute to crop productivity. As such, interactions and responses are extremely complex. For example, strong genotypic effects on the root microbiome have been observed between chickpea (*Cicer arietinum*) and wheat in tilled systems but not in undisturbed, no-till systems (Yang *et al.*, 2020). *Pseudomonas* has been found to inhibit root growth of direct-drilled (no-till) wheat but not wheat on cultivated soil (Simpfendorfer *et al.*, 2002). Other studies have confirmed the effect of host genotype (Mauchline *et al.*, 2015; Mahoney *et al.*, 2017), fertilisation (Kavamura, 2018), land management and seed load (Mauchline *et al.*, 2019), irrigation (Mavrodi, 2018), seed germination and host age (Huang *et al.*, 2016) on the rhizosphere microbiome. Studies are rarely carried out in identical environmental conditions (soil type, crop management, crop species and variety, temperature, soil moisture), and the huge number of factors that influence the microbiome means that studies are often difficult to compare. There has not yet been a coordinated effort among academics, industry researchers and farmers to elucidate plant genotype x environment x microbiome x management interactions, develop model crop-microbiome interactions systems and turn these into practical solutions (Busby *et al.*, 2017). This leaves a large, mostly untapped target for improved crop function.

Food security is reliant on growing crops that are capable of maintaining sufficient yield in spite of environmental pressures, such as water stress, high temperatures and salinity. Furthermore, the excessive and indiscriminate use of fertilisers and pesticides has led to negative environmental and health impacts, which could be alleviated by developing more sustainable farming methods (Singh and Trivedi, 2017). Exploiting the plant microbiome has the potential to reduce pathogenic burden, reduce chemical inputs and greenhouse gas emissions, and increase yield (Turner *et al.*, 2013). The role of microorganisms in promoting resilience to climate change in plants is illustrated at the molecular scale: for example, several studies have shown that the production of the enzyme, ACC deaminase, by various plant growth promoting bacteria increases biomass and yield in tomato, pepper, pea and maize by lowering the endogenous level

of ethylene production under mild drought stress (Mayak *et al.*, 2004; Dodd *et al.*, 2004; Arshad *et al.*, 2008; Naveed *et al.*, 2014). In studies testing the effect of bacterial inoculation on temperature stress, the alleviation of stress has been attributed to the accumulation of proline, sugars and amino acids in sorghum and *Vitis vinifera* L. (grape vine) (Ali *et al.*, 2009; Barka *et al.*, 2006).

With appropriate understanding of the rhizosphere microbiome, it may be possible to deliver tailored microbial cultures to crops as a so-called "biofertiliser". Alternatively, the evidence that genotypes of the same plant species differ in their rhizosphere microbial community composition indicates the possibility of breeding crops for more beneficial microbiomes. Chapter 4 provides a comprehensive review of the rhizosphere microbiome and its interactions with plants.

# 1.4 Wheat germplasm resources

There are numerous genetic and genomic resources for wheat available, developed by projects including the Wheat Genetic Improvement Network (WGIN), the International Wheat Genome Sequencing Consortium (IWGSC), the Wheat Genetics Resource Centre (WGRC) and EnsemblPlants.

## 1.4.1 The Avalon x Cadenza doubled haploid population

The Avalon x Cadenza doubled haploid (AxC) wheat population benefits from good genetic resources and has been used as the UK reference population for quantitative trait locus (QTL) analysis. It is derived from F1 progeny of a cross between the UK cultivars (cvs.) Avalon and Cadenza, and was developed by Clare Ellerbrook, Liz Sayers and the late Tony Worland (John Innes Centre, JIC), as part of a Defra funded project led by ADAS. The parents were originally chosen to contrast for canopy architecture traits by Steve Parker (Central Science Laboratory), Tony Worland and Darren Lovell (Rothamsted Research). The genome sequence for Cadenza has recently been published (Walkowiak *et al.*, 2020), and is available via the Grassroots Infrastructure project website: https://wheatis.tgac.ac.uk/grassroots-portal/blast. The Avalon genome sequence is expected to be released in the future. These varietal genome sequences will be of use for genetic investigations.

## 1.4.2 Chinese Spring deletion lines

Deletion lines are a useful genetic tool to identify regions of the genome that are associated with specific phenotypes. Thanks to its polyploidy nature, the wheat genome can tolerate major chromosomal deletions and rearrangements. This allows the development of genetic stocks exhibiting aneuploidy or sub-chromosomal deletions. Whole chromosome deletions were described by Sears (1954) and later there were reports of deletions of different sizes in wheat (Endo and Tsunewaki, 1975; Endo and Gill, 1996; Endo, 1998). The Wheat Genetics Resource Centre (WGRC) located at Kansas State University has developed wheat deletion lines of cv. Chinese Spring.

## 1.4.3 Paragon gamma deletion Lines

Gamma ray irradiation has been used widely as a mutagenising agent in breeding programmes for many crops. Out of 3362 officially released mutant crops, 1702 were produced by gamma irradiation (FAO-IAEA Mutant Variety Database, 2020). Besides using mutagenesis as a direct mechanism to bring about new crop varieties, it is a valuable tool for studying crop genetics and applying findings in conventional breeding programmes. At high dosages, gamma irradiation causes double-strand DNA breaks, which result in genomic insertions and deletions (Datta *et al.*, 2018). Previous studies have reported deletions of up to 3.8 Mbp in banana (Datta *et al.*, 2018). A collection of gamma ray deletion lines has been generated at the John Innes Centre using the UK spring wheat cultivar, Paragon.

## 1.4.4 Near-isogenic Lines

NILs with a desired allele of a specific genotype in a nearly uniform genotypic background from another genotype allow the characterisation of identified QTLs independently of the parental background (Figure 1.2) (Marcel *et al.*, 2007). The target QTL is considered mendelised and constitutes the major source of variation due to the absence of other segregating QTLs (Alonso-Blanco and Koorneef, 2000; Paterson *et al.*, 1990). The Simon Griffiths group at the JIC has generated a population of NILs derived from an initial cross between cvs. Avalon and Cadenza and successive rounds of backcrossing to one parent.
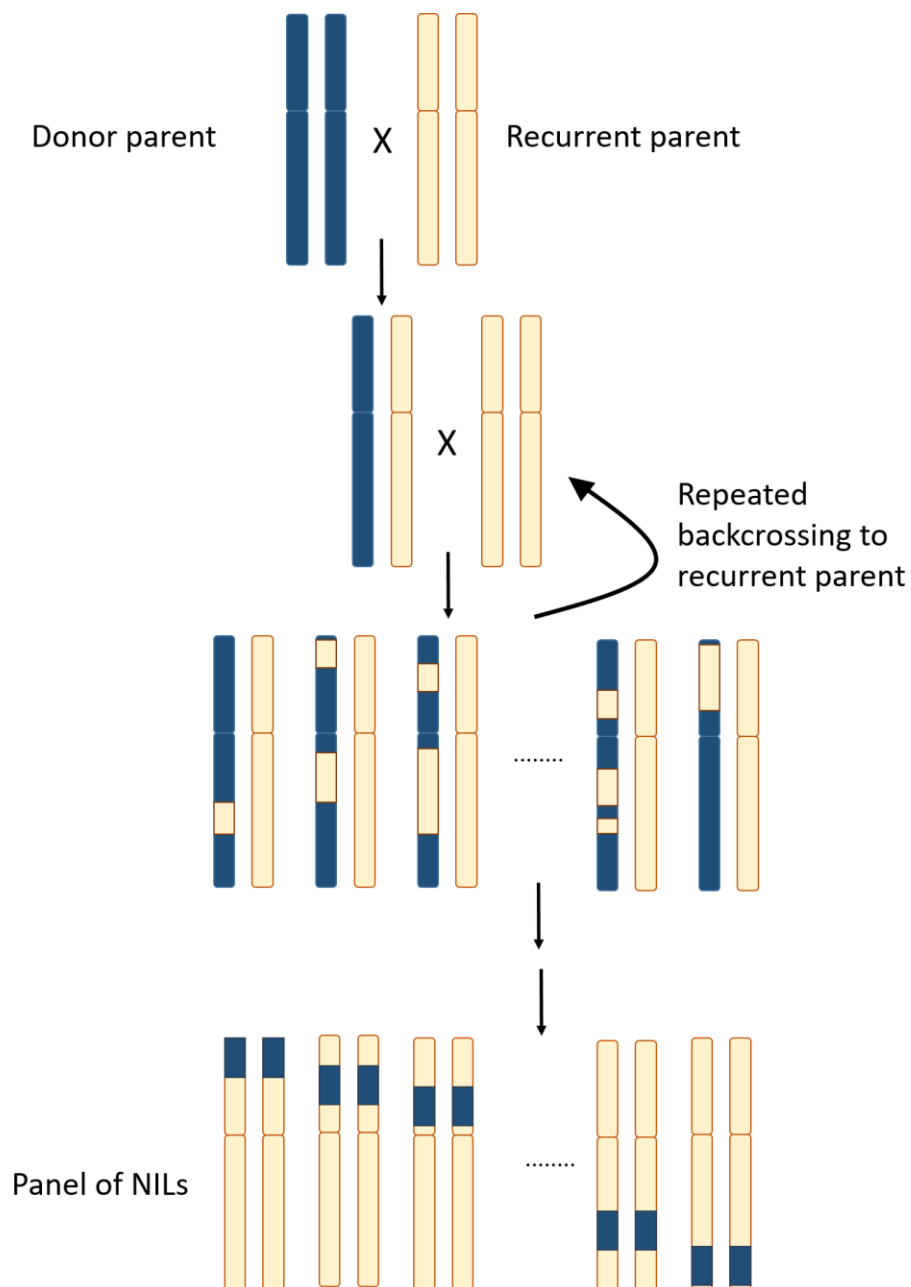
**Figure 1.2 Illustration of the process for near-isogenic line development.** A donor and recurrent parent are crossed. Subsequent repeated backcrossing to the recurrent parent leads to a reduction of the donor genome contribution. With marker-assisted selection, a panel of NILs can be constructed.

# 1.5 Aims

The overarching aims of the doctorate are to:

- Use forward genetic screening to map loci controlling root system architecture in a wheat mapping population.
- Determine the root secretions landscape in a wheat mapping population and its association with rhizosheath formation.
- Dissect the microbiome of the rhizosheath of a wheat mapping population.
- Test for genetic diversity in the ability of wheat lines from the same mapping population to recruit distinct microbiomes.
- Establish appropriate agronomical root and rhizosphere traits that can be used for large-scale phenotyping and breeding.

# 2

# Root System Architecture

## 2.1 Abstract

Wheat root system architecture is critical to ensure efficient uptake of nutrients and water from the soil to support crop development and grain filling. However, root system architecture (RSA), the spatial configuration of roots in the soil is overlooked in crop breeding due to the challenge of phenotyping organs below ground. Here I explore the genetic control of RSA with a particular focus on root growth angle, a trait that is associated with deeper rooting. Using forward genetic screens, I locate RSA quantitative trait loci (QTL) in the Avalon x Cadenza doubled haploid wheat mapping population. I determine the correlation between the traits of mature plants in the field and those of seedlings grown in pots. Replicable QTLs were associated with root angle and mapped to chromosomes 3A and 4D, explaining 7% of phenotypic variation. After extensive root phenotyping, the tails displaying phenotypes at the extremes of the population distribution were taken forward for field trials. Correlations between seedling root phenotypes, yield and the root and canopy phenotypes of mature plants in the field were calculated.

# 2.2 Introduction

Climate change models project increases in drought incidence while soil nutrient losses contribute to environmental damage and lost profits (for example, N fertilisers represent ~30% of cereal production costs) (Gilbert, 2012). It is estimated that global fertiliser production releases 575 million tonnes of greenhouse gases each year, and P fertilisers are made from finite reserves that may be exhausted in the next 50-100 years (Cordell *et al.*, 2009; Gilbert, 2012). Nutrient losses can be reduced and water capture increased by developing more resilient and efficient crop cultivars with improved root systems. However, root system architecture (RSA), the spatial configuration of roots in the soil, has often been overlooked in crop breeding due to the challenge of phenotyping organs below ground.

Most modern wheat (*Triticum aestivum* L.) varieties were bred under high input conditions, which may have masked the negative selection of RSA traits (McGrail, 2020). Modern varieties tend to have smaller root systems than landraces (Subbiah *et al.*, 1968; Virmani, 1971; Gupta and Virmani, 1973; Mac Key, 1973; Waines and Ehdaie, 2007; Fradgley *et al.*, 2020), McGrail *et al.*, 2020). Although small root systems are metabolically advantageous in well-irrigated, fertile conditions, they can have a negative impact on yield in low input scenarios if they are shallow and do not explore deeper soil strata (McGrail *et al.*, 2020). Optimal root systems differ depending on the environment. However, for the sustainable intensification of agriculture in conditions of unpredictable weather, the overarching requirement is to develop wheat RSA capable of coping with low inputs and periods of drought. The root ideotype, "steep, cheap and deep" proposed in *Zea mays* (maize) by Lynch (2013), and adopted by the wheat research community, focuses on N and water capture, through rapid and deep exploration of the sub-strata. The model does not take into consideration P uptake, which is limited to the topsoil, and the authors recognise that elements of the ideotype need to be optimised. Narrow seminal root angles result in deeper rooting, enhanced deep water and N capture and an increased chance of survival in drought (Bruce *et al.*, 2002). In addition, narrow root angles are desirable in an agricultural setting of high population density as they reduce competition between neighbours (Zhu *et al.*, 2018). An optimal root system achieves a balance between metabolic cost and effective foraging. Root density should balance the trade-off between exhaustive soil exploration and the metabolic cost of high root biomass (Ge *et al.*, 2000; Rubio *et al.*, 2001; Postma and Lynch, 2012).

16

For example, a study on the effect of terminal drought demonstrated that a variety with a large root system (total length and biomass) experienced a greater reduction in grain yield than a variety with a small root system due to poorer water use efficiency (Figueroa-Bustos *et al.*, 2020). In maize (Gao and Lynch, 2016) and *Vicia faba* (bean) (Ho *et al.*, 2005), genotypes with a steeper angle of root growth have an increased rooting depth for a given elongation rate and perform better in terminal drought conditions than genotypes with wider angles of root growth.

Crop breeding involves the selection of plants displaying advantageous traits using a combination of phenotyping and genotyping. A quantitative trait locus (QTL) is a region of the genome that encompasses one or more allelic variants that affect a phenotypic trait (Miles *et al.*, 2008). Agriculturally important QTLs often constitute complex traits – traits that are controlled by multiple genes – with gene x environment (GxE) interactions (Ross-Ibarra *et al.*, 2007; Collard *et al.*, 2005). These factors complicate the effectiveness of traditional phenotypic evaluation for crop improvement. QTL analysis is an informative approach which makes use of phenotypic data alongside genetic markers for the identification and positioning of QTLs in the genome (Ross-Ibarra *et al.*, 2007; Collard *et al.*, 2005). Genetic maps assign positions to genes or genetic markers relative to each other given their patterns of inheritance and independent assortment (Sturtevant, 1913). Integrated composite interval mapping (ICIM) is one of the most advanced statistical mapping methods and incorporates additive, dominant and epistatic QTL effects (Furbank and Tester, 2011). The genome is scanned by stepwise regression to identify markers and marker interactions, while the two markers flanking the scanning position are omitted from the calculation of phenotypic value for background control (Manschadi *et al.*, 2006).

QTL analysis requires the use of a mapping population, usually derived from parents which differ for the trait of interest. This enables the identification of linkage between the trait and regions of the genome in the progeny (Ross-Ibarra *et al.*, 2007; Collard *et al.*, 2005). F1-derived bi-parental mapping populations are most commonly used in crop genetics and include F2, recombinant inbred lines (RIL) and doubled haploid (DH) populations. F2 lines are derived from selfed F1 progeny of a cross and are suitable for preliminary mapping but less for fine mapping (Mackay and Powell, 2007). RILs arise from inbreeding the progeny of a cross to isogeny over several generations (Pollard, 2012). F1-derived DH populations have the advantage of attaining homozygosity after just one generation (Kasha and Maluszynski, 2003). DHs are generated by inducing chromosome doubling in the gametophytes of F1 individuals. Here I use the Avalon x

Cadenza Doubled Haploid (AxC) population after identifying significant differences in root angle between cultivars (cvs.) Avalon and Cadenza. The population benefits from a high-density genetic map with a mean inter-marker distance of 3.31 cM and 1793 markers (Downie *et al.*, unpublished).

The phenotyping component of QTL analysis can be laborious and technically challenging (Wasson *et al.*, 2012). The magnitude of the root network below ground makes it very difficult to determine traits in mature plants. As the early stages of plant development have been shown to be critical for the performance of the mature plant, seedling root traits represent important agronomic targets (Lynch, 2007; Lopes and Reynolds, 2010; Smith and Smet, 2012). Furthermore, seedling screens are completed on a shorter time-scale. Most phenotyping techniques that have been developed for roots are low throughput such as soil sampling (Wasson *et al.*, 2012), thermography (Lopes and Reynolds, 2010), x-ray computed tomography (Gregory *et al.*, 2003) and rhizotrons (Nagel *et al.*, 2012). Recently, two high-throughput root phenotyping methods for seedlings have been developed: the growth of seedlings between layers of germination paper contained in a plastic pouch and the growth of seedlings in soil-filled clear pots (Richard *et al.*, 2015). While the growth pouch uses less space, the clear pot method has been shown to have greater heritability and consistency across experiments (Richard *et al.*, 2015). Although such laboratory methods do not emulate field conditions, root measurements tend to be more precise and reproducible compared with heterogeneous field conditions (Bolot *et al.*, 2009). Shovelomics is a method considered to have one of the highest throughputs among field phenotyping techniques. It involves the excavation of root crowns from the field and the removal of soil to analyse traits such as root angle, crown root number, nodal root number, root span, tiller diameter and tiller number (Trachsel *et al.*, 2011). Although shovelomics is labour intensive and requires a large area, it provides useful information about root architecture in the field (Trachsel *et al.*, 2011).

The fact that the five most socio-economically important arable crops (wheat, *Hordeum vulgare* [barley], maize, *Oryza sativa*, [rice] and *Sorghum bicolor* L. [sorghum]) share a common ancestor and display genomic macro- and micro-colinearity (Bolot *et al.*, 2009) facilitates the characterisation of novel genes that have previously been described in a related crop. Numerous studies have reported QTLs for RSA in rice (Uga *et al.*, 2013; MacMillan *et al.*, 2006; Steele *et al.*, 2006; Steele *et al.*, 2007; Yue *et al.*, 2006; Shimizu *et al.*, 2004) and maize (Li *et al.*, 2015;

Tuberosa *et al.*, 2002; Landi *et al.*, 2007). However, few RSA QTLs have been cloned due to the lack of precision in positioning QTLs in mapping populations (Mai *et al.*, 2014).

In rice, a cloned gene, *DEEPER ROOOTING 1* (*DRO1*), was found to control root angle through an increased gravitropic response (Uga *et al.*, 2013). The *DRO1* QTL was detected on chromosome 9 using 117 RILs derived from a cross between a shallow-rooting rice cultivar, IR64 and a deep-rooting rice cultivar, Kinandang Patong (KP) (Uga *et al.*, 2011). *DRO1* was initially fine-mapped to a 608.4 kb interval using $BC_2F_3$ recombinant lines (Uga *et al.*, 2011). Subsequently, the region was narrowed to 6.0 kb using near-isogenic lines (NILs). Lines homozygous for the KP allele have increased root biomass in deep soil layers, and have significantly greater grain filling than IR64 in conditions of drought (Uga *et al.*, 2013). Transforming a genomic fragment containing *DRO1* into IR64 increased the degree of deep-rooting (Uga *et al.*, 2013). *DRO1* is regulated by auxin, as seen by the interaction of auxin-response factors (ARFs) with an auxin response element (ARE) in the *DRO1* promoter and the reduction of *DRO1* expression after auxin (2,4-dichlorophenoxyacetic acid, 2,4-D) treatment (Uga *et al.*, 2013). The difference between the IR64 and KP alleles appears to be a single base pair deletion resulting in a premature stop codon in the IR64 allele (*DRO1-IR*). The truncated DRO1-IR protein loses plasma membrane specificity, potentially due to the lack of a C-terminal localisation signal (Uga *et al.*, 2013). Studies have revealed the functionality of DRO1 in Arabidopsis (*Arabidopsis thaliana*) and plum (*Prunus domestica*) (Guseman *et al.*, 2017). However, little work has yet been conducted in other cereal species. In spite of the hexaploidy and complexity of the wheat genome, this success story can inspire similar goals in wheat.

# 2.2.1 QTL identification in the Avalon x Cadenza doubled haploid population

Using the genetically-characterised AxC population, this QTL analysis aimed to:

- Determine the extent of genetic variation for RSA in the Avalon x Cadenza doubled haploid population.
- Use forward genetic screening to map loci controlling root system architecture in a wheat mapping population.
- Find major effect loci controlling root system architecture.

## 2.2.1.1 Materials and methods

### 2.2.1.1.1 Germplasm

The AxC DH population was developed by and sourced from Clare Ellerbrook, Liz Sayers and the late Tony Worland (John Innes Centre, JIC), as part of a Defra funded project led by ADAS.

### 2.2.1.1.2 Experimental design

Experimental design was undertaken using the "Blockdesign" package in R (R Core Team, 2016; Edmondson, 2016). To phenotype the AxC population, parental lines and their 201 DH progenies were characterised using fifteen replicates per line per experiment, divided over three sets with five replicates per experiment. Sets were grown in consecutive weeks. A total of three experiments were undertaken in February 2019 (Exp1), June 2019 (Exp2) and September 2019 (Exp3), resulting in up to 45 replicates per line depending on germination rate and phenotyping possibility. Individuals were allocated across 90 pots, 12 individuals per plot, in a random block design with five main levels and eighteen sublevels using the R "blocksdesign" package (Figure 2.1).
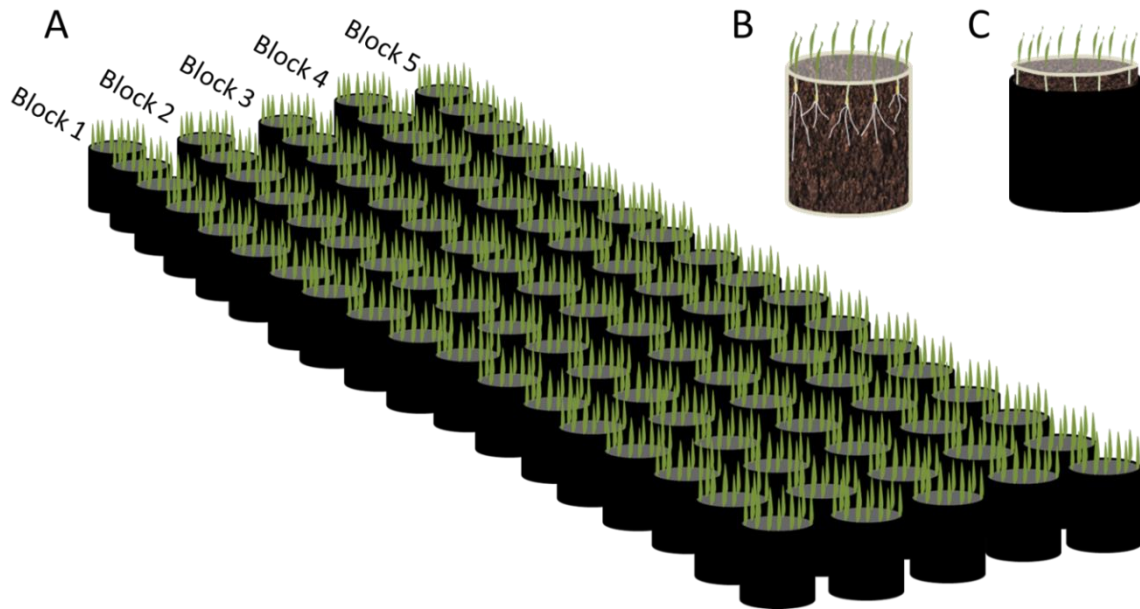
**Figure 2.1. Layout of the clear pot screen of the Avalon x Cadenza doubled haploid population.** (A) Each line had one replicate in each of five blocks, resulting in a total of five replicates per line per set. Three sets of screens totalled one experiment. The eighteen pots per block represented sub-blocks containing twelve different genotypes per sub-block. (B) Seeds were sown against the surface of clear pots (C) Clear pots were inserted into black pots to protect the seeds and roots from light.

## 2.2.1.1.3 Root phenotyping

Wheat seedlings were grown in 4 L clear pots (ANOVApot®, 200 mm diameter, 190 mm height) as per Richard *et al.* (2015) with the following conditions: a daytime temperature of 18-24 ºC and night time temperature of 15-18 ºC, 10,000 lux supplementary sodium vapour lights ensuring a 16 hour day length. Twelve genetically-different seeds per pot were sown vertically against the pot wall with the embryo pointing down. Seeds were not pre-germinated to select for uniformity in seed size and stage of germination due to limited seed supply and the prohibitive time requirement associated with processing such large numbers of seeds. However, this step would otherwise have been recommended. Seeds were sown in Levington M2 compost (pH range, 5.3 - 6.0; particle size, 0-10 mm; conductivity, 228-414 s; nutrient added, 192 mg $L^{-1}$ N, 98 mg $L^{-1}$ P, 319 mg $L^{-1}$ K) (ICL, Suffolk) at a depth of 2 cm with a four-cm separation between seeds. The clear pots were placed in black pots to shield the roots from light during growth. The pots were gently watered until the soil was saturated. One layer of empty black pots was positioned around the block of planted pots and surrounded by foil-backed insulation material to minimise edge effects. To photograph seedlings, clear pots were removed from the black pot

and placed on a rotating stage in front of a fixed Olympus TG-4 camera (Essex, UK) in an open-sided black box to shield from excessive extraneous light. Each seedling was photographed by rotating the stage incrementally, including the numbered position on the pot in each image and the pot label at the beginning of the image series for the pot. The camera was remotely-triggered with a phone using the OLYMPUS Image Share app. Photographs were taken four, five and six days after sowing. Processing time was around 25 minutes for the imaging of twenty pots. To assign images to genotypes on the computer, images were renamed using an Excel script. ImageJ software (Schneider *et al.*, 2012) was used to measure root angles and root length at a rate of around three images per minute. Automation was not used so as to mitigate for computational error (e.g. oblique seed orientation that prevented accurate measurement of root angle would not be considered by automated software; root length could be underestimated by software when the root disappeared into the soil). Root angle was measured for each day as the angle between the first pair of seminal roots at half the seminal root length (Figure 2.2). The seminal root length of each plant was fixed as the mean of the two seminal roots on day 5. Total root length (cm) was calculated as the sum of the lengths of the primary root and the two seminal roots on day 5. Root growth rate was calculated as the increase in root length (cm) per day, based on the mean difference in root length over a 24 h period on an individual plant measured on days 4, 5 and 6.
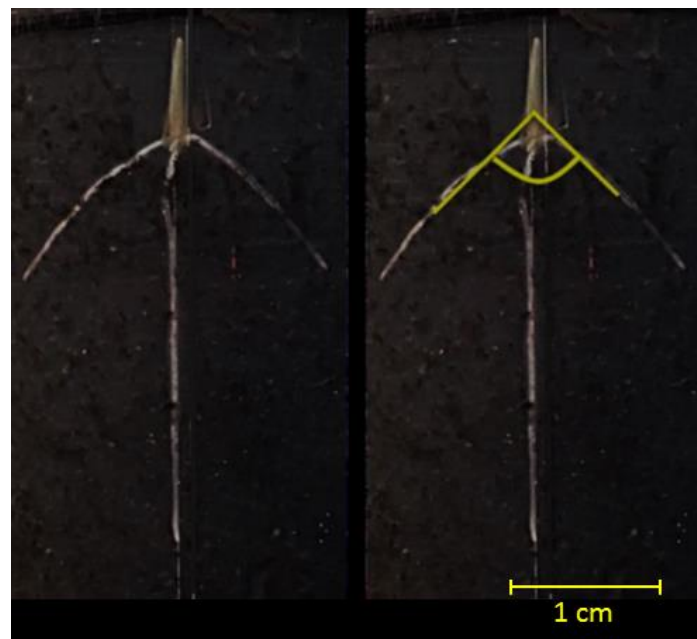


**Figure 2.2. Angle between the first pair of seminal roots in wheat seedlings.**

## 2.2.1.1.4 Statistical analysis

Statistical analysis was performed using the R software suite (version 3.3.2; R Core Team, 2016). To test for differences between wheat lines and for correlations between phenotypes across three sets of three experiments, best linear unbiased predictions (BLUPs) were generated for each line using the lme4 package, assigning *Set* and *Experiment* as random variables, totalling observations for ~8400 groups (Bates *et al.*, 2015; R Core Team, 2016; Edmondson, 2016). Block did not have a significant effect so spatial variation was not added to the model as a random effect. Analysis of variance (ANOVA) was performed on the BLUPs using the R package, lmerTest. The Pearson correlation test was applied to the BLUPs to test the strength of relationships between traits in R (R Core Team, 2016). Heritability for each root trait was calculated in GenStat based on the model with the lowest Akaike information coefficient out of a series of iterations (Line x Experiment x Block).

## 2.2.1.1.5 QTL mapping and sequence analysis

ICIM software (Li *et al.*, 2015) was used for the construction of a linkage map (Downie *et al.*, unpublished) and QTL analysis in the AxC population. The threshold for QTL detection was determined with 1000 permutations at α=0.05 (Churchill and Doerge, 1994), and a step of 1 cM was used. Manhattan plots were generated using the ggplot2 R package (Wickham, 2009). The physical position of markers was determined by mapping to the *Triticum aestivum* (Chinese Spring) IWGSC RefSeq v1.0 assembly (Alaux *et al.*, 2018). The number of F2 testcross progeny required to be genotyped to detect sufficient crossovers to achieve a desired kilobase or gene block resolution for QTL mapping was calculated as described in Dinka *et al* (2007):

$$N = \log(1-P)/\log(1-T\text{-marker}/100R)$$

where N is the number of meiotic gametes (chromosomes) that must be genotyped in which it can be determined whether a crossover is located proximal or distal to the targ*et al*lele, P is threshold probability of success (e.g., 0.95), T-marker is expected distance between flanking molecular markers (kilobases or candidate genes), and R is local or genome-wide average recombination frequency (kb/cM or genes/cM).

# 2.2.1.2 Results

## 2.2.1.2.1 Root phenotypic variation

In a preliminary clear pot screen (ten replicates per cultivar) of the parents of multiple mapping populations, cvs. Avalon (A) and Cadenza (C) were noted for their contrasting root angle and length (data not shown). Consequently, the AxC population was taken forward for QTL analysis. Approximately 9000 seedlings (~45 per line) were screened for root angle, root length and root growth rate across three independent experiments. Root angle measurements were not taken for seedlings whose orientation made it challenging to measure angle accurately, and root length was not measured for seedlings whose roots did not grow fully against the clear surface of the pot. As such, measurements for approximately 8400 seedlings were retained and BLUPs calculated for each line to account for random variation between experiments and blocks. Root length measurements from five days after sowing were taken forward to analysis as the roots of many lines had reached the bottom of the pot by the sixth day. The AxC population displayed transgressive segregation for all the measured traits with the presence of phenotypes more extreme than the parental phenotypes (Figure 2.3). Primary root length was an exception with most of the progeny displaying a longer primary root than both parents (Figure 2.3.b). Avalon had a narrower seminal root angle than Cadenza (ANOVA, $p = 0.031$), longer seminal roots (ANOVA, $p = 0.025$), and a longer primary root, although the latter did not reach statistical significance in these clear pot experiments (ANOVA, $p = 0.075$, Figure 2.4). The GxE effect was significant and accounted for by BLUP calculation. Primary root length and seminal root length had a strong, positive correlation (Pearson, $\rho = 0.43$, $p < 0.001$, Figures 2.5 and 2.6). There was no correlation between root growth rate and root angle. Seminal root length at 5 days after sowing was negatively correlated with root angle: plants with narrow root angles tended to have longer roots (Pearson, $r^2 = -0.17$, $p = 0.018$). The significant correlation between angle and length but not rate could reflect earlier germination in lines with narrow angles. The correlation of root angle and primary root length did not quite reach statistical significance, although tended towards a negative trend ($p = 0.07$). Total root length was negatively correlated with root angle, presumably resulting from the greater contribution of seminal roots than the primary root to overall root length (Pearson, $r^2 = 43$, $p < 0.001$). Among the seminal root traits, root angle displayed the highest heritability at 0.60 (Table 2.1). Primary and seminal root length were

moderately heritable (0.27 and 0.33 respectively). Total root length was not heritable in spite of being a function of primary and seminal root length (0.096), potentially due to the error variances from each trait being combined for total root length. Root growth rate had negligible heritability. As this trait is dominated by temperature, future experiments could express relative root growth rate on a thermal-time basis (degree-hours) using mean soil temperature per pot measured by a temperature probe.
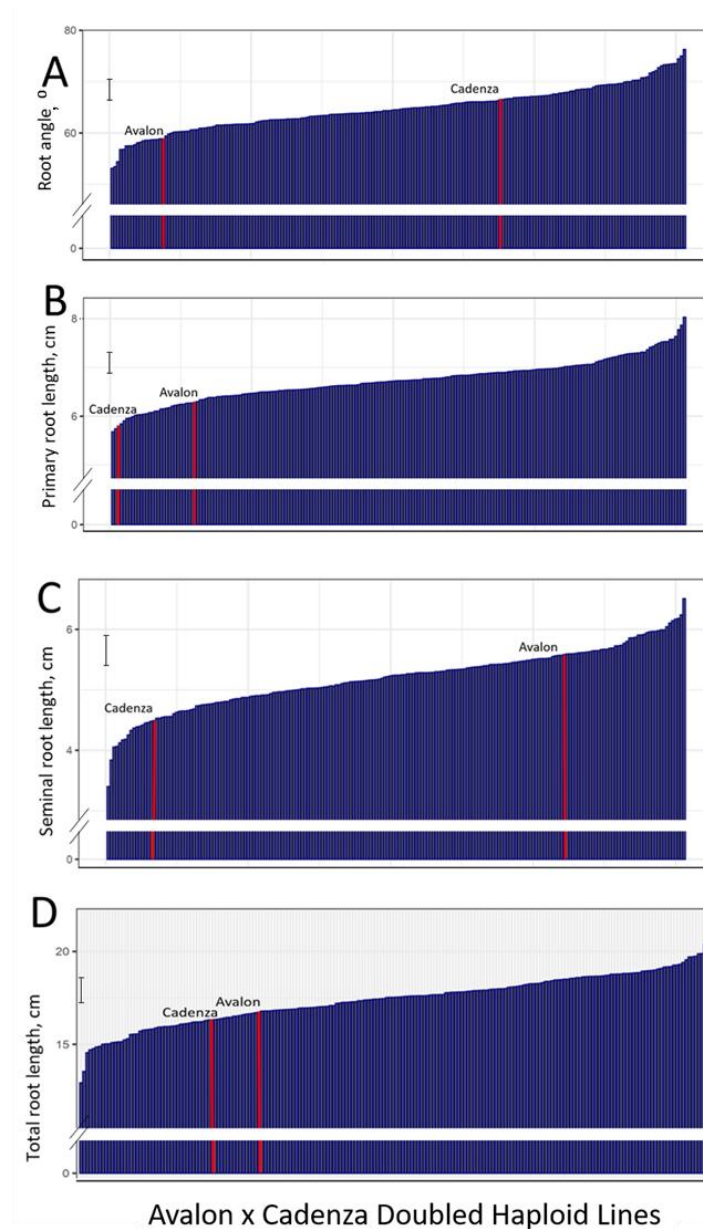


**Figure 2.3 Phenotypic variation in RSA traits of the AxC DH mapping population**. (A) Angle between the first pair of seminal roots. (B) Primary root length. (C) Seminal root length (D) Total root length. Plotted are BLUPS for each line, with standard deviation among BLUPs shown above the plot. Parental line means are shown in red.
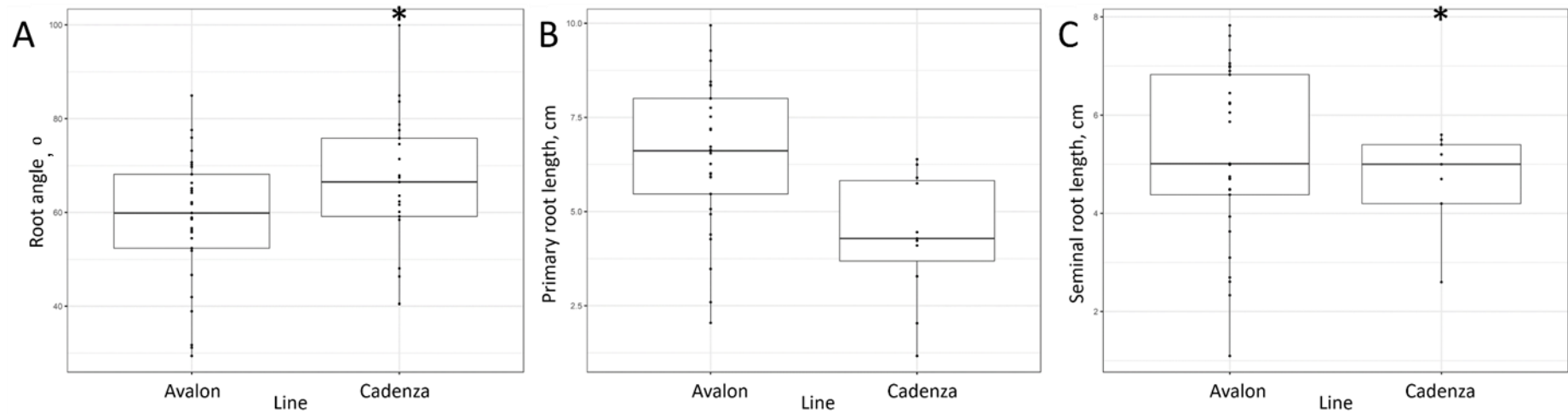
**Figure 2.4 Phenotypic variation in RSA traits of the wheat varieties, Avalon and Cadenza**. Phenotypes of pot-grown plants were measured five days after sowing in multiple sets of experiments. (A) Angle between the outer pair of seminal roots, n = 50 (B) Primary root length, n = 40 (C) Seminal Root Length, n = 38. Boxes comprise the interquartile range (25% - 75%). The line inside the boxes is the median value. The whiskers display the minimum and maximum values after removing outliers. The asterisk indicates a statistically significant difference (p < 0.05) between genotypes.
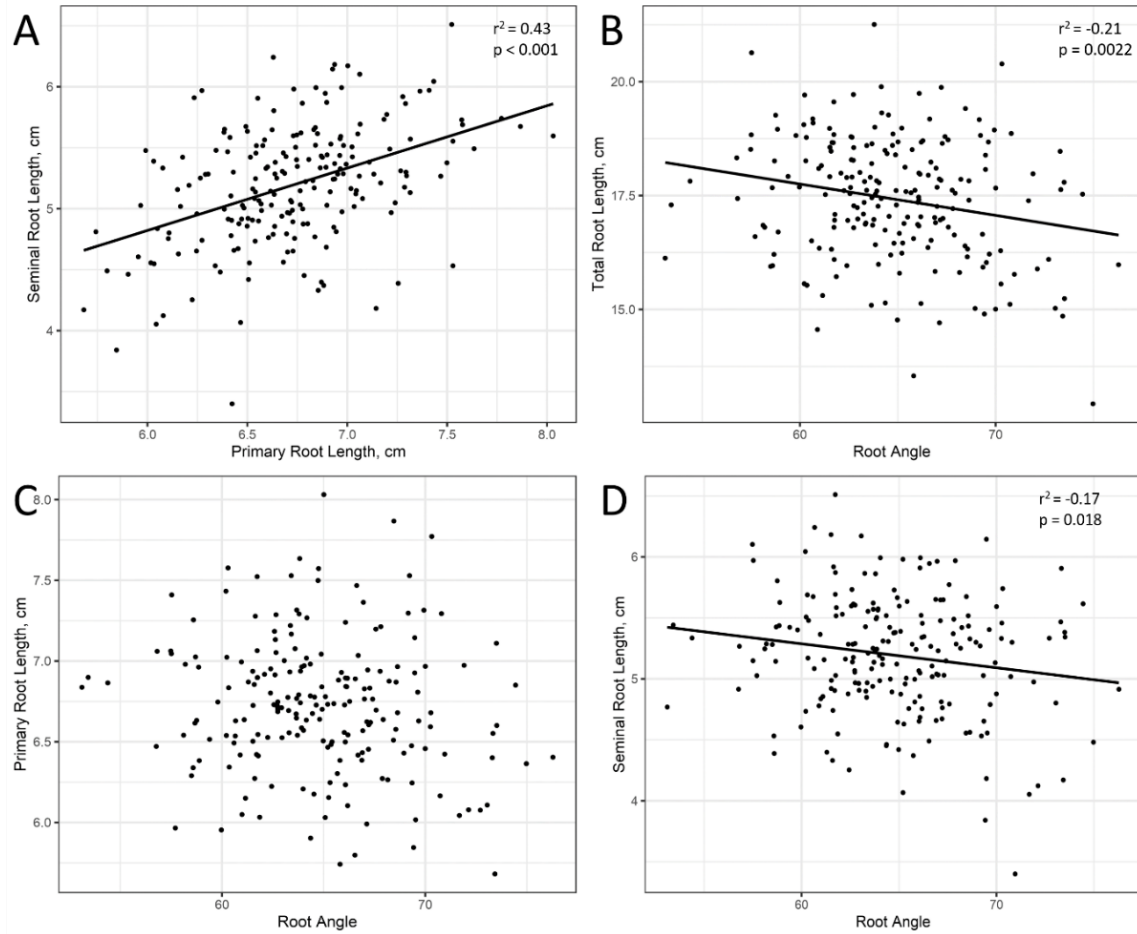
**Figure 2.5 Relationship between root traits in five-day old seedlings of the Avalon x Cadenza doubled haploid mapping population.** Plotted are BLUPS for each line. The Pearson correlation coefficient ($r^2$), alongside the associated level of significance (p), is displayed for each panel.
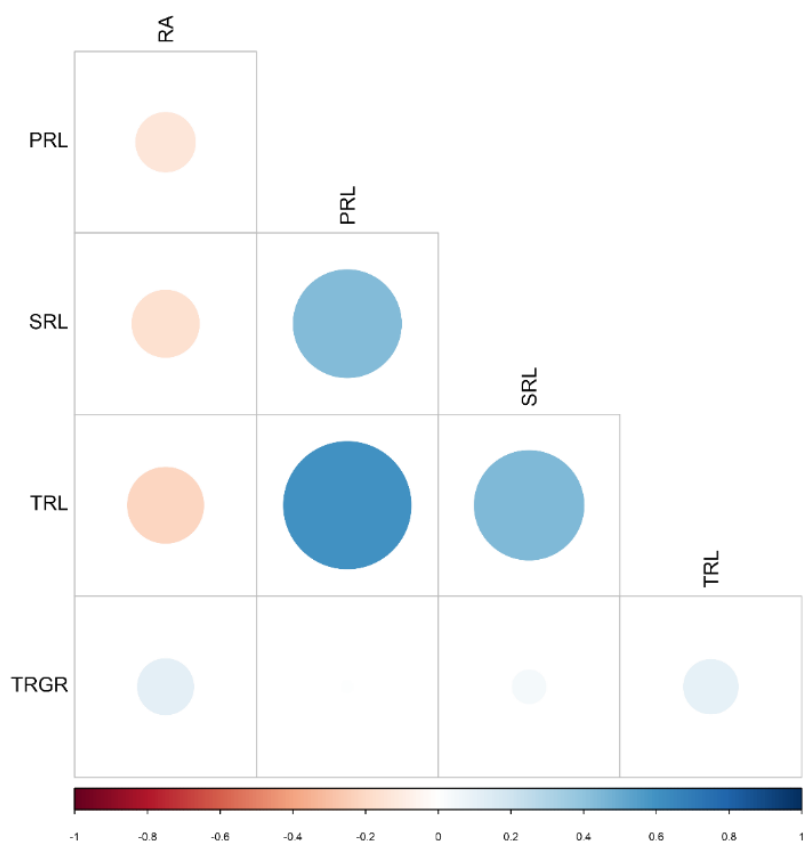
**Figure 2.6 Correlation matrix of seedling root traits in the Avalon x Cadenza doubled haploid population.** BLUPs for each of 203 wheat lines were calculated and the strength of the correlation between phenotypes was tested using the Pearson Correlation. RA, root angle; PRL, primary root length; SRL, seminal root length; TRL, total root length; TRGR, total root growth rate.

**Table 2.1. Heritability of seedling traits.** Heritability was calculated in GenStat based on the model with the lowest Akaike information coefficient out of a series of iterations (Line x Experiment x Block).

| Trait | Root angle | Primary Root Length | Seminal Root Length | Total Root Length | Primary Root Growth Rate | Seminal Root Growth Rate | Total Root Growth Rate |
|---|---|---|---|---|---|---|---|
| Heritability | 0.60 | 0.27 | 0.33 | 0.096 | 0.083 | 0.049 | 0.14 |

## 2.2.1.2.2 QTL analysis

An initial clear pot screen of 15 replicates per line (Exp1) was undertaken to screen for QTLs relating to seminal root angle, primary root length, seminal root length, total root length, and the growth rate of these root classes. Nine QTLs were identified across the traits in Exp1 (Table 2.2). In order to validate the QTLs, the experiment was repeated twice more, identifying thirteen QTL in total. Of these, the root angle QTL, *QRa.niab.4D-1,* on chromosome 4D was the only QTL identified in all three screens (Figure 2.7). One other QTL for root angle, *QRa.niab.3A-1,* located on Chromosome 3A, was identified in two out of three experiments (Figure 2.7). All remaining QTLs were only identified in a single experiment. Additive effects indicated the independent contribution of the allele to genetic variability (Awata *et al.*, 2020). Source and effect of favourable alleles were determined depending on signs of the QTL additive effects (Liu *et al.*, 2014; Awata *et al.*, 2020). The additive effects score of both of the replicated QTLs was positive, indicating that the presence of the allele at both loci increased root angle. The QTLs for root length and growth rate were identified in just one screen, Exp1. They tended to have very low additive effects (-0.18-0.47 %) but contributed a larger (3–14 %) proportion of phenotypic variance (PVE).

**Table 2.2 Root system architecture QTLs identified in the Avalon x Cadenza doubled haploid population.** QTLs displayed were identified in at least one of three clear pot experiments undertaken on a total of 9000 seedlings. QTLs were identified using IciMapping software and a genetic map constructed by Downie (unpublished). CHR, chromosome; LOD, logarithm of the odds; PVE, proportion of phenotypic variance (%); ADD, additive effect score (%).

| QTL | Trait | CHR | Position (cM) | LOD | PVE | ADD | Left Marker | Right Marker | Threshold LOD | Experiment |
|---|---|---|---|---|---|---|---|---|---|---|
| *QRa.niab.3A-1* | Root Angle | 3A | 122 | 4.8 | 7.32 | 2.1 | Tdurum_contig25642_92 | Ra_c38505_544 | 4.05 | Exp1, Exp3 |
| *QRa.niab.4D-1* | | 4D | 7 | 4.8 | 7.36 | 2.1 | BS00094770_51 | RAC875_c19666_85 | | Exp1, Exp2, Exp3 |
| *QPr.niab.5B-1* | Primary Root Length | 5B | 259 | 5.8 | 12.11 | -0.18 | Ra_c10633_2155 | Excalibur_c88113_139 | 5.25 | Exp1 |
| *QPr.niab.3A-1* | | 3A | 112 | 3.9 | 0.61 | 0.096 | D_contig22919_290 | Ex_c5858_1992 | 3.7 | Exp2 |
| *QRp.niab.7B-1* | Rate of Primary Root Growth | 7B | 108 | 5.2 | 12.79 | 0.02 | BS00110528_51 | BS00049961_51 | 5.08 | Exp1 |
| *QRp.niab.6D-1* | | 6D | 163 | 5.9 | 6.3 | 0.14 | BS00022206_51 | D_contig37522_188 | 5.7 | Exp2 |
| *QSr.niab.3A-1* | Seminal root length | 3A | 136 | 7.8 | 10.05 | -0.13 | BS00021909_51 | BS00047668_51 | 4.24 | Exp1 |
| *QSr.niab.3B-1* | | 3B | 164 | 9.4 | 12.26 | -0.15 | Excalibur_c48047_90 | BS00010083_51 | | Exp1 |
| *QSr.niab.5A-1* | | 5A | 84 | 6.7 | 14.05 | 0.17 | BobWhite_c4004_61 | BS00029347_51 | 4.47 | Exp1 |
| *QRs.niab.7B-1* | Rate of Seminal Root Growth | 7B | 117 | 3.2 | 0.58 | -0.12 | BS00110584_51 | Tdurum_contig30082_197 | 3.1 | Exp2 |
| *QRs.niab.3B-1* | | 3B | 162 | 8.5 | 12.7 | -0.5 | BS00037225_51 | IACX11202 | 4.53 | Exp1 |
| *QTr.niab.3B-2* | Total length | 3B | 189 | 4.7 | 4.87 | -0.1 | Kukri_c14967_836 | Tdurum_contig42366_818 | 4.31 | Exp1 |
| *QTr.niab.5A-1* | | 5A | 83 | 4.5 | 3.53 | 0.47 | GENE-1265_290 | BobWhite_c4004_61 | | Exp1 |
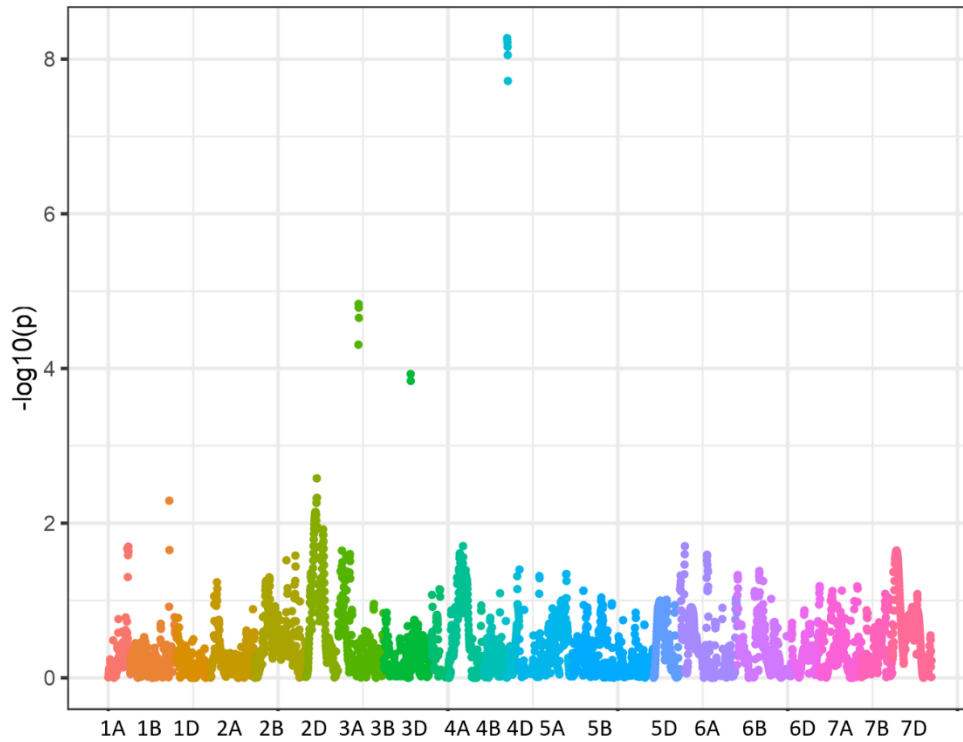
**Figure 2.7 Manhattan plot for root angle QTL identification in the Avalon x Cadenza doubled haploid population.** Seedlings (8400 individuals) were phenotyped for seminal root growth angle in three clear pot screens and BLUPs calculated for each line (random variable = experiment). Phenotypic data were combined with a genetic map (Downie *et al.*, unpublished) for integrated composite interval mapping in IciMapping software. Logarithm of odds score is plotted against the marker position (cM). Chromosomes, distinguished by colour, are indicated on the x-axis.

Given the lack of reproducibility of the QTLs for root length and growth rate, and the low heritability for these traits, only *QRa.niab.4D-1* and *QRa.niab.3A-1* were taken forward for further analysis. *QRa.niab.4D-1* and *QRa.niab.3A-1* spanned 204.1 Mb and 42.8 Mb respectively, and were predicted to contain 12400 and 6000 high confidence genes respectively using the URGI Jbrowse platform (Table 2.3) (Alaux *et al.*, 2018). In order to determine whether the QTLs were located in regions of high or low genetic recombination, the physical and genetic distances of markers on each chromosome were plotted against each other (Figure 2.8). As seen by the large jump in physical distance relative to genetic distance, *QRa.niab.4D-1* spanned a region of low genetic recombination, with a ratio of 0.03 cM/Mb. The semi-dwarfing allele, *Rht-D1b* (previously known as *Rht2*), is found on the short arm of chromosome 4D, located at 18.8 Mbp (Börner *et al.*, 1996). This does not overlap with QRa.niab.4D-1, which is found on the long arm between 131.8 and 335.9 Mbp. *QRa.niab.3A-1* did not span a region of such low genetic recombination, with a ratio of 0.054 cM/Mb.

**Table 2.3. Physical position of the genetic markers flanking the two replicated root system architecture QTLs identified in the Avalon x Cadenza doubled haploid population.** Location was determined using *Triticum aestivum* (Chinese Spring) IWGSC RefSeq v1.0 assembly.

| QTL | Flanking marker | Physical position (Mb) | QTL size (Mb) | Position (cM) |
|---|---|---|---|---|
| *QRa.niab.4D-1* | BS00094770_51 | 131.8 | 204.1 | 122 |
| | RAC875_c19666_85 | 335.9 | | |
| *QRa.niab.3A-1* | Tdurum_contig25642_92 | 522.9 | 42.8 | 7 |
| | Ra_c38505_544 | 565.7 | | |
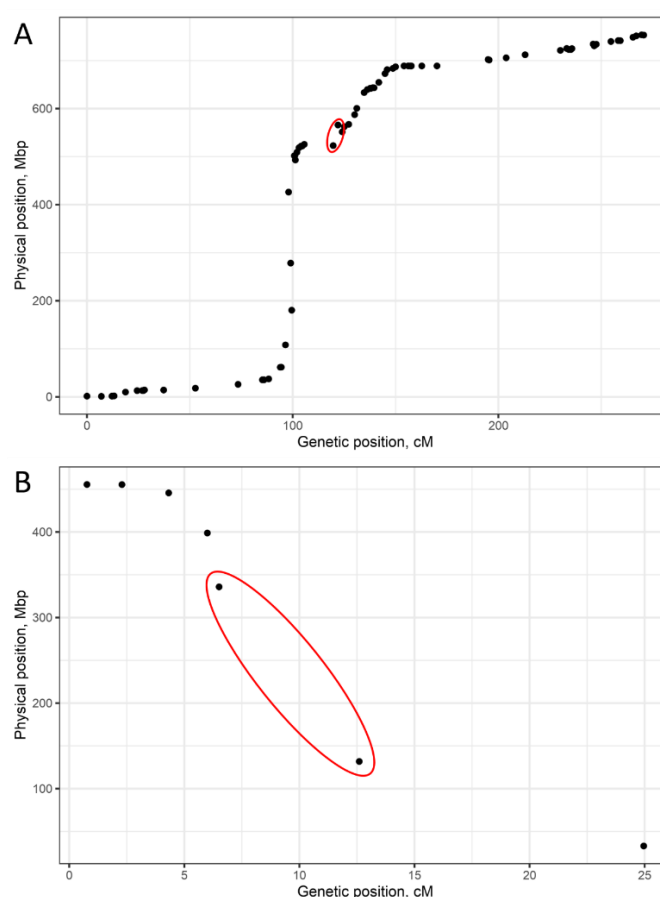


**Figure 2.8 Locating the positions of *QRa.niab.3A-1* and *QRa.niab.4D-1* on the wheat physical and genetic maps.** Plots of the physical versus genetic distances of molecular markers on chromosomes 3A (A) and 4D (B) are shown. Genetic distances are based the genetic map produced by Downie *et al.* (unpublished). Physical distances were determined by mapping markers to the wheat reference genome assembly of cv. Chinese Spring (RefSeq.1; Alaux *et al.*, 2018). The locations of QTLs are indicated by red circles

# 2.2.1.3 Discussion

## 2.2.1.3.1 Root phenotypic variation

The clear pot method used to phenotype the roots proved to be high throughput, space efficient, and easily accessible in terms of set-up, allowing one person to screen 1080 seedlings in one 10-day experiment using 3.6 m$^2$. This contrasts with other methods such as rhizotrons, which are lower throughput, occupy more space and can be difficult to handle (Bekkering *et al.*, 2020). Furthermore, clear pots allowed the growth in soil, unlike high throughput pouch methods where seedlings grow on paper, or plants grown hydroponically, where RSA will invariably differ relative to soil-grown plants (Richard *et al.*, 2015; Volder *et al.*, 2019; Bekkering *et al.*, 2020). However, the clear pot method is limited to phenotyping seedlings at a very early stage and does not provide information on the root system after more than six days of growth when the roots hit the bottom.

The AxC DH population displayed transgressive segregation for root angle and seminal root length (Figure 2.3). This is likely to be due to the combined effect of multiple loci controlling these traits, and their epistatic and additive effects. The progeny may be less fit than the parents as predicted by the Dobzhansky-Muller model, or fitter as predicted by the Bateson model (Dittrich-Reed and Fitzpatrick, 2013). The Dobzhansky-Muller model posits that reduced fitness arises from negative epistatic interactions between alleles of two parents of different species, populations or varieties (Dobzhansky, 1936; Muller, 1939). Alternatively, Bateson's model (1984, 2002) describes the situation where two alleles from different populations or varieties complement each other and lead to enhanced effects. This offers potential for selecting positive recombinants for breeding programmes.

Nearly all the progeny displayed greater primary root length than the parents, indicating heterosis. Given the polygenic regulation of the root system, it is surprising that the many combinations of parental alleles produced only positive effects on primary root length. Furthermore, mean seminal root length of the progeny exceeded the parents in both a positive and a negative direction, in contrast to the transgressive segregation predominantly in a single direction exhibited by primary root length.

Although they are both part of the seedling root system, the primary and seminal roots display different characteristics and are likely to be controlled by different genetic factors, at least in part. First to emerge from the coleorhiza, the primary root grows vertically through the soil and has been shown to contribute ~60% of the whole plant transpiration rate in early developmental stages (Golan *et al.*, 2018). The later emerging seminal roots grow at an angle in the soil. It is possible that seminal roots are subject to greater genetic control due to the importance of the gravitropic setpoint angle (GSA). As suggested by the relationship between seminal root length and root angle, there is a likely co-regulation between the GSA and elongation of the seminal roots, a process in which auxin is heavily involved (Roychoudhry *et al.*, 2013). Studies in Arabidopsis have shown that asymmetrical distribution of auxin in the roots sets the growth angle by modulating the rate of cell elongation on opposing sides of the root (Rosquete *et al.*, 2013; Ruiz Rosquete *et al.*, 2018). In Arabidopsis, shorter lateral roots exhibit a greater curvature response to clinorotation (Roychoudhry *et al.*, 2013). The same study found that placing primary roots at an angle to the axis of rotation did not alter their direction of growth but did for lateral roots, and the modulation of auxin signalling in the columella statocytes altered lateral root GSA without affecting primary root GSA (Roychoudhry *et al.*, 2013). The more complex gene interactions in seminal root development could offer greater potential for positive and negative allelic interactions compared with the primary root. Besides co-regulation, the correlation between root angle and root length may reflect the co-selection of these two traits during breeding.

Although the phenotypic observations of the AxC population presented here do not provide concrete evidence of the mechanism of genetic control of primary and seminal roots, they do support existing evidence and provide a base for discussion that can inform further investigation.

The correlations identified here corroborate findings in other studies and enhance a building body of evidence of the trends between root length and root angle (Zhu *et al.*, 2018). Seminal root growth angles were significantly negatively correlated with the length of seminal roots and with the total root length of the seedling root system.

The reasonably high heritability of seedling root angle indicates that there would be a large response to selection and high transmissibility to the next generation (Mohsin *et al.*, 2009). This is useful for accelerating selection of cultivars for breeding by allowing selection at the seedling

stage. Root length at an early developmental stage is indicative of seedling vigour and can also be selected for during breeding (Lopes and Reynolds, 2010). However, the higher heritability of root angle makes it a more important and reliable target for selection. Negligible heritability of root growth rate reflects the large environmental effect on this root trait, where the genetic variation in root growth rate was outweighed by environmental factors. To minimise environmental effects, a growth system with stricter control of soil temperature, more insulation from radiative heat and air temperature fluctuations could be installed. Another point to note is that root length and growth rate are affected by embryo and seed size, which could be due to environmental effects on the mother plant or position of the grain within the spike (Elwell *et al.*, 2011). Seeds were not preselected to select for uniformity in seed size due to limited seed supply and the prohibitive time requirement associated with processing such large numbers of seeds.

## 2.2.1.3.2 QTL identification

QTL analysis for RSA in grass crop species has largely been dominated by work on rice and maize (Dorlodot *et al.*, 2007). Until recently much less attention has been given to identifying RSA QTLs in wheat. Furthermore, few studies have addressed the implications of seedling RSA QTLs on field performance in wheat (Sanguineti *et al.* 2007; Bai *et al.* 2013; Cané *et al.*, 2014). There is evidence that QTLs identified at the young seedling stage correspond to phenotypes observed in the field at more mature stages (Tuberosa *et al.*, 2002; Landi *et al.*, 2010; Bai *et al.*, 2013; Li *et al.*, 2015; Richard *et al.*, 2015; Uga *et al.*, 2015). This justifies the validity of undertaking QTL mapping in seedlings and opens the door towards rapid screening of genotypes.

Soil heterogeneity and root plasticity make QTL identification and reproducibility challenging. It was therefore not unexpected that most QTLs could not be reproduced across experiments. The QTLs that were not reproducible related to root length and growth rate and were located on chromosomes 3B, 5A, 5B, 6D and 7B. Nonetheless, other studies have reported root length QTLs on chromosome 6D, but not in the same region (Zhang *et al.*, 2013, Atkinson *et al.*, 2015).

One QTL for root angle, *QRa-niab-4D-1,* was identified in all three experiments and another, *QRa-niab-3A-1,* was found in two out of three experiments. The higher heritability of root angle, compared with other traits, coincided with the more robust identification of these QTLs. Both root angle QTLs, donated by Cadenza, led to increased root angle and each contributed around

7% of PVE and 2% of additive effects. The smaller additive effect relative to PVE suggests that these QTLs were subject to genetic interactions. There are a few examples of QTL that individually explain up to 30% of phenotypic variation in rice and maize but RSA in most cases is governed by a suite of small-effect loci that interact with the environment (Price *et al.*, 1997; Price *et al.*, 2002, *et al.*, Giuliani *et al.*, 2005).

Root angle QTLs identified here were located on chromosomes 3A and 4D. This contrasts with previous studies, which identified wheat root angle QTLs on 2B, 3B, and 3D (Atkinson *et al.*, 2015); 2A, 3D, 5D, 6A, and 6B (Christopher *et al.*, 2013); 1A, 2B, 3A, 3B, and 7D (Liu *et al.*, 2013); 6A (Alahmad *et al.*, 2019). The large number of different QTLs found in different locations by each of these studies highlights the fact that root angle is regulated by a collection of small-effect genes. Furthermore, the identification of different QTLs using different mapping populations shows that there are relatively large amounts of natural genetic variation for the regulation of root angle in the elite wheat genepool (Hamada *et al.*, 2012; Bai *et al.*, 2013; Atkinson *et al.*, 2015).

Atkinson *et al.* (2015) identified a QTL on 4D for the ratio between the maximum width and depth of the root system, but it was located on the short arm, distant from *QRa-niab-4D-1*. Bai *et al.*, detected root length QTLs on chromosome 4D in AxC seedlings but did not investigate root angle. These QTLs were associated with *Rht-B1b*, highlighting the potential effect of dwarfing on the root system. *Rht-B1b* did not co-localise with the QTLs identified in the present study, meaning that *QRa-niab-4D-1* is a novel target for selection. Atkinson *et al.* (2015) reported a larger proportion of seedling root trait QTLs on the D genome than on the other two genomes, suggesting that the D genome has a major influence on root system development. However, the D genome is known for its low genetic diversity, as observed here in the AxC population and this has hindered the development of D genome molecular markers (Hao *et al.*, 2005).

As seen by the large jump in physical distance relative to genetic distance, *QRa.niab.4D-1* spanned a region of low genetic recombination. Low recombination complicates attempts to fine-map a gene due to the co-inheritance of many genes within that region. Besides the development of additional markers, the physical to genetic distance at the QTL (33.5 Mb/cM) would require the screening of 1000 additional meioses (based on the formula of Dinka *et al.*, 2007) to provide the chance of observing any additional recombination events at a 10 Mb resolution, or 10,000

meioses to achieve a 1 Mb resolution. This limits the possibility of resolving the correct candidate gene by genetics and recombination. *QRa.niab.3A-1* was in a zone of greater recombination frequency, with a physical to genetic distance of 18.4 Mb/cM. This would nonetheless be predicted to require the screening of 5510 additional meiosis to provide the chance of observing any additional recombination events at a 1 Mb resolution (Dinka *et al.*, 2007).

The D genome is known for its low genetic diversity, and the low marker density on chromosome 4D meant that the 6.1 cM QTL region was large and covered 204 Mb. Based on the wheat reference genome of cv. Chinese Spring, 12 400 high confidence genes were identified in the *QRa.niab.4D-1* region. This led to an estimated average density of 61 genes/Mb in the region, which would suggest it contains gene-poor regions if considering that gene-rich regions of the Triticaceae have an average of 100-200 genes per Mb (Sandhu and Gill, 2002). Such a large number of genes combined with the low genetic recombination in the region makes it unfeasible to narrow down a list of candidate genes based on annotation functional domains.

With the Cadenza genome already sequenced ([https://wheatis.earlham.ac.uk/grassroots-portal/blast](https://wheatis.earlham.ac.uk/grassroots-portal/blast)), the expected release of the Avalon genome will allow sequence alignment and the identification of polymorphisms within QTL regions. As QTL analysis identified the QTL on 4D and not 4A or 4B, this would suggest that the gene(s) either have no homeologues or the D genome homeologue is dominant. This could help narrow down the candidates. Gene expression information can be used to prioritise candidate genes underlying the QTL, and RNA silencing, complementation or TILLING could carry the QTLs forward for the experimental validation and functional analysis of candidate genes (Adamski *et al.*, 2020).

# 2.2.2 Using genetic resources for QTL validation

## 2.2.2.1 Introduction and aims

Different genetic material, such as NILs and deletion lines, is useful to complement QTL analysis. NILs carrying a single introgression in an otherwise largely homogeneous genetic background are a valuable resource to validate the effect of a particular genomic region. For example, in the recent discovery that *VERNALIZATION1* (*VRN1*) regulates RSA, NILs carrying different combinations of winter and spring *VRN1* alleles in a common genetic background were used to verify the effect of the gene on root angle (Voss-Fels *et al.*, 2018). The presence of the winter alleles consistently reduced root angle at all growth stages under greenhouse and field conditions (Voss-Fels *et al.*, 2018). NILs are currently being used to further dissect RSA: a panel of ~80 NILs in four elite spring wheat backgrounds contrasting for root biomass and root angle in four different combinations are being developed with a combination of marker-assisted selection for biomass and phenotyping in each cycle for root angle (L. Hickey, personal communication). Similarly, chromosome deletion lines can enable the identification of regions of the genome that are associated with specific phenotypes through loss of function. Thanks to its polyploidy nature, the wheat genome can tolerate major chromosomal deletions and rearrangements. This allows the development of genetic stocks exhibiting aneuploidy or sub-chromosomal deletions. Chromosomal breaks can be induced during crossing schemes via the inheritance of chromosomes in the monosomic condition (Endo *et al.*, 1996) or through gamma ray irradiation which causes double-strand breaks resulting in genomic insertions and deletions (Datta *et al.*, 2018).

The aims of the using different genetic resources were to:

- Use near-isogenic lines to validate the effect on root angle of cvs. Avalon and Cadenza alleles in identified QTL regions.
- Use a combination of sequencing and bioinformatics techniques to genotype cv. Chinese Spring deletion lines in order to:
- Validate the location and effect of identified QTLs on root angle by phenotyping lines containing deletions spanning the QTL region.

- Phenotype Paragon gamma deletion lines in order to validate the location and effect of identified QTLs on root angle.

# 2.2.2.2 Materials and methods

## 2.2.2.2.1 Germplasm

### 2.2.2.2.1.1 Near-isogenic lines

NILs derived from cvs. Avalon and Cadenza were sourced from the Simon Griffiths group at the JIC (Table 2.4). The NILs represent most of the identified QTLs on the 820 K Axiom Wheat HD Genotyping Array, a high-density array containing 819 571 exome-captured single-nucleotide polymorphism (SNP) sequences derived from hexaploid, tetraploid and diploid wheat accessions and wheat relatives.

**Table 2.4 List of AxC near-isogenic lines phenotyped in this study.**

| Near Isogenic Line | Background genotype | Introgression location (chromosome) |
|---|---|---|
| CSSL 1 | Avalon | 4D |
| CSSL 20 | Avalon | 3A |
| CSSL 21 | Avalon | 3A |
| CSSL 26 | Avalon | 3B |
| CSSL 63 | Cadenza | 4D and 3B |
| CSSL 68 | Cadenza | 3B |
| CSSL 79 | Cadenza | 3B |
| CSSL 93 | Cadenza | 3A |
| CSSL 94 | Cadenza | 3A |

### 2.2.2.2.1.2 Chinese Spring deletion lines

Deletion lines generated in the cv. Chinese Spring were received from the Wheat Genetics Resource Centre (WGRC) located at Kansas State University (Table 2.5). The deletion lines arise from a cross between *T. aestivum* cv. Chinese Spring and an individual of *Ae. cylindrica* containing

a chromosome present in the monosomic condition (Endo *et al.*, 1996). As a result of the cross, chromosomal breaks are induced in the gametes not inheriting the monosomic *Ae. cylindrica* chromosome (Figure 2.9). These breaks are rapidly stabilised by the gain of a telomere structure and can be inherited by offspring.
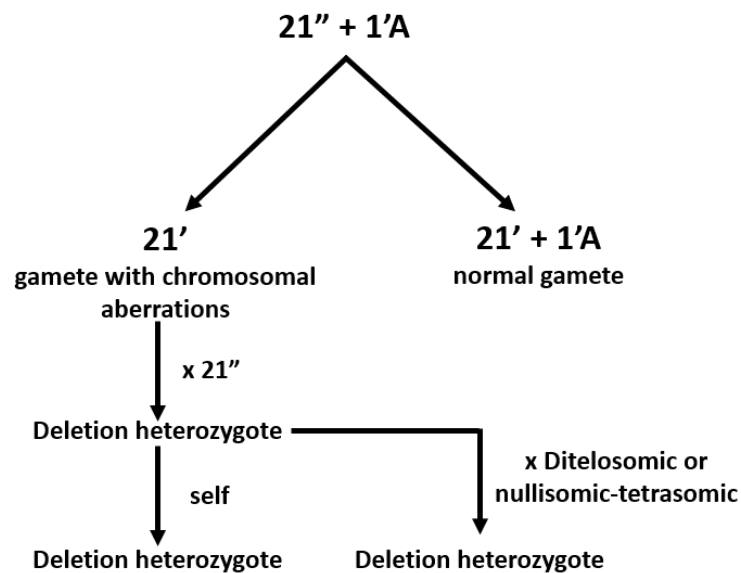


**Figure 2.9. A scheme showing the production of the deletion stocks in common wheat**. "A", *Aegilops* chromosome or chromosome segment causing chromosomal aberrations; ", diploid; ' haploid. Adapted from Endo *et al.*, 2016.

**Table 2.5 List of Chinese Spring deletion lines sequenced and phenotyped in this study.** Lines were developed at the Wheat Genetics Resource Centre (WGRC) located at Kansas State University.

| Abbreviation | Full identifier |
|---|---|
| 4DS-1 | 4532 , 1 , CS del4DS-1 |
| 4DS-2 | 4532 , 2 , CS del4DS-2 |
| 4DS-3 | 4532 , 3 , CS del4DS-3 |
| 4DS-4 | 4532 , 4 , CS del4DS-4 |
| 4DS-5 | 4532 , 5 , CS- del4DS-5 |
| 4DL-1 | 4533 , 1 , CS- del4DL-1 |
| 4DL-2 | 4533 , 2 , CS- del4DL-2 |
| 4DL-3 | 4533 , 3 , CS del4DL-3 |
| 4DL-5 | 4533 , 5 , CS del4DL-5 |
| 4DL-6 | 4533 , 6 , CS del4DL-6 |
| 4DL-7 | 4533 , 7 , CS del4DL-7 |
| 4DL-8 | 4533 , 8 , CS del4DL-8 |
| 4DL-9 | 4533 , 9 , CS del4DL-9 del1BS-18 |
| 4DL-11 | 4533 , 11 , CS del4DL-11 |
| 4DL-12 | 4539 , 9 , CS del5DL-9 del4DL-12 |
| 4DL-13 | 4533 , 13 , CS del4DL-13 |
| 4547_4DL-14 | 4547 , 10 , CS del7AL-10 del4DL-14 |
| 4533_4DL-14 | 4533 , 14 , CS del4DL-14 del7AL-10 |

## 2.2.2.2.1.3 Paragon gamma deletion lines

Gamma deletion lines generated using the cv. Paragon were obtained from the Germplasm Resources Unit (GRU) at the JIC. The collection consists of the M4 generation of the UK spring wheat cultivar, Paragon, which was subjected to irradiation with gamma rays to induce chromosome breakage and deletions. The resulting lines were skim-sequenced by the JIC to provide an overview of the deletions present in each line. Twelve lines were selected for deletions across the QTL region identified on chromosome 3A and twenty-seven lines were selected for

deletions across the QTL region on chromosome 4D (Table 2.6). The disparity between the number of lines covering the 3A and 4D QTL regions was due to the greater size of the 4D QTL.

**Table 2.6 List of Paragon gamma deletion lines phenotyped in this study.** Lines were developed at the John Innes Centre and made available via the Germplasm Resource Unit.

| Abbreviation | Full Identifier | Chromosome of interest |
|---|---|---|
| J1-29 | J1-29 (WParG0026) | 4D |
| J1-38 | J1-38 (WParG0034) | 4D |
| J1-50 | J1-50 (WParG0046) | 4D |
| J1-7 | J1-7 (WParG0006) | 4D |
| J2-28 | J2-28 (WParG0113) | 4D |
| J3-11 | J3-11 (WParG0179) | 4D |
| J3-16 | J3-16 (WParG0184) | 4D |
| J3-39 | J3-39 (WParG0204) | 4D |
| J3-52 | J3-52 (WParG0217) | 4D |
| J3-59 | J3-59 (WParG0224) | 4D |
| J4-47 | J4-47 (WParG0304) | 4D |
| J4-64 | J4-64 (WParG0318) | 4D |
| J4-74 | J4-74 (WParG0328) | 4D |
| J4-89 | J4-89 (WParG0342) | 4D |
| J4-9 | J4-9 (WParG0269) | 4D |
| J5-28 | J5-28 (WParG0376) | 4D |
| J5-30 | J5-30 (WParG0378) | 4D |
| J6-59 | J6-59 (WParG0499) | 4D |
| J6-68 | J6-68 (WParG0508) | 4D |
| J6-71 | J6-71 (WParG0511) | 4D |
| J6-88 | J6-88 (WParG0527) | 4D |
| J7-21 | J7-21 (WParG0554) | 4D |
| J7-56 | J7-56 (WParG0587) | 4D |
| J7-6 | J7-6 (WParG0540) | 4D |
| J7-64 | J7-64 (WParG0595) | 4D |
| J7-77 | J7-77 (WParG0608) | 4D |
| J7-91 | J7-91 (WParG0622) | 4D |
| J8-19 | J8-19 (WParG0644) | 4D |
| J1-55 | J1-55 (WParG0049) | 3B |
| J2-75 | J2-75 (WParG0155) | 3B |
| J3-16 | J3-16 (WParG0184) | 3B |
| J3-66 | J3-66 (WParG0231) | 3B |
| J3-91 | J3-91 (WParG0256) | 3B |
| J5-67 | J5-67 (WParG0415) | 3B |
| J5-7 | J5-7 (WParG0356) | 3B |
| J6-11 | J6-11 (WParG0453) | 3B |
| J6-23 | J6-23 (WParG0463) | 3B |
| J6-46 | J6-46 (WParG0486) | 3B |
| J7-66 | J7-66 (WParG0597) | 3B |

## 2.2.2.2.2 Phenotyping

Plants were phenotyped using the clear pot method described in Chapter 2, Section 2.2.1.1.3.

## 2.2.2.2.3 DNA extraction and sequencing

At least 0.4 µg of high quality DNA at a concentration > 10 ng/µg, (OD 260/280 close to 1.8) in an AE buffer ([Tris·Cl] = 10 mM, [EDTA] = 0.5 mM, pH 9.0) were isolated from three-week old leaf tissue of each deletion line using the DNeasy Plant Mini kit (Qiagen, Manchester, UK). The following change was made to the protocol: samples were incubated for 60 minutes at room temperature before elution in Buffer AE (60 µg).

Whole genome sequencing was carried out at Novogene with an Illumina PE150 sequencing strategy. Sequencing was undertaken on 22.6 M - 29.6 M paired 150 bp reads, resulting in a predicted depth of 0.40-0.52x assuming a wheat genome size of 17 Gb.

## 2.2.2.2.4 Sequence data processing

To prepare the sequences for alignment, reads were trimmed of their adapters using the wrapper script, Trim Galore! (https://www.bioinformatics.babraham.ac.uk/projects/trim_galore/), and reads shorter than 100 bp or with a quality score lower than 25 were filtered out.

The reads were mapped to the *Triticum aestivum* (cv. Chinese Spring) IWGSC RefSeq v1.0 assembly using the Burrows-Wheeler Aligner (BWA) tool, BWA-MEM (Li 2013). BWA finds the best positions of reads aligned to a reference sequence. Potential polymerase chain reaction (PCR) duplicates were removed using 'rmdup' command in the Picard software (https://broadinstitute.github.io/picard/). Genome coverage rate for each sample was calculated by SAM tools over jumping windows of 1 M, 10 K and 2 K bases. Sequencing depth was plotted against physical position in R.

# 2.2.2.3 Results

## 2.2.2.3.1 Phenotyping near-isogenic lines for QTL validation

The nine NILs (4 for chromosome 3A, 4 for chromosome 3B and 2 for chromosome 4D) were phenotyped and tested for differences with the parental phenotypes (Table 2.7, Figure 2.10). A phenotype that contrasted with the parental background but was similar to that of the introgressed parent would validate the presence of the QTL.

With low genetic diversity on chromosome 4D, only nine markers were genotyped to characterise the NILs. Out of 94 NILs, only 7 were found to contain an introgression based on those 9 markers, and they had significant introgressions located on other chromosomes. None of the 9 markers were located within the *QRa-NIAB-D-1* region, but spanned it either side. It had to be assumed that they were indicative of the genomic region between them based on the low rates of genetic recombination across the QTL region. Two NILs, CSSL 1 (Avalon background) and CSSL 63 (Cadenza background), were selected for the validation of *QRa-NIAB-4D-1*. The justification for selection of CSSL 1 was that there was minimal introgression on other chromosomes and all markers on chromosome 4D were introgressed from Cadenza. This would make it likely that the region between the markers flanking the QTL was also of Cadenza genotype, given its low recombination rate (a physical to genetic distance ratio of 33.5 Mb/cM). CSSL 63 was chosen for the lowest number of introgressions elsewhere on the genome.

The introgressions on chromosomes 3A and 3B were characterised to a finer resolution than those on 4D, due to the higher number of genetic markers available for these chromosomes. Four NILs were selected for *QRa.niab.3A-1*. NILs were selected for 3B on the premise that CSSL 63 (selected for *QRa-NIAB-4D-1* validation) also contained an introgression on 3B. Phenotyping NILs of 3B could act as a negative control.

For chromosome 4D, CSSL 1 (putative Cadenza-4D region in an Avalon background) did not differ significantly from Avalon for the seminal root angle phenotype, but almost reached significant difference with Cadenza (p = 0.84). CSSL 63 (Avalon 4D region in Cadenza background) did not differ significantly from either parents. The fact that these NILs did not differ significantly from their parental background does not validate *QRa-NIAB-4D-1*. However,

44

it does not give grounds to reject the hypothesis that there is a QTL for root angle on Chromosome 4D because the very low marker density meant that large regions of the chromosome were not genotyped. An introgression may not have been identified or the assumed introgression could have been interspersed with the background genotype.

For the chromosome 3A QTL, CSSL 93 and CSSL 94 (Avalon 3A region in a Cadenza background) had significantly larger root angles than Avalon but did not differ from Cadenza. CSSL 21 (Cadenza 3A region in an Avalon background) had significantly narrower root angles than Cadenza but did not differ from Avalon, while CSSL 20 (Cadenza 3A region in an Avalon background ) displayed intermediate root angles. As the NILs for chromosome 3A did not differ significantly from their parental background, *QRa-NIAB-3A-1* was not validated using this approach.

In conclusion, none of the NILs differed from their parental background, indicating that the introgressions did not modify the root angle relative to the parental background under the experimental conditions used.

**Table 2.7 Significance of variation between the mean root angle of near-isogenic lines and the parents, Avalon and Cadenza.** Level of significance based on a Student's T-test is denoted by * ($< 0.05$).

| Near Isogenic Line | Background genotype | Introgression location (chromosome) | Root angle difference to Avalon (p-value) | Root angle difference to Cadenza (p-value) |
|---|---|---|---|---|
| CSSL 1 | Avalon | 4D | 0.97 | 0.084 |
| CSSL 20 | Avalon | 3A | 0.26 | 0.57 |
| CSSL 21 | Avalon | 3A | 0.98 | 0.034* |
| CSSL 26 | Avalon | 3B | 0.85 | 0.15 |
| CSSL 63 | Cadenza | 4D and 3B | 0.68 | 0.32 |
| CSSL 68 | Cadenza | 3B | 0.22 | 0.44 |
| CSSL 79 | Cadenza | 3B | 0.034* | 0.91 |
| CSSL 93 | Cadenza | 3A | 0.074 | 0.72 |
| CSSL 94 | Cadenza | 3A | 0.076 | 0.48 |
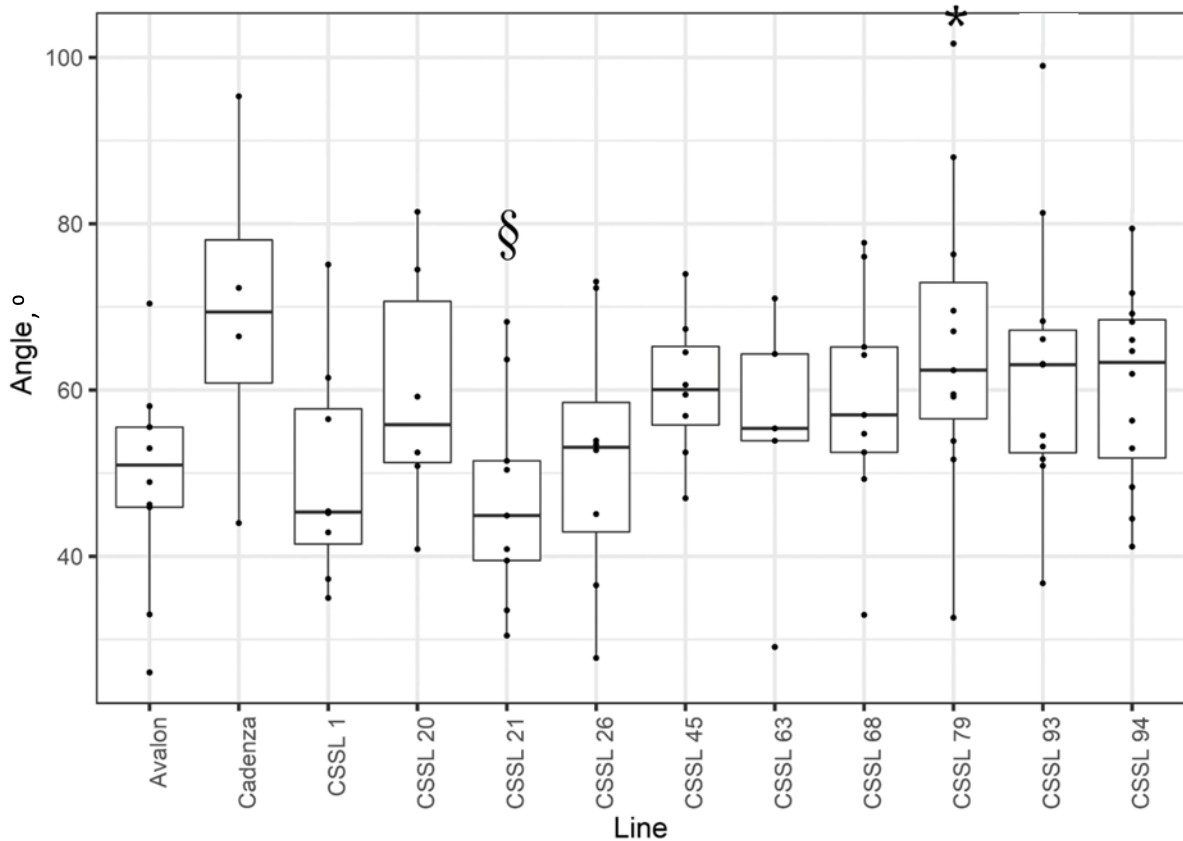
**Figure 2.10 Seminal root angle of near-isogenic lines and the parents, cvs. Avalon and Cadenza.** Significant differences from the mean root angle of Avalon (*) and Cadenza (§) are based on a Student T-test, p < 0.05, n > 5 per line.

## 2.2.2.3.2 Sequencing Chinese Spring deletion lines

In order to refine the QTL region, Chinese Spring deletion lines carrying terminal deletions were phenotyped with the aim of comparing the location of the deletion with the effect of the deletion on root angle. Information was lacking and unreliable on the physical position of the breakpoints. C-banding, followed by expressed sequence tag (EST) mapping, had previously been used to determine the breakpoint locations (https://www.k-state.edu/wgrc/genetic_resources/Germplasm/Deletions/group4.html). However, neither method determined the precise location of the breakpoints, and blasting the ESTs against the *Triticum aestivum* (Chinese Spring) IWGSC RefSeq v1.0 assembly revealed sparse coverage of the chromosome and a large number of EST preferentially aligning to chromosomes 4A and 4B.

Therefore for the present study, the lines were skim sequenced using 22-29.6 M paired 150 bp reads, with a predicted depth of 0.4-0.52 X.

Sequencing depth (the number of times a particular base is represented within the sequencing reads) was plotted against the position along the chromosome to illustrate the location of the deletions. Results for the short and long arms of chromosome 4D are shown in Figures 2.11 and 2.12 respectively. Chromosomal break points were clearly identified by the drop in sequence depth, and the precise location of the breaks was determined using a 2 Kbp jumping window (Table 2.8; Figure 2.13). Two lines, 4DS-5 and 4DL-3, described by KSU as 4D deletion lines were actually found not to have any deletions on chromosome 4D (Table 2.8). 4DL-9 was heterozygous for the 4D deletion, as seen by the 50 % reduction of read counts at the position of the break (Figure 2.12). The order in which the lines have their deletions corresponds between the KSU assignments and the results presented here with the exception of 4DL-1 (Figure 2.14). Here, I found the breakpoint to be nearer the centromere than previously described. 4DL-4 and 4DL10 displayed in Fig 2.14A were not used in this work as they are described as heterozygous by the Wheat Genetics Resource Centre at KSU. Eight lines had deletions or duplications on chromosomes in addition to a deletion on 4D (Figure 16, Table 2.8). These were 4DS-1, 4DS-5, 4DL-1, 4DL-3, 4DL-8, 4DL-9, CS del4DL-14 (4533) and 4DL-14 (4547).
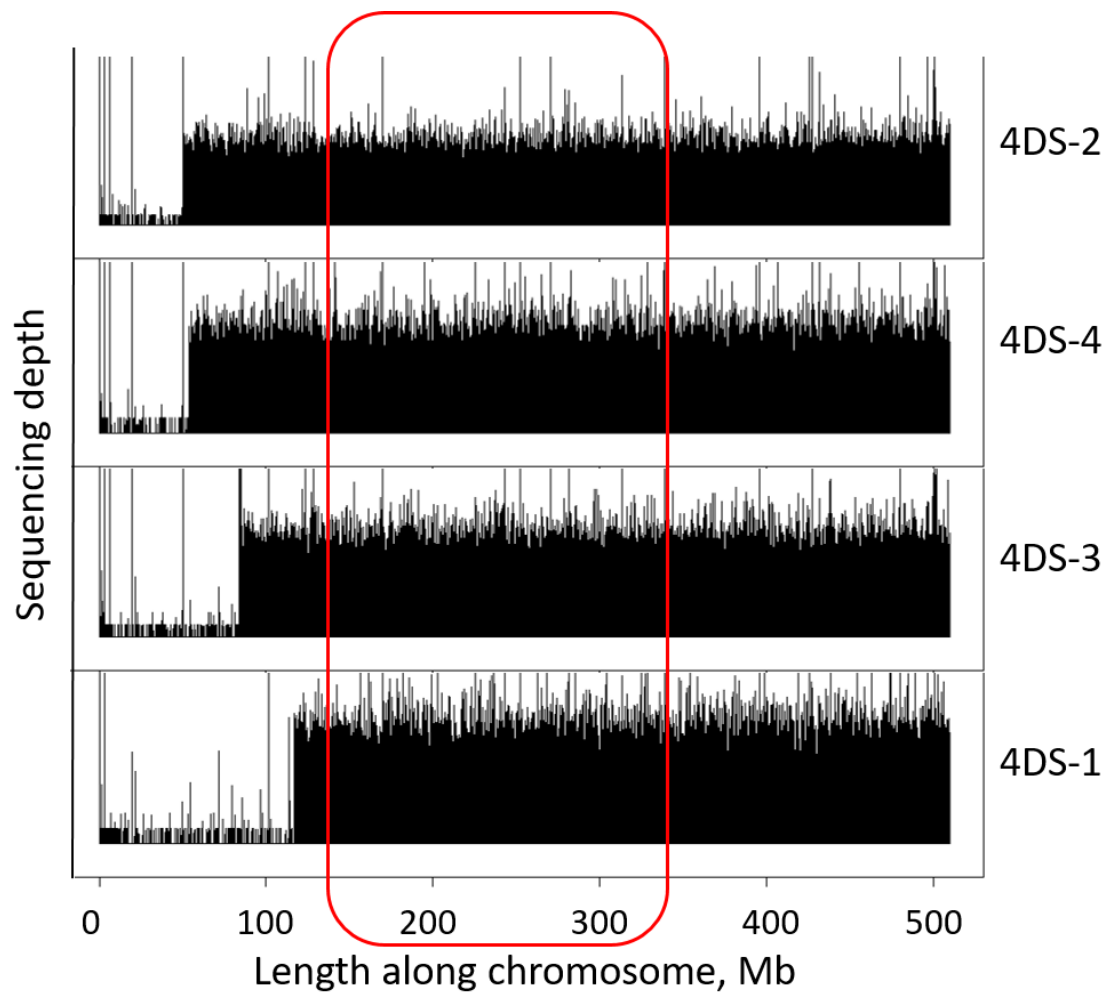
**Figure 2.11 Distribution of sequence reads on Chromosome 4D of Group 4 Chinese Spring deletion lines carrying deletions on the short arm.** Reads were mapped to the *Triticum aestivum* (cv. Chinese Spring) IWGSC RefSeq v1.0 assembly and genome coverage was calculated over 1 Mb jumping windows. Each panel displays the sequencing depth of lines with a short arm deletion. The red box displays the location of the *QRa.niab.4D-1* QTL.
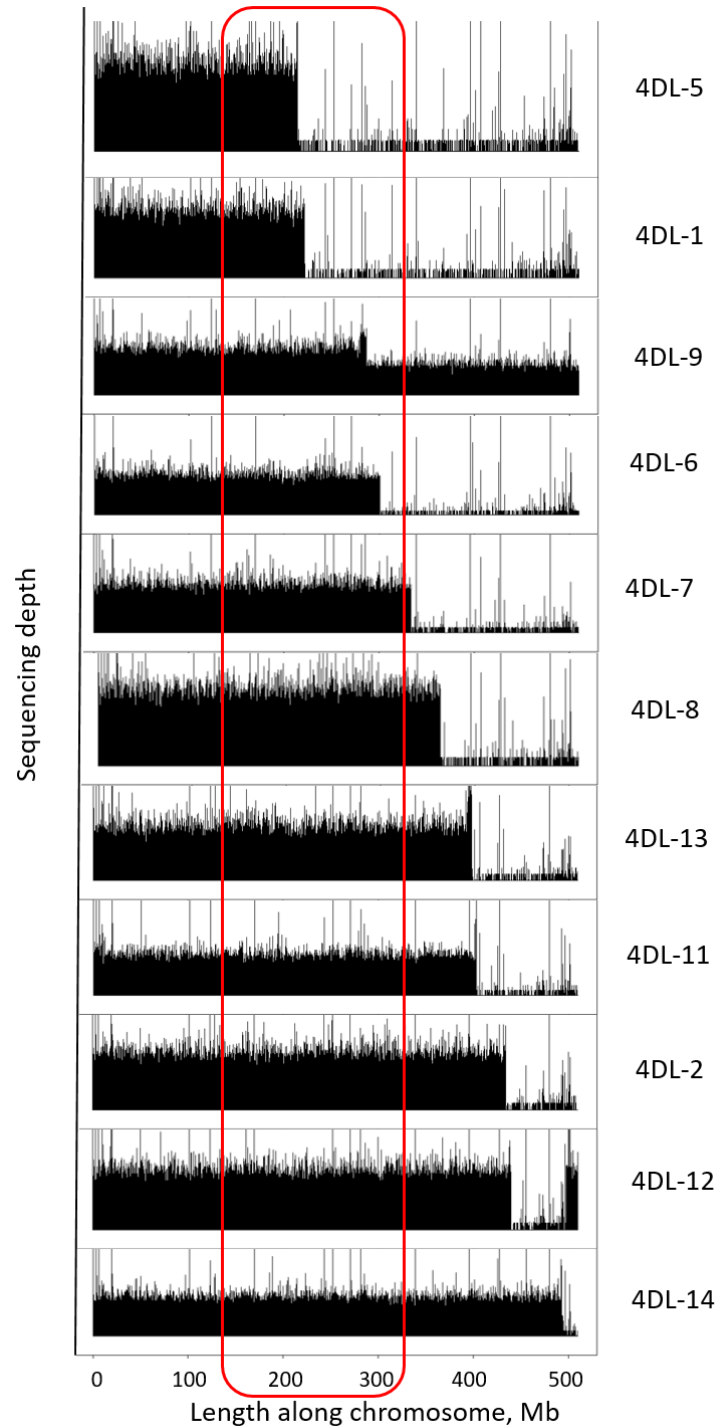
**Figure 2.12 Distribution of sequence reads on Chromosome 4D of Group 4 Chinese Spring deletion lines carrying deletions on the long arm.** Reads were mapped to the *Triticum aestivum* (cv. Chinese Spring) IWGSC RefSeq v1.0 assembly and genome coverage was calculated over 1 Mb jumping windows. Each panel displays the sequencing depth of lines with a long arm deletion. The red box displays the location of the *QRa.niab.4D-1* QTL.

**Table 2.8. Chromosomal modifications of the Group 4 Chinese Spring deletion Lines.** The lines were skim-sequenced and reads were mapped to the *Triticum aestivum* (Chinese Spring) IWGSC RefSeq v1.0 assembly. Chromosome breakpoints were determined using 2 Kb jumping windows. Hom, homozygous; het, heterozygous; WT, wild type.

| Line | Chr 4D | | Other chromosomal modifications | |
|---|---|---|---|---|
| | Deletion start (bp) | Deletion end (bp) | Chromosome | Effect |
| 4DS-1 | 0 | 116735000 | 7B | Duplication (hom), 620-735 Mb; Deletion (het), 735-751 Mb |
| 4DS-2 | 0 | 51025000 | NA | NA |
| 4DS-3 | 0 | 83963000 | NA | NA |
| 4DS-4 | 0 | 53945000 | NA | NA |
| 4DL-7 | 33833000 | 510000000 | NA | NA |
| 4DL-5 | 213793000 | 510000000 | NA | NA |
| 4DL-9 | 286470000 | 510000000 | 6D | Duplication (hom), 340-454 Mb; Deletion (het), 454-474 Mb |
| 4DL-6 | 300533000 | 510000000 | NA | NA |
| 4DL-8 | 363581000 | 510000000 | 3B | Deletion (het), whole chromosome |
| 4DL-13 | 398275000 | 510000000 | NA | NA |
| 4DL-11 | 403052000 | 510000000 | NA | NA |
| 4DL-2 | 434465000 | 510000000 | NA | NA |
| 4DL-12 | 439589000 | 497953000 | NA | NA |
| 4547_4DL-14 | 493200000 | 510000000 | 7A | Deletion (hom), 543-736 Mb |
| 4533_4DL-14 | 493209000 | 510000000 | 7A | Deletion (hom), 543-736 Mb |

| 4DL-1 | 221531000 | 510000000 | 4A | Duplication (hom), 0-120 Mb |
|-------|-----------|-----------|-----|-----------------------------|
| 4DL-3 | NA | NA | 6D | Deletion (het), 213-356 Mb |
| 4DS-5 | NA | NA | NA | NA |
| CS WT | NA | NA | NA | NA |
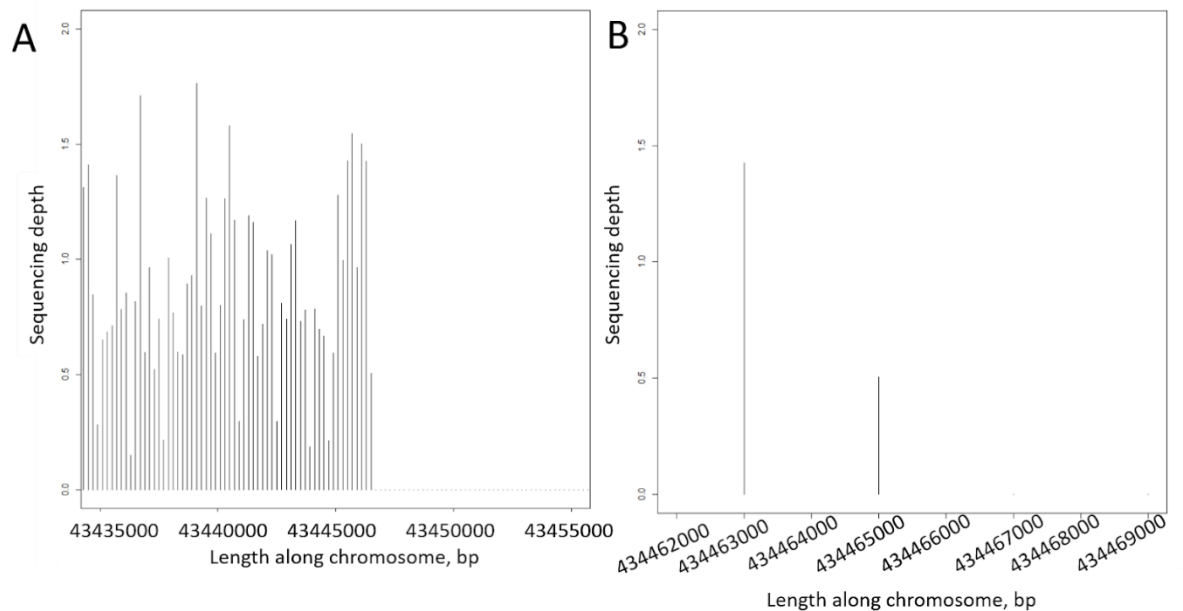


**Figure 2.13. Distribution of sequence reads in a section of Chromosome 4D of an example Group 4 Chinese Spring deletion line.** Illustration of the high-resolution identification of the position of breakpoints. Reads were mapped to the *Triticum aestivum* (Chinese Spring) IWGSC RefSeq v1.0 assembly and genome coverage was calculated over 2 Kb jumping windows. (A) a graph of a section of chromosome 4D, higher in resolution that the whole chromosome (B) a higher resolution graph showing a drop-off in base calls between 434465 and 434466 Kbp.
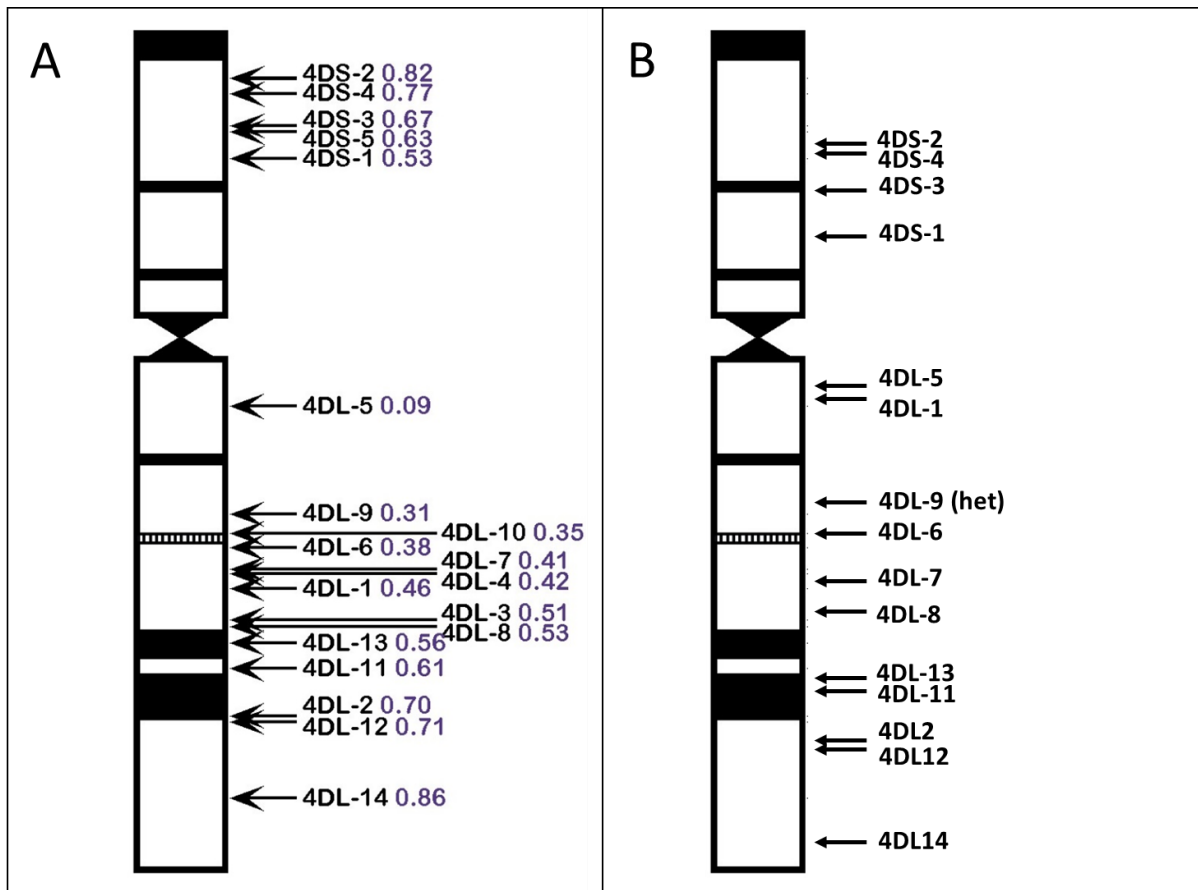
**Figure 2.14 Location of breakpoints in Chinese Spring deletion lines.** (A) Figure adapted from Kansas State University. Breakpoint locations were determined by EST mapping. Purple numbers represent FL values. (B) Locations of breakpoints as presented in this thesis by skim-sequencing.
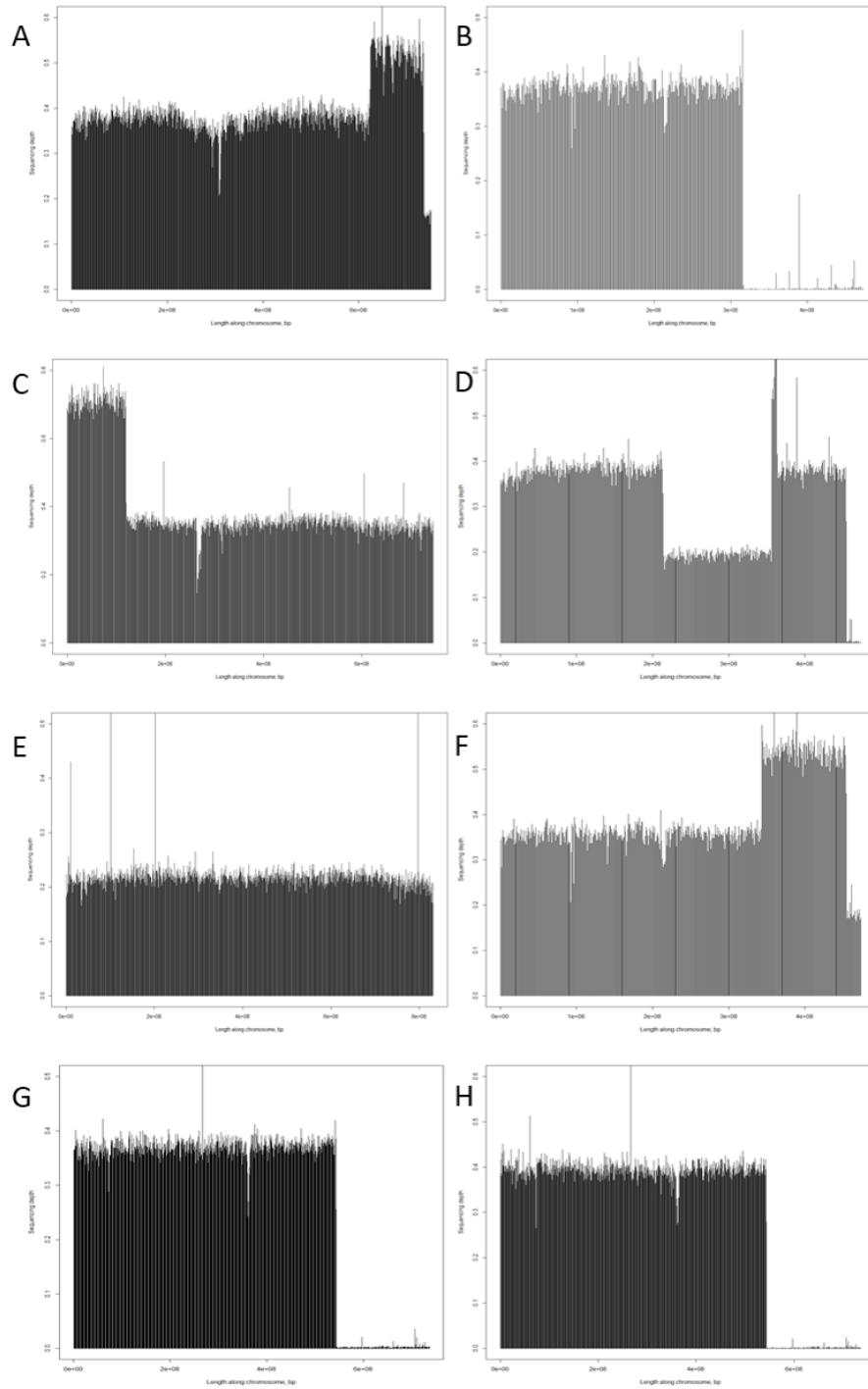
**Figure 2.15 Non-target chromosome modification of the Group 4 Chinese Spring deletion lines investigated.** The lines were skim-sequenced and the number of base calls were used to identify duplications and/or deletions. (A) CS del4DS-1 (B) CS del4DS-5 (C) CS del4DL-1 (D) CS del4DL-3 (E) CS del4DL-8 (F) CS del4DL-9 del1BS-18 (G) CS del4DL-14 del7AL-10 (H) CS del7AL-10 del4DL-14

# 2.2.2.3.3 Root phenotyping of Chinese Spring deletion lines

Using a clear pot screen, root angle was recorded for 10-14 reps per line (Figure 2.16). Variation in the number of reps per line arose from the difficulty in accurately measuring the angle of certain roots which did not grow against the clear pot surface. The lines with deletions spanning the QTL region were 4DL-5, 4DL-1, 4DL-9 and 4DL-6. The deletion present in line 4DL-7 was located on the very edge of the QTL region.

The only line to display a significant difference compared with wild-type (WT) was 4DL-7 (ANOVA, p = 0.014). The section deleted in 4DL-7 was also missing from 4DL-5, 4DL-1, 4DL-9 and 4DL-6. If the deletion in 4DL-7 contained genes regulating root angle, one would expect those lines to display the same wide-angle phenotype as 4DL-7. As this was not the case, the results of this screen remain inconclusive.

The 4DS lines had significantly less variation in root angle than the 4DL lines (p = 0.013) and had very similar means and standard deviations to each other and to WT CS. In contrast, 4DL lines displayed greater inter-line and intra-line variation. Furthermore, the lines with deletions corresponding to the location of the QTL had significantly greater standard deviation to the other lines (p = 0.049).
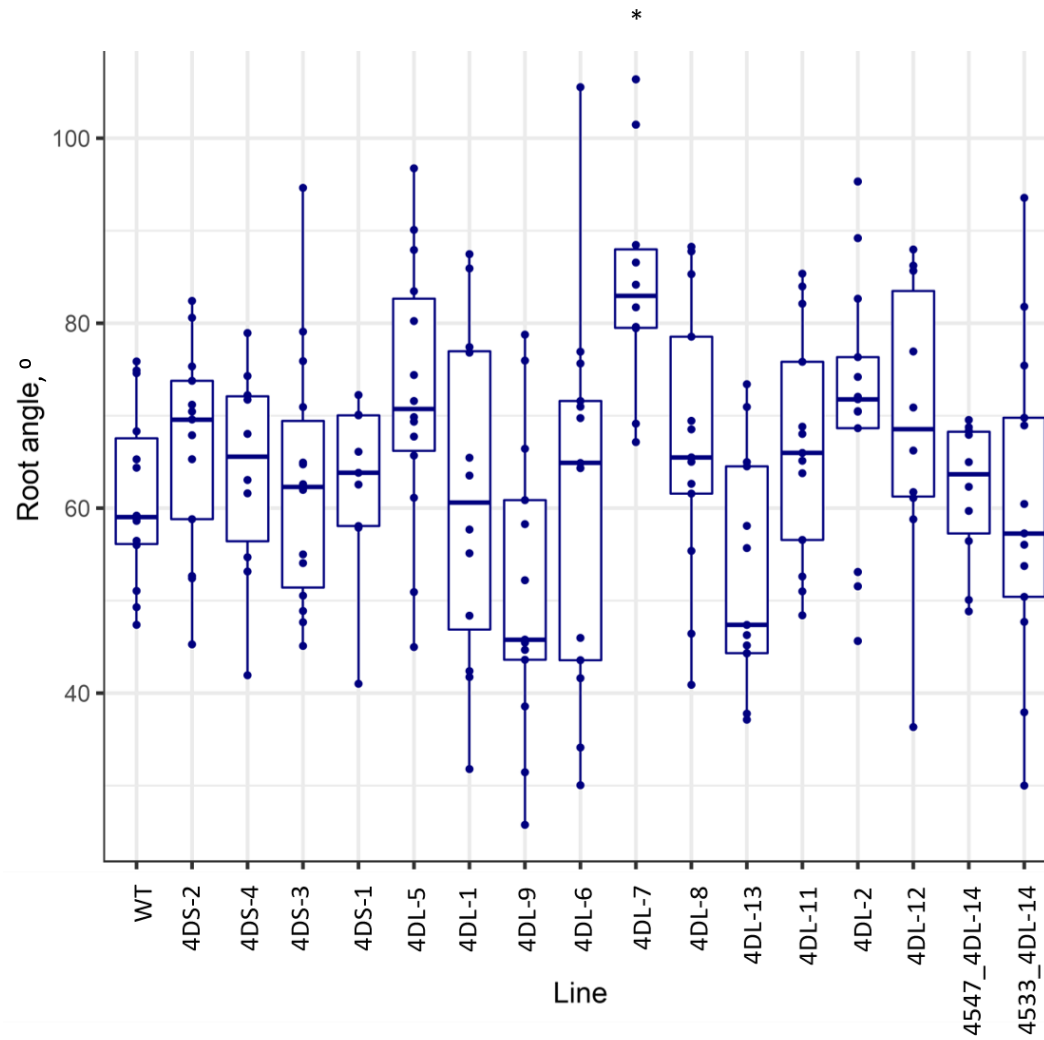
**Figure 2.16 Seminal root angle in group 4 Chinese Spring deletion lines investigated.** Lines are ordered according to the deletion startpoint. WT, wildtype; 4DS, short-arm deletions; 4DL, long arm deletions. Levels of significance relative to wild type cv. Chinese Spring are indicated as follows: *, < 0.05; **, < 0.01; ***, < 0.001.

# 2.2.2.3.4 Genotyping Paragon gamma deletion lines

Information obtained from the John Innes Centre (R. Ramirez-Gonzalez, personal communication) on the location of the deletions on chromosomes 4D and 3A in the Paragon deletion lines was combined into one graph for each chromosome to demonstrate a non-saturated tiling path of deletions across the QTL region (Figure 2.17). Chromosome 3A unfortunately had lesser coverage across the QTL region, making it more challenging to draw definitive conclusions about the location of genes involved in the QTL and increasing the likelihood of false negative results from the screen.
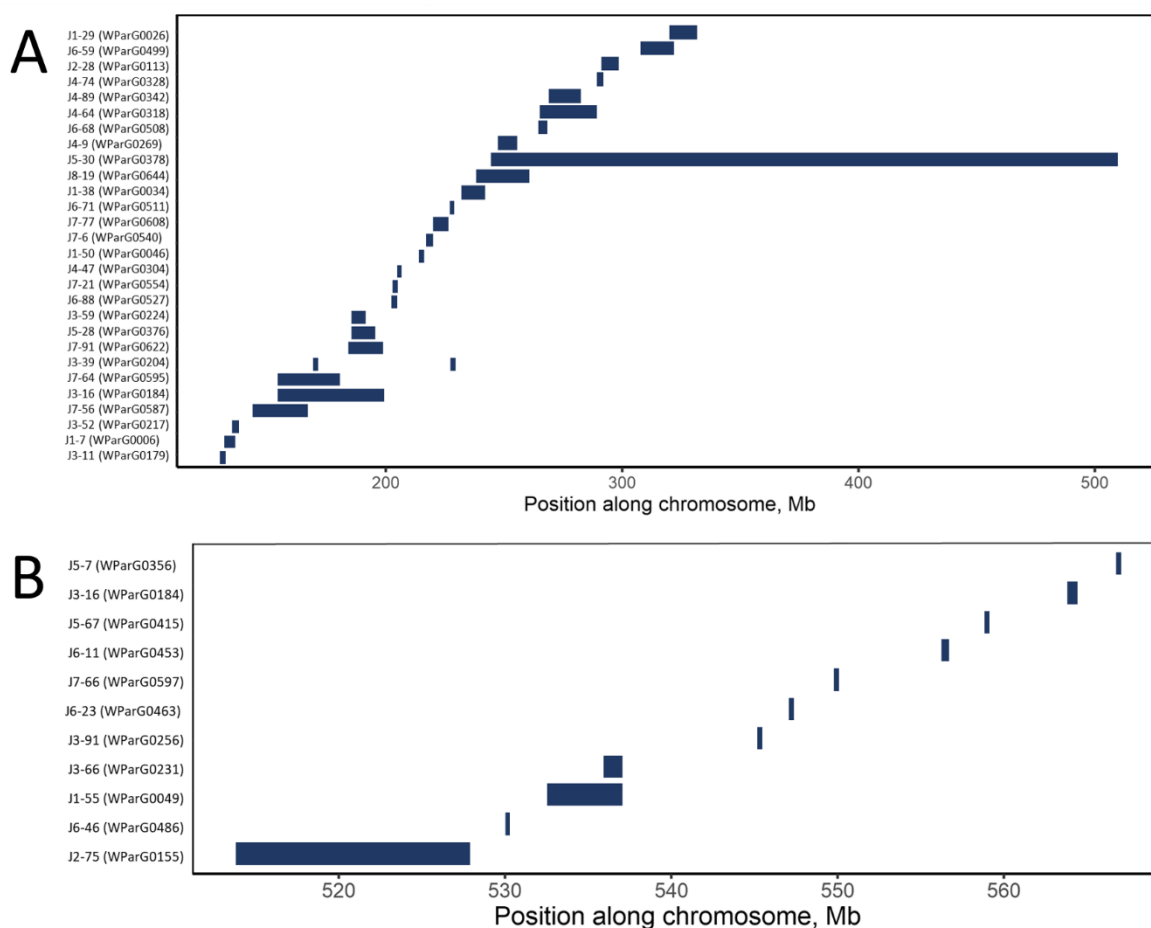


**Figure 2.17 The position of deletions along sections of Chromosomes 3A and 4D of Paragon gamma deletion Lines.** Lines are listed with their GRU code on the y-axis. Deletion locations were determined by skim-sequencing (Ramirez-Gonzalez *et al.*, unpublished). The chromosome section displayed covers the QTL region, *QRa.niab.4D-1* (A) and *QRa.niab.3A-1* (B).

# 2.2.2.3.5 Phenotyping Paragon gamma deletion lines

## 2.2.2.3.5.1 *Ra-niab-4D-1*

The Paragon gamma deletion lines phenotyped in clear pots varied significantly for root angle. Nine deletion lines had significantly wider root angles than WT cv. Paragon (Figures 2.18 and 2.19): J3-52, J3-39, J5-28, J3-59, J6-88, J7-21, J6-71, J7-6, J5-30. No deletion line had a significantly narrower root angle than WT.

The results remain inconclusive. Lines that had significantly wider angles than WT did not necessarily indicate that the gene regulating root angle was located in the deleted region because other lines with an overlapping deletion did not display a significant phenotype. For example, the wide-angled group of lines with consecutive deletions comprising J5-28, J3-59, J6-88 and J7-21, overlapped with J7-91, which did not display a significant difference to the WT phenotype.

J3-39, which displayed the most significant phenotype had two deletions. One deletion overlapped with lines which did not display any phenotype. The other deletion in J3-39 was located in relatively close proximity to that of J6-71, which displayed a significant phenotype (230.5 - 231 Mb and 227.5 - 228.37 Mb respectively). However, the lack of overlap means it is unlikely that this is related to the QTL.
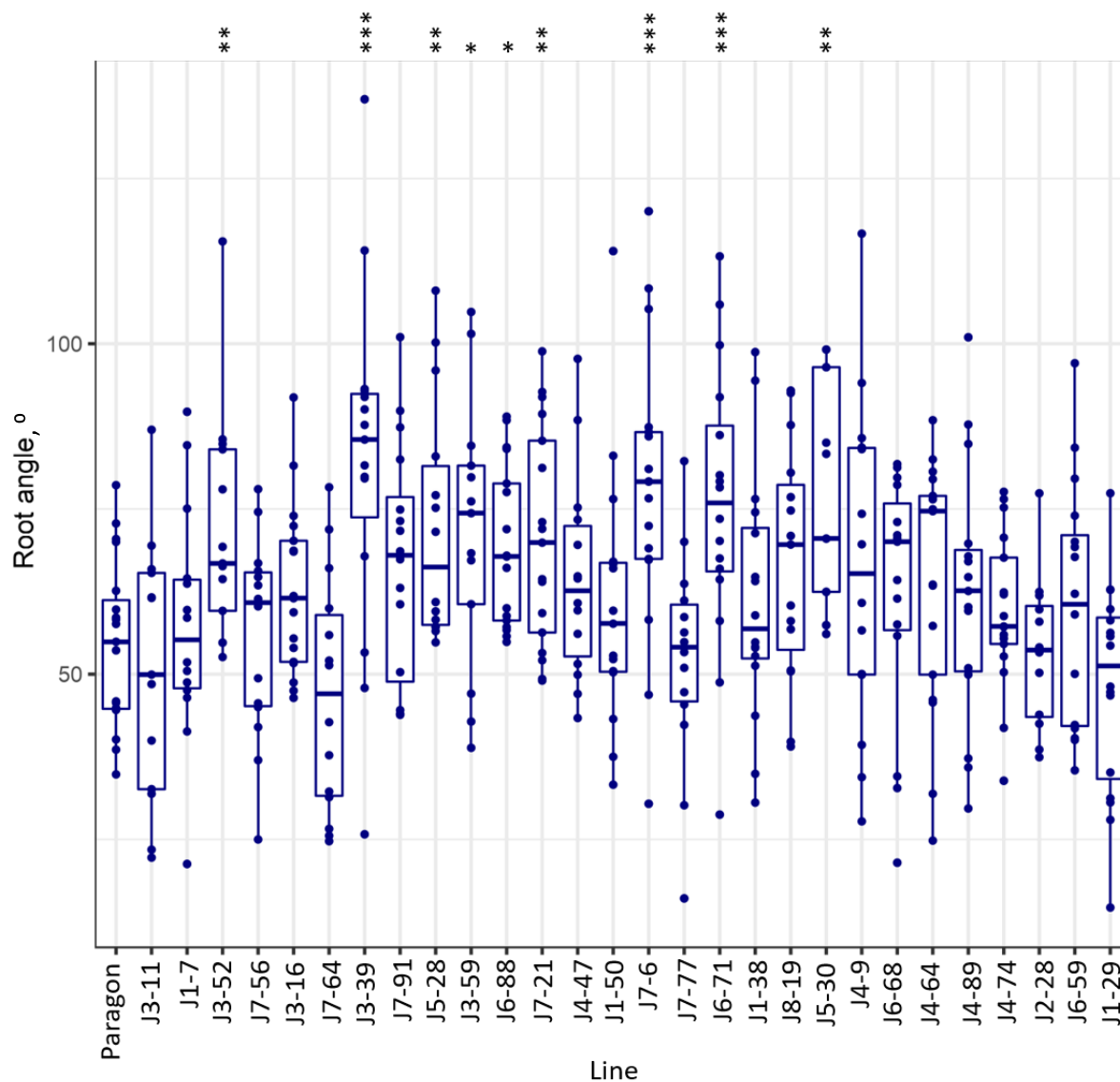
**Figure 2.18 Seminal root angle in Paragon gamma lines.** Lines were selected for containing one or more deletions between 130 and 340 Mb on Chromsome 4D. Seeds obtained from the John Innes Centre were grown in clear pots, photographed, and the angle between the first two seminal roots was measured in ImageJ software. Lines are ordered according to the deletion startpoint. Levels of significance relative to wild type cv. Paragon are indicated as follows: *, < 0.05; **, < 0.01; ***, < 0.001.
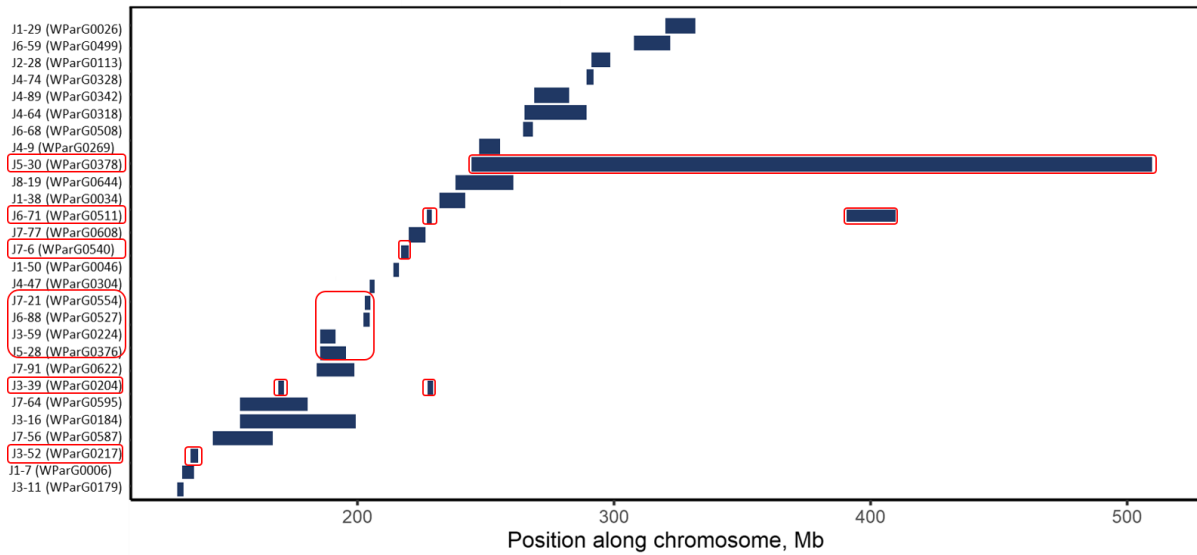
**Figure 2.19 The position of deletions along a section of Chromosome 4D of Paragon gamma deletion lines.** Lines that differed significantly from wild type Paragon for root angle are outlined by a red box. Lines are listed with their GRU code on the y-axis. The chromosome section displayed covers the QTL region, *QRa.niab.4D-1*.

## 2.2.2.3.5.2 Ra-niab-3A-1

The only line to differ significantly in its root angle phenotype from WT was J3-66, which had a significantly wider root angle than Paragon (p < 0.01, Figures 2.20 and 2.21). The chromosomal deletion possessed by J3-66 overlapped with the deletion of J1-55 and was in fact contained within the J1-55 region. However, J1-55 did not display any difference in root angle compared to WT.
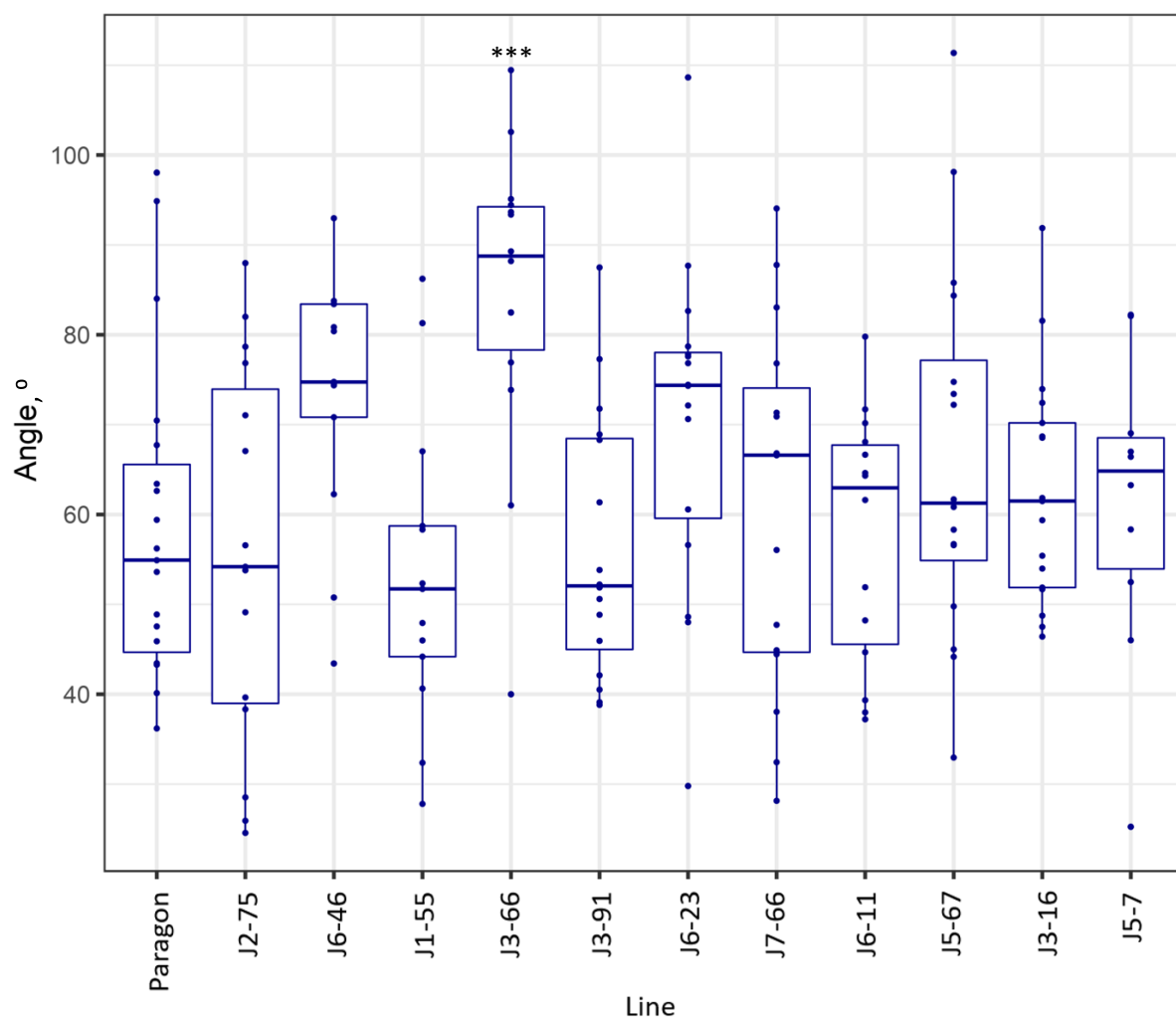


**Figure 2.20 Seminal root angle in Paragon gamma deletion lines.** Lines contain one or more deletions between 511.6 - 558.9 Mb on Chromsome 3A. Seeds obtained from the John Innes Centre were grown in clear pots and the angle between the first two seminal roots and the seed was measured in ImageJ software. Lines are ordered according to the deletion startpoint. *** indicates the level of significance relative to wild type cv. Paragon is < 0.001.
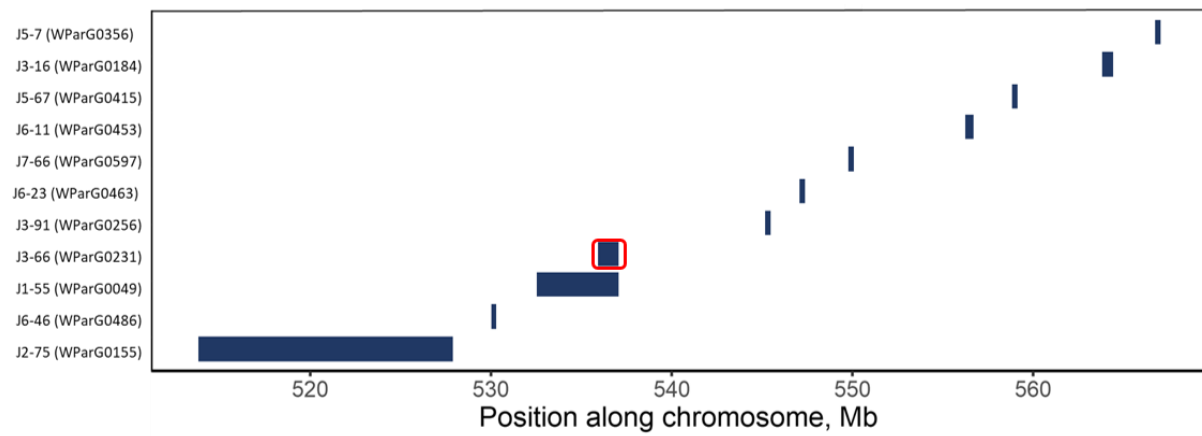
**Figure 2.21 The position of deletions along a section of Chromosome 3A of Paragon gamma deletion lines.** Lines that differed significantly from wild type Paragon for root angle are outlined by a red box. Lines are listed with their GRU code on the y-axis. The chromosome section displayed covers the QTL region, *QRa.niab.3A-1*.

## 2.2.2.4 Discussion

### 2.2.2.4.1 Near-isogenic lines for QTL validation

Here, AxC NILs carrying large introgressions putatively containing the target QTL for *Ra.niab-3A.1* or *Ra.niab-4D.1* were screened for root angle to test the hypothesis that the QTL would confer the root angle phenotype originating from the QTL allele from the donor parent. However, the root angle phenotypes were not significantly different to the recurrent genetic background. It is possible that because of the small contribution of the QTLs to overall root angle, the phenotyping experimental design used did not have enough power to identify the relatively small changes in root angle that the target QTLs were predicted to confer, based on the QTL mapping. This further highlights the complexity of RSA, and particularly root angle, regulation. If there were enough ground to believe that these NILs could lead to QTL validation, the NILs would undergo a backcrossing scheme to refine the introgression region to the size of the identified QTLs. Kompetitive Allele-Specific PCR (KASP) genotyping using primers specific to the QTL markers would provide a basis for the selection of progeny to be used for backcrossing. Through glasshouse and field validation of a phenotype associated with a particular introgression, QTLs can be tracked within breeding programmes.

### 2.2.2.4.2 Chinese Spring deletion lines for QTL region refinement

The Chinese Spring Deletion Lines are a valuable resource for physically mapping genes to regions within a chromosome, although the large size of the deletions means they lack precision. The lines were initially characterised using C-banding, a method of chromosome staining to reveal heterochromatic regions (Endo and Gill, 1996). The deletion size was reported as a fraction length (FL) value; the proportion of the chromosome arm estimated to have been retained. Certain lines were subsequently used in the NSF Wheat EST Genomics Project, where ESTs were mapped to the deletion lines and assigned to physically determined bins along the chromosome arms. Open access tools are available to search for the mapped ESTs and order them by location. However, not all deletion lines were included in the mapping project. Since

then, Hales *et al.*, (2020) genotyped four lines containing terminal deletions of 4DS, using 37 homeologous non-specific markers. In their technique, homeologous genes were simultaneously amplified using a single pair of primers and were distinguished due to differences in the size of the PCR product corresponding to the A, B and D copies (Hales *et al.*, 2020). The retained homeologues acted as controls for a deletion in the 4D homeologue. This allowed them to refine the physical position of the deletion endpoints to intervals of < 1 Mbp.

Here, I characterise all Group 4 Deletion Lines to a resolution of 2 Kbp, making this the most comprehensive characterisation of the Group 4 Chinese Spring Deletion Lines to date. In addition to determining the location of the 4D deletion breakpoints, I identified modifications on other chromosomes.

I performed a clear pot screen on the 18 genotyped deletion lines plus WT Chinese Spring. This demonstrated that one line, 4DL-7 had increased root angle relative to the WT. 4DS deletions had no visible effect on root angle and these lines had smaller standard deviations and similar means to each other and to WT Chinese Spring. In contrast, 4DL lines were more variable in their root angles. QRa.niab.4D-1 spans the interval 131-335 Mb which is located on the long arm of chromosome 4D. The lack of significant root angle phenotype relative to WT in the 4DS lines was therefore expected and indicated that the QTL was not located on the short arm. However, the phenotypic analysis of the 4DL deletion lines did not bring conclusive evidence on the location of the QTL. The greater variation among 4DL lines with deletions overlapping the QTL region could indicate that the loss of the gene(s) within the QTL region removed some level of regulation on root angle. Without this level of control, root angle was less genetically specified and plants within the same line could display narrow or wide angles. The extreme phenotype of 4DL-7 is challenging to explain as the section deleted in 4DL-7 was also missing from 4DL-5, 4DL-1, 4DL-9 and 4DL-6, yet these lines displayed no obvious phenotype. The breakpoint of the deletion of 4DL-7 was on the cusp of the QTL region but did not overlap.

## 2.2.2.4.2 Paragon gamma deletion lines for QTL region refinement

The finding that no deletion line investigated had a narrower root angle than Paragon could suggest that the genes that regulate root angle primarily function by promoting gravitropic growth and that aberrations caused by irradiation may dampen the gravitropic response. However, it is difficult to draw any conclusions from this study because the lines which varied significantly from wild type Paragon, also varied significantly from deletion lines with overlapping deletions. Deletion lines comprised a non-saturated tiling path of deletions across the QTL region. Therefore, it is possible that an important gene falling in a region not covered by the deletions went undetected.

# 2.2.3 Field characterisation of RSA

## Aims

To have meaningful impact on agriculture, undertaking research in a field setting is a highly valuable progression from controlled glasshouse experiments. The aims of this field study were to test the following hypotheses:

- Lines with narrow seminal root angles in controlled seedling screens have narrow root angles at maturity in the field.
- The differential ability of genotypes to extract soil moisture, using canopy senescence as an indicator, is linked to root system architecture of the seedling and/or the mature plant.
- Lines with a narrow root growth angle invest less biomass in upper soil layers.
- Narrow seminal root angles and vigorous root growth in seedlings are indicative of increased canopy biomass in the field.
- Narrow seminal root angles are good predictors of high grain yield.

## 2.2.3.1 Methods

## 2.2.3.1.1 Germplasm

The value of testing a subset of lines displaying phenotypes at the extremes of a population distribution was demonstrated by Rebetzke *et al.* (2017). Eighteen lines from the AxC DH population that displayed root phenotypes (angle and growth rate) at the tail ends of the population distribution in the clear pot screen were selected on the basis of having the greatest number of replicates within the top 1 % or bottom 1 % of BLUPs (Table 2.9), calculated from ~8400 individuals depending on the trait (angle, primary root length and seminal root length).

## 2.2.3.1.2 Trial design and statistics

Field trials were prepared following an alpha design with two replicates per line in the first year and three replicates per line in the second year. To test for differences between wheat lines and for correlations between phenotypes across two years, BLUPs were generated for each line using the lmer package in R, assigning *year* and *plot position* (row and column) as random variables, totalling observations for 668 groups, 95 plots and 2 years (Bates *et al.*, 2015; R Core Team, 2016; Edmondson, 2016). The Pearson correlation test was applied to the BLUPs to test the strength of relationships between traits in R. Heritability was calculated in GenStat using a linear mixed model, selecting the model with the lowest Akaike information coefficient (AIC).

## 2.2.3.1.3 Trial management

Field trials were sown on 11th Oct 2018 at the NIAB site in Cambridge, UK (Lat, Long: 52.247, 0.0918) and on 2nd December 2019 at Hinxton, near Cambridge (52.096, 0.173). The soil at the Cambridge site was a clay loam (St Lawrence series) overlaying clay, while the Hinxton was a freely draining lime-rich sandy clay loam (20.5% clay, 60.5% sand and 19% silt) overlaying chalk rubble. Plots were 6 x 2 m with 12 rows per plot spaced at 14 cm, drilled to achieve a target population of 280 plants $m^{-2}$. The weight of seed per plot was calculated for each line as:

$$g \text{ seed/plot} = TGW * \text{plant pop} / \text{germination} / \text{survival} / 1000)$$

where TGW = thousand grain weight, germination proportion in 0.95 and survival proportion is 0.75 rate (the proportion of germinated seeds that yield viable plants post-winter).

Trials received standard husbandry to control weeds, diseases and pests as needed. In 2019, nitrogen was applied as ammonium nitrate in spring in three splits totalling 190 kg N/ha (2019) and 214 kg/ha in 2020. Phosphorous was applied as triple super phosphate, totalling 83 kg/ha (2019) and 125 kg/ha (2020). Weather data were acquired from weather stations located in proximity to each trial site: NIAB (52.245, 0.103) and Hinxton (52.101, 0.177).

**Table 2.9 Seedling phenotypes of the AxC tails selected for field trials.** See text for explanation of the phenotypes.

| GRU Store Code | Accession Name | Phenotype |
|---|---|---|
| AxC0001 | AxC1 | Long roots |
| AxC0005 | AxC5 | Short roots, wide angle |
| AxC0006 | AxC6 | Long roots, narrow angle |
| AxC0007 | AxC7 | Short roots |
| AxC0009 | AxC9 | Short roots |
| AxC00028 | AxC28 | Short roots |
| AxC00043 | AxC43 | Short roots, wide angle |
| AxC00056 | AxC56 | Short roots, wide angle |
| AxC00080 | AxC80 | Long roots, narrow angle |
| AxC000102 | AxC102 | Long roots, wide angle |
| AxC000108 | AxC108 | Short roots, wide angle |
| AxC000131 | AxC131 | Short roots, narrow angle |
| AxC000146 | AxC146 | Short roots, narrow angle |
| AxC000156 | AxC156 | Short roots, wide angle |
| AxC000179 | AxC179 | Short roots, wide angle |
| AxC000181 | AxC181 | Long roots, narrow angle |
| AxC000182 | AxC182 | Long roots, narrow angle |
| AxC000198 | AxC198 | Narrow angle |
| AxC000207 | AxC207 | Narrow angle |
| AxC000208 | AxC208 | Short roots |

# 2.2.3.1.4 Phenotyping

## 2.2.3.1.4.1 Leaf canopy cover

The extent of green canopy cover was estimated using a RapidScan spectral ratio meter (Holland Scientific, USA) held at approximately 1.4 m above the ground. Measurements were made from mid-February (when the wheat was in its foundation stage, approximately growth stage 20, GS20) until mid-July (late grain filling stage, approximately GS87). In 2019, three measurements per plot were taken every two weeks from February until May, after which the trial was scanned every week. In 2020, data could not be acquired due to safeguarding strategies during the COVID-19 pandemic. The RapidScan is a handheld device that provides a measure of the green foliage within the field of views. It measures the Normalised Difference Vegetation Index (NDVI) and Normalised Difference Red Edge (NDRE). NDVI is the ratio of near infrared (NIR) light (0.7-1.1 um) to visible (VIS) red light (0.4-0.7 um) reflected from the surface being measured. Chlorophyll absorbs visible (predominantly red and blue) light while leaf cell structure reflects NIR strongly. Thus, a high NIR to VIS light ratio indicates a large proportion of green canopy within the field of view.

$$NDVI = (NIR - VIS)/(NIR + VIS)$$

*where NDVI ranges from 0 - 1, with higher values indicating a denser canopy.*

NDRE measures the ratio of NIR light (0.7-1.1 um) to red edge light (0.7 um) reflected from the surface being measured and gives measurements further down into the canopy.

$$NDRE = (NIR - RE)/(NIR + RE).$$

The RapidScan is an 'active' sensor type, containing its own light source, which provides illumination to supplement natural light and thus minimises error due to variations in incoming solar radiation (Fitzgerald, 2010). Over the growth of the wheat crop, the typical trend is for an increase in NDVI as canopy density increases, with saturation of the signal at full canopy cover, followed by a decline as the leaves senesce.

Due to the inherent variability of NDVI values resulting from varying sky conditions and leaf wetness, smoothing of data was carried out using the Loess function in R, a locally weighted non-parametric regression with a smoothing parameter ($\alpha$) of 0.5 (Figure 2.22). The large number of data points across the season made it possible to accurately fit the curve with a 95 % confidence interval.

For each individual plot, the rate of change of green leaf canopy was calculated as the change in NDVI per day for three time brackets: (i) from the start of the foundation phase to the start of the construction phase (NDVI.FP); (ii) from the start of the construction phase to the peak (NDVI.CP) (iii) from the peak to the mid/end of the production phase (NDVI.PP). The time of the peak differed between lines by a maximum of 29 days.
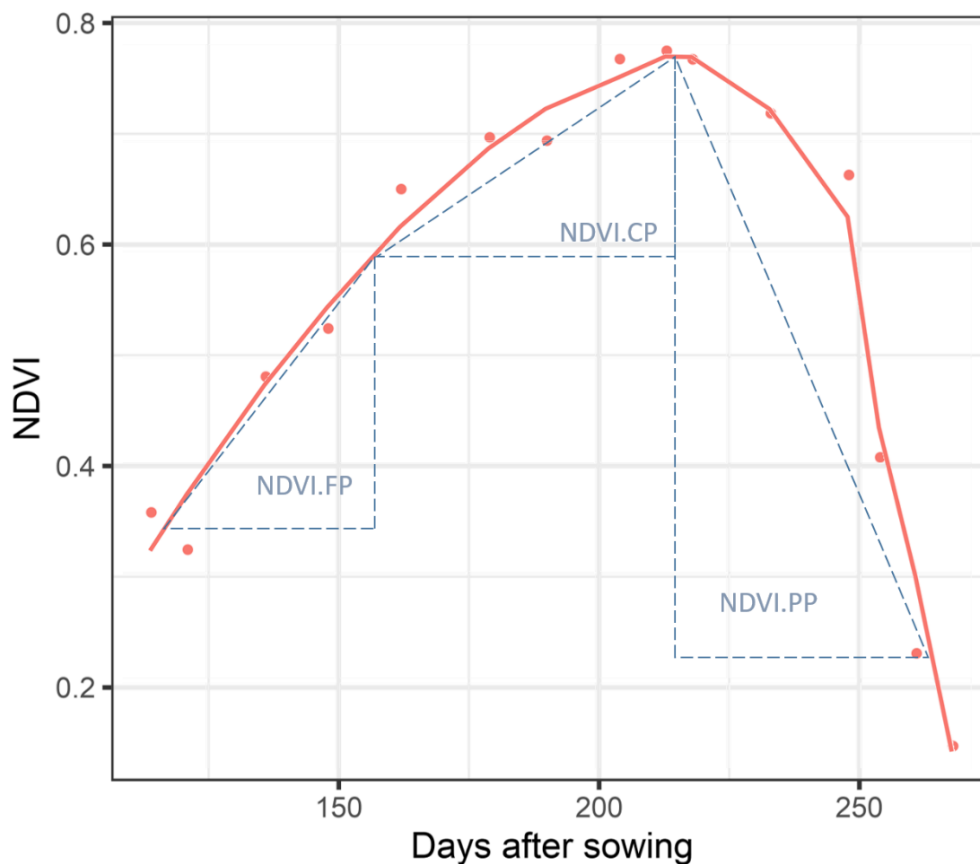


**Figure 2.22 Change in NDVI over time in an example plot of field-grown wheat from February (T114) to July (T264).** Shown for comparison are raw NDVI values (points) and fitted NDVI curve (line) from the same wheat plot. The curve was fitted by locally weighted smoothing to NDVI data, based on mean values with a 95% confidence interval. The metrics for rate of change in NDVI are indicated with dotted lines as NDVI.FP, NDVI.CP and NDVI.PP.

## 2.2.3.1.4.2 Grain harvesting

Plots were harvested on 21$^{st}$ August 2019 and 21$^{st}$ August 2020 with a Hege or Haldrup plot combine. Grain weights were adjusted to 85% dry matter using moisture contents measured on board the combine.

## 2.2.3.1.4.3 Root crown excavation

Plants were sampled for root phenotyping post-harvest on 23rd August 2019 and 29th August 2020 (316 and 270 days after sowing, respectively). Three clumps of plants per plot were gently pulled out of the soil, each clump consisting of the root crown and tillers of up to eight plants. In the typical shovelomics method (Traschel *et al.*, 2011; Fradgley *et al.*, 2020; York *et al.*, 2018), a shovel is used to excavate the root crowns, but in these experiments, it was faster to pull the plants, and roots remained as intact as those excavated with a shovel. Clumps were bagged and brought to the lab where most of the soil was removed by soaking the roots in soapy water, and the closely associated soil aggregates were detached by washing the roots under running water. Eight to twelve plants per line were randomly selected for analysis. They were stored in water-filled plastic pouches at 4 °C for up to a week until further processing. The root crowns were photographed in two planes at 90° to each other using a digital camera (Olympus, model TG-4) (Figure 2.23). Root angle was defined as the angle between the outermost crown roots and was measured using ImageJ software (Schneider *et al.*, 2012). Other measurements taken were total tiller number and total root number.
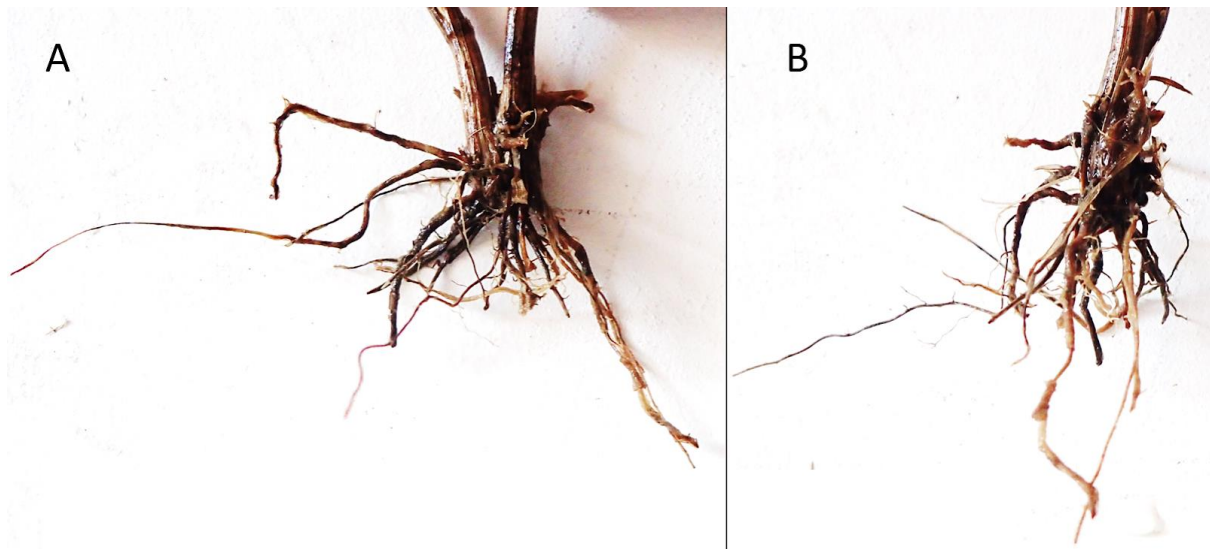
**Figure 2.23 Images of an example wheat root crown taken in two planes.** Plants were excavated after harvest and the root crown of each plant was photographed twice, each plane at 90⁰ to the other. Figures A and B are two planes of the same plant.

# 2.2.3.2 Results

## 2.2.3.2.1 Environmental conditions

2018-19 experienced greater precipitation and higher temperatures than 2019-20 (Figure 2.24). Total precipitation in the trial locations between November and July was 316 mm in 2018-19 compared with 178 mm in 2019-20. Average Temperature in the trial locations was higher across all seasons from sowing to harvest in 2018-19, averaging 11.2 ⁰C compared with 9.6 ⁰C in 2019-20.
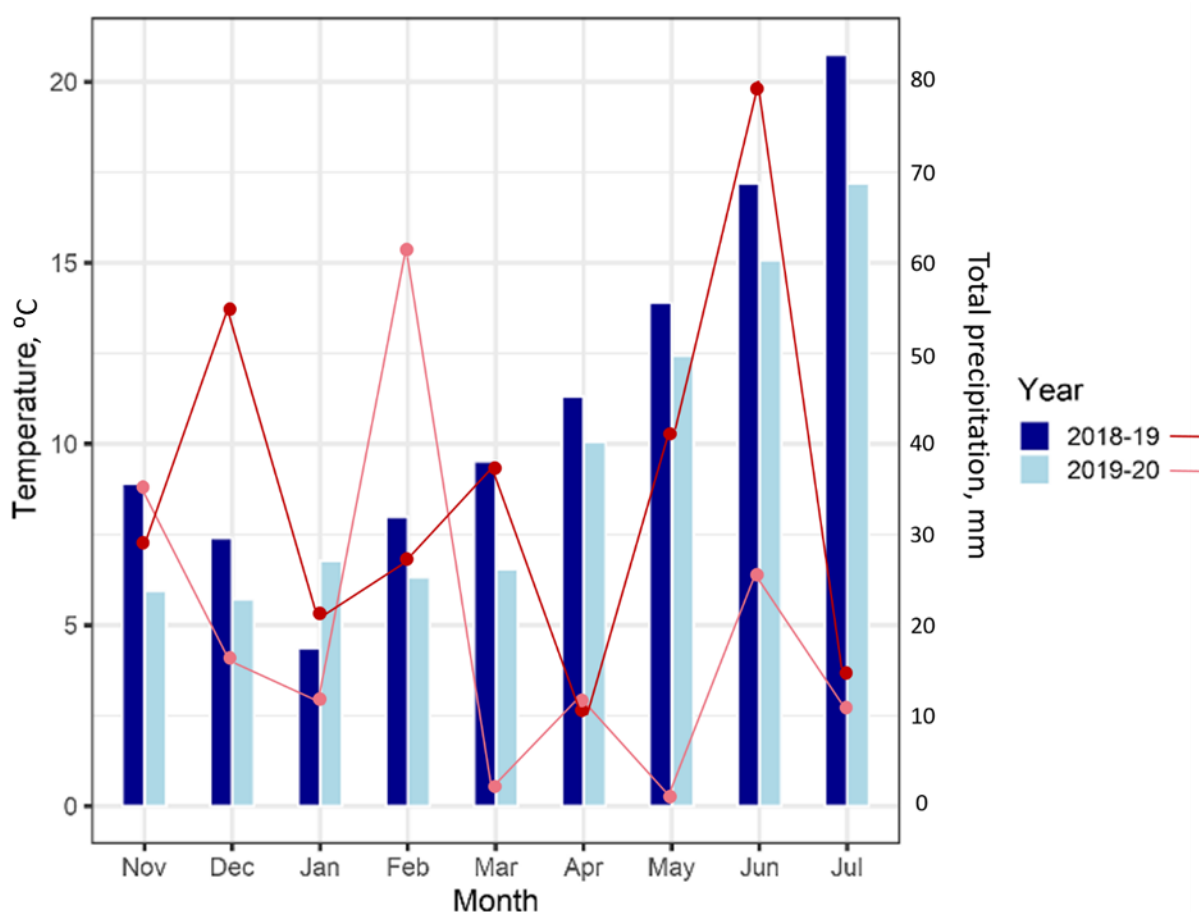
**Figure 2.24 Monthly average daily temperature and monthly summed precipitation during the winter wheat seasons from 2018 - 2020.** Data shown for the 2018-19 (dark blue bars, red dots) and 2019-2020 (light blue bars, pink dots) field seasons from weather stations located in proximity to each trial site: NIAB (52.245, 0.103) and Hinxton (52.101, 0.177).

## 2.2.3.2.2 Leaf canopy dynamics

NDVI provides an estimate of the extent of green canopy, indicative of the growth of the canopy and N status of a crop stand. NDVI increases over the foundation (sowing to GS31) and construction phases (GS31 to GS59), measured here from February (late foundation) to early June (Figure 2.25). During this time, wheat stem extension and leaf production contribute to increasing canopy density and light interception approaches 100% (AHDB, 2018). A peak in NDVI occurs between GS47 and GS59 in late May/early June, after which leaf and stem N is translocated towards the grain and the leaves senesce during the production phase. The presence of weeds below the canopy can contribute to the NDVI signal and lead to overestimates of the wheat canopy, but in these trials weed density was negligible as weed control was effective. Also,

diseases can cause leaf senescence, and genotypes can differ in levels of resistance to pathogens. In these trials diseases were well controlled with fungicides.

In this study, NDVI was recorded in each plot at fifteen time points between February and July. At each time point, NDVI did not vary significantly between lines until the peak in leaf canopy. The three time points measured during senescence showed significant genotypic variation in NDVI (ANOVA, $F_{(20, 19)}$ > 6.9, p < 0.001). Although there was greater variation between lines for the mean NDVI prior to the peak than after the peak, the variance between lines of the same genotype was larger before the peak, hence the lack of significance.

The rate of change of NDVI was calculated for the foundation-construction phase transition (NDVI.FP), the construction phase (NDVI.CP), and the production phase (NDVI.PP). While there was no genotypic effect on NDVI.FP, there was a significant effect on NDVI.CP and NDVI.PP (p = 0.043 and 0.045 respectively).
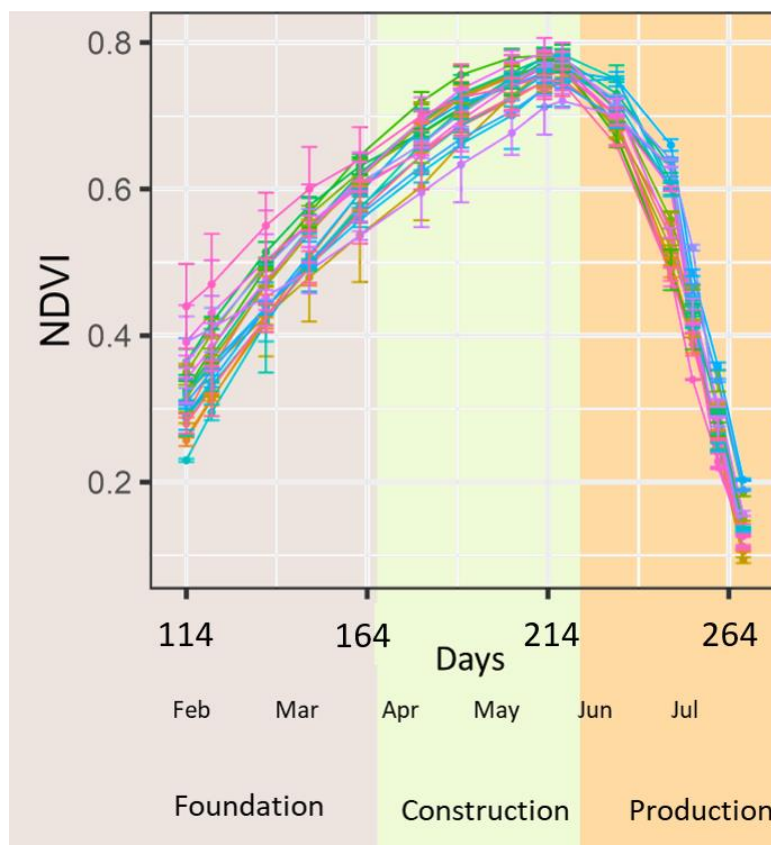


**Figure 2.25 Change in NDVI of field-grown wheat from February to July 2019.** Curves fitted to genotypic means at each measurement date are plotted for each line in the AxC tails subset, including the parents.

73

## 2.2.3.2.3 Root crown excavation

The number of roots per tiller varied significantly between lines (Table 2.10). This variation was matched by the significant difference between the parents, whereby Avalon had on average 1.6 more roots per tiller than Cadenza (p = 0.022). There was no genotypic effect on the crown root angle of the narrowest plane but there was a significant effect on the widest angle (p = 0.049). There was a significant year effect (p = 0.023) and a significant genotype:year interaction (p = 0.017) for the smallest root angle, but not the widest root angle plane. In addition there were significant year effects and genotype:year interaction for the number of tillers and number of roots per tiller, indicating that genotypes responded differently to conditions in each year. Although there was a year effect on yield, there was no genotype:year interaction, suggesting a uniform response in grain yield across the lines to environmental conditions.

For the traits with significant genotypic variation, particular lines of note were AxC 179 with the smallest crown root angle from the wide plane and AxC 6 with the widest angle from the wide plane. AxC 1 had the fewest roots per tiller and AxC 198 the most. AxC 146 and AxC 179 had the smallest yield whereas AxC 56 and AxC 198 had the greatest yield. AxC 179 was both the lowest yielding line and the line with the narrowest crown root angle (imaged at the widest plane). AxC 198 was both the highest yielding line and that with the most roots per tiller.

**Table 2.10 BLUPs for crown root traits of lines from the AxC population and parental lines.** The F-probability from a one-way ANOVA for the effect of genotype is shown and was carried out on BLUPs calculated from 668 individuals and accounting for the random variables, year (x2) and trial design (95 plots).

| Line | Smallest angle | Widest angle | Average angle | Roots per tiller | Tiller number | Yield, t ha$^{-1}$ |
|---|---|---|---|---|---|---|
| AxC 1 | 73 | 95 | 84 | 4.2 | 3.0 | 6.6 |
| AxC 5 | 66 | 92 | 83 | 6.3 | 2.5 | 6.1 |
| AxC 6 | 87 | 114 | 101 | 6.6 | 2.1 | 6.9 |
| AxC 7 | 82 | 106 | 94 | 6.5 | 2.3 | 6.0 |
| AxC 9 | 76 | 102 | 89 | 6.6 | 2.2 | 6.3 |
| AxC 28 | 68 | 94 | 82 | 6.3 | 2.8 | 6.8 |
| AxC 43 | 81 | 97 | 89 | 5.4 | 2.9 | 6.9 |
| AxC 56 | 72 | 93 | 81 | 6.4 | 2.7 | 7.2 |
| AxC 80 | 75 | 96 | 85 | 5.6 | 2.6 | 6.5 |
| AxC 102 | 69 | 97 | 84 | 6.6 | 2.2 | 6.9 |
| AxC 108 | 80 | 100 | 90 | 6.1 | 2.0 | 6.3 |
| AxC 131 | 80 | 104 | 93 | 7.3 | 2.0 | 6.1 |
| AxC 146 | 76 | 94 | 85 | 6.1 | 2.6 | 5.6 |
| AxC 156 | 74 | 100 | 87 | 5.2 | 3.6 | 6.3 |
| AxC 179 | 71 | 90 | 81 | 5.8 | 2.9 | 5.6 |
| AxC 181 | 89 | 107 | 96 | 6.6 | 3.2 | 6.3 |
| AxC 182 | 76 | 103 | 90 | 5.9 | 3.8 | 6.9 |
| AxC 198 | 80 | 107 | 94 | 7.9 | 2.1 | 7.1 |
| **Avalon** | 74 | 98 | 88 | 7.5 | 2.0 | 6.4 |
| **Cadenza** | 77 | 101 | 89 | 5.9 | 2.5 | 7.0 |
| **Mean of AxC Tails** | 76 | 100 | 88 | 6.2 | 2.6 | 6.5 |
| **Genotypic effect p-value** | 0.37 | 0.049* | 0.14 | 0.028* | 0.76 | < 0.001*** |
| **Year effect p-value** | 0.023* | 0.35 | 0.075 | < 0.001*** | 0.0086** | < 0.001*** |
| **Genotype:Year effect p-value** | 0.017* | 0.10 | 0.024* | 0.001** | < 0.001*** | 0.09 |
| **Genotype LSD** | 9.3 | 9.9 | 8.5 | 1.6 | 0.76 | 0.74 |
| **Year LSD** | 2.9 | 3.2 | 2.7 | 0.40 | 0.24 | 0.23 |
| **Genotype:Year LSD** | 13.1 | 14.0 | 11.9 | 1.77 | 1.1 | 1.0 |

Genotypic effects on each phenotype coincided with heritability: the traits that experienced a genotypic effect had higher heritability (Table 2.11). Heritability was calculated from the model with the lowest Akaike information coefficient out of a series of iterations (Line x Experiment x Block). In addition to yield, which showed the greatest heritability among the measured traits, the number of roots per tiller also showed good heritability. The wider crown root angle of the two planes displayed greater heritability than the narrower angle, presumably as the outer boundary marker of the root system. Tiller number displayed little to no heritability.

**Table 2.11 Heritability of phenotypes in mature field-grown lines of the AxC tails.** Data were collected from field-grown plants over 2019 and 2020 among twenty lines of the AxC DH population.

| Angle of smallest plane | Angle of widest plane | Average crown Root Angle | Tiller number per plant | Roots per Tiller | Yield |
|---|---|---|---|---|---|
| 0.29 | 0.42 | 0.25 | 0.016 | 0.47 | 0.60 |

# 2.2.3.2.4 Relationship between roots and shoots in seedlings and mature plants

I compared the seedling phenotypes of the AxC tails grown in a clear pot screen with their phenotypes measured in the field at later stages of development in two field trials. In Figure 2.26, 2019 data are used in a correlation matrix for the comparison of NDVI values with the root crown phenotypes of that season and the seedling root phenotypes of the clear pot experiments. Figure 2.27 plots the correlation matrix of 2019 and 2020 field data minus the NDVI values as these were not fully measured in 2020.

Seedling root growth rate was positively correlated with the rate of NDVI increase during the construction phase (NDVI.CP), the rate of NDVI decrease during the production phase (NDVI.PP) and the peak NDVI value. The greater the seedling root growth rate and length, the faster the gain and loss of canopy density and the greater the peak NDVI ($p < 0.01$). Seedling root growth rate and length also correlated significantly with the timing of peak canopy density: genotypes displaying faster root elongation rates peaked later ($p < 0.001$).

There was a significant negative correlation ($p=0.046$) between seedling seminal root angle and crown root angle at maturity. The narrower the seedling seminal root angle, the wider the crown root angle.

There was a strong negative correlation between the number of roots per tiller and seedling seminal root angle ($P < 0.001$). The narrower the seedling seminal root angle, the greater the number of roots per tiller observed at maturity. The correlation between the number of roots

per tiller and crown root angle did not reach statistical significance with one year's worth of data but adding a second year of data pushed it to statistical significance, with wider crown root angles being associated with a greater root number (p = 0.014, Figure 2.26). Furthermore, genotypes with narrow seminal root angles and many roots per tiller displayed a higher peak canopy density (p = 0.0021).

There was a significant negative correlation between seedling root angle and the rate of NDVI increase from February to the peak (p = 0.014), while crown root angle correlated positively with the rate of NDVI increase during the construction phase until the peak (P = 0.049). Neither correlated with the rate of canopy senescence. NDVI.FP correlated negatively with seedling root angle, while NDVI.CP correlated positively with crown root angle. In other words, early in the season, narrow seminal root angles were associated with higher rates of canopy gain while later on during the construction phase, high canopy gain was associated with wide crown root angles.

Interestingly, there was a significant correlation between crown root angle and the timing of the peak NDVI whereby genotypes with narrower crown root angles peaked later (p = 0.016). Fewer roots per tiller were moderately associated with a later peak in canopy density (p = 0.07).

The number of roots per tiller correlated positively with NDVI.FP, NDVI.CP and maximum NDVI but not with NDVI.PP. A greater root number was also associated with higher yields in 2019 but not in 2020.

In 2019, a greater root number and narrower seedling root angle was significantly associated with higher yields. However, combining the 2019 and 2020 yield data eliminated any relationship, indicating the importance of multiple field trials to confirm observed phenotypes and relationships.
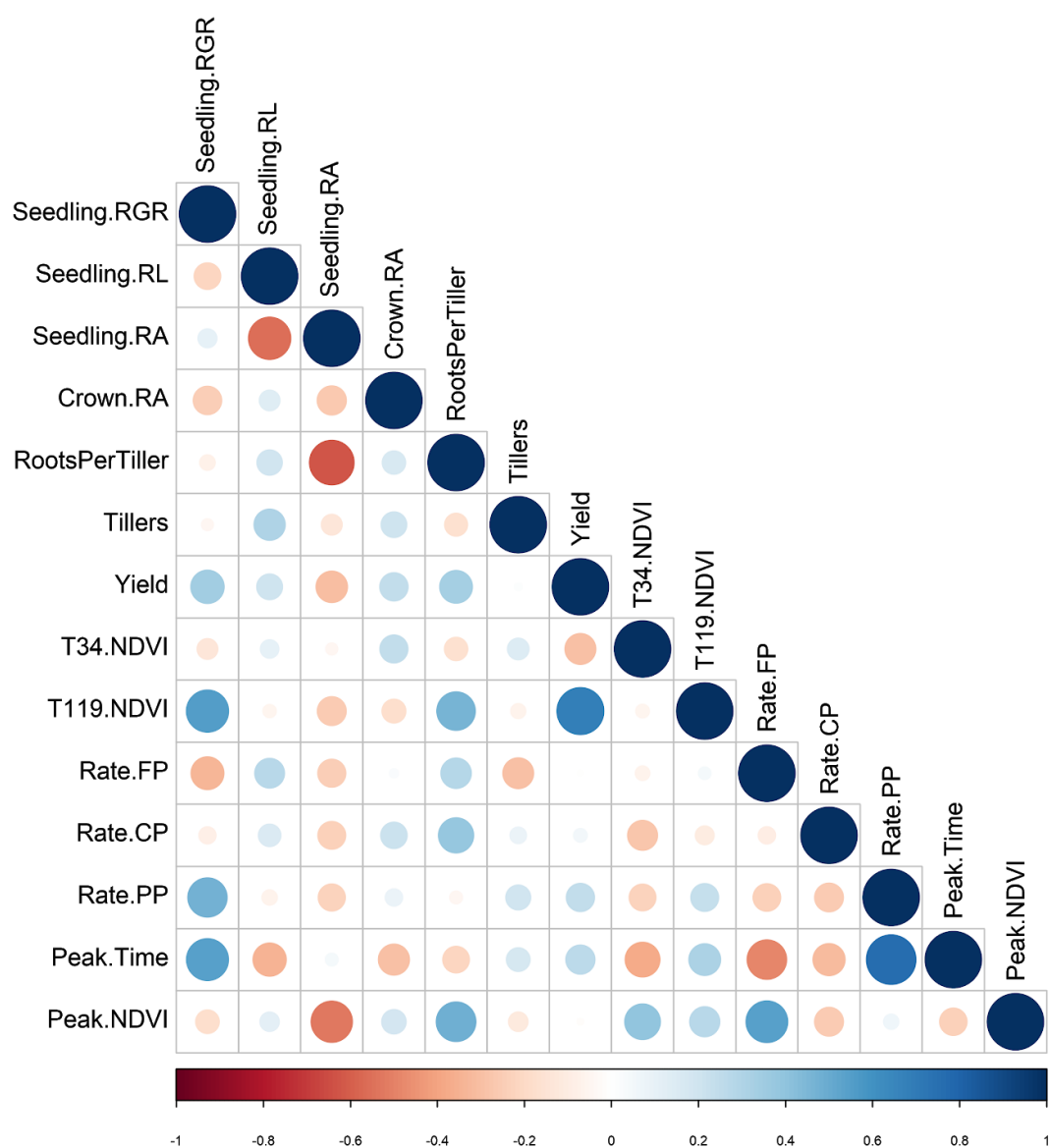
**Figure 2.26 Correlation matrix of seedling and field root and canopy traits in the AxC DH population.** BLUPs for each of twenty wheat lines were calculated from 2019 field data (Crown.RA, Roots.per.Tiller, Tillers, Yield and NDVI values [measured at T = 34 days and T = 119 days]) and three independent clear pot experiments (Seedling.RGR, Seedling.RL, Seedling.RA). The strength of the correlation between phenotypes was tested using the Pearson Correlation. RGR, total root growth rate; RL, total root length; RA, root angle; Rate = rate of change in NDVI during the foundation phase (FP), construction phase (CP) and production phase (PP); Peak.time, day on which maximum NDVI was measured; Peak.NDVI, maximum value of NDVI measured.
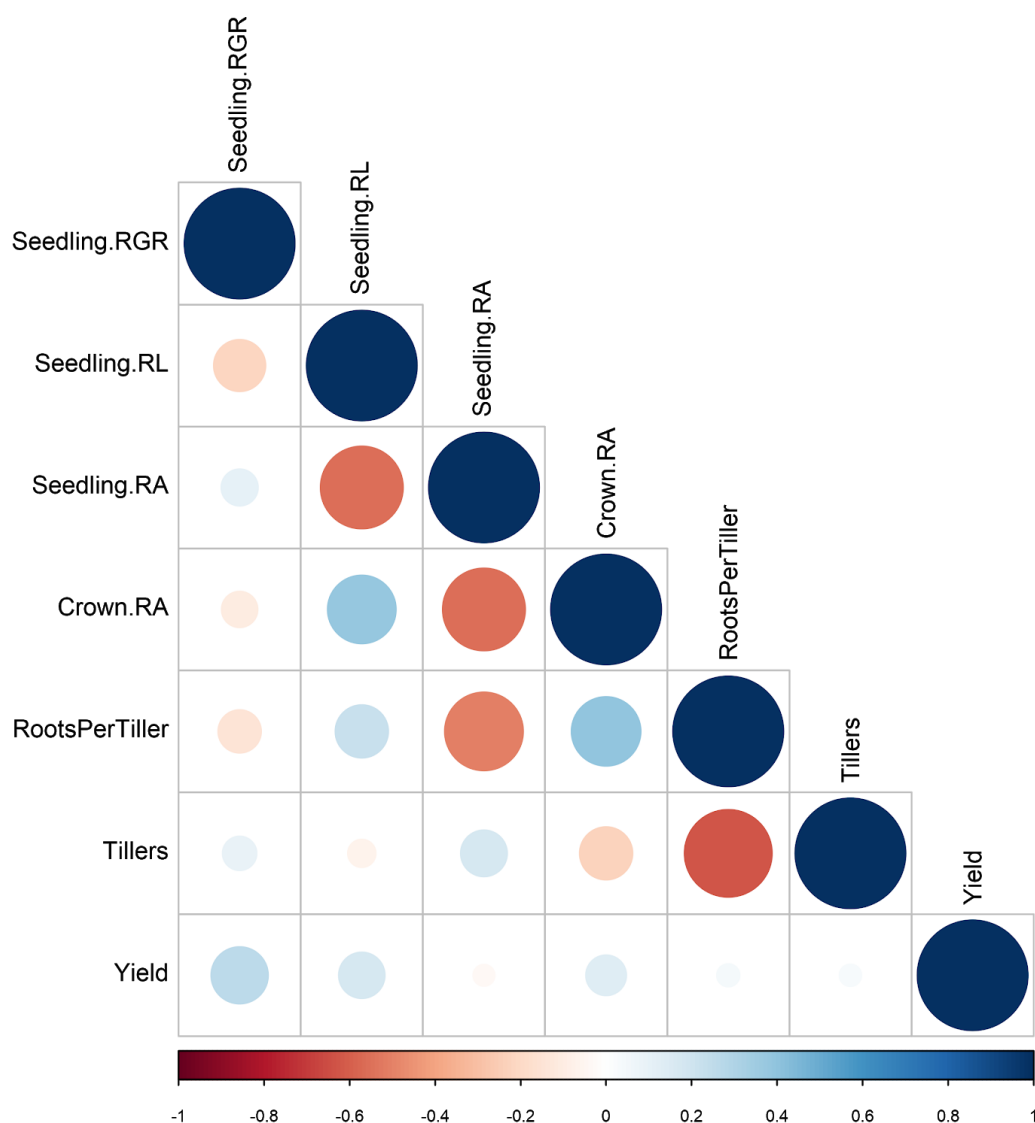
**Figure 2.27 Correlation matrix of seedling and field traits in the AxC DH population.** BLUPs for each of twenty wheat lines were calculated from two years of field data (Crown.RA, Roots.per.Tiller, No..tillers and Yield) and four clear pot experiments (Seedling.RGR, Seedling.RL, Seedling.RA). The strength of the correlation between phenotypes was tested using the Pearson Correlation. RGR, total root growth rate; RL, total root length; RA, root angle; FP, foundation phase; CP, construction phase; PP, production phase; Peak.time, day on which maximum NDVI was measured; Peak.NDVI, maximum value of NDVI measured.

## 2.2.3.3 Discussion

The use of "tails" representing the phenotypic extremes of a population is an approach that is well suited to assessing complex, polygenic traits (Rebetzke *et al.*, 2017). The smaller set of tails can be evaluated with methods that would otherwise be too expensive or laborious on a whole population. Rebetzke *et al.* (2017) found that the power of tail comparison tests is related to trait heritability, meaning that it is possible to compare indirect selection on two different traits from a common selection study with confidence that the difference in tails is strongly related to the underlying genetic correlation. This observation is supported in the present study whereby genotypic effects on each phenotype coincided with heritability: root angle of the wider plane, roots per tiller and yield showed significant genotypic differences and had higher heritability.

Indoor screens for specific wheat RSA phenotypes are more rapid and controlled than field trials and make it possible to attribute phenotypes to genotypes while attempting to minimise environmental factors. Furthermore, it is possible to determine the effect of a single environmental factor while keeping all other factors constant. However, glasshouse pot experiments are not representative of field conditions. It is not necessarily desirable to select for a particular trait in a controlled environment due to the wider range of environmental scenarios under field conditions, especially so under future climate scenarios. There is benefit to identifying genotypes that can adapt to a changing climate and perform consistently in a range of climatic conditions.

The field trials undertaken here aimed to corroborate the phenotypes observed in the clear pot seedling screens, test whether seedling phenotypes translated into those of mature plants, test the relationship between root traits and canopy traits, determine the reproducibility of root crown phenotypes and determine the contribution of RSA to grain yield.

## 2.2.3.3.1 Leaf canopy dynamics

NDVI measurements are often reported at fixed time points without taking into account the leaf canopy dynamics across the growing season. Here, the static measurements were found to reveal little while the rate of change of NDVI provided a greater insight into leaf canopy dynamics. Leaf canopy dynamics importantly indicate the rate of biomass accumulation and leaf senescence,

which ultimately determines the capacity for grain filling. During the period of slow biomass accumulation early in the year, all lines responded similarly and could not be differentiated for canopy development. However, in the longer days of increasing solar radiation that characterise the subsequent growth phases, the rate of canopy accumulation varied significantly between the lines up to the peak NDVI, demonstrating varying capacity to intercept abundant light resources. Similarly, there was significant variation in the rate of NDVI reduction due to leaf senescence in the production phase. The varying NDVI values and rate of canopy loss during the production phase may demonstrate a genotypic effect on the speed or duration of grain filling, each of which may be controlled separately and respond differently to the supply of photosynthate.

Building and maintaining a green canopy, which is essential for realising a good grain yield, depends on the root system supplying sufficient N and water from the soil. Although there were no strong relationships between root traits measured in the field and yield, a positive correlation between NDVI 233 days after sowing and seedling RGR may suggest that root RGR, as an indicator of vigour, supports this interaction between root activity and shoot growth, or between below-ground and above-ground activity. More testing would be required to see how robust seedling RGR would be as a proxy for desirable shoot growth traits of older plants in the field.

In contrast to the UK trend across these years (https://ahdb.org.uk/harvestresults), yield in the AxC DH trials was lower in 2019 than 2020 (an average of 5.3 t/ha and 7.6 t/ha, respectively). Due to a lack of NDVI data in 2020 due to Covid-19 restrictions, it was not possible to examine the canopy dynamics of 2020 relative to 2019. However, it is likely that, in comparison with 2019, a combination of higher rates of fertiliser application, colder winter temperatures and higher precipitation in July 2020 contributed to accelerated plant development relative to the previous year.

## 2.2.3.3.2 Root crown excavation

Root crown excavation was an effective, high-throughput method to phenotype the root system of mature crop plants. Although phenotypic information was limited to the top soil layers, unlike pot-, pipe- or rhizotron-based methods, it enabled root observations in the field on a large scale.

Heritability is the proportion of phenotypic variance among individuals in a population that is due to heritable genetic effects as opposed to environmental effects (Smidt *et al.*, 2019). High heritability facilitates selection in plant breeding as traits are highly likely to be passed on to the subsequent generation. The large environmental variation from 2019 to 2020 (e.g. soil type, climatic effects, nutrient levels and sowing time) would have reduced the likelihood of observing high heritability in the field phenotypes. As a consequence, observing high heritability *in spite* of environmental variation would have greater value than observing high heritability across uniform environments, as this would give a researcher or breeder confidence that selected traits could perform over a range of field conditions. To truly make wider inferences about traits and their relationships, they need to be tested in more than one environment as demonstrated here.

Yield saw the greatest heritability at 60%. Grain yield heritability in multi-environment scenarios are generally reported between 45 - 70% (Condon and Richards, 1992; Ortiz *et al.*, 2001; Eid, 2009).

Out of the two photographed planes from the field excavated root systems, the widest observed crown root angle had higher heritability than the narrow-angled plane. It is possible that the narrower plane was trickier to measure accurately and had greater error, hence the lower heritability. The different angles that are apparent on the same plant depending on how the plant is viewed could be due to the orientation of the plant in the row as the plant is closer to the adjacent plant in the same row than the adjacent plant in the next row. The wider spread may arise from roots having more space to grow and less competition with roots from neighbouring plants in the inter-row space.

As the outer boundary of the root system, the wider plane is a truer indicator of root spread. For meaningful phenotyping, these results indicate that the widest plane is the more useful measure. For greater accuracy and information, measuring root system spread in 3D by rotating the plant and imaging it could be recommended if a high-throughput system were achieved.

The number of roots per tiller had relatively high heritability while the number of tillers had negligible heritability. As heritability estimates can be affected by the degree of variation for the trait in the panel, it is possible that the low heritability of tiller number arose from small variation (BLUP range of 2.0 – 3.8).

The significant effect of genotype, year and their interaction on the number of roots and their growth angle indicated genotypic differences among the lines in the response to environmental factors. It has previously been seen that different wheat cultivars respond differently to drought. Ehdaie *et al.* (2012) reported three responses: an increase in root biomass, a decrease in root biomass and no change in root biomass in different wheat genotypes exposed to drought. Furthermore, the effect on root length density varied according to genotype. In that experiment, the increase in root biomass led to a reduction in grain yield (Ehdaie *et al.*, 2012). As per the "cheap, steep and deep" ideotype, less metabolically costly ("cheap") roots ensured that more resources were directed to the grain and not diverted to the roots (Lynch, 2013). RSA ideotypes differ among environmental and management scenarios (Ehdaie *et al.*, 2012; Tardieu *et al.*, 2017). The effect of on plant performance of having a fast-growing, deep root system may be positive or negative depending on the rainfall patterns and soil type of a particular region (Tardieu *et al.*, 2017). For example, the "steep, cheap and deep" ideotype with deep growing roots of low metabolic cost is not necessary in shallow soils (Lynch, 2013; Tardieu *et al.*, 2017). In drought scenarios, an efficient root system may not lead to the best performance if the efficiency means that the plant depletes available water very quickly (Messina *et al.*, 2015).

Climate change is leading to more and more unpredictable growth environments and plastic roots systems are more than ever crucial to stabilising grain yield. A root system capable of modulating root length density as a direct response to drought could be a key to mitigating the negative effects of unpredictable climate on yield. The genotype x environment interaction could provide a lead on identifying the way RSA is modulated between environments in genotypes with consistent yield and canopy traits. This would require several years of data with varying levels of available soil moisture across the years.

2018-19 experienced greater precipitation and higher temperatures than 2019-20. Crown root angle was significantly wider, root number significantly lower and yield significantly higher in 2019-20. Two years of data where precipitation and temperature are neither controlled nor unique environmental inputs are insufficient to draw conclusions about the effect of precipitation and temperature on root angle and number. However, it is an observation that provides a base for further research.

Further research could include soil coring, which enables the quantification of root length density up to depths of 1-2 m (Wasson *et al.*, 2016; Whalley *et al.*, 2017). The limited ability of roots to access water is commonly attributed to low root length density at depth (Gregory *et al.*, 1978a, Gregory *et al.*, 1978b). Equipment breakdowns with the coring rig limited the collection of sufficient core data for reliable assessment. As illustrated by measurements taken on seedlings and excavated root crowns, the large variability of root traits means a large number of replicates is required to study the root system. Core break imaging (Wasson *et al.*, 2016) significantly increases throughput by avoiding the need to wash soil core sections to weigh and measure roots. Future work could utilise soil coring to characterise the root length density of the AxC DH population, and identify co-inheritance of root angle and root length density. Root length density has been found to be higher in drier years than more humid ones (Hamblin *et al.*, 1990).

Drought trials are key to evaluating whether genotypes demonstrate a change in root angle and root length density in response to soil moisture in the field and to determining whether the phenotypic response is genetically determined. Consistent genotype x environment interactions are desirable to stabilise grain production under unreliable rainfall patterns.

Until now, studies have primarily examined seedlings growing in artificial growth environments (Manschadi *et al.*, 2008; Ehdaie *et al.*, 2012). However, field experiments to test the effect of drought on root angle and root length density, and to test for related QTLs are lacking. This is in part due to the difficulty of preventing rainfall in open fields. The problem could be overcome by collecting data over several years of varying rainfall, undertaking field trials in different climatic zones or installing a polytunnel rainout shelter over the field trial to intercept rainfall.

The genotypic variation in field RSA observed here has functional implications for water and nutrient capture. The genotypic differences in response to environmental factors (between the years) provide a basis for selection, depending on the desired RSA ideotype for given climatic conditions.

## 2.2.3.3.3 The relationship between roots and shoots in seedlings and mature plants

Few studies have directly compared the root traits of seedlings grown in a controlled environment with those of mature plants grown in the field. Additionally, there are discrepancies between studies for the correlation between young and old plants. Watt *et al.* (2013) found positive significant relationships between root traits of seedlings grown in rolled tubes of germination paper and the roots in the field at early growth stages. However, no correlations were found between paper-based assays and mature plants grown in the field, nor between field-grown seedlings and mature plants. Rich *et al.* (2020) found some correlations between seedling root traits and mature field-grown roots but correlations were inconsistent across trials and season. They found that soil-based seedling screens showed a stronger relationship than paper-based screens with mature field traits. Other studies reporting no correlation between seedling root traits and those of mature plants in the field used paper-based seedling assays (Bai *et al.*, 2019). The relationships that I found between seedlings and mature plants could arise because seedling screens were conducted in soil.

The negative correlation between seminal root angle and crown root angle may reflect the different roles of these two classes of roots (Ahmed *et al.*, 2018). For example, maize seminal roots exhibit a greater contribution to water uptake in young plants only, whereas crown roots are the major contributors after (or earlier than) 5 weeks. In maize, this was attributed to the greater hydraulic conductivity of crown roots and the fact that they are attached to the shoot above the seminal roots (Ahmed *et al.*, 2018). The negative correlation implies that the genetic program that governs how cells within the root tip respond to gravity (the gravitropic setpoint angle) differs in these two root tissues. It multiplies the number of potential targets for breeders: this may be considered a complication or it may be used for the ability to fine tune a desired RSA for a specific environment.

Root growth angle has a different impact depending on the function of the root. Seminal roots are important for the establishment of the seedling (Manske *et al.*, 2002). At germination, it could be beneficial to rapidly establish a presence in deeper soil horizons to explore areas beyond the topsoil. Furthermore, a seedling is less likely to encounter competition from other plants by foraging in a vertical plane than spreading out laterally towards potential neighbours. This is critical at a young stage when there are few roots and the contribution of each root to the nutrient status of the plant is of greater importance. Accessing deeper soils also quickly establishes early anchorage for the plant. Zhu *et al.* (2018) suggest that breeding has selected for plants that do

not compete with their neighbours, resulting in a collective higher yield while preventing a given plant from outcompeting its neighbours.

In contrast to seminal roots, crown roots emerge at the first foliar node and from successive higher nodes thereon (Klepper *et al.*, 1984). Crown roots comprise the root plate which is important for anchoring the root in the soil and minimising lodging. The spreading of crown roots forms a net that captures rain as it falls onto the topsoil. It is known that the deep root system comprises mainly seminal roots while the shallow root system comprises crown and seminal roots (Watt *et al.*, 2008; Ehdaie *et al.*, 2012). If root angle represents rooting depth, the results presented herein corroborate this observation.

The correlation between seminal root angle and crown root angle was significant but not strong, suggesting that the link between seminal and crown root angles can be broken in some instances. For example, Avalon displayed both a narrow seminal root angle and a narrow crown root angle, while AxC 156 displayed both a wide seminal root angle and a wide crown root angle.

The strong correlation of seminal root angle and canopy density suggests enhanced water and nutrient foraging in genotypes with narrow seminal root angles. As angle is a proxy for rooting depth, it is predicted here that deeper rooting genotypes were able to support greater canopy biomass. The results from this study complements that of Rebetzke, who conducted a study on recurrent selection lines (RSL) bred for early seminal root vigour (Palta *et al.*, 2011). He noted that those lines with greater elongation rate of seminal roots (and presumably greater rooting depth) had lower canopy temperature, indicative of a better water status (Blum *et al.*, 1989; Palta *et al.*, 2011). In another study of a panel of wheat lines grown in the UK, all lines with deep roots were high yielding (Bai *et al.*, 2019).

Given the negative correlation between seminal and crown root angle, the genotypes with narrower crown root angles may have experienced inter-root competition within the same plant as crown and seminal roots overlapped.

Root number per tiller, seminal root angle and crown root angle correlated with rates of NDVI increase up until the peak. However they did not seem to correlate with canopy density during the production phase. This corresponds to the fact that nitrogen during grain filling is typically sourced from the leaves, not the roots, although in some situations post-anthesis, N uptake can

bypass the leaves and move into the grain (Bogard *et al.*, 2010; AHDB, 2018; S. Swarbeck, personal communication). Once the maximum canopy density is reached, the root system plays a lesser role in the rate of translocation of nutrients from the leaves to the seed. While I identified a close connection between root system phenotypes in the seedlings, mature plants and leaf canopy growth, there was more disconnect between the root system, and grain filling and senescence.

There was a significant relationship between the number of roots per tiller and the timing of senescence onset: a larger root system was linked to earlier senescence. An early onset of senescence can be an indicator of drought stress (Larbi and Mekliche, 2004). It is possible that genotypes with more roots per tiller were less resilient to low soil moisture in the summer months. In Mediterranean environments, or environments with terminal drought, a large root system that depletes too much soil moisture early in development leaves too little moisture available for grain filling. In these environments, more moderate water use is desirable to extend the time frame for extraction of stored soil moisture (since rainfall ceases after a certain point in these environments).

Alternatively, genotypes with more roots per tiller may have had a shallower root system (number of roots per tiller showed a strong negative correlation with crown root angle) and were therefore less able to extract water from deeper soil layers and avoid stress and senescence. Genotypes with more roots per tiller may also have had more efficient early uptake of N into the plant, leaving less soil N available post anthesis. Thus translocation of stored N to the grain may have depleted N from the leaves more quickly and hastened senescence.

Those genotypes which peaked earlier also ended with a lower final canopy density, potentially compensating for early senescence: drought-induced senescence may increase remobilisation of pre-anthesis stored carbohydrates from the stem and leaves to developing grains, and compensate for possible losses in grain yield (Yang *et al.*, 2006, 2007; Plaut *et al.*, 2004).

# 3

# Root mucilage and the rhizosheath

## 3.1 Abstract

The rhizosheath is the soil-polysaccharide complex that adheres to roots and has demonstrated benefits for plants, particularly during biotic and abiotic stress. Interactions between root system architecture and the formation and function of the rhizosheath are poorly understood, and filling the knowledge gap may have potential benefits to agriculture. The polysaccharide component of the rhizosheath originates in part from root secretions and represents a significant proportion of carbon fixed by photosynthesis. This research quantifies and tests relationships between a suite of key polysaccharides released from the roots of lines of the Avalon x Cadenza doubled haploid mapping population. There was significant genotypic variation among the Avalon x Cadenza lines for rhizosheath size, root length, shoot length and the concentration of polysaccharides in the rhizosheath. The findings demonstrated that genotypes of the same species

are capable of forming distinct polysaccharide secretion profiles. Furthermore, plants with higher levels of heteroxylan and arabinogalactan protein had a significantly larger rhizosheath. Genotypic differences in components of the rhizosheath lay the foundation for breeding for improved root systems.

# 3.2 Introduction

The rhizosheath is the soil-polysaccharide complex that adheres to roots and is thought to provide benefits to plants during abiotic stress and to soil microorganisms in the rhizosphere. Rhizosheath formation relies on mucilage secretion and the presence of root hairs, which enmesh soil particles (Watt *et al.*, 1994; Moreno-Espíndola *et al.*, 2007; Haling *et al.*, 2010, 2014; Brown *et al.*, 2012; Delhaize *et al.*, 2012; George *et al.*, 2014). It was first documented in 1887 by Volkens, who observed it on the roots of xerophytic grasses. This led to the idea that the rhizosheath is a feature of drought adaptation (Price, 1911). Indeed, rhizosheath thickness has been observed to increase under drought conditions in xerophytic grasses, aiding the uptake of water from the soil (Hartnett *et al.* 2012), and mucilage has a high water holding capacity and ensures that rhizosphere hydraulic conductivity declines less rapidly during soil drying (Zickenrott *et al.*, 2016). Since their documentation in 1887, rhizosheaths have been observed in other plant families, suggesting their occurrence is not limited to chronically arid areas. Various studies have shown their influence on microbial populations, nutrient acquisition, water uptake and metal toxicity (Morel *et al.*, 1986; Archambault *et al.*, 1996; Read *et al.*, 2003; Pausch *et al.*, 2016). In addition, the focus of research on members of the Poales may have led to the misconception that the rhizosheath is a feature unique to this order, but it has been observed in other orders, including species of cacti (McCully 1999), soybean (Sprent 1975), lupin (Unno *et al.* 2005) and fig (North and Nobel 1997).

Mucilage is mainly composed of a matrix of highly-branched, heterogeneous polysaccharides of both plant and microbial origin, with glycoproteins and lipids accounting for a smaller component. The composition and properties of mucilage can vary according to species, climatic conditions, soil properties, water status, nutrient deficiency, exposure to pathogens and herbivory, and can even vary on a diurnal basis (Yang and Crowley, 2000; Hertenberger *et al.*, 2002; Carminati *et al.*, 2013). The rhizosheath can also differ between varieties of the same

species, as seen in cvs. Avalon and Cadenza, which differ in their level of polysaccharide secretion and in the degree of rhizosheath formation (P. Knox, personal communication). Developmental stage of the plant is an important factor: *Oryza sativa* (rice) and *Lupinus* spp. (lupin) seedlings have been observed to exude less material than mature plants and fast growing seedlings exude more as they are more metabolically active (Badri *et al.*, 2009). Garcia *et al.* (2001) showed that root exudation was positively correlated with root growth, suggesting that actively growing root systems secrete more exudates.

Regarding drought tolerance, there is controversy over the mode of action of rhizosheath mucilage although it is clear that it is a function of the properties of its constituent polysaccharides, glycoproteins and phospholipids. Presumably, the effects of mucilage on hydraulic conductivity also depend on the type of soil including pore size, and the degree of saturation. Several experiments on lupin (Carminati, 2013), *Triticum aestivum* L. (wheat, Young, 1995) and *Zea mays* (maize) (Read *et al.*, 2003) indicate that typically the rhizosphere is wetter than bulk soil, and therefore mucilage increases the water holding capacity of soil. It ensures that rhizosphere hydraulic conductivity declines less rapidly during soil drying (Zickenrott *et al.*, 2016) as it mitigates the formation of air gaps when soil dries and roots shrink. The small amount of phospholipids within mucilage confer surfactant properties (Carminati and Veterlein, 2013). Experiments on commercial lecithin, an amphiphilic phospholipid, to mimic the mucilage lipids have revealed that the surface tension decreases and viscosity increases as mucilage dries (Read *et al.*, 2003). As surface tension decreases, the water holding capacity decreases. Reduced surface tension might allow the roots to better drain water from small soil pores (Carminati and Veterlein, 2013). The increased viscosity restricts soil particle movement and stabilises the rhizosheath, maintaining root-soil contact (Carminati *et al.*, 2013). Overall, mucilage seems to promote hydraulic conductivity during soil drying and restrict it during re-wetting of dry soil (Read *et al.*, 2003). The restriction of hydraulic conductivity during re-wetting may not necessarily have a benefit but it could mitigate the potentially detrimental effects of too rapid an increase in water in the roots.

Besides being a drought adaptive trait, the rhizosheath confers benefits in relation to biotic factors: Hiltner (1904) made the first observation that microorganisms are more abundant in the rhizosphere than bulk soil and subsequently, Knudson (1920) and Lyon and Wilson (1921) identified a link between root exudation and microbe abundance (Hartmann *et al.*, 2008). Root

mucilage provides a nutrient-rich environment for micro-organisms and could be involved in recruiting beneficial microorganisms such as Rhizobia, and maintaining a diverse "disease-suppressive" environment, whereby a diverse microbial community inhibits the development of pathogenic microbes (Sujkowska-Rybkowska and Borucki, 2014; Haas *et al.*, 2005; Fatima *et al.*, 2019). The relationship between the rhizosheath and microorganisms is further discussed in Chapter 4.

The two principal agents for modulating rhizosheath presence and size are root hairs and the quantity and composition of mucilage, both of which are discussed below (Watt *et al.*, 1994; Moreno-Espíndola *et al.*, 2007; Haling *et al.*, 2010, 2014; Brown *et al.*, 2012; Delhaize *et al.*, 2012; George *et al.*, 2014).

# 3.2.1 Role of mucilage in rhizosheath formation

Compounds released by the roots account for 5-70 % of total carbon fixed by the plant during photosynthesis, although these figures vary by species (wheat, *Hordeum vulgare* [barley], maize and *Solanum lycopersicum* [tomato] reviewed here) and study (Whipps and Lynch,1983; Whipps, 1984; Newman, 1985; Whipps, 1987; Badri and Vivanco, 2009). Secreted compounds comprise mucilage, root exudates and up to 6% proteins (Nguyen, 2003). Mucilage tends to be defined as the complex of large plant polysaccharides which are acidic, highly-branched and heterogeneous (Badri and Vivanco, 2009). They are insoluble and hydrophilic thanks to numerous hydroxyl (OH) groups capable of forming hydrogen bonds with the soil particles and they trap water in their cage-like structure to form a gel (Read *et al.*, 2003; Carminati and Veterlein, 2013). Examples of mucilage constituents include mannans, hemicelluloses, pectins. Exudates comprise low-molecular weight sugars, amino acids, organic and inorganic acids, secondary metabolites, phenolics and phytosiderophores, many of which can be rapidly metabolised by micro-organisms (Jones *et al.*, 2005; Fischer *et al.*, 2010; Dippold *et al.*, 2014; Gunina and Kuzyakov, 2015).

The mechanism underpinning secretion of polysaccharides and glycoproteins has yet to be fully characterised but it is possible that it involves one or the other or both of the following: (i) as roots grow through the soil, the friction exerted on the root cap results in the lysis of root cap cells, border cells and tip cells. As the cells lyse, they release the polysaccharides contained in the

cell wall matrix (Read and Gregory 1997; Iijima *et al.* 2004). (ii) Active secretion of the polysaccharides via specialised cell wall pores (Badri and Vivanco, 2009).

A study of the spatial distribution of mucilage in maize using infrared spectroscopy demonstrated an increasing concentration of mucilage on the root surface as distance from the root tip increased (Holz *et al.*, 2018). The study did not propose an explanation for this observation. It is possible that the greater levels of mucilage in older root zones could arise from multiple sources: the root cap is widely acknowledged to be the primary location of mucilage release as border cells are sloughed off as a result of root meristem cell division (Pearson and Parkinson, 1961). As the root grows through the soil, it pushes through these rhizodeposits, plausibly resulting in older zones to become sheathed in mucilage. In addition to this mucilage, it is likely that mucilage on these parts of the root are derived from the degradation of epidermal cell walls (Foster, 1982) and secretion from root hairs and epidermal cells. While there is no clear evidence that the epidermis and root hairs of plants secrete mucilage, Werker and Kislev (1978) reported small drops of mucilage secreted by root hairs and a mucilage layer secreted by the epidermal cells of sorghum.

The properties of the rhizosheath are a function of the properties of its constituent polysaccharides, glycoproteins and phospholipids. Several studies have characterised the carbohydrate component of the rhizosheath, particularly in maize (Bacic *et al.* 1986; Guinel and McCully 1986; Moody *et al.* 1988; Read and Gregory 1997). Recent studies have shown more interest in wheat (Galloway *et al.*, 2018, 2020). Monosaccharide linkage analysis of two-day old wheat grown on filter paper has suggested that these species release high amounts of heteroxylan and low amounts of pectic polysaccharides (Moody *et al.*, 1988). A more recent study of hydroponic-grown wheat suggested that concentrations of xyloglucan were higher than those of xylans (Galloway *et al.*, 2020). If relative concentrations differed, both studies concurred on the presence of heteroxylans, AGP, xyloglucan and pectic polysaccharides in wheat root mucilage. There appears to be similarity between the polysaccharides present within the root body and those released by roots (Bacic *et al.* 1986; Guinel and McCully 1986; Moody *et al.* 1988; Read and Gregory 1997).

Based on literature data of the high molecular weight polysaccharides found in the wheat rhizosheath, xyloglucan, extensin, AGP, homogalacturonan and xylan/heteroxylans were chosen

for this study. An insight into the structure and function of these high molecular weight polysaccharides is provided below.

# 3.2.1.1 Xylan and heteroxylans

Xylans or heteroxylans are a group of hemicellulose polysaccharides made up of β-1,4-linked xylose (a pentose sugar) with a variety of possible decorations (side branches). Heteroxylans can occur in three main forms, depending on the decoration: glucuronoxylan (GX), neutral arabinoxylan (AX) and glucuronoarabinoxylan (GAX) (Table 3.1). They tend to have structural roles, notably forming hydrogen bonds with cellulose microfibrils in cell walls (Simmons *et al.*, 2016).

**Table 3.1 Structure and occurrence of three main types of heteroxylans.** Heteroxylans consist of a xylose backbone substituted with decorations.

| Polysaccharide | Decoration | Occurrence | Reference |
|---|---|---|---|
| Glucuronoxylan (GX) | 1,2-α-linked glucuronic acid residue for every 10 xylosyl residues | Mainly secondary cell wall of eudicotyledons | Albersheim *et al.*, 2010; Hao and Mohnen 2014 |
| Neutral arabinoxylan (AX) | α-L arabinofuranose | Secondary cell walls of all plants and endosperm of cereal grains | Albersheim *et al.* 2010 |
| Glucuronoarabinoxylan (GAX) | α-L arabinofuranose and a glucuronic acid residue for every 5 to 6 xylosyl residues | Cell walls of commelinid monocotyledons e.g. Bromeliads and Poaceae | Vogel 2008; Burton *et al.* 2010 |

# 3.2.1.2 Extensin

Extensins are a family of flexible, rod-like, hydroxyproline-rich glycoproteins (HRGPs), typically with two major repetitive peptide motifs, one hydrophilic and the other hydrophobic. These motifs can crosslink with other compounds such as pectins and hemicelluloses, which is important for supporting the structure of cell walls (Castilleux *et al.*, 2018). Extensins are O-

glycosylated and are decorated with arabinose residues and display significant structural variation (Castilleux *et al.*, 2018).

Extensins are reported to occur ubiquitously in plants and are involved in a range of processes such as embryo development (Hall and Cannon, 2002; Zhang *et al.*, 2008), root hair growth (Ringli, 2010; Velasquez *et al.*, 2011, 2015), cell wall assembly (Cannon *et al.*, 2008; Lamport *et al.*, 2011; Pereira *et al.*, 2011; Chormova and Fry, 2016), biotic and abiotic stress responses (Merkouropoulos and Shirsat, 2003; Deepak *et al.*, 2010; Sujkowska-Rybkowska and Borucki, 2014; Zhang *et al.*, 2016) and plant defence (Deepak *et al.*, 2010; Rashid, 2016). The structure (epitope) that the extensin-specific antibody, LM1, binds to remains relatively unknown, although it is a sequence of sugar residues (Castilleux *et al.*, 2018). Studies on extensin using the LM1 antibody identified a change in extensin expression in response to pathogen inoculation and wounding, suggesting a role for extensins in plant immunity (Castilleux *et al.*, 2018). Extensin is found in all plant tissues. Specifically, studies in Arabidopsis (*Arabidopsis thaliana*) and flax (*Linum usitatissimum*) show LM1 epitopes in the cell wall of root border-like cells (Sujkowska-Rybkowska and Borucki, 2014). Root border-like cells are derived from root caps and are released into the rhizosphere. One role attributed to them is the protection of the root from pathogenic attack (Hawes *et al.*, 2000; Hawes *et al.*, 2002; Vicré *et al.*, 2005; Driouich *et al.*, 2010). Furthermore, the *ext1* gene, primarily expressed in roots and involved in extensin synthesis, is upregulated during pathogen infection in potato (*Solanum tuberosum*) (Koroney *et al.*, 2016). On the other hand, extensin may also play a positive role in microbial interactions: pea (*Pisum sativum* L) root nodules infected with *Rhizobium* contain LM1 epitopes, leading to the suggestion that extensins may be involved in the attachment of *Rhizobium* to nodules (Sujkowska-Rybkowska and Borucki, 2014).

## 3.2.1.3 Xyloglucan

Xyloglucan is a hemicellulose polysaccharide, made up of a β 1-4-linked glucose backbone with side-chains containing xylose, galactosyl and fucosyl. The variety of possible decorations leads to scope for multiple structural conformations and interactions, and therefore multiple functional roles. Xyloglucan is present in the cell walls of all land plants and is a common feature of root secretions, as documented in wheat, barley, maize, tomato, and Arabidopsis (Galloway *et al.*,

2018; Piqué *et al.*, 2018). The different structural forms of xyloglucan are present in varying abundance in different tissues, plant clades and species (Hayashi 1989; York *et al.*, 1996; Peña *et al.*, 2008; Albersheim *et al.*, 2010). Thanks to its gel-like properties, xyloglucan is widely used for food, cosmetics and drug delivery (Piqué *et al.*, 2018). Concerning the rhizosheath, xyloglucan has been shown to promote soil aggregation, indicating its likely importance for rhizosheath formation (Galloway *et al.*, 2018).

# 3.2.1.4 Arabinogalactan protein

Arabinogalactan protein (AGP) is typically composed of 90% glycan and 10% protein (Chen *et al.*, 1997). The glycan backbone is formed of 1,3- and 1,6-β-linked galactose residues with side-chains of 1,6-β-linked galactose that holds 1,3-α-linked L-arabinose residues, 1,6-β-glucuronic acid and 1,4-α-linked L-arabinose residues (Ellis *et al.*, 2010). The protein domain ranges from 5 KDa to 30 KDa and is rich in alanine, proline and hydroxyproline and is heavily glycosylated (Bacic *et al.* 1997; Kieliszewski, 2001). It is soluble and diffusible (Kreuger *et al.*, 1993).

Ubiquitously present in cell walls, plasma membranes and extracellular secretions, AGP is known for its role in cell expansion, division, death, seed germination, pollen tube growth and resistance to infection (Nguema-Ona *et al.*, 2012). It is widely reported that AGP contributes to positive and negative plant-microbe interactions. For example, several studies in Arabidopsis and pea have shown that AGP is involved in recognition of host roots by beneficial microbes and contributes to successful root colonisation by symbiotic bacteria (Gaspar *et al.*, 2004; Nguema-Ona *et al.*, 2013). Furthermore, many micro-organisms produce AGP glycan-degrading enzymes and rhizobacteria grow well on AGP-rich mucilage, indicating its role as a food source (Nguema-Ona *et al.*, 2013). Conversely, AGP is postulated to contribute to defence against pathogenic microorganisms in the "extracellular trap" (Driouich *et al.*, 2019). The release of mucilage and border cells from the root results in a physical barrier to microorganisms, which may also contain anti-microbial compounds (Goldberg *et al.*, 1989; Cannesan *et al.*, 2011; Curlango-Rivera *et al.*, 2011). An increase in AGP production and release has been recorded following the treatment of pea and potato with a pathogen or elicitor (Cannesan *et al.*, 2012; Koroney *et al.*, 2016).

# 3.2.1.5 Homogalacturonan

Homogalacturonan is one of five classes of pectic polysaccharides, alongside xylogalacturonan, apiogalacturonan, rhamnogalacturonan I and II. Collectively, they constitute 2-10% of grass primary cell walls and homogalacturonan is the most abundant pectin across studied plant species (Mohnen, 2008; Wolf *et al.*, 2009). Structurally, homogalacturonan consists of α-1,4-linked galacturonic acid residues (Caffall and Mohnen, 2009). These residues may be methyl-esterified on the carboxyl groups or acetylated on the hydroxyl groups (Carpita and McCann, 2000). Methylesterifaction and acetylation are important for regulating the structural and signalling properties of pectin (Wolf *et al.*, 2009). Pectin has been shown to contribute to cell extension, wall porosity, plant defence, cell-cell adhesion, seed hydration (Ridley *et al.*, 2001; Willats *et al.*, 2001; Driouich *et al.*, 2013; Basińska-Barczak *et al.*, 2020). For example, evidence for cell-cell adhesion by homogalacturonan is provided by the Arabidopsis *QUASIMODO 1-1* mutant, which is deficient in homogalacturonan biosynthesis. Border-like cells in these mutants are released as individual border cells instead of in complex (Driouich *et al.*, 2013). In defence signalling, Vorwerk *et al.* (2004) found that Arabidopsis homogalacturonans are broken down to oligogalacturonans to activate plant defence mechanisms. While much molecular work has been undertaken in Arabidopsis, less is known about mechanisms in wheat, particularly in the rhizosphere.

# 3.2.2 Role of root hairs in rhizosheath formation

Multiple studies in different species have demonstrated that root hairs are required for rhizosheath formation (Moreno-Espinola *et al.*, 2007; Shane *et al.*, 2011; Delhaize *et al.*, 2012; George *et al.*, 2014 Brown *et al.*, 2017). In an extensive glasshouse study of 58 plant species, the rhizosheath was absent in all species that lacked root hairs (Brown *et al.*, 2017). A study comparing wild type barley with mutant barley lacking root hairs demonstrated that a substantial rhizosheath was only present if root hairs were present (George *et al.*, 2014). Studies using wheat mapping populations derived from parents contrasting for rhizosheath size substantiated this (Haling *et al.*, 2010; Delhaize *et al.*, 2012).

The same is not true for root hair length. There is conflicting evidence on the importance of root hair length for rhizosheath formation. Across the 58 plant species, Brown *et al.* (2017) did not find a relationship between root hair length and rhizosheath weight. In their study on barley, George *et al.* (2014) suggested that root hair length was irrelevant because the size of the rhizosheath was related to the presence of root hairs regardless of environmental conditions that would alter root hair length, for example phosphorous (P) availability (George *et al.*, 2014). However, this does not eliminate the possibility that in environmental scenarios not tested in this experiment, root hair length is of importance. Supporting the importance of root hair length, a study in a wheat back-cross population derived from parents with contrasting rhizosheath size identified a strong relationship between root hair length and rhizosheath weight per unit root length (Delhaize *et al.*, 2012). A previous study in wheat had also identified a link between the length of root hairs and the ability to maintain a rhizosheath (Haling *et al.*, 2010). The inconsistency in the results of studies testing the effect of root hair length on the rhizosheath could be due to the different species or differences in the growth conditions: for example, both studies on wheat used acid soil, with elevated aluminium, manganese and hydrogen ions (Delhaize *et al.*, 2012). Water moisture in the various experiments may also play a part, as it has been demonstrated in rice that the role of root hairs is more pronounced under soil drying conditions (Zhang *et al.*, 2020). Therefore, there is a need for further, carefully designed and controlled experiments to understand the role that root hairs play in the formation of the wheat rhizosheath. The basis for root hair involvement in rhizosheath formation is not fully understood but it is likely to be a combination of physical and biochemical factors. Increased root hair density (and potentially length) allows greater propensity for enmeshing soil particles. Greater root hair density also provides a greater surface area over which compounds can be secreted (Holz *et al.* 2018).

# 3.2.3 Methods for rhizosheath and mucilage collection

Historical data on rhizosheath presence and size has often been anecdotal and prone to subjective observations and it is only in recent years that quantitative records are being made (Brown *et al.*, 2017). Furthermore, rhizosheath measurement has not been standardised and methodologies

can vary. In this thesis, the rhizosheath is defined as the soil that remains bound to the root after carefully removing the seedling from soil and gently shaking for two seconds.

Despite significant advances in the past decades, the sampling and analysis of root secretions still remains a major challenge. A balance is required between achieving growth conditions that are relevant to the field and enabling the detection of mucilage and exudates, which often can be done more easily in artificial conditions. Past approaches have involved growth on germination paper (Bacic *et al.* 1986; Moody *et al.* 1988; McCully and Sealey 1996; Read and Gregory 1997; Ray *et al.* 1988; Osborn *et al.* 1999; Narasimhan *et al.* 2003), hydroponics (Galloway *et al.*, 2018; 2020) and soil-based growth set-ups (Morel *et al.* 1986; Mounier *et al.* 2004).

Although non-soil-based systems allow the direct collection of secreted compounds into solution and avoid the adsorption of compounds to soil particles, they do not replicate true field conditions. For example, the root is not exposed to mechanical impedance, which could affect root system architecture (RSA), metabolism and the stimulation of secretion processes (Neumann and Römheld, 1999; Liao *et al.*, 2006). Furthermore in these artificial systems, the root is not exposed to typical soil microorganisms, which exert an influence over root secretions (Driouich *et al.*, 2013). As such, root secretions characterised by these methods may not be representative of naturally-occurring mucilage. Aeration of a liquid growth medium can be necessary to prevent the roots becoming hypoxic. However, the agitation of the growth medium by aeration has been shown to elicit a stress response in plants (Smallwood *et al.*,. 1995). Stress responses are visible in root secretions, for example through the release of extensins (Smallwood *et al.*,. 1995). Conversely, quantification of compounds in the mucilage of soil-grown plants may not be accurate due to the adsorption of compounds on soil particles, and soil heterogeneity may expose roots to different local conditions that affect secretion (Oburger *et al.*, 2013). Compounds are also exposed to microbial degradation (Oburger *et al.*, 2013). Nonetheless, the plants are exposed to conditions more representative of those in the field and measures can be taken to minimise sampling artefacts.

For compound detection, methods can include different types of mass spectrometry, enzyme-linked immunosorbent assays (ELISAs) and immunoblotting. Various forms of mass spectrometry (e.g. gas chromatography, liquid chromatography) exist and separate molecules from each other based on size, allowing the identification of compounds based on known

molecular weights (Pettolino *et al.* 2012). Mass spectrometry provides a very comprehensive analysis but can be limiting in terms of cost and requires fairly large amounts (1 – 10 mg) of material for analysis (Pattathil *et al.*, 2012; Pettolino *et al.*, 2012). ELISAs are highly sensitive, affordable tests, which detect polysaccharides released by roots using monoclonal antibodies directed to specific compounds. These assays utilise the property of monoclonal antibodies to be highly specific to a particular antigen. In animals, antibodies form part of the immune response to recognise and bind to specific foreign substances (Medzhitov and Janeway 1997). The immune response can be exploited to produce desired antibodies: an animal (typically a rat or a mouse) injected with a particular antigen (e.g. a plant polysaccharide) will produce a range of antibodies, each of which binds a specific epitope of that antigen, typically an oligosaccharide motif of 3-6 monosaccharides (Moller *et al.* 2008; Lee *et al.* 2011). An antibody is selected and cultured to produce exact clones of this type (a monoclone) so that each antibody in an ELISA reacts to exactly the same epitope in the same way. Briefly, the antigen (here, the polysaccharide) is immobilised on an assay plate, then complexed with an antibody that is linked to an enzyme that catalyses a reaction producing a coloured end product. This enzyme activity, which is proportional to the number of antibody-enzyme complexes, is determined by colorimetric measurement of the amount of product after incubation with a chromogenic substrate. The detection strategy relies on a highly specific antibody-antigen interaction. Quantitative data on the concentration of the antigen can be obtained by comparing the results with a standard curve produced by a dilution series of a pure reference standard. Monoclonal antibodies can also be used in diagnostic tests such as immunoblotting and chromatography. ELISA offers the advantage of requiring small quantities of antibody, inexpensive reagents, and enables the processing of a large number of samples at a time.

## 3.2.4 The rhizosheath as a target for crop improvement

Interactions between root architecture and the formation and function of the rhizosheath are poorly understood, implying that this area of research has potential for benefits to agriculture. The existence of genotypic variation for root secretions within a species suggests that it amenable to breeding, and that genetic gains can be achieved through selection (Halings *et al.*, 2010; Delhaize *et al.*, 2012; P. Knox, personal communication). Targets for selective breeding relating

to the rhizosheath include root hair density, root hair length, rhizosheath size, mucilage abundance and composition. Root hair length and root hair density have a demonstrated importance for functions like P acquisition. However, root hair traits are challenging to screen for and rhizosheath size could be used as a proxy for selection as it is easier to measure. There is currently strong evidence that the presence of root hairs leads to a larger rhizosheath ((Moreno-Espinola *et al.*, 2007; Shane *et al.*, 2011; Delhaize *et al.*, 2012; George *et al.*, 2014 Brown *et al.*, 2017). There is conflicting evidence on the relationship between root hair length and rhizosheath size and more research would be required to validate this.

Quantitative trait loci (QTL) relating to rhizosheath weight have been identified in barley (George *et al.*, 2014) and wheat (Delhaize *et al.*, 2015; James *et al.*, 2016). This opens the possibility of developing genetic markers for rhizosheath size and improve the ability of crop plants to cope with rhizosphere stresses. With sufficient heritability, a "rhizosheath QTL" may be useful as a practical marker of an underlying trait (e.g. root hairs, secretion composition) or collective traits.

The composition of wheat mucilage and its interaction with biogeochemical factors has potential to be integrated into breeding programmes or field management strategies (McGrail *et al.*, 2020). Tapping into root secretions is not the unique solution for developing climate resilient crops, but it is an important player. The root system is a Swiss-army knife for the functioning of plants and a holistic approach to engineering an optimal root system should include secretions as well as other traits such as components of root system architecture, the root microbiome etc. Root secretions have many roles, including nutrient acquisition, drought tolerance and interactions with microorganisms (Parker *et al.*, 2000; Fan *et al.* 2017; Grierson *et al.*, 2001; Michael, 2001). There is a risk that selecting for a desired trait within the root mucilage could negatively affect another process governed by root secretions. For example, the secretion of organic acids is important for P acquisition on calcareous soils but the secretion of chelators and phytosiderophores is more important for phosphorous acquisition in iron- and aluminium-heavy soils (McGrail *et al.*, 2020). Breeding programmes may need to select phenotypes for specific environmental conditions and take into account the interaction between secretions and root system architecture. For example, the different properties of different soil horizons means that deep and shallow root systems benefit from the secretions of different compounds. Multi-faceted, trait-based, resource-specific screening can lead to the selection of desired root phenotypes

(McGrail *et al.*, 2020). Breeders need to have a better understanding of the trait and these interactions before resources in a breeding programme are diverted to selections specifically for these traits. The research presented here helps to build that foundation of understanding.

## 3.2.5 Aims

The rhizosheath and root secretions have been studied for quite some time, but there is still relatively little known about the exact composition of wheat mucilage, which could be important for agriculture. In order for farmers and breeders to develop and use a variety that has the optimal mucilage for a given farming system or growing environment, breeders need a) genetic variation and b) a selection method. There is some evidence that there is intraspecific, varietal variation for root mucilage in wheat, but little has been published. An inexpensive, relatively high throughput method is needed, either for phenotypic selection or for marker development, which requires phenotyping large mapping populations. The same is true of the rhizosheath. In order to test for genetic variation in the Avalon x Cadenza (AxC) mapping population using a minimum of resources, a subset of the population that captured sufficient genetic variation was used.

The aims of this study were to test the following hypotheses:

- There is genotypic variation for rhizosheath size, mucilage secretion and root hair density in lines from the Avalon x Cadenza doubled haploid population
- The secretion of high molecular weight polysaccharides contribute to rhizosheath size
- Certain polysaccharides are secreted in proportional amounts, indicating their potential linkage in the mucilage matrix
- Genotypes with higher root hair density have a larger rhizosheath
- The location of root hairs along the root determines rhizosheath formation
- The rhizosheath is an accessible and appropriate agronomical trait for large-scale phenotyping

# 3.3 Materials and methods

# 3.3.1 Germplasm

The Avalon x Cadenza doubled haploid (AxC DH) population was used. It is derived from F1 progeny of a cross between cvs. Avalon and Cadenza developed by Clare Ellerbrook, Liz Sayers and the late Tony Worland (John Innes Centre, JIC), as part of a Defra funded project led by ADAS. Eighteen lines from the AxC population that displayed root phenotypes (angle and growth rate) at the tail ends of the population distribution in a series of clear pot screens (Chapter 2, section 2.2.1) were selected on the basis of having the greatest number of replicates within the top 1 % or bottom 1 % of best linear unbiased predictions (BLUPs, Table 2.9), calculated from ˜8400 individuals depending on the trait (angle, primary root length and seminal root length). These lines are hereon referred to as the "AxC tails". The use of tails representing the phenotypic extremes of a population is well suited to assessing complex, polygenic traits (Rebetzke *et al.*, 2017).

# 3.3.2 Plant growth conditions

The AxC tails, plus cvs. Avalon and Cadenza, were grown in Falcon tubes (50 mL) in an equal mix of Norfolk native field loam and sports sand (Renovation Mix, Bailey's, Norfolk; pH 6.5-7.5, screened to 4 mm particle size). The sieved mix was not sterilised in order to approach field microbial conditions as much as possible. One seed was sown per tube (depth of 5 mm) to ensure that exudate samples were distinct biological replicates. Lines were randomised within the layout using the "Blockdesign" package in R (R Core Team, 2016). Five replicates per line were randomised in five blocks, each block comprising two rows (Figure 3.1). Each line had one replicate per block. Glasshouse conditions were maintained at a daytime temperature of 18-24 ⁰C and night-time temperature of 15-18 ⁰C, 10 000 lux supplementary sodium lights ensuring a 16-hour day length. Containers were watered daily to maintain moisture content and care was taken not to flood the tubes by avoiding pooling water on the soil surface. Results presented here are from two separate experiments, referred to as Exp1 (November 2018) and Exp2 (December 2018). The parents, cvs. Avalon and Cadenza, were phenotyped for rhizosheath size, root length and shoot length in an additional experiment (Exp3, June 2019).
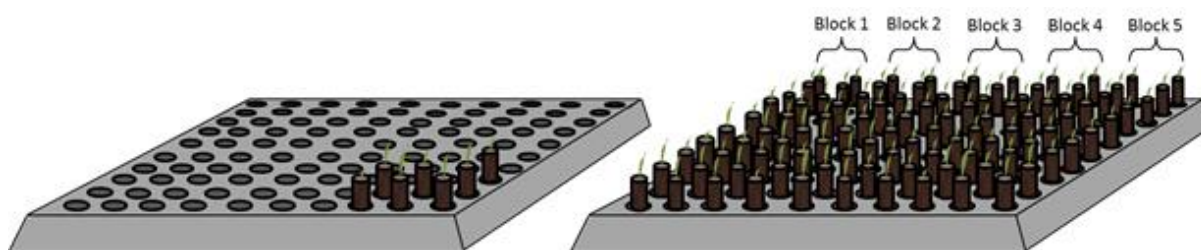
**Figure 3.1 Growth set-up of selected lines for analysis of the rhizosheath.** Seedlings from cv. Avalon, cv. Cadenza and the AxC tails were grown in a randomised block design in Falcon tubes (50 mL) secured in a custom-made holder matrix consisting of an inverted tray perforated with holes (10 rows x 10 columns). One seedling was grown per tube.

# 3.3.3 Mucilage collection

Seedlings that germinated within a day of each other were harvested seven days after sowing. Those with delayed germination were discarded. Seedlings were carefully removed from the growth tubes and gently shaken for two seconds to remove soil that was not attached to the rhizosheath. They were laid on white paper and photographed with an Olympus TG-4 camera. The shoot was separated from the roots at the junction with the seed. The shoot was weighed and the leaf length measured from base to tip (only one leaf emerged at this stage). The roots with attached rhizosheath soil were weighed and transferred to flat-bottomed, screw-cap tubes (15 mL) on ice. They were transferred to -80 ⁰C with no more than a delay of 30 minutes. This was considered appropriate to feasibly minimise polysaccharide degradation as microbial uptake of the high molecular weight compounds studied here is slowed by the need for exoenzymes (Jones *et al.*, 2005; Fischer *et al.*, 2010; Dippold *et al.*, 2014; Gunina and Kuzyakov, 2015). Once all samples were collected, UltraPure™ distilled DNase/RNase free water (4 mL, Invitrogen) was added to the tubes. The tubes were gently vortexed for 5 seconds (Vortex-Genie 2, Scientific Industries, Inc. USA) to fractionate the rhizosheath and release the compounds into the water. Although efforts were made to minimise disruption of the root, it is possible that there was leakage from ruptured cells and the assayed material could have contained some compounds that diffused out of root cells during the extraction process. The soil was allowed to sediment for 15 minutes on ice and the water was pipetted off and transferred to Eppendorf tubes (2 mL). They were stored at -20 ⁰C for up to a month until further processing.

# 3.3.4 Enzyme-linked immunosorbent assay (ELISA)

The ELISA technique was learned from the Paul Knox group (University of Leeds), which set up the antibody distribution service, PlantProbes. The ELISA was performed using 96-well microtitre plates, manufactured to promote adhesion of the polysaccharide components of the rhizosheath extract to the plastic walls of the wells (NUNC Maxisorp, Life Technologies, Thermo Fisher Scientific, UK). Aliquots of the thawed root/rhizosheath aqueous wash (10 μL) were added to each well with 90 μL 1x phosphate buffered solution (PBS, 8 mg mL$^{-1}$ NaCl, 0.2 mg mL$^{-1}$ KCl, 1.4 mg mL$^{-1}$ Na$_2$HPO$_4$, 0.2 mg mL$^{-1}$ KH$_2$HPO$_4$) and incubated at 4°C overnight to allow adsorption of the compounds to the surface of the wells. Plates were washed by plunging them three times in tap water and tapping them dry to remove excess rhizosheath solution. They were incubated for 2 h at room temperature using 300 μL per well of MP/PBS (5% w/v skimmed milk powder) in 1x PBS to block any surface of the ELISA plate not coated with antigen. The washing step was repeated. A 1:10 dilution of rat MAb (hybridoma cell supernatant; PlantProbes, Leeds, UK) specific to the chosen antigen was added to each well in MP/PBS (100 μL). The plates were incubated for 1 h at room temperature and washed six times as previously described. A 1:1,000 dilution of anti-rat secondary antibody coupled with horseradish peroxidase (HRP; A9037; Sigma-Aldrich, US) was added to MP/PBS (100 μL per well) for 1 h at RT. The washing step was repeated thrice. The following chromogenic substrate (100 μL) was added to each well with 10 μL H$_2$O$_2$: 9 mL water, 1 mL 1 M sodium acetate pH 6.0, 100 μL 3,3',5,5'-tetramethylbenzidine (10 mg mL$^{-1}$ dimethyl sulphoxide, DMSO). After 5 minutes, 50 μL 2.5 M sulphuric acid was added to the wells to stop the reaction. Absorbance was measured at 450 nm with a microplate reader (Elx800, Bio-figureTEK instruments, U.S.A.). Assays were carried out with three technical replicates on the same plate. Replicates with a coefficient of variability greater than 15 % were discarded. A standard curve was generated for each ELISA plate using commercial standard polysaccharides of concentrations ranging from 0.05 - 10 μg mL$^{-1}$ (Appendix 1). Absorbances were plotted against the known concentrations. An equation to fit the curve was calculated using mycurvefit.com, with a goodness of fit of 99%. The equation was then used to determine polysaccharide concentrations in the root/rhizosheath aqueous wash. The majority of absorbances fit into the linear part of the curve. There was no additional advantage to using a log or logit transformation of the standard curves. Table 3.2 lists the commercial standards and their origin.

**Table 3.2 Commercially produced polysaccharides used in ELISAs.** The commercial purified polysaccharides were used to construct a standard curve; the antigen refers to the corresponding target polysaccharide in the rhizosheath samples whose concentration was determined using the standard curve of the corresponding commercial polysaccharide. The antibody label refers to the catalog ID from the supplier (PlantProbes, Ltd UK). XLLG, xyloglucan nonasaccharide (Glc$_4$Xyl$_3$Gal$_2$); XXXG, xyloglucan heptasaccharide; XXLG, xyloglucan octasaccharide; XY, xylan; Gal, galactose.

| Commercial polysaccharide | Supplier | Antibody | Antigen | Specificity | Antibody reference |
|---|---|---|---|---|---|
| Xylan (Beechwood) | Megazyme | LM11 | Xylan | Unsubstituted and low-substituted xylans, particular affinity for arabinoxylan. beta-XY-(1->4)-beta- XY-(1->4)-beta- XY-(1->4)-beta- XY | McCartney *et al.*, 2005 |
| Xyloglucan (from Tamarind seed) | Megazyme | LM25 | Xyloglucan | Xylosyl/galactosyl residues, XLLG, XXLG and XXXG | Pedersen *et al.*, 2012 |
| Gum Arabic | Sigma Aldrich | LM2 | Arabinogalactan protein | Beta-linked glucuronic acid | Smallwood *et al.*, 1996; Yates *et al.*, 1996 |
| Citrus Pectin (galacturonic acid) | Sigma Aldrich | JIM7 | Homogalacturonan | Partially methyl-esterified homogalacturonan. GalA1->4MeGalA1->4MeGalA1->4MeGalA1->4MeGalA1->4GalA | Knox *et al.*, 1990; Willats *et al.*, 2000; Clausen *et al.*, 2003 |
| Citrus Pectin (galacturonic acid) | Sigma Aldrich | LM19 | Homogalacturonan | De-esterified homogalacturonan alpha-GalA(1-4)alpha-GalA(1-4)alpha-GalA(1-4)alpha-GalA | Verhertbruggen *et al.*, 2009 |
| Gum Arabic | Sigma Aldrich | LM1 | Extensin | Most likely includes glycan components of extensins | Smallwood *et al.*, 1995 |
| Xylan (Beechwood) | Megazyme | LM27 | Heteroxylan | Most likely a complex substitution of grass heteroxylan, especially glucuronoarabinoxylan (GAX) | Cornuault *et al.*, 2015 |

## 3.3.5 Image analysis and statistics

Image J software (Schneider *et al.*, 2012) was applied to measure root length, shoot length and rhizosheath projected area using photos of the plants harvested for the ELISA. As rhizosheath area correlated strongly with rhizosheath weight (Pearson, $r_{(72)}$ = 0.81, p < 0.001), rhizosheath area was chosen as an indicator of rhizosheath size to minimise damage to the samples through handling during the weighing process. Total root length was calculated as the sum of the lengths of the primary root and the seminal roots. The epitope concentrations determined by ELISA were adjusted for root length to give concentrations per unit root length for each plant.

Data were tested for normality (Shapiro-Wilk test in R) and log-transformed for statistical analysis if they did not fit the normal distribution. To investigate the genetic effect on rhizosheath polysaccharide concentration, log-transformed data were analysed with a mixed model using restricted maximum likelihood (REML) in GenStat 19 (VSN International, 2017). As data from repeated experiments were combined in the analyses, the fixed model Line x Experiment accounted for a possible interaction. Heritability of the traits was also calculated in GenStat 19. Analyses of the differences between cvs. Avalon and Cadenza were undertaken in R with a linear mixed model fit by REML using the lmm package, assigning Experiment as a fixed factor (Bates *et al.*, 2014; R Core Team, 2016). To test correlations between traits across all experiments, BLUPs were generated for each line using the lmer package, assigning Experiment as a random variable (Bates *et al.*, 2014; R Core Team, 2016). The Pearson correlation test was applied to the BLUPs to test the strength of relationships between traits in R (R Core Team, 2016).

## 3.3.6 Root hair measurement

The AxC tails, plus Avalon and Cadenza, were tested for patterns in root hair growth. Eight seeds per line were placed on wet germination paper which was folded over and placed in a clear unsealed plastic Polybag. The Polybags were stacked vertically to maintain gravitropic growth and the germination paper remained wet until the imaging of the seedlings five days later using a Canon EOS 100D camera. The seedlings were placed on black card and the camera was adjusted at 10 cm above the seedlings in order to capture the root hairs. Multiple photographs were taken to capture the entire length of the roots as each image framed a section of the root system (Figure

3.2). Root hair number was measured manually in ImageJ software (Schneider *et al.*, 2012). Resolution was not sufficient to accurately measure root length.



**Figure 3.2 Example wheat plant photographed for root hair count**.

# 3.4 Results

## 3.4.1 Genotypic variation of root and shoot traits

There was significant variation in rhizosheath size, total root length, shoot length and shoot mass among the AxC tails (Table 3.3). There was a strong experiment effect and a strong genotype:experiment interaction for all traits, except shoot length. BLUPs for each line can be found in Appendix 2. Rhizosheath size displayed a moderate heritability of 0.39 (Table 3.3). In these experiments, total root length had a high heritability of 0.81, in contrast with results from clear pot experiments (Chapter 2, section 2.2.1). Much greater heritability was observed for shoot length (0.54) than shoot mass (0.071).

In separate experiments phenotyping cvs. Avalon and Cadenza alone for increased replication, Avalon was found to have a larger rhizosheath than Cadenza: the amount of adhered soil per length of root in plants of the Avalon genotype was significantly greater than for plants of the Cadenza genotype ($p < 0.001$, Figures 3.3 and 3.4, Table 3.4). There was a significant "experiment" effect for all traits but no genotype:experiment interaction for any traits. Based on experiments in different growth media (Chapter 2), Avalon generally had a longer primary root than Cadenza, but Cadenza generally produced a greater number of seminal roots than Avalon. The net effect is that Cadenza seedlings displayed a greater total length of the seminal root system within seven days after sowing. This trend was repeated in this set of experiments, although the differences in length did not reach statistical significance.

**Table 3.3 Mean values for root and shoot phenotypes of the AxC tails and parental lines.** Values are based on two independent experiments. Statistics were carried out on log transformed data to account for a non-normal distribution. Degrees of freedom ranged from [19, 164] to [19, 254]. Rhizosheath size is quantified by projected area using image analysis.

| Phenotype | Rhizosheath size ($cm^2$ area $cm^{-1}$ root length) | Shoot length (cm) | Shoot dry mass (mg) | Total root length (cm) |
|---|---|---|---|---|
| AxC tails | 0.25 | 10 | 0.040 | 31 |
| Avalon | 0.35 | 11 | 0.050 | 38 |
| Cadenza | 0.29 | 10 | 0.030 | 36 |
| Genotype p-value | <0.001*** | 0.0050** | 0.0030** | 0.001*** |
| Experiment p-value | <0.001*** | <0.001*** | <0.001*** | <0.001*** |
| Genotype:Experiment p-value | <0.001*** | 0.074 | 0.0020** | 0.034* |
| Genotype LSD | 0.11 | 2.6 | 0.018 | 9.8 |
| Experiment LSD | 0.024 | 1 | 0.0068 | 3.8 |
| Genotype:Experiment LSD | 0.063 | 4.4 | 0.029 | 17 |
| Heritability | 0.39 | 0.54 | 0.071 | 0.81 |

**Table 3.4 Mean values for root and shoot phenotypes of wheat cultivars Avalon and Cadenza.** Values based on three independent experiments. Statistics calculated from a linear mixed model fit by REML, accounting for experiment as a factor. Degrees of freedom were (3, 41).

| Trait | Primary Root length (cm) | Total Root length (cm) | Rhizosheath size (cm$^2$ cm$^{-1}$ root length) | Shoot length (cm) | Total root number |
|---|---|---|---|---|---|
| Avalon | 13 | 40 | 0.29 | 11 | 3 |
| Cadenza | 11 | 43 | 0.22 | 11 | 4 |
| Genotype p-value | 0.02* | 0.41 | < 0.001*** | 0.94 | 0.002** |
| Experiment p-value | 0.033* | 0.014* | < 0.001*** | 0.009** | 0.043* |
| Genotype:Experiment p-value | 0.78 | 0.18 | 0.065 | 0.2 | 0.23 |
| Genotype LSD | 1.6 | 7.4 | 0.050 | 1.8 | 0.52 |
| Experiment LSD | 2.1 | 9.7 | 0.064 | 2.3 | 0.69 |
| Genotype:Experiment LSD | 2.9 | 13.5 | 0.088 | 3.2 | 0.96 |
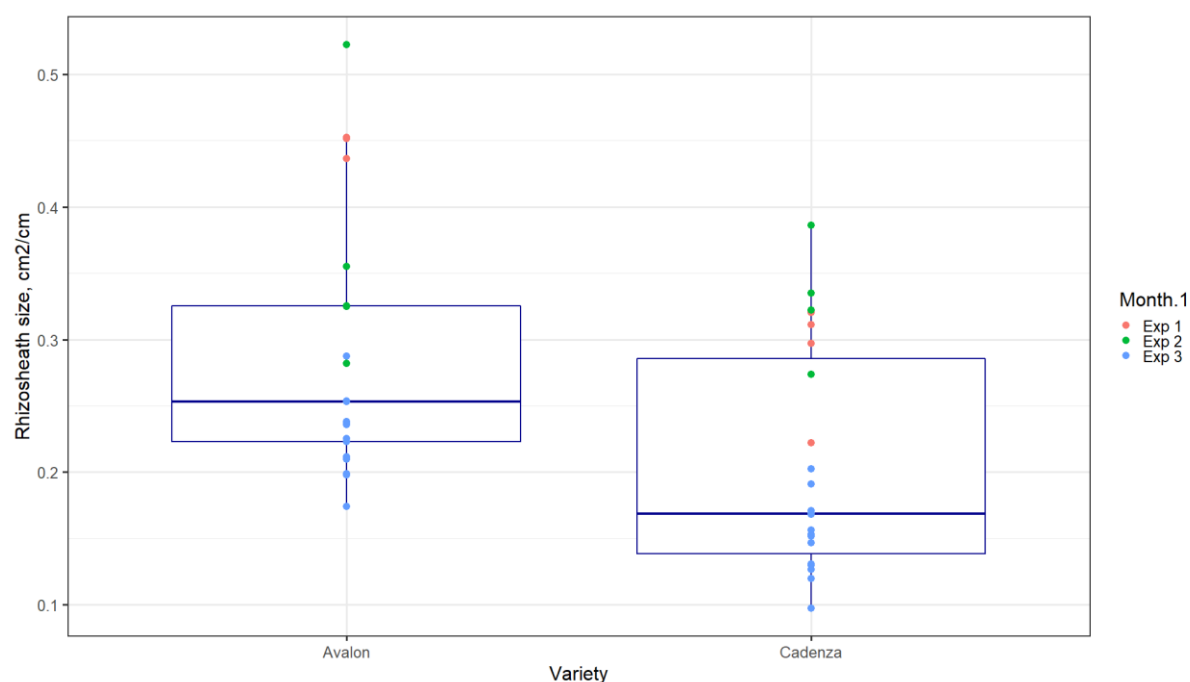


**Figure 3.3 Rhizosheath area of wheat cultivars cvs. Avalon and Cadenza**. Rhizosheath area was measured in ImageJ using photos of plants from three independent experiments. Area was adjusted for root length, to give area per total root length.
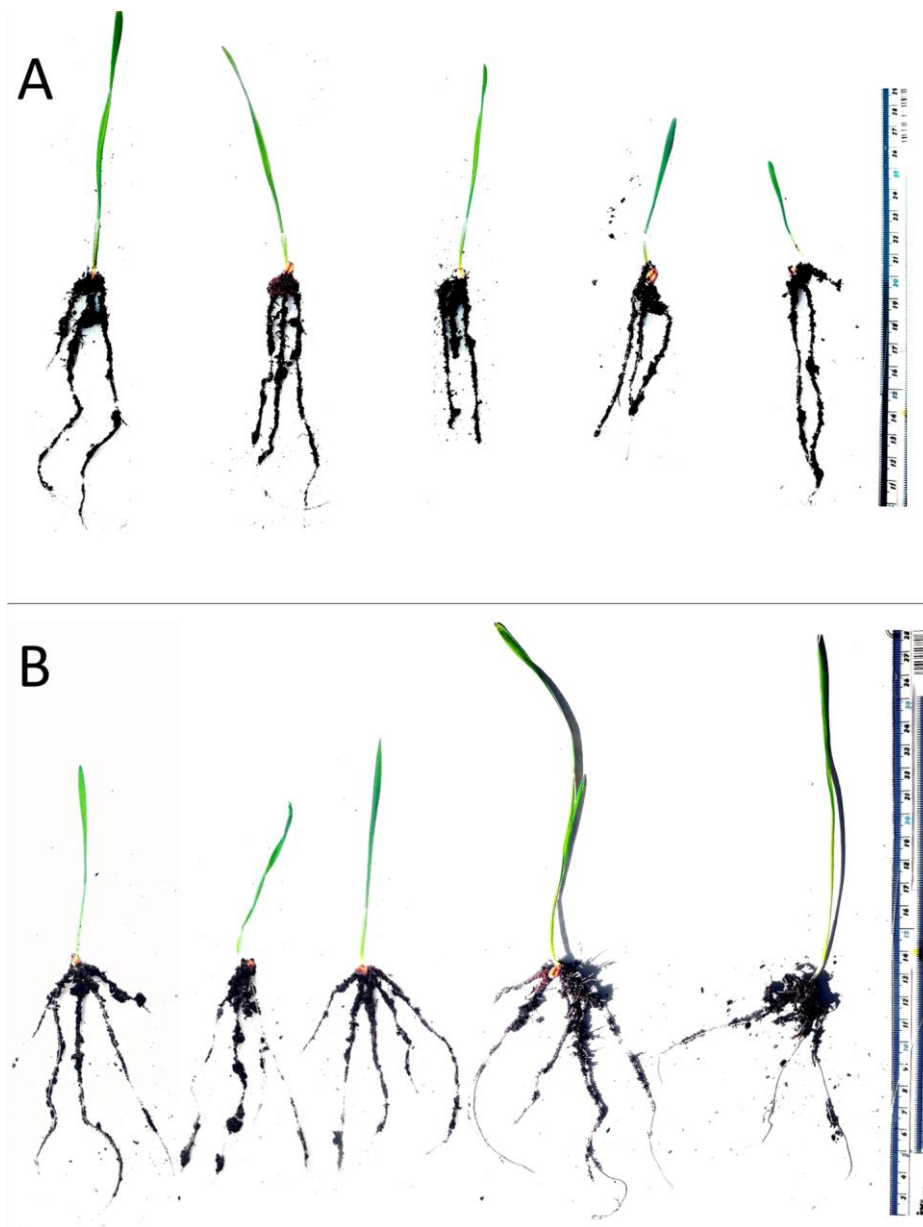
**Figure 3.4 The rhizosheath of wheat cultivars, Avalon and Cadenza**. Image shows examples of Avalon (A) and Cadenza (B).

# 3.4.2 Genotypic variation in polysaccharide concentrations

There was a significant environmental effect on the secretion of xylan, AGP, extensin and homogalacturonan and this was taken into account by the calculation of BLUPs. The AxC tails varied significantly for all epitopes (Table 3.5). The strongest genotypic effect was for the LM27 (heteroxylan), LM1 (extensin) and LM19 (homogalacturonan) epitopes. The LM11 epitope, xylan, had the smallest genotypic effect, which was nonetheless significant.

The most relevant method to calculate polysaccharide concentration was to report the concentration per unit root length, reflecting the degree of secretion along the length of the root. Different epitopes varied in concentration (Figure 3.5, Table 3.5). The LM27 epitope, heteroxylan, was the most abundant polysaccharide in the rhizosheath of tested plants (1.3 μg cm$^{-1}$). The LM2 epitope, AGP, was the second most abundant compound among those tested (0.11 μg cm$^{-1}$). Negligible levels of the JIM7 homogalacturonan epitope were identified compared with the LM19 homogalacturonan epitope. JIM7 binds to partially methyl-esterified homogalacturonan while LM19 binds to de-esterified homogalacturonan. The results indicate low amounts of partially methyl-esterified homogalacturonan in the wheat rhizosheath. Fairly low levels of xylan (LM11) and extensin (LM1) were detected compared with heteroxylan (LM27), AGP (LM2) and homogalacturonan (LM19). Avalon and Cadenza did not vary significantly for the concentration of the tested epitopes in their rhizosheath relative to the length of the root ($t_{(5)}$, p > 0.1).

Heritability of polysaccharide concentration varied (Table 3.5). Xylan, AGP, heteroxylan and xyloglucan (LM25) had moderate heritability ranging between 0.38 and 0.56. Homogalacturonan (LM19) had the highest heritability of 0.66. Extensin (LM1) had negligible heritability of less than 0.1.

**Table 3.5 Mean epitope concentration detected in the rhizosheath of the AxC tails and parental lines.** Displayed are the combined results from two independent experiments for the AxC tails. Statistics were carried out on log transformed data to account for a non-normal distribution with degrees of freedom of (19, 70). XY, xylan; HX, heteroxylan; AGP, arabinogalactan protein; EX, extensin; HG, homogalacturonan; XG, xyloglucan. The antibody ID is shown in brackets.

| Epitope (µg ml-1 cm-1) | XY (LM11) | HX (LM27) | AGP (LM2) | EX (LM1) | HG (LM19) | HG (JIM7) | XG (LM25) |
|---|---|---|---|---|---|---|---|
| AxC tails | 0.0096 | 1.3 | 0.11 | 0.011 | 0.23 | 0.0014 | 0.078 |
| Avalon | 0.0064 | 2.3 | 0.21 | 0.0078 | 0.15 | 0.00083 | 0.092 |
| Cadenza | 0.0033 | 2 | 0.16 | 0.0081 | 0.18 | 0.00068 | 0.1 |
| Genotypic variation p-value | 0.022 * | <0.001 *** | 0.001 ** | <0.001 *** | <0.001 *** | 0.0015 ** | 0.004** |
| Experiment effect p-value | 0.005 ** | <0.001 *** | <0.001 *** | <0.001 *** | <0.001 *** | <0.001 *** | <0.001 *** |
| Line:Experiment effect p-value | 0.007 | 0.12 | 0.037 | <0.001 *** | <0.001 *** | 1 | 0.33 |
| Genotypic variation LSD | 0.0050 | 1.2 | 0.049 | 0.017 | 0.38 | 0.99 | 0.067 |
| Experiment effect LSD | 0.0016 | 0.38 | 0.015 | 0.0057 | 0.12 | 0.3 | 0.022 |
| Line:Experiment effect LSD | 0.0070 | 1.5 | 0.068 | 0.023 | 0.47 | 1.2 | 0.082 |
| Heritability | 0.38 | 0.40 | 0.40 | 0.050 | 0.66 | NA | 0.56 |
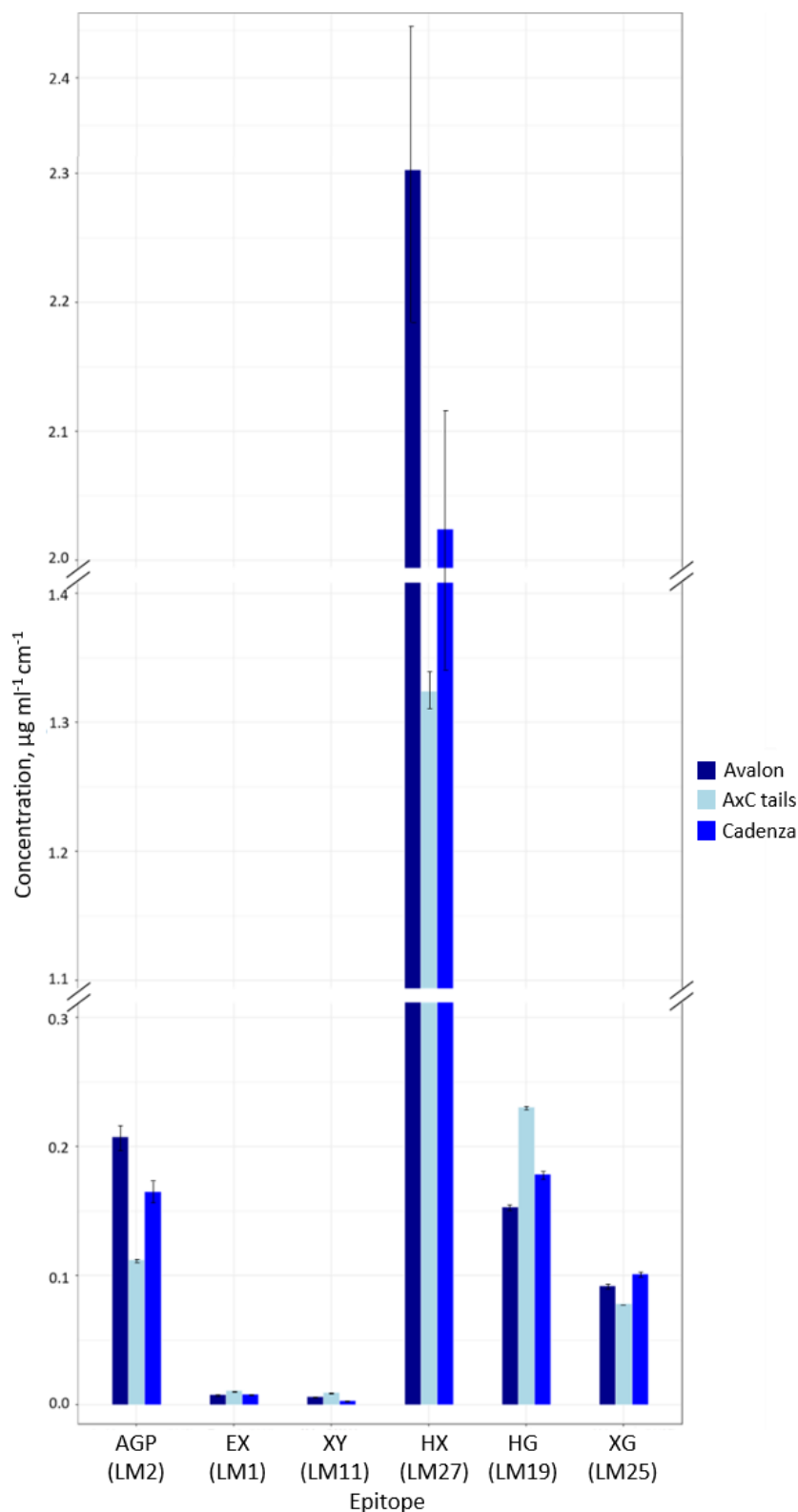
**Figure 3.5 Concentration of tested polysaccharides (µg/mL) in the rhizosheath extract, adjusted for the length of root (cm) in the sample.** Bars are the mean of the BLUPs across all lines ± se (navy blue), and BLUPs of Avalon (sky blue) and Cadenza (bleu Breton). AGP, arabinogalactan protein; EX, extensin; XY, xylan; HX, heteroxylan; HG, homogalacturonan; XG, xyloglucan. The antibody ID is shown in brackets.

### 3.4.3 Correlations between the levels of different polysaccharides

There was a significant environmental effect on the concentration of epitopes determined in different experiments (p<0.001). However, correlations were replicable between experiments and the data reported here comprise BLUPs calculated from both experiments. Shoot mass and length were significantly, negatively correlated with xylan and extensin concentration (Table 3.6). Shoot mass but not length was significantly, negatively correlated with homogalacturonan (LM19). There was a significant positive correlation between the size of the rhizosheath per unit root length and the concentration of LM27 and LM2 epitopes, heteroxylan and AGP. There was a moderate, non-significant correlation between the size of the rhizosheath and xyloglucan concentration (r = 0.34). Total root length displayed a significant, negative correlation with the LM11 epitope, xylan (r = -0.49). As negligible amounts of the JIM7 epitope were detected, no correlations were determined.

There were significant positive correlations between levels of AGP and heteroxylan, and between xylan, extensin and homogalacturonan (Table 3.7). In other words, genotypes that had greater concentrations of AGP in their rhizosheath, also had higher concentrations of heteroxylan. Likewise, xylan, extensin and homogalacturonan tended to co-occur. Xyloglucan concentration did not correlate with the concentration of other tested polysaccharides.

To determine the relationship between RSA and secretion, genotypes were grouped on the basis of being in the top or bottom tertile for root angle measured in a series of clear pot screens (Chapter 1, section 2.2.1), or grain yield measured over two seasons of field trials (Chapter 1, section 2.2.3). There was no significant difference in the level of polysaccharides between genotypes with wide seedling root angles and genotypes with narrow seedling root angles (Appendix 3, Supplementary Figure 3.1). There was equally no significant difference between high- and low-yielding genotypes (Appendix 3, Supplementary Figure 3.2).

**Table 3.6 Correlations between phenotypes and epitope concentration in the rhizosheath of the AxC tails.** Displayed are the Pearson correlation coefficients (r). Degrees of freedom are 18. * indicates a 0.05 significance threshold. ** indicates a 0.01 significance threshold.

| Epitope | Rhizosheath size | Shoot length | Shoot mass | Total root length |
|---|---|---|---|---|
| Xylan (LM11) | 0.16 | -0.52* | -0.79** | -0.49* |
| Heteroxylan (LM27) | 0.64** | -0.12 | -0.25 | -0.14 |
| Arabinogalactan protein (LM2) | 0.52* | 0.12 | 0.042 | 0.12 |
| Extensin (LM1) | 0.11 | -0.63** | -0.68** | -0.28 |
| Homogalacturonan (LM19) | -0.18 | -0.36 | -0.50* | -0.41 |
| Homogalacturonan (JIM7) | NA | NA | NA | NA |
| Xyloglucan (LM25) | 0.34 | 0.20 | 0.11 | -0.10 |

**Table 3.7 Correlations between the concentrations of different epitopes in the rhizosheath of the AxC tails.** Pearson correlation coefficients ($r^2$) are displayed in the bottom left (purple) and corresponding p-values are displayed in the top right (blue) of the table.

| $r^2$ / p-value | LM25 | LM2 | LM27 | LM1 | LM11 | LM19 |
|---|---|---|---|---|---|---|
| LM25 | | 0.12 | 0.28 | 0.60 | 0.96 | 0.96 |
| LM2 | 0.36 | | 0.00030*** | 0.23 | 0.81 | 0.59 |
| LM27 | 0.25 | 0.73*** | | 0.07 | 0.33 | 0.81 |
| LM1 | -0.13 | 0.28 | 0.41 | | 0.0001*** | 0.0021** |
| LM11 | -0.01 | 0.06 | 0.23 | 0.76*** | | 0.013* |
| LM19 | 0.01 | 0.13 | 0.06 | 0.64** | 0.55* | |

# 3.4.4 Genotypic variation in root hairs

For root hair measurements, plants were grown on germination paper to ensure the visibility of root hairs. Root hair length is not reported as the small size of root hairs made measurements too inaccurate. The macro setting on the DSLR camera was sufficient to accurately measure hair density, and throughput using microscopy would have been too low. However, greater magnification for root hair length than used here using the camera would be required for accurate determination. In future experiments, an inexpensive digital microscope could be used for image acquisition.

Root hair density was highest in the basal third of the seminal root system, nearest the root/shoot junction and was lowest in the apical third, nearest the root apical meristem (Figure 3.6, Table 3.8). There was significant genotypic variation in root hair density across the AxC tails in all portions of the root (Table 3.8). The difference in root hair density along the whole length of the roots of the parental lines, Avalon and Cadenza, did not reach statistical significance ($p = 0.067$). However, Cadenza had significantly more root hairs than Avalon in the basal third of the root system, nearest the seed ($p = 0.04$).

There was no significant correlation between the root hair density measured in the germination paper and the concentration of polysaccharides determined in the rhizosheath of soil-grown plants ($p > 0.1$). Furthermore, there was no correlation between the root hair density measured in the germination paper and the size of the rhizosheath per unit root length of soil-grown plants ($p > 0.1$).
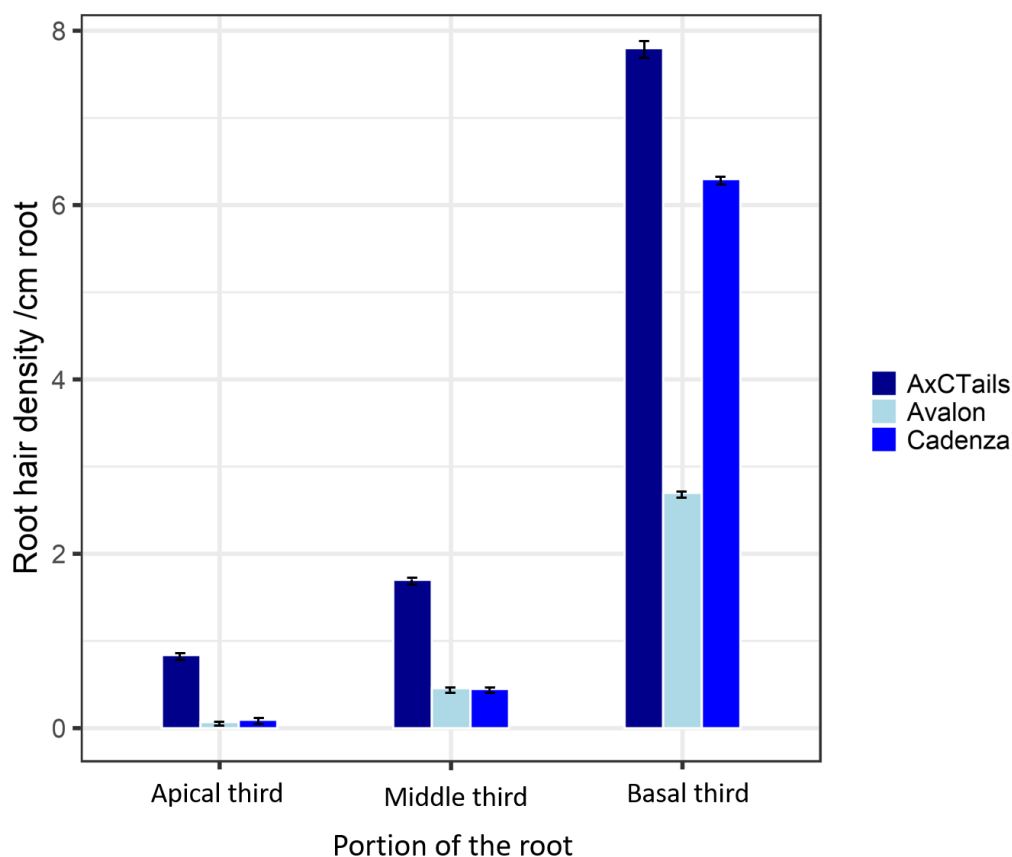
**Figure 3.6 Root hair density in different portions of the seminal root system of five-day old wheat seedlings.** Bars are genotypic means ± se (n = 133 total number of plants) for the apical third (near root apical meristem), middle third and basal third (nearest the root/shoot junction).

**Table 3.8 Mean root hair density in AxC tails and the associated genotypic variation.** Root hair density was measured five days after sowing on moist germination paper. Degrees of freedom for the whole subset of lines were (19, 132). Degrees of freedom for the parents ranged from 10-14.

| Root section | Root hair density (number of hairs cm⁻¹ root) | | | p-value | | LSD |
|---|---|---|---|---|---|---|
| | AxC Tails | Avalon | Cadenza | AxC Tails | Avalon and Cadenza | |
| Total root length | 3.4 | 1.1 | 2.3 | 0.001*** | 0.067 | 2.5 |
| Basal third | 7.8 | 2.7 | 6.3 | 0.001*** | 0.040* | 6.2 |
| Middle third | 1.7 | 0.46 | 0.45 | 0.001*** | 0.14 | 2.1 |
| Apical third | 0.84 | 0.072 | 0.097 | 0.029* | 0.63 | 1.3 |

# 3.5 Discussion

## 3.5.1 Methodology

The growth of plants in soil-filled Falcon tubes enabled a rapid, low-tech and space-efficient set-up for a high throughput screen. Growth set-up and seed sowing were relatively rapid, totalling around 3 hours for 100 seeds (100 minutes to fill 100 Falcon tube with soil; 60 minutes to arrange seeds of different genotypes in a randomised order; 15 minutes to sow seed). However, sampling was more laborious, totalling around 9-10 hours for 100 seeds (removal of the plant from the soil, photography, transfer of the roots and rhizosheath to a collection tube). Soil moisture had to be closely monitored due to rapid evaporative loss from the small soil volumes in the Falcon tubes. The standardisation of the growth conditions minimised variation in many environmental factors that are known to affect rhizosheath formation, such as temperature, soil moisture content, soil type, soil pH and nutrient availability (Watt *et al.*, 1994; Brown *et al.*, 2017). Soil moisture and temperature probes would be advised to ensure uniformity within the soil for all seedlings. By monitoring germination time, the harvesting of plants at a given growth stage was standardised. All plants were harvested by one person to ensure that plants were extracted from the soil in the same way. It is possible that polysaccharides were not fully extracted into water due to adsorption onto soil particles. Furthermore, the possible contribution of microbe-derived polysaccharides cannot be eliminated. However, this was a necessary trade-off to ensure that the growth medium approached that of the field. I also argue that the interaction between the plant and soil microorganisms influences the secretion of compounds from the roots. In the absence of microorganisms, mucilage characteristics may be different and so the presence of micro-organisms provides a more representative picture of rhizosheath mucilage in nature. To determine the contribution of microorganisms to rhizosheath mucilage, it would be interesting to undertake an experiment with sterilised soil conducted under axenic conditions.

## 3.5.2 Genotypic variation of root and shoot traits

Avalon displayed a larger rhizosheath than Cadenza and significant variation was observed among the AxC lines. In spite of the parents having relatively small variation in root length and

shoot length/mass, the progeny showed transgressive segregation. This means there would be potential to carry out QTL analysis on these traits using the entire population.

The apparent trend for cv. Avalon seedlings is to have a longer primary root but fewer seminal roots than Cadenza within the first week of development. The net effect is that Cadenza seedlings display a greater total length of the seminal root system. This could reflect different strategies for establishment, whereby Avalon puts energy into rapidly achieving depth, while Cadenza puts more energy into spread of the root system. Future work could determine the respective benefits of each strategy and how the RSA of each cultivar changes further along in development. For example, it has previously been recorded that better water status is achieved in wheat recurrent selection lines with greater elongation of seminal roots (Blum *et al.*, 1989; Palta *et al.*, 2011). The moderate heritability of the rhizosheath size means that it could be suitable as a trait for breeding. Using the Falcon tube set-up with sandy loam, there was high heritability for total root length ($H^2$ = 0.81). This contrasts with the heritability of 0.096 identified in the clear pot experiment (Chapter 2, section 2.2.1). This could arise from a greater uniformity in environmental conditions between Falcon tubes than between clear pots.

# 3.5.3 Genotypic variation of polysaccharide concentration

Heteroxylan (LM27) was the most abundantly detected polysaccharide in the rhizosheath of AxC lines, followed by homogalacturonan (LM19), AGP (LM2) and xyloglucan (LM25). LM27 is thought to bind to GAX, which is the abundant form of heteroxylan in the secondary cell walls of monocotyledons (Cornuault *et al.*, 2015). The heteroxylan detected here could be a component of the cell walls of border cells that were sloughed off from growing root tips. The comparatively lower abundance of xylan (LM11) indicates the lower abundance of the less branched form of xylan in rhizosheaths compared with highly branched heteroxylan (LM27). Presumably, the unbranched LM11 epitope is less recalcitrant and may be more prone to microbial degradation. This may make it less favourable as a component of mucilage or indicate that its low levels results from degradation post-sampling. The abundance of AGP and homogalacturonan supports the evidence that these polysaccharides play an important role in plant defence (Nguema-Ona *et al.*, 2013). For example, AGP is a proposed constituent of the

"extracellular trap" which forms a protective barrier around the root and de-esterified pectins are involved as signalling molecules in the defence strategy of a plant (Basińska-Barczak *et al.*, 2020).

Galloway *et al.* (2018) reported high concentrations of xyloglucan, xylan, extensin, AGP and homogalacturonan in wheat root secretions. The relative abundances of these polysaccharides differed from the present study: Galloway *et al.* (2018) found that xyloglucan was most abundant, followed by extensin, xylan, AGP and homogalacturonan. It is possible that differences arise because the study by Galloway *et al.* involved a hydroponic system whereas here, I use soil. For example, changes in root cell wall composition have been shown to change in response to environmental factors such as salt concentration (Byrt *et al.*, 2017). In particular, the lower-than-expected concentration of xyloglucan in the present study may be due to methodology: Galloway *et al.* (2019) previously reported that xyloglucan has strong soil-binding properties. It is possible that in the present study, xyloglucan was not fully extracted into solution due to strong binding to soil particles, leading to an underestimation of concentration in the ELISA assay. This would not, however, affect relative concentrations of xyloglucan between samples as all samples were treated in the same way. Further research could use alkali treatment for fuller extraction of xyloglucan (Galloway *et al.*, 2017).

The significant variation in epitope concentration among the eighteen lines, along with moderate heritability, demonstrated a genotypic effect on the concentration of polysaccharide secretion for xylan, AGP, homogalacturonan and xyloglucan. Although REML analysis identified significant variation between lines for extensin concentration, the low heritability of extensin suggests that genotypic variation was relatively small compared with the environmental influence on extensin secretion. The parents, cvs. Avalon and Cadenza, did not vary significantly for the concentration of the tested epitopes in their rhizosheath. This differs from reports that they contrast for xyloglucan secretion, although the observations were carried out in different growth media (P. Knox, personal communication). Furthermore, there is a discrepancy between the significant difference in rhizosheath size and the apparent lack of variation in polysaccharide secretion between Avalon and Cadenza. These parental lines do not follow the trend seen among the other lines, for an associated increase in rhizosheath size with the increase in the concentration of heteroxylan and AGP. This may be due to other factors, such as root hairs or another component of mucilage not measured here.

# 3.5.4 Correlations associated with polysaccharide concentration

There were significant positive correlations between levels of AGP and heteroxylan, and between xylan, extensin and homogalacturonan (Table 3.7). Xyloglucan concentration did not correlate with the concentration of other tested polysaccharides. The correlation of the concentrations of different polysaccharides indicates that they are present in the rhizosheath in proportional amounts. This may be a result of co-secretion, common biosynthetic pathways, involvement in common processes or physical linkage to each other in a common structure or matrix.

A range of models have previously been proposed for the organisation of cell wall polymers (Keegstra *et al.*, 1973; McCann and Roberts 1994; Carpita and Gibeaut 1993; Somerville *et al.*, 2004; Baba 2006). These all present a matrix of cellulose microfibrils crosslinked to a greater or lesser extent with various molecules including xyloglucans, heteroxylans and pectic polysaccharides (Zykwinska *et al.*, 2007; Burton *et al.*, 2010; Cosgrove, 2014). The crosslinking of these molecules in the cell wall indicates that they may also form a matrix in the rhizosheath, or are secreted at levels proportional to that in which they are found in the plant cell wall.

Galloway *et al.*, (2020) found strong evidence that xylan links xyloglucan and AGP in wheat exudates. Cornuault *et al.*, (2015) demonstrated a potential attachment of heteroxylan to AGP in potato tuber cell walls. Here correlations between heteroxylan and AGP could indicate these form polysaccharide complexes. Furthermore, correlations between xylan, extensin and homogalacturonan could suggest that their co-occurrence in proportional levels is a sign that they are all part of common complexes. It is known that pectic polysaccharides interlink other compounds. Homogalacturonan is known for its role in cell extension, cell-to-cell adhesion and wall porosity. It is possible that through modulation of cell wall porosity, it regulates the secretion of other compounds (Durand *et al.*, 2009). Further work is required to determine its role in the rhizosphere. Epitope detection chromatography, which involves chromatographic separation of polysaccharides can indicate links between epitopes. It could reveal whether the correlations observed here were due to physical binding of the polysaccharides together.

Rhizosheath size per unit root length displayed a significant positive correlation with heteroxylan and AGP, and a moderate, non-significant correlation with xyloglucan. This indicates that

genotypes exuding large amounts of these polysaccharides were able to develop larger rhizosheaths. Heteroxylan (LM27), but not xylan (LM11), had a positive correlation with rhizosheath size, potentially because the LM11 epitope is relatively unbranched. The diverse branching pattern of heteroxylan (LM27) may promote binding opportunities with AGP and with soil particles through increased opportunity for interactions with other molecules. Studies would be required to verify this as different degrees of branching have different effects in different compounds. For example, a survey of soil adhesion properties of multiple polysaccharides demonstrated that the most effective tested polysaccharide was a highly branched gum tragacanth (Akhtar *et al.*, 2018). However, the same study showed that an unbranched arabinan was more effective than a branched arabinan at soil adhesion.

A study on soil aggregation demonstrated that xyloglucan is capable of increasing soil particle size (Galloway *et al.*, 2018). This study did not report the potential for other polysaccharides to aggregate soil. However, the results presented herein indicate that heteroxylan and AGP may also be soil aggregators. The lack of significance between xyloglucan concentration and rhizosheath size does not necessarily contradict the finding of Galloway *et al.*, (2018) that xyloglucan is a potent soil aggregator. The authors recognise that they used much higher xyloglucan concentrations ($10 \, g \, kg^{-1}$) than would be present in the soil. They used concentrations that were higher than the xyloglucan detected here in the rhizosheath of AxC lines. No study has yet made a direct link between rhizosheath size and polysaccharide concentration. My results support the hypothesis that heteroxylan and AGP, and perhaps xyloglucan could interlink in a matrix which promotes soil agglutination and rhizosheath formation. Additional work could further explore the roles of the enzymes involved in the synthesis of these polysaccharides. For example, the enzyme, xyloglucan endotransglycosylase, regulates cell expansion in the elongation zone of root tips. It catalyses the breakdown of cell wall microfibril tethers that permit relaxation of the cell wall under turgor pressure and appears to be regulated under drought to permit continued root elongation in dry soil (Wu and Cosgrove, 2000; Boyer, 2009).

The negative correlation between shoot length/mass and the concentrations of xylan, AGP and extensin could be an indicator of the cost of directing photosynthate towards root secretions as opposed to above-ground growth. The same could be true for the negative correlation between root length and xylan exudation, whereby root growth may be slowed by the diversion of carbon from root growth to processes involving polysaccharide synthesis. Breeding for root traits should

achieve a balance between high functioning, resource-demanding roots and a more parsimonious root system. The negative correlation observed here could demonstrate the trade-off between favouring root processes and favouring above-ground biomass. Presumably, exudation provides a significant benefit to plants, and it would be interesting to undertake a meta-analysis to determine at which point the cost outweighs the benefit. It would also be interesting to see if trade-off lessens as the plant matures: in the first week, there is little leaf area to supply assimilate and seed reserves are being depleted, whereas later developmental stages may be able to spare more carbon without significant cost to growth.

# 3.5.5 Genotypic variation of root hairs

Root hair density was highest nearest the seed (Figure 3.6). The canonical root system is described to have fewer hairs in older portions of the roots (i.e. nearest the soil surface) (Goron *et al.*, 2015). However, as 5-day old seedlings were measured here, it is likely that root hairs had not yet reached their maximum longevity and had not yet died in older parts of the root: for example, Brown *et al.* (2013) estimate root hair longevity is typically five days and the root hairs of barley seedlings grown in germination pouches have been shown to have a longevity of up to 55 hours at temperatures between 15 and 25 °C (McElgunn and Harrison, 1969). There was significant genotypic variation in root hair density in all portions of the root. This supports existing evidence for strong genotypic regulation in the production of root hairs (Brown *et al.*, 2017). There was no relationship between the root hair density measured on germination paper and the size of the rhizosheath of the same genotypes grown in soil. The lack of correlation between root hair density and rhizosheath size in different growth environments suggests that there may be a genotype x environment interaction. Alternatively, if variation in root hair density does not explain the variation in rhizosheath size, root secretions may play a more important role. Numerous studies in older plants demonstrate that genotypes with greater root hair density have the capacity to form larger rhizosheaths (Moreno-Espinola *et al.*, 2007; Shane *et al.*, 2011; Delhaize *et al.*, 2012; George *et al.*, 2014; Brown *et al.*, 2017). Assuming this was also true in seedlings, the genotypes that produced many root hairs on germination paper would have had fewer root hairs in soil. Similarly, there was no correlation between root hair density on germination paper and polysaccharide concentration in the rhizosheath of the soil-grown plants. This suggests that root hair density may not be an important factor for the amount of mucilage

formed in wheat seedlings. However, it is likely that due to genotype x environment interactions, this comparison was not meaningful. Future studies using immunoblotting could measure root hairs growing on paper, then blot the root to determine whether increased root hair density could lead to increased secretion. It could also give spatial information on where polysaccharides were located.

# 3.6 Concluding remarks

There was significant variation among the AxC tails for rhizosheath size, root length, shoot length and the concentration of polysaccharides in the rhizosheath. Heritability was moderate for most traits, negligible for shoot mass and extensin concentration, and high for homogalacturonan (LM19). The high heritability and large abundance of homogalacturonan in the rhizosheath could support its role as an important target for breeding once its role in the rhizosphere is better established. However, although it was seen to correlate with xylan and extensin, it did not correlate with rhizosheath size. The moderately high heritability of xyloglucan ($H^2 = 0.56$), along with previous evidence of its soil adhesion (Galloway *et al.*, 2019) could support xyloglucan as a breeding target. Rhizosheath size was positively correlated with AGP and heteroxylan, which were abundant in the rhizosheath. This experiment demonstrated the value of undertaking larger-scale QTL mapping for polysaccharide concentration in the AxC population.

# 4

# The wheat rhizosheath microbiome

## 4.1 Abstract

The tripartite interaction between crops, soil microorganisms and the environment has gained attention for its potential impact on crop breeding. Microbial activity in the rhizosphere exerts positive, negative and neutral influences on a variety of plant processes including nutrition, water uptake, growth and pathogenesis. The challenge of meeting the demand for wheat yield in a changing climate could be met by leveraging the beneficial properties of the microbiome, yet relatively little is known on the effects of host genetics on the rhizosphere microbiome. A 16S and ITS metagenomics analysis was undertaken on the rhizosheath of 25 lines of the Avalon x Cadenza (AxC) doubled haploid wheat mapping population. Rhizosheath bacterial and fungal diversity was tested at the seedling stage; good establishment and vigorous early growth of the crop are an essential foundation for realisation of yield potential, and seedlings allow simple

experiments with high throughput. AxC lines did not vary in their rhizosheath microbiome according to various diversity indices but they did vary in the species composition of their microbiome. Lines grouped according to high or low grain yield from multiple field studies showed that higher-yielding lines differed significantly from lower-yielding lines for fungal species composition but not bacterial species composition. Genotypic differences in root system architecture and root polysaccharide secretion were associated with differences in bacterial and fungal species composition. Combining metagenomics data with information on the genetic control of RSA and mucilage composition in a mapping population begins to provide a more complete picture of rhizosphere dynamics, with the potential to engineer beneficial crop rhizospheres, reduce pathogenic burden, reduce chemical inputs and greenhouse gas emissions, increase climate resiliency and the sustainable production of yield.

# 4.2 Introduction

There is an ever-growing body of research into cross-biome microbial diversity and it is well known that ecosystems across continents harbour distinct microbial communities (Fierer *et al.*, 2012). However, within the same biome and in fact, between parts of the same organism, different microbial communities exist (Turner *et al.*, 2013). The plant microbiome is composed of an array of prokaryotic and eukaryotic microorganisms, including bacteria, fungi, archaea, viruses and protozoans. The plant microbiome can be broken down to smaller levels as distinct microbial communities inhabit different parts of the phyllosphere (plant aerial surfaces), the rhizosphere (the soil around the roots), and the endosphere (internal plant tissue) (Turner *et al.*, 2013). Microbial activity exerts an influence on nearly all aspects of biogeochemical processes such as nutrient cycles, water cycles and more. Of particular relevance to plants, microbes collectively play a role in controlling plant nutrition, metabolism, physiology, pathogenesis and the immune response (Christian *et al.*, 2015). They can provide beneficial services to plants thanks to the production of compounds including phytohormones, exopolysaccharides, osmolytes, antioxidants, hydrogen cyanide, antibiotics and hydrolytic enzymes (Fatima *et al.*, 2019). They facilitate the uptake of minerals that are often present in forms inaccessible to plants (Bais *et al.*, 2006); they can contribute to drought tolerance (Kim *et al.*, 2012), heat tolerance (Castiglioni *et al.*, 2008), salt tolerance (Zhang *et al.*, 2008; Fatima *et al.*, 2019) and protection from pathogens (Berendsen *et al.*, 2012); they can enhance plant growth and photosynthesis

through the production of phytohormones (Ali *et al.*, 2009a; Ali *et al.*, 2009b; Ulrich *et al.*, 2019). Global fertiliser use is economically and environmentally costly and waste is high. For example, China, the world's largest consumer of fertiliser has an estimated overuse of more than 30%, leading to high greenhouse gas emissions, groundwater nitrate contamination, soil acidification and eutrophication (Chen *et al.*, 2019). Roots play an important role in the efficient use of nitrogen for yield formation, which is a key target for increasing the sustainability of agriculture. High nitrogen-use efficiency in wheat is a target for variety improvement and increasing the sustainability of agriculture. The interplay of microorganisms with plants and the environment has garnered attention for their potential impact on crop breeding for responses to resource inputs. For example, the challenge of increasing nutrient uptake efficiency or drought tolerance could be overcome by leveraging the interactions between host plant genetics and the properties of the microbiome.

# 4.2.1 An overview of the rhizosphere microbiome

Although archaea, viruses and protozoans are also major players in the soil microbiome, I focus here on bacteria and fungi. Microorganisms can establish beneficial (mutualistic), neutral (commensal) or detrimental (pathogenic) associations of varying intimacy with the plant (Turner *et al.*, 2013). More than 80% of higher plant species form mutualistic relationships with symbiotic mycorrhizas, benefiting from enhanced nutrient and water uptake as well as protection from pathogenic attack (Schüßler and Walker, 2011). However, plant roots are also exposed to a broad spectrum of free-living micro-organisms, each of which likely plays a more or less important role in the rhizosphere ecosystem.

The rhizosphere is the soil directly influenced by root and root function and the term was first coined by Lorenz Hiltner over a century ago (Hiltner, 1904; Hartmann *et al.*, 2008). Roots are veritable engineers of the rhizosphere, engendering a microecosystem distinct from bulk soil, through secretion of mucilage, sloughed off cells and exudates, particularly organic acids, sugars, amino acids, fatty acids, vitamins, growth factors, hormones and antimicrobial compounds (Bertin *et al.*, 2003). Root secretions provide a nutrient-rich habitat for microorganisms, and many studies have found an enrichment of microorganisms in the rhizosphere relative to the bulk soil (Donn *et al.*, 2015; Fan *et al.*, 2017). Indeed, as free-living soil microorganisms are

strongly carbon limited, they are highly responsive to increases in carbon delivered as plant exudates (Wardle, 1992; Semenov *et al.*, 1999). Carbon labelling studies demonstrate that $^{13}CO_2$ taken up by plants and fixed by photosynthesis becomes metabolised by the microbial community (Lu *et al.*, 2006; Haichar *et al.*, 2008). Compounds released by roots account for 5-70 % of total carbon fixed by the plant during photosynthesis (Whipps and Lynch,1983; Newman, 1985; Badri and Vivanco, 2009).

While the rhizosphere does not have a specifically defined boundary because factors like exudate concentration diminish over a spatial gradient, the region of highest influence identified by non-destructive visualisation techniques typically englobes the 0.4-5 mm layer of soil extending from the root surface (Kuzyakov and Razavi, 2019). The composition of the rhizosphere microbiome varies according to environmental factors such as climatic conditions, soil structure and soil type (Buyer *et al.*, 1999, Dalmastri *et al.*, 1999, Kowalchuk *et al.*, 2000). In particular, we know bacteria to be strongly influenced by pH (Rousk *et al.*, 2010; Fierer *et al.*, 2012). From this perspective alone, it is clear that plants must exert an influence on the bacterial composition of the rhizosphere as the flux of organic acids and H+ into and out of roots modulate soil pH. Fungal communities appear to be less strongly affected by pH, tolerating a wider pH range for optimal growth (Rousk *et al.*, 2010).

As per the Baas Becking hypothesis, which states that "organisms are everywhere and the environment selects", microorganisms have the opportunity to thrive if they contain the right genetic makeup to withstand environmental pressures. Plant roots have a direct influence on a microenvironment distinct from bulk soil, resulting in the shift of the bulk soil microbiome to an assembly of microorganisms suited to the rhizosphere environment (Fitzpatrick *et al.*, 2018; Chen *et al.*, 2019). There is evidence that the resulting rhizosphere modified by the root provides adaptive advantages to the plant. Numerous studies in different plant species demonstrate the effect of root exudates on the microbiome (Bakker *et al.*, 2012).

It is likely that there are variations in the relative importance of soil characteristics and the effect of the plant on the rhizosphere in shaping the microbial community. For example, a study on sand sedge (*Carex arenaria*) in multiple contrasting locations showed that the rhizosphere bacterial community was determined to a large extent by the bulk soil community composition (Ridder-Duine *et al.*, 2005). Furthermore, plants from different original locations developed

similar communities when grown in the same soil (Ridder-Duine *et al.*, 2005). This does not contradict studies demonstrating strong genotypic effects on the rhizosphere microbiome but demonstrates another layer of control, which can – in some instances – dominate plant genotypic effects. The effects of host plant genotype on the microbiome is discussed later.

Indeed, many studies demonstrate that different plant species (and even ecotypes or cultivars of the same species) grown under similar conditions are found to have different rhizosphere microbiomes (Marschner *et al.*, 2001, Smalla *et al.*, 2001, Kowalchuk *et al.*, 2002, Marschner *et al.*, 2002; Costa *et al.*, 2006; Garbeva *et al.*, 2008; Aira *et al.*, 2010; İnceoğlu *et al.*, 2010, 2011; Bouffaud *et al.*, 2012; Teixeira *et al.*, 2010; Dias *et al.*, 2012). While different plant species often harbour similar relative abundances of each microbial phylum, variation is seen at the microbial species level (Lundberg *et al.*, 2012; Inceoglu *et al.*, 2011).

# 4.2.2 Contribution of the rhizosphere microbiome to food security

In an agricultural setting, it is known that the wheat rhizosphere microbiome is influenced by host genotype (Mauchline *et al.*, 2015; Mahoney *et al.*, 2017), fertilisation (Kavamura, 2018), land management and seed load (Kavamura, 2019), irrigation (Mavrodi, 2018), seed germination and host age (Huang *et al.*, 2016). The relevance of microorganisms to nutrient uptake by the roots is put into perspective with the observation that all nutrients absorbed by plants pass through a region of intense microbial activity (Bonkowski, 2004). Plants have considerable dependence on microbial activity for access to nutrients in a form they can absorb.

The most widely known plant-microbe interactions in the soil occur with symbiotic mycorrhizal fungi and nitrogen-fixing rhizobia bacteria (symbiotic *Rhizobium* spp. and free-living *Azotobacter* spp.) (Young *et al.*, 2006; Bonfante, 2010). The symbiosis between these microorganisms and plants assists in the uptake of nutrients, most notably phosphorous by fungi and nitrogen by bacteria. Furthermore, arbuscular mycorrhizal symbioses are known to assist crops in coping with drought stress (Lehnert *et al.*, 2018). However, the advent of metagenomics has opened the door to exploring the enormous *omnium-gatherum* of species, many or all of which are important players in plant processes.

There are reports that intensive wheat breeding, particularly subsequent to the Green Revolution, has affected the wheat microbiome (Kavamura *et al.*, 2020). There are multiple strands of evidence for this, although each comprises relatively few varieties and replicates: the abundance of eukaryotes in *Pisum sativum* (pea) and *Avena sativa* (oat) rhizospheres is five-fold higher than the rhizosphere of modern hexaploid wheat (Turner *et al.*, 2013). A study examining three wheat lines found that ancient wheat landraces have more diverse rhizosphere microbiomes than modern cultivars (Germida and Siciliano, 2001). Further research is needed to determine whether their findings extend to a greater number of landraces and modern cultivars. Supporting this, a recent study reported that three tall wheat cultivars (developed pre-green revolution) have distinct rhizosphere bacterial communities from five modern semi-dwarf cultivars, and wheat breeding from tall to semi-dwarf plants resulted in plants less able to select a complex rhizosphere (Kavamura *et al.*, 2020). Collectively, these results indicate a reduction in microbial diversity as a result of the green revolution, but also highlight the need for more extensive research to validate the hypothesis.

Management practices affect soil microbes. For example, a field trial of wheat (cv. Cadenza) using four different nitrogen (N) regimes found that high levels of inorganic fertilisers negatively affected bacterial richness and diversity (Kavamura *et al.*, 2018). A study on legume-*Rhizobium* mutualism in a long-term (22-year) N fertilisation experiment demonstrated that wheat breeding in high-input conditions resulted in the evolution of rhizobia that are less mutualistic, providing fewer benefits to the host (Weese *et al.* 2015). Global calorie demands cannot currently be met without the addition of inorganic fertiliser. However, reducing excess fertiliser in line with optimal doses could promote mutualism with rhizobia.

Microorganisms are most often associated with pathogenesis and can be implicated in severe yield losses. Despite some fungi causing plant disease, others are known to antagonise plant pathogens (Gomes *et al.*, 2003). Furthermore, non-pathogenic microbes have been shown to increase the level of disease resistance in plants, giving rise to induced systemic resistance (Bittel and Robatzek, 2007). Through induced systemic resistance, higher levels of jasmonic acid and ethylene signalling prime plants for defence (Newman *et al.* 2013). There is extensive research on the role of plant growth-promoting rhizobacteria (PGPR), particularly strains of *Pseudomonas* and *Bacillus* species, in triggering systemic resistance in plants (Van der Ent *et al.* 2009). However, less is known about non-pathogenic fungal strains. Nonetheless, while bacteria are more

functionally prominent than fungi in the animal microbiome, the opposite appears to be true among plants (Christian *et al.*, 2015). Studies on Arabidopsis suggest that despite being scarcer than bacteria, fungi appear to exert a greater influence on plant health (Lundberg *et al.*, 2012; Bulgarelli *et al.*, 2012).

It has been postulated that changes in root system architecture (RSA) as a side-effect of breeding for above-ground traits such as high yield and lodging resistance may have affected the rhizosphere microbiome (Micallef *et al.*, 2009). A study into the microbiome of different root categories in peach trees discovered that fine or small roots recruited more rich and diverse bacterial communities than large roots (Pervaiz *et al.*, 2020). As different root classes have different functions and physiological characteristics, it is intuitive to suppose that they foster different local soil environments. Furthermore, larger populations of bacteria and fungi were isolated from the rhizosphere of seminal roots than nodal roots of the same wheat plant, although it is likely that the nodal roots were younger (Sivasithamparam *et al.*, 1979). Overall, there is very little research into the relationship between RSA and the microbiome, notably in relation to root angle and depth. However, it is possible that hormonal signals that modulate root development also affect microbial growth. Here, I address the possible interaction between wheat root angle and the rhizosphere microbiome.

# 4.2.3 The study of the microbiome: species identification

Until recent years, studies have been hampered by the fact that most soil microorganisms cannot be cultured (Bakker *et al.*, 2013) and technologies had not been developed for *in situ* studies. Furthermore, classic culturing techniques miss a vast proportion of microbial diversity in an environment. The rise of genomics brought with it techniques which accelerated microbiology, making it increasingly feasible to build an *in situ* picture of the microbiome from a taxonomic and a functional point of view (Turnbaugh *et al.*, 2007; Gilbert *et al.*, 2010). High throughput sequencing technologies allow the identification of thousands to millions of sequences in a single sample (Margulies *et al.*, 2005; Bentley *et al.*, 2008). The study of genetic material on a large scale in environmental samples is known as metagenomics.

For studying prokaryotes, PCR amplification of 16S ribosomal RNA (rRNA) is commonly used. Universally present in prokaryotes, the 16S rRNA gene represents a good marker for taxonomic research because it has both highly conserved regions that can act as primer binding sites in a large number of taxonomic groups, and hypervariable regions which can provide species-specific signature sequences (Britschgi, 1990; Case *et al.*, 2007).

The study of fungal communities has lagged behind the study of bacterial communities because fungal evolution and morphological diversity are not intimately associated with a single genetic marker (Usyk *et al.*, 2017). However, inspired by molecular bacterial taxonomy, the development of primers for fungal molecular taxonomy focused on the fungal ribosomal operon, yielding primers specific to the large subunit, small subunit (18S) and internal transcriber spacer (ITS) (Cheng *et al.*, 2016). The more variable ITS1 region is preferred because the 18S rRNA does not provide sufficient taxonomic discrimination. The now classic paper by White *et al.* (1990) included universal primers still widely used for amplifying three main components of the fungal ribosomal operon: (i) the large subunit (LSU) (ii) the small subunit (SSU, or 18S), separated by (iii) the ITS, comprising two sections (ITS1, ITS2).

Thanks to databases of the taxonomy of known microorganisms, the potential of metagenomics is vast. One of its limitations, however, is that PCR amplification is biased by primer design. For example, some primers which yield long amplicons may result in few sequences being amplified, while others may skew the results towards a particular phylum or not amplify a certain phylum (Peiffer *et al.*, 2013). Thus, the choice of primers depends on the application and may involve a certain trade-off.

Metagenomics can reveal the functional potential of the microbiome – i.e. the presence of genes involved in particular processes (Turner *et al.*, 2013). On the other hand, metatranscriptomics and metaproteomics reveal the expression of genes and proteins in the microbial community at a particular moment in time. Data from metatranscriptome/metaproteome analyses can thus describe which of the genes annotated in the metagenomic analysis are transcribed/translated and to what extent (Bashiardes *et al.*, 2016).

# 4.2.4 Understanding microbial diversity

Biological diversity is widely defined as the variability among living organisms and their ecological complexes, and comprises species richness and relative species abundance in space and time (Kim *et al.*, 2017; Schloss *et al.*, 2006). The two main factors which are taken into account to measure biological diversity are richness and evenness. Richness counts the number of species: an environment containing a greater number of species is considered richer than an environment with fewer species (Kim *et al.*, 2017). This does not count the number of individuals of each species. Evenness compares the uniformity of the population sizes, taking into account relative abundances of different species. An environment with a more even distribution of species is considered more diverse than an environment with the same number of species, where one species dominates and other species are less abundant (Schloss *et al.*, 2006; Schloss *et al.*, 2009). The four widely used measures of diversity in a sample (also known as alpha diversity) are the Chao1, ACE, Shannon-Weaver and Simpson indexes.

Chao1 and ACE are measures of species richness. Chao1 is a non-parametric method which estimates species richness by placing weight on the rarer species and using them to estimate the missing species (Chao *et al.*, 1984; 2002; 2006). ACE is a non-parametric method of estimating the number of species using sample coverage, which is the sum of the probabilities of the observed species (Chao and Lee, 1982; Chao *et al.*, 1993).

Shannon-Weaver and Simpson diversity indices measure community diversity by taking into account both richness and evenness. The Shannon-Weaver index places greater weight on species richness, whereas the Simpson index places greater weight on species evenness (Schloss *et al.*, 2006, Schloss *et al.*, 2009). Furthermore, the Shannon-Weaver index takes into account the average degree of uncertainty in predicting a species chosen at random. The uncertainty increases with an increasing number of species and uniformity (Magurran *et al.*, 2004; Lemos *et al.*, 2011). On the other hand, the Simpson index accounts for species dominance by measuring the probability that two randomly chosen individuals belong to the same species (Simpson, 1949).

Due to the many facets of biological diversity, it is most informative to report all four indices and use them to build a picture of the microbial landscape within a specific environment.

Beta diversity refers to intra-group diversity and involves the comparison of different groups of samples based on the composition of their microbial communities (Baselga, 2007). A square matrix of distance can be calculated to reflect the dissimilarity between samples based on weighted and unweighted UniFrac. UniFrac measures the phylogenetic distance between sets of taxa as the fraction of the branch length of a phylogenetic tree that leads to descendants from either one environment or the other, but not both (Lozupone and Knight, 2005). Weighted UniFrac takes into account species abundance, and unweighted UniFrac determines variation in the presence or absence of taxa.

# 4.2.5 Considerations for analysis

Given a list of counts, statistical comparison of metagenomes is used in order to detect differences (Tringe *et al.*, 2005). Unfortunately the statistical analysis is complicated by high levels of both biological and technical variability (Wooley and Ye, 2009). The biological variability stems from the high diversity and complexity of microbial communities (Delmont *et al.*, 2011). The bacterial species composition is for example known to vary considerably between samples (David *et al.*, 2014). In addition, many bacterial species have plastic genomes and exhibit large variability in the gene content, even between individual members of a population (Kashtan *et al.*, 2014). There is also a considerable variation in the presence of other organisms including viruses (Reyes *et al.*, 2010). Technical sources of errors include the handling of samples and extraction of DNA which can introduce biases towards certain species (Morgan *et al.*, 2010). The sequencing is also known to introduce errors as well as be biased with respect to the GC-content and repetitive contents (Benjamini and Speed, 2012). Furthermore the number of genes being investigated is typically very large (tens of thousands) while the number of replicates are low requiring methods that have the power to detect differences yet the specificity to avoid false positives. All these factors contribute to making statistical inference of metagenomic data complex. However, thanks to an increasing body of literature as well as statistical developments, the use of multiple tests and the selection of the appropriate test for the data in question, it is possible to make interesting discoveries.

# 4.2.6 Engineering the rhizosphere microbiome

Manipulation of the plant microbiome has the potential to reduce pathogenic burden, reduce chemical inputs and greenhouse gas emissions, and increase yield (Turner *et al.*, 2013). Biological control as opposed to chemical application could involve exogenous application of microbial organisms to the plant rhizosphere. Comparisons of oat, pea and *Triticum aestivum* (bread wheat) show that oat and pea have increased microbial abundance in the rhizosphere than wheat (Turner *et al.*, 2013). Furthermore, in crop rotation systems, wheat yield often increases after seasons of oat or pea, the former being attributed to reduced disease incidence (oat reduces take-all pressure because it is resistant to the pathogen) and the latter to increased soil nitrogen (Seymour *et al.*, 2012). The mechanisms underlying beneficial plant-microbe may have applications in wheat.

With appropriate understanding of the rhizosphere microbiome, it may be possible to deliver tailored microbial cultures to crops as a so-called "biofertiliser". Inoculation in isolation with a specific microbe possessing a desired function may not have a beneficial effect whereas combinations of microbes may be more effective. For example, the black queen hypothesis refers to the advantage of reductive evolution in a community. Organisms may undergo genomic streamlining and become beneficiaries of a minority of "helpers" which retain an important function. The beneficiaries are relieved of a metabolic burden and have a growth advantage at no cost to the helper. A similar phenomenon is the synergy between microorganisms whereby the product or by-product of the metabolism of a compound by one species may be a food source for another (Leng *et al.*, 2019). For example, the decomposition of pectin exuded by roots releases methanol, which can be used as a carbon source by other microbes (Galbally *et al.*, 2002; Knief *et al.*, 2012). On a larger scale, certain species, termed keystone species exert a large influence on shaping the microbiome and may be instrumental to cultivating a beneficial microbiome (Shi *et al.*, 2016; Brinker *et al.*, 2019). In this vein, inoculating the wheat rhizosphere with the arbuscular mycorrhizal *Rhizophagus irregularis* increased the phosphorous (P) content of plant biomass compared with non-inoculated plants (Elliott *et al.*, 2020). However, the increased P was not due to an increase in fungal-derived P but due to an increase in direct assimilation via the root. It is possible that increasing *R. irregularis* abundance increased root uptake efficiency or affected the rhizosphere microbiome, which in turn increased available soil P. For example, through the release of organic acids, some bacteria chelate cations bound to phosphate anions, thus releasing the compound into the soil and making it available to plants (Vassilev *et al.*, 2006). Furthermore,

the effect of inoculation is genotype-specific: in contrast to the other tested cultivars, the P content of Avalon did not respond favourably to inoculation (Elliott *et al.*, 2020). To successfully engineer the microbiome, it may be most beneficial to tailor specific innocula to specific cultivars and soils so that there is a measurable benefit to cultivar performance.

# 4.2.7 Aims

This study tested the following hypotheses:

- The genotype of individuals in the AxC tails determines bacterial and fungal alpha diversity and beta diversity in the rhizosheath
- Genotypes contrasting for root system architecture harbour different microbial communities in the rhizosheath
- The microbial community composition of the rhizosheath varies between genotypes that secrete different levels of high molecular weight polysaccharides
- Differences in microbial abundance between AxC lines are less prevalent at the phylum level but more apparent at lower taxonomic levels

# 4.3 Materials and Methods

## 4.3.1 Germplasm

The Avalon x Cadenza doubled haploid (AxC DH) population was used. It is derived from F1 progeny of a cross between cvs. Avalon and Cadenza developed by Clare Ellerbrook, Liz Sayers and the late Tony Worland (John Innes Centre, JIC), as part of a Defra funded project led by ADAS. Twenty-five lines from the AxC DH population that displayed root phenotypes (angle and growth rate) at the tail ends of the population distribution in a series of clear pot screens (Chapter 2, section 2.2.1) were selected on the basis of having the greatest number of replicates within the top 1.1 % or bottom 1.1 % of BLUPs (Table 4.1), calculated from ˜8400 individuals depending on the trait (angle, primary root length and seminal root length). These lines are hereon referred to as the "AxC tails". The use of tails representing the phenotypic extremes of a population is well suited to assessing complex, polygenic traits (Rebetzke *et al.*, 2017).

## 4.3.2 Experimental set-up

Metagenomics analysis was undertaken on rhizosheath soil of twenty-five AxC lines (set A), on soil supplemented with commercial polysaccharide (set B, Table 4.2), on soil supplemented with an isolate of root secretions from cvs. Avalon and Cadenza (set C) and on untreated soil (control). Commercial polysaccharide solutions and root secretion isolates were applied to non-sterile soil and sterile soil that had been autoclaved at 120 ⁰C for 20 minutes.

For set A, seedlings of cvs. Avalon, Cadenza and twenty-five AxC lines (Table 4.1) were grown in Falcon tubes (50 mL) in an equal mix of Norfolk native field loam and sports sand (Renovation Mix, Bailey's, Norfolk; pH 6.5-7.5, screened to 4 mm particle size) (Figure 4.1). One seed was sown per tube in three reps per line randomised using the "Blockdesign" package in R (Edmondson, 2016). Glasshouse conditions were maintained at a daytime temperature of 18-24 ⁰C and night-time temperature of 15-18 ⁰C, 10 000 lux supplementary sodium lights ensuring a 16 hour day length.

For set B, commercial polysaccharide (1 mL, 0.5 µg/mL) was applied to soil in Eppendorf tubes (2 mL). The concentration of each pure carbohydrate in water was adjusted so that the final amount of carbohydrate added per gram of soil was equivalent to that found in native rhizosphere samples using the enzyme-linked immunosorbent assay (ELISA) (Chapter 3). The samples were incubated at the same time and in the same conditions as set A.

For set C, root secretions were isolated as described for the ELISAs in *Materials and Methods, Chapter 3*. Aliquots (1 mL) of secretions from cvs. Avalon and Cadenza were added to soil in Eppendorf tubes. In this case the concentrations of compounds in solution derived from the root exudate wash and added to the soil were determined by the secretion capacity of the genotype. The samples were incubated at the same time and in the same conditions as set A.
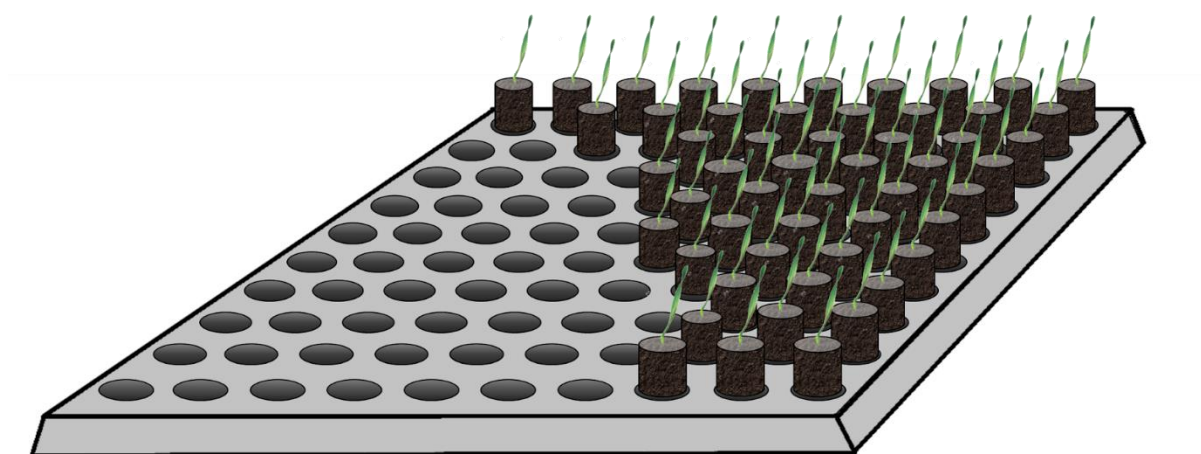


**Figure 4.1 Growth set-up of selected lines for analysis of the rhizosheath.** Seedlings from Avalon, Cadenza plus twenty-five lines of the Avalon x Cadenza doubled haploid population were grown in Falcon tubes (50 mL) secured in a dark grey plastic box perforated with holes (10 rows x 10 columns). One seedling was grown per tube. Plants were grown for seven days in a glasshouse (18-24 ⁰C, day; 15-18 ⁰C, night).

**Table 4.1 Seedling phenotypes of the subset of the AxC DH population selected for metagenomics analysis.** Phenotypes were determined as described in Chapters 2 and 3. A phenotype was described as "high" or "low" if it fell into the top or bottom tertile for the trait. Antibodies indicate the concentration of epitopes: LM25, Xyloglucan; LM2, arabinogalactan protein; LM27, heteroxylan; LM1, extensin; LM11, xylan; LM19, homogalacturonan. The accession code from the Germplasm Resource Unit (GRU) is given for each line (www.seedstor.ac.uk).

| GRU Accession | Accession | Yield | Root angle | Rhizosheath size | LM25 | LM2 | LM27 | LM1 | LM11 | LM19 | Shoot length | Total root length |
|---|---|---|---|---|---|---|---|---|---|---|---|---|
| AxC0001 | AxC1 | | | high | low | low | low | low | low | low | high | high |
| AxC0005 | AxC5 | low | wide | low | low | low | low | low | low | low | low | low |
| AxC0006 | AxC6 | high | narrow | low | low | low | low | low | high | low | low | low |
| AxC0007 | AxC7 | low | | high | low | high | high | high | high | low | | low |
| AxC0009 | AxC9 | | | | | | | | | | | |
| AxC00013 | AxC13 | | | | | | | | | | | low |
| AxC00014 | AxC14 | | | | | | | | | | | low |
| AxC00028 | AxC28 | | | low | low | low | low | low | low | low | low | |
| AxC00043 | AxC43 | high | wide | high | low | low | low | low | high | low | | |
| AxC00047 | AxC47 | | | | | | | | | | | |
| AxC00056 | AxC56 | high | wide | low | low | high | low | low | low | low | high | |
| AxC00080 | AxC80 | | narrow | high | low | low | low | low | low | high | | |
| AxC00096 | AxC96 | | | | | | | | | | | |
| AxC000102 | AxC102 | high | | | | | | | | | | |
| AxC000108 | AxC108 | low | wide | | high | high | high | low | | low | | low |
| AxC000131 | AxC131 | low | narrow | low | high | low | high | high | high | high | | low |
| AxC000140 | AxC140 | | | | | | | | | | | low |
| AxC000146 | AxC146 | | narrow | low | low | high | high | high | low | high | low | low |
| AxC000156 | AxC156 | low | wide | high | low | high | high | high | high | high | low | |
| AxC000179 | AxC179 | low | wide | high | high | high | high | low | high | low | high | |
| AxC000181 | AxC181 | | narrow | high | | high | high | low | high | low | high | |
| AxC000182 | AxC182 | high | narrow | | high | low | low | low | low | low | high | high |
| AxC000198 | AxC198 | high | narrow | low | high | low | low | high | | | low | high |
| AxC000205 | AxC205 | | | | | | | | | | | high |
| AxC000206 | AxC206 | | | | | | | | | | | high |

| AxC000207 | AxC207 |  | narrow | high | high | high | high | low | low | low | high | high |
|---|---|---|---|---|---|---|---|---|---|---|---|---|
| AxC000208 | AxC208 | high | wide | high | high | high | high | low | low | low |  | high |

**Table 4.2 Commercially produced polysaccharides applied to soil.** The antigen refers to the epitope contained in the commercial polysaccharide which is specific to the corresponding antibody.

| Commercial polysaccharide | Supplier | Antibody | Antigen | Antibody reference |
|---|---|---|---|---|
| Xylan (Beechwood) | Megazyme | LM11 | Xylan | McCartney *et al.*, 2005 |
| Xyloglucan (from Tamarind seed) | Megazyme | LM25 | Xyloglucan | Pederson *et al.*, 2012 |
| Gum Arabic | Sigma Aldrich | LM2 | Arabinogalactan protein | Smallwood *et al.*, 1996; Yates *et al.*, 1996 |
| Citrus Pectin (galacturonic acid) | Sigma Aldrich | JIM7 | Homogalacturonan (partially methyl-esterified) | Knox *et al.*, 1990; Willats *et al.*, 2000; Clausen *et al.*, 2003 |
| Citrus Pectin (galacturonic acid) | Sigma Aldrich | LM19 | Homogalacturonan (de-esterified) | Verhertbruggen *et al.*, 2009 |
| Gum Arabic | Sigma Aldrich | LM1 | Extensin | Smallwood *et al.*, 1995 |
| Xylan (Beechwood) | Megazyme | LM27 | Heteroxylan | Cornuault *et al.*, 2015 |

# 4.3.4 DNA extraction

Collection microtubes (2 mL, Quiagen) were prepared with 0.15-0.25 g of autoclaved (120 ºC, 20 minutes) Garnet particles (Stratech, UK). Plants were pulled out of the soil and the soil adhering to the roots (~250 mg) was shaken and gently scraped into collection microtubes using tweezers sterilised in ethanol. Tubes were stored at -80 ºC for up to one month until further processing. Solution C1 (60 µL) from the DNeasy PowerSoil Kit (Qiagen) was added to each thawed tube. Cells were disrupted by shaking the tubes in a 1600 MiniG® (1500 rpm, 2 x 1 minute). Tubes were centrifuged (10,000 g, 30 seconds) and the supernatant was transferred to clean collection tubes (DNeasy PowerSoil Kit). The rest of the extraction proceeded using the DNeasy PowerSoil Kit (Quiagen). The final step was modified to elute the DNA in 60 µL of

Solution C6, resulting in a minimum concentration of 17 ng/ μL. DNA was quantified using a Qubit dsDNA HS (High Sensitivity) Assay Kit and quality-checked by agarose gel electrophoresis.

# 4.3.5 Library preparation and sequencing

16S rRNA and ITS rRNA gene PCR amplification and sequencing were performed by Novogene (UK) Company Limited using primers outlined in Table 4.3. For the bacterial 16S rRNA gene, the V5-V7 hypervariable region was amplified using the specific primers 799F and 1193R, chosen because they have low amplification of non-target DNA and retrieve a high number of operational taxonomic units (OTU) (Beckers *et al.*, 2016). For the sequencing of fungi, the ITS1 region of the eukaryotic ribosomal cluster was chosen for amplification as it has features allowing for wide taxonomic coverage and has high species- and genus-level classification accuracy (Bokulich and Mills, 2013; Usyk *et al.*, 2017).

PCR reactions were undertaken with Phusion® High-Fidelity PCR Master Mix (New England Biolabs). PCR products were quantified and qualified by electrophoresis on a 2% agarose gel, using an equal volume of 1 x loading buffer containing SYBR green. PCR products were purified with the Qiagen Gel Extraction Kit (Qiagen, Germany). Libraries were generated with NEBNext® UltraTM DNA Library Prep Kit for Illumina and quantified via Qubit and qPCR. The samples were sequenced using paired-end Illumina sequencing (2 x 250 bp) on the NovaSeq 6000 platform (Illumina, USA).

**Table 4.3 16S and ITS primers used for amplicon sequencing.**

| Region | Length | Primer | Sequence |
|--------|--------|--------|----------|
| 16S | 395bp | 799F | AACMGGATTAGATACCCKG |
| | | 1193R | ACGTCATCCCCACCTTCC |
| ITS ITS1-1F | 321bp | ITS1-1F-F | CTTGGTCATTTAGAGGAAGTAA |
| | | ITS1-1F-R | GCTGCGTTCTTCATCGATGC |

# 4.3.5 Sequencing data processing

OTU processing was carried out at NIAB EMR with the UPARSE 10.0 OTU clustering pipeline (Edgar, 2013), as outlined previously (Deakin, 2018). FASTQ reads were demultiplexed into bacterial (16S) and fungal (ITS) datasets based on their primer sequences. Sequences with incorrect barcodes or primers, or with adaptor contamination, or with less than 250 bases were discarded. Forward and reverse sequences were merged with a maximum difference in overlap of 5% (Edgar, 2013). Merged sequences less than 400 bp for bacteria and 250 bp for fungi were discarded. Quality filtering removed sequences with > 0.5 expected error per sequence (Edgar and Flyvbjerg, 2015). Sequences were demerged, leaving only one representative of each sequence.

These unique sequence reads were clustered into OTUs at the level of 97% similarity and a representative sequence for each OTU was generated. Chimeras were removed during the clustering process. The UTAX algorithm (http://drive5.com/usearch/manual/tax_conf.html) then assigned each OTU representative sequence to taxonomic ranks by alignment with the gene sequences in the reference databases 'Unite V7' (fungal ITS) (Koljalg *et al.* 2013) and 'RDP training set 15' (16S) (Cole *et al.* 2014). To generate an OTU frequency table, all unfiltered sequences were aligned with the OTU representative sequences at the level of 97% similarity.

# 4.3.6 Data analysis

All statistical analyses were undertaken in R 3.6.1 (R Core Development Team, 2008). To test for differences in microbial diversity between the rhizosphere of plants with contrasting phenotypes, lines of the AxC population were grouped if they fell into the top or bottom tertile of a particular phenotypic measurement (Table 4.1). In most cases, this resulted in the same number of lines in each group. For homogalacturonan concentration, there was a greater number of lines with a low concentration. For the purpose of metagenomics group comparison, surplus lines were not included to ensure equal numbers in both groups. Phenotypes were measured as described in Chapters 2 and 3 and included seedling root angle, grain yield of field-grown plants, rhizosheath size per cm root length, and the concentration of the root exudates xyloglucan

(LM25), xylan (LM11), heteroxylan (LM27), homogalacturonan (LM19), arabinogalactan protein (AGP, LM2) and extensin (LM1).

# 4.3.6.1 Alpha diversity

Alpha diversity (diversity within a sample) was calculated using R bioconductor packages *Phyloseq* (McMurdie and Holmes, 2013) and *vegan* (Dixon, 2003). The four indices of alpha diversity considered were Chao1, ACE, Shannon-Weaver and Simpson. The difference in alpha diversity between samples was determined using a Pairwise Wilcoxon test.

# 4.3.6.2 Beta diversity

Weighted and unweighted UniFrac distances between samples were calculated and analysed with permutational multivariate analysis of variance (PERMANOVA), executed by the *adonis* function in the *vegan* package. This tested which plant phenotypes (exudate concentration, root system architecture, plant genotype, grain yield) may be correlated with differences in beta diversity (difference in microbial community composition between samples) (Anderson, 2011).

# 4.3.6.3 Differential abundance

Differential abundance of taxa between factors was tested using the R bioconductor package, *Deseq*, on OTU counts normalised for library size using the median of ratios method (Anders and Huber, 2010, Love *et al.*, 2014). A Wald p-value was generated where the estimated standard error of a log-2 fold change was used to test if it was equal to zero.

# 4.3.6.4 Data visualisation

Principal component analysis (PCA) was applied to library size normalized reads using the DESeq2 variance stabilisation transformation (VST).

The *phyloseq* package was used to construct heatmaps to display the abundance of OTUs at varying taxonomic levels in different samples or groups of samples (McMurdie and Holmes, 2013).

The *metacoder* package was used to visualise differential abundance between factors (different levels of exudate concentration, root system architecture, plant genotype) through the construction of heat trees (Foster *et al.*, 2017). Significant differences between the median proportion of reads for different samples were identified using a Wilcox rank-sum test followed by a Benjamini-Hochberg (FDR) correction for multiple testing (Foster *et al.*, 2017). The intensity of colour used to visualise significant differences in taxa between groups varied relative to the log-2 ratio of difference in median proportions (Foster *et al.*, 2017).

# 4.3.6.5 Lifestyle

The taxonomy assigned to OTUs was used to infer the organism's lifestyle using FUNGuild (Nguyen *et al.*, 2016). The results presented include only the lifestyle assignments that were considered "probable" or "highly probable" by FUNGuild.

# 4.4 RESULTS

## 4.4.1 General sequencing results

Sequencing data were obtained for 81 16S samples and 66 ITS samples. There were high numbers of raw sequence reads ranging from 130,000 to 150,000 for 16S rhizosphere reads and 105,000 to 150,000 for 66 ITS rhizosphere reads. The lack of asymptote indicated on the 16S rarefaction curve indicated that the soil was not sampled exhaustively and rarer species may not be represented (Figure 4.2). Most rarefaction curves in the ITS samples for fungi were nearer to reaching a plateau than the bacteria, indicating a greater depth of species representation (Figure 4.3). There was greater variation in species abundance between ITS samples than 16S samples (standard deviation of OTUs of 23,990 and 16,670 respectively).



**Figure 4.2 Rarefaction curve showing the bacterial diversity in 81 soil samples.** The accumulated proportion of sequence reads is plotted against the number of OTUs.
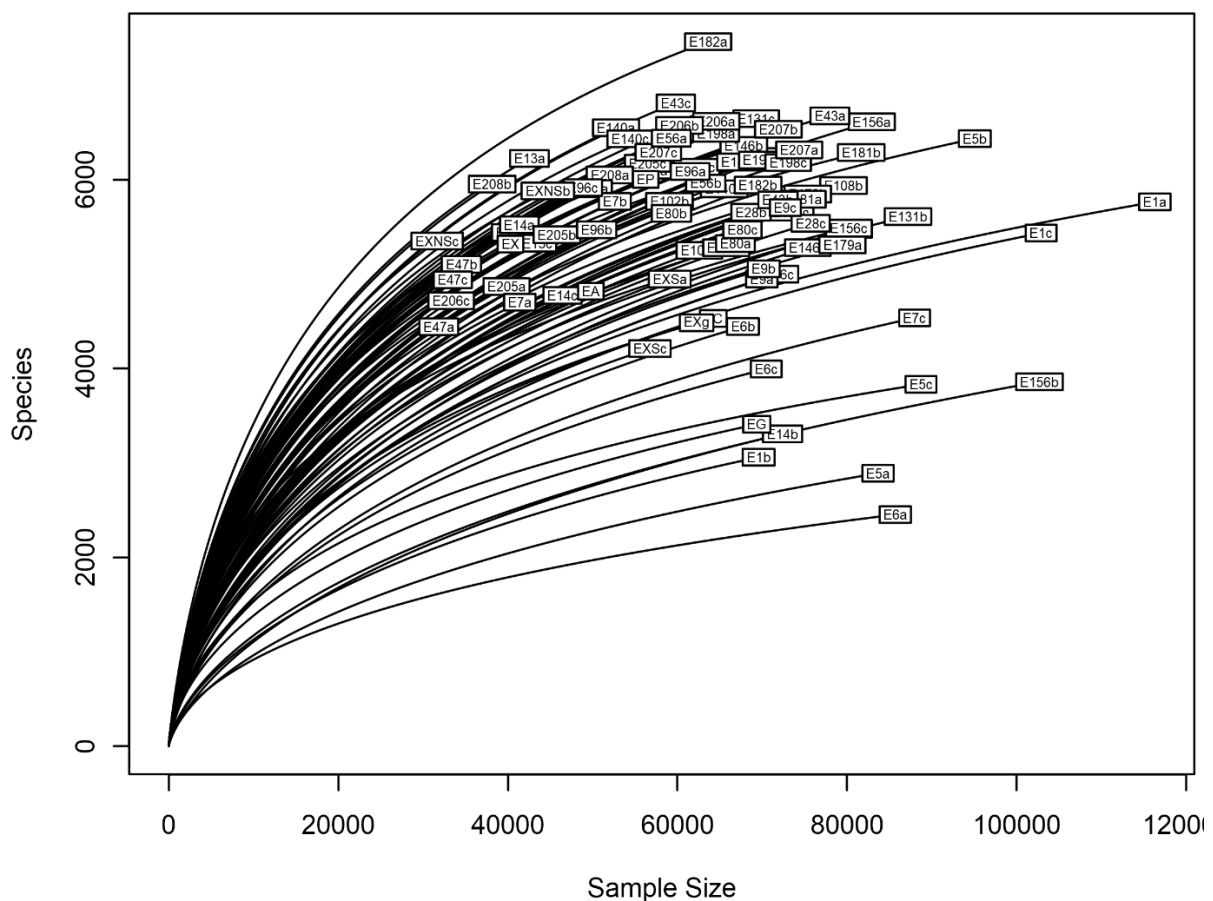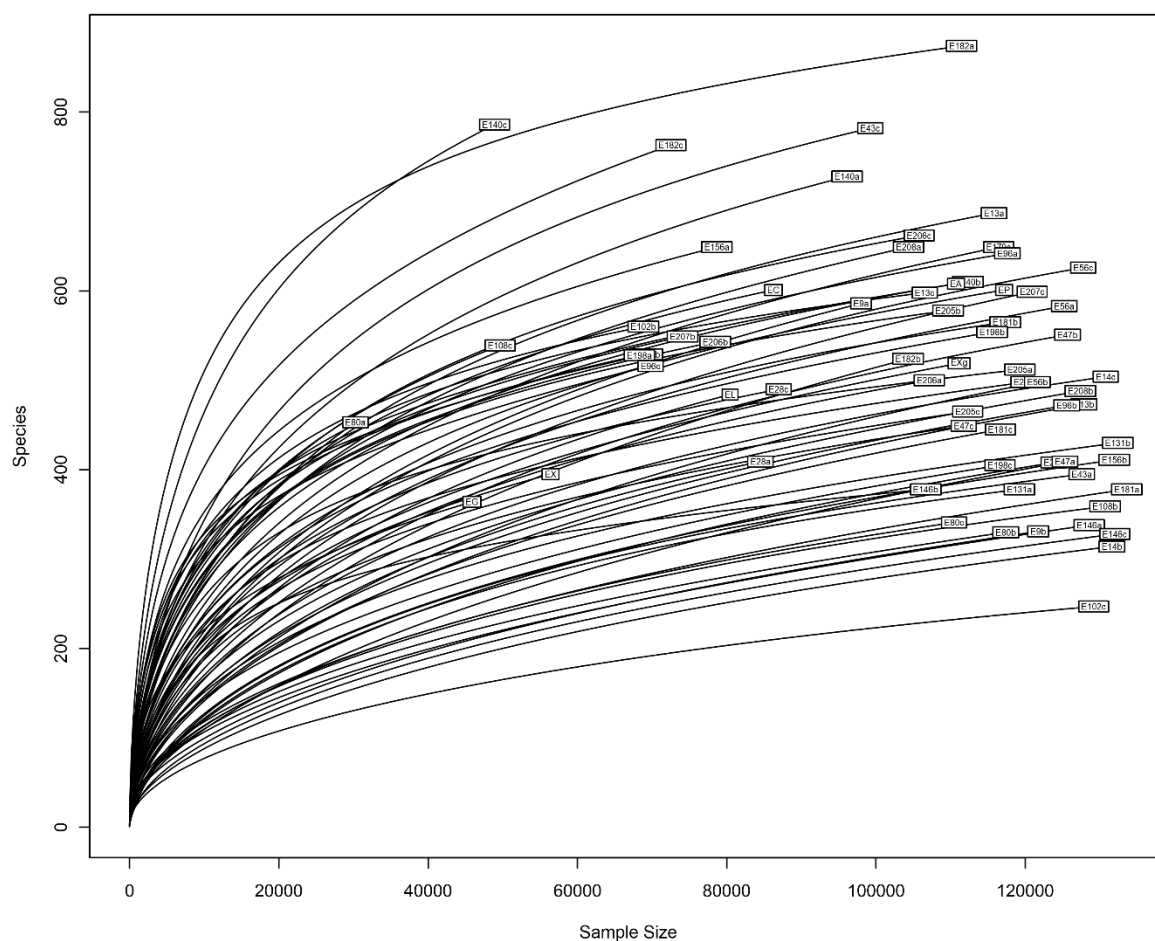
**Figure 4.3 Rarefaction curve showing the fungal diversity in 66 soil samples.**

# 4.4.2 Overview of species and abundance

## 4.4.2.1 Fungi

Out of the seven phyla identified in the samples, the Ascomycota accounted for 85% of reads (Figure 4.4, Table 4.4). Glomeromycota and Rozellomycota were the least abundant, accounting for 0.02%. There were 302987 unassigned reads, accounting for 2.9% (i.e. had less than 97% sequence similarity with sequences on the reference database, or had at least 97% similarity with more than one taxonomic unit, or had at least 97% similarity with an unidentified fungal strain

in the database). Each phylum tended to be dominated by one or two classes, which contributed 56-96% and 25-30% respectively to total taxa abundance (Table 4.4). The Ascomycota classes, Sordariomycetes and Dothideomycetes were the most abundant classes in the samples, representing 79% of reads (Figure 4.5).

**Table 4.4 Reads assigned to each class of fungi in all tested rhizosheath samples of lines from the Avalon x Cadenza population.** Reads were normalised for the calculation of percentage abundance.

| Phylum | Class | Percentage Abundance across all taxa | Percentage Abundance within phylum |
|---|---|---|---|
| Ascomycota | Sordariomycetes | 57 | 67 |
| | Dothideomycetes | 23 | 27 |
| | Eurotiomycetes | 3.4 | 3.9 |
| | Pezizomycetes | 1.1 | 1.2 |
| | Agaricomycetes | 0.85 | 1.0 |
| | unknown | 0.20 | 0.23 |
| | Saccharomycetes | 0.12 | 0.15 |
| | Leotiomycetes | 0.062 | 0.074 |
| | Glomeromycetes | 0.055 | 0.065 |
| | Mortierellomycotina_cls_Incertae_sedis | 0.048 | 0.056 |
| | Pezizomycotina_cls_Incertae_sedis | 0.0055 | 0.0065 |
| | Archaeorhizomycetes | 0.0052 | 0.0061 |
| | Orbiliomycetes | 0.0027 | 0.0032 |
| | Lecanoromycetes | 0.00051 | 0.00060 |
| | Schizosaccharomycetes | 0.00047 | 0.00050 |
| | Pneumocystidomycetes | 0.00023 | 0.00030 |
| | **Total** | **85** | |
| Basidiomycota | Tremellomycetes | 3.4 | 71 |
| | Agaricomycetes | 1.2 | 26 |
| | Microbotryomycetes | 0.057 | 1.2 |

| | | | |
|---|---|---|---|
| | Glomeromycetes | 0.035 | 0.74 |
| | Wallemiomycetes | 0.027 | 0.57 |
| | Ustilaginomycotina_cls_Incertae_sedis | 0.0067 | 0.14 |
| | Ustilaginomycetes | 0.0055 | 0.12 |
| | Cystobasidiomycetes | 0.0014 | 0.030 |
| | Pucciniomycetes | 0.0010 | 0.022 |
| | Pucciniomycotina_cls_Incertae_sedis | 0.00096 | 0.020 |
| | Atractiellomycetes | 0.00094 | 0.020 |
| | unknown | 0.00056 | 0.012 |
| | Exobasidiomycetes | 0.00041 | 0.0087 |
| | Mucoromycotina_cls_Incertae_sedis | 0.00029 | 0.0060 |
| | Sordariomycetes | 0.000090 | 0.0020 |
| | Entorrhizomycetes | 0.000050 | 0.0011 |
| | **Total** | **4.8** | |
| **Cercozoa** | unknown | 0.13 | 67 |
| | Agaricomycetes | 0.050 | 25 |
| | Eurotiomycetes | 0.0082 | 4.2 |
| | Glomeromycetes | 0.0057 | 2.9 |
| **Chytridiomycota** | Chytridiomycetes | 0.57 | 97 |
| | Agaricomycetes | 0.0044 | 2.3 |
| | Glomeromycetes | 0.013 | 2.1 |
| | unknown | 0.0074 | 1.3 |
| | Saccharomycetes | 0.00037 | 0.063 |
| | Monoblepharidomycetes | 0.00012 | 0.020 |
| | **Total** | **0.2** | |
| **Glomeromycota** | Glomeromycetes | 0.023 | 100 |
| | **Total** | **0.02** | |
| **Rozellomycota** | unknown | 0.0086 | 56 |
| | Agaricomycetes | 0.0046 | 30 |
| | Glomeromycetes | 0.00079 | 5.1 |
| | Tremellomycetes | 0.00062 | 4.1 |

| | Sordariomycetes | 0.00044 | 2.9 |
|---|---|---|---|
| | Pucciniomycetes | 0.00015 | 0.97 |
| | Leotiomycetes | 0.000070 | 0.47 |
| **unknown** | unknown | 2.9 | 30 |
| | **Total** | **0.02** | |
| **Zygomycota** | Mortierellomycotina_cls_Incertae_sedis | 6.5 | 69 |
| | Sordariomycetes | 0.0028 | 0.030 |
| | Zoopagomycotina_cls_Incertae_sedis | 0.0010 | 0.011 |
| | Mucoromycotina_cls_Incertae_sedis | 0.00051 | 0.0054 |
| | Glomeromycetes | 0.00012 | 0.0013 |
| | Kickxellomycotina_cls_Incertae_sedis | 0.000080 | 0.00080 |
| | **Total** | **6.5** | |
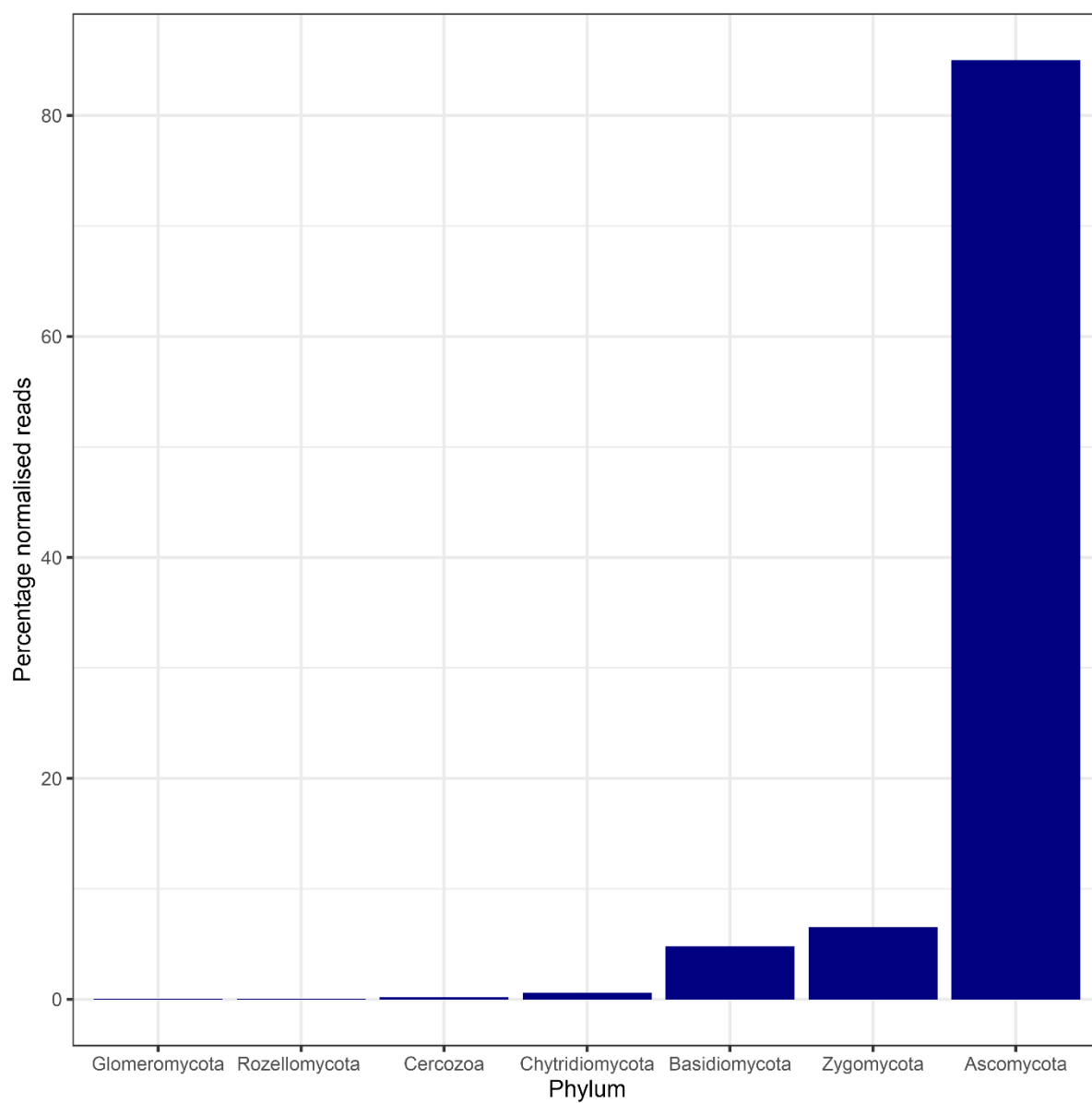
**Figure 4.4 Abundance of fungal phyla in all rhizosheath samples.** The number of reads per sample were normalised using median sequencing depth.

**Figure 4.5 Abundance of fungal classes across all samples.** The number of reads per sample were normalised using median sequencing depth.

## 4.4.2.2 Bacteria

Out of a total of 16 identified phyla (5,770,000 observations), the four phyla Proteobacteria, Actinobacteria, Bacteroidetes and Firmicutes accounted for 96.6% of the total bacterial microbiome (Table 4.5, Figure 4.6). The Proteobacteria were the most abundant, comprising 53%, of which the classes Gammaproteobacteria, Alphaproteobacteria and Betaproteobacteria were most abundant (Figure 4.7). The four least represented phyla, Crenarchaeota, Parcubacteria, Tenericutes and BRC1 collectively accounted for 0.005% of total bacterial phyla identified.

**Table 4.5 Reads assigned to each class of bacteria in all tested rhizosheath samples of lines from the Avalon x Cadenza population.** Reads were normalised for the calculation of percentage abundance.

| Phylum | Class | Percentage Abundance across all taxa | Percentage Abundance within phylum |
|---|---|---|---|
| Acidobacteria | Acidobacteria_Gp6 | 2.63 | 22 |
| | Acidobacteria_Gp3 | 15 | 19 |
| | Acidobacteria_Gp7 | 4.6 | 17 |
| | Acidobacteria_Gp10 | 0.20 | 15 |
| | Acidobacteria_Gp5 | 0.092 | 6.4 |
| | Acidobacteria_Gp4 | 0.51 | 5.6 |
| | Acidobacteria_Gp11 | 0.31 | 4.6 |
| | Acidobacteria_Gp22 | 0.10 | 3.3 |
| | Acidobacteria_Gp1 | 3.3 | 2.6 |
| | Acidobacteria_Gp25 | 1.6 | 1.6 |
| | Deltaproteobacteria | 19 | 0.57 |
| | Acidobacteria_Gp17 | 5.6 | 0.51 |
| | Acidobacteria_Gp2 | 6.2 | 0.31 |
| | Acidobacteria_Gp9 | 22 | 0.23 |
| | Acidobacteria_Gp13 | 17 | 0.20 |
| | Holophagae | 0.24 | 0.16 |
| | Actinobacteria | 0.14 | 0.14 |
| | Endomicrobia | 0.025 | 0.13 |
| | Negativicutes | 0.57 | 0.12 |
| | Acidobacteria_Gp21 | 0.045 | 0.10 |
| | Acidobacteria_Gp15 | 0.13 | 0.092 |
| | Gemmatimonadetes | 0.053 | 0.053 |
| | Elusimicrobia | 0.16 | 0.045 |
| | Clostridia | 0.12 | 0.025 |
| | **Total** | **2.8** | |
| Actinobacteria | Actinobacteria | 22.079 | 99.959 |
| | Thermoleophilia | 0.0027 | 0.0121 |
| | Gemmatimonadetes | 0.0065 | 0.0292 |

|  | Total | 22 |  |
|---|---|---|---|
| **Armatimonadetes** | Fimbriimonadia | 0.075 | 70 |
|  | Chthonomonadetes | 0.013 | 12 |
|  | unknown | 0.0075 | 7 |
|  | Armatimonadia | 0.0071 | 6.7 |
|  | Negativicutes | 0.0020 | 1.9 |
|  | Clostridia | 0.0011 | 1.0 |
|  | Actinobacteria | 0.0010 | 0.94 |
|  | **Total** | **0.11** |  |
| **Bacteroidetes** | Flavobacteriia | 8.1 | 56 |
|  | Cytophagia | 4.1 | 28 |
|  | Sphingobacteriia | 2.2 | 15 |
|  | Bacteroidia | 0.19 | 1.3 |
|  | **Total** | **14.6150** |  |
| **BRC1** | unknown | 0.0011 | 59.6 |
|  | Deltaproteobacteria | 0.00050 | 24.8 |
|  | Actinobacteria | 0.00030 | 15.6 |
|  | **Total** | **0.0019** |  |
| **candidate_division_WPS-1** | Phycisphaerae | 0.0047 | 100 |
|  | **Total** | **0.0047** |  |
| **Candidatus_Saccharibacteria** | unknown | 0.10 | 96 |
|  | Clostridia | 0.0018 | 1.6 |
|  | Deltaproteobacteria | 0.0014 | 1.3 |
|  | Bacilli | 0.00080 | 0.73 |
|  | **Total** | **0.11** |  |
| **Chlamydiae** | Chlamydiia | 0.21 | 100 |
|  | **Total** | **0.21** |  |
| **Chloroflexi** | Caldilineae | 0.096 | 34 |
|  | Chloroflexia | 0.086 | 30 |
|  | Ardenticatenia | 0.037 | 13 |
|  | Actinobacteria | 0.030 | 10 |
|  | Thermomicrobia | 0.022 | 7.7 |
|  | Deltaproteobacteria | 0.0063 | 2.2 |
|  | Dehalococcoidia | 0.0050 | 1.7 |

|  | Ktedonobacteria | 0.0012 | 0.44 |
|  | Dehalococcoidetes | 0.00090 | 0.31 |
|  | Clostridia | 0.00070 | 0.25 |
|  | **Total** | **0.28** |  |
| **Crenarchaeota** | Thermoprotei | 0.00080 | 100 |
|  | **Total** | **0.00080** |  |
| **Cyanobacteria/Chloroplast** | Cyanobacteria | 0.30 | 100 |
|  | **Total** | **0.30** |  |
| **Deinococcus-Thermus** | Deinococci | 0.0033 | 100 |
|  | **Total** | **0.0033** |  |
| **Elusimicrobia** | Elusimicrobia | 0.024 | 75 |
|  | Endomicrobia | 0.0081 | 25 |
|  | **Total** | **0.032** |  |
| **Firmicutes** | Bacilli | 3.7 | 93 |
|  | Clostridia | 0.24 | 6.1 |
|  | Deltaproteobacteria | 0.0060 | 0.15 |
|  | Actinobacteria | 0.0036 | 0.089 |
|  | Nitrospira | 0.0034 | 0.086 |
|  | Thermodesulfobacteria | 0.0029 | 0.071 |
|  | Negativicutes | 0.0023 | 0.057 |
|  | Erysipelotrichia | 0.0010 | 0.024 |
|  | Endomicrobia | 0.00080 | 0.021 |
|  | Flavobacteriia | 0.00030 | 0.0082 |
|  | **Total** | **4.0** |  |
| **Gemmatimonadetes** | Gemmatimonadetes | 0.94 | 100 |
|  | **Total** | **0.94** |  |
| **Ignavibacteriae** | Ignavibacteria | 0.15 | 100 |
|  | **Total** | **0.15** |  |
| **Latescibacteria** | Bacilli | 0.038 | 41 |
|  | Negativicutes | 0.021 | 24 |
|  | Deltaproteobacteria | 0.019 | 21 |
|  | Actinobacteria | 0.0042 | 4.6 |
|  | Clostridia | 0.0036 | 4.0 |
|  | Acidobacteria_Gp6 | 0.0017 | 1.9 |

| | | | |
|---|---|---|---|
| | Alphaproteobacteria | 0.0010 | 1.1 |
| | unknown | 0.00080 | 0.86 |
| | Nitrospinia | 0.00070 | 0.76 |
| | Gemmatimonadetes | 0.00050 | 0.57 |
| | Gammaproteobacteria | 0.00030 | 0.31 |
| | **Total** | **0.091** | |
| **Nitrospirae** | Nitrospira | 0.38 | 100 |
| | **Total** | **0.38** | |
| **Parcubacteria** | Clostridia | 0.0010 | 100 |
| | **Total** | **0.0010** | |
| **Planctomycetes** | Planctomycetia | 0.089 | 64 |
| | Phycisphaerae | 0.048 | 35 |
| | Actinobacteria | 0.00040 | 0.32 |
| | **Total** | **0.14** | |
| **Poribacteria** | Actinobacteria | 0.0068 | 51 |
| | Deltaproteobacteria | 0.0054 | 41 |
| | Clostridia | 0.0010 | 7.6 |
| | **Total** | **0.013** | |
| **Proteobacteria** | Gammaproteobacteria | 19 | 35 |
| | Alphaproteobacteria | 16 | 30 |
| | Betaproteobacteria | 13 | 25 |
| | Deltaproteobacteria | 4.5 | 8.5 |
| | Gemmatimonadetes | 0.24 | 0.45 |
| | Actinobacteria | 0.095 | 0.18 |
| | Clostridia | 0.037 | 0.070 |
| | Deferribacteres | 0.025 | 0.046 |
| | Bacilli | 0.0082 | 0.015 |
| | Thermomicrobia | 0.0031 | 0.0058 |
| | Ignavibacteria | 0.0031 | 0.0058 |
| | Acidobacteria_Gp7 | 0.0029 | 0.0054 |
| | Oligoflexia | 0.0028 | 0.0053 |
| | Nitrospira | 0.0021 | 0.0040 |
| | Phycisphaerae | 0.0019 | 0.0036 |
| | Caldilineae | 0.0014 | 0.0026 |

| | | | |
|---|---|---|---|
| | Planctomycetia | 0.0012 | 0.0022 |
| | Chloroplast | 0.0011 | 0.0022 |
| | Elusimicrobia | 0.0011 | 0.0020 |
| | Acidobacteria_Gp10 | 0.0010 | 0.0019 |
| | Thermodesulfobacteria | 0.00090 | 0.0017 |
| | Halobacteria | 0.00040 | 0.00080 |
| | **Total** | **53** | |
| **Spirochaetes** | Spirochaetia | 0.0068 | 100 |
| | **Total** | **0.0068** | |
| **Tenericutes** | Mollicutes | 0.0016 | 100 |
| | **Total** | **0.0016** | |
| **Verrucomicrobia** | Subdivision3 | 0.54 | 90 |
| | Spartobacteria | 0.048 | 8.0 |
| | Opitutae | 0.0055 | 0.90 |
| | Verrucomicrobiae | 0.0028 | 0.46 |
| | Subdivision5 | 0.0023 | 0.37 |
| | **Total** | **0.60** | |

**Figure 4.6 Proportion of DESeq2 normalized sequence reads assigned to different bacterial phyla across all samples.**
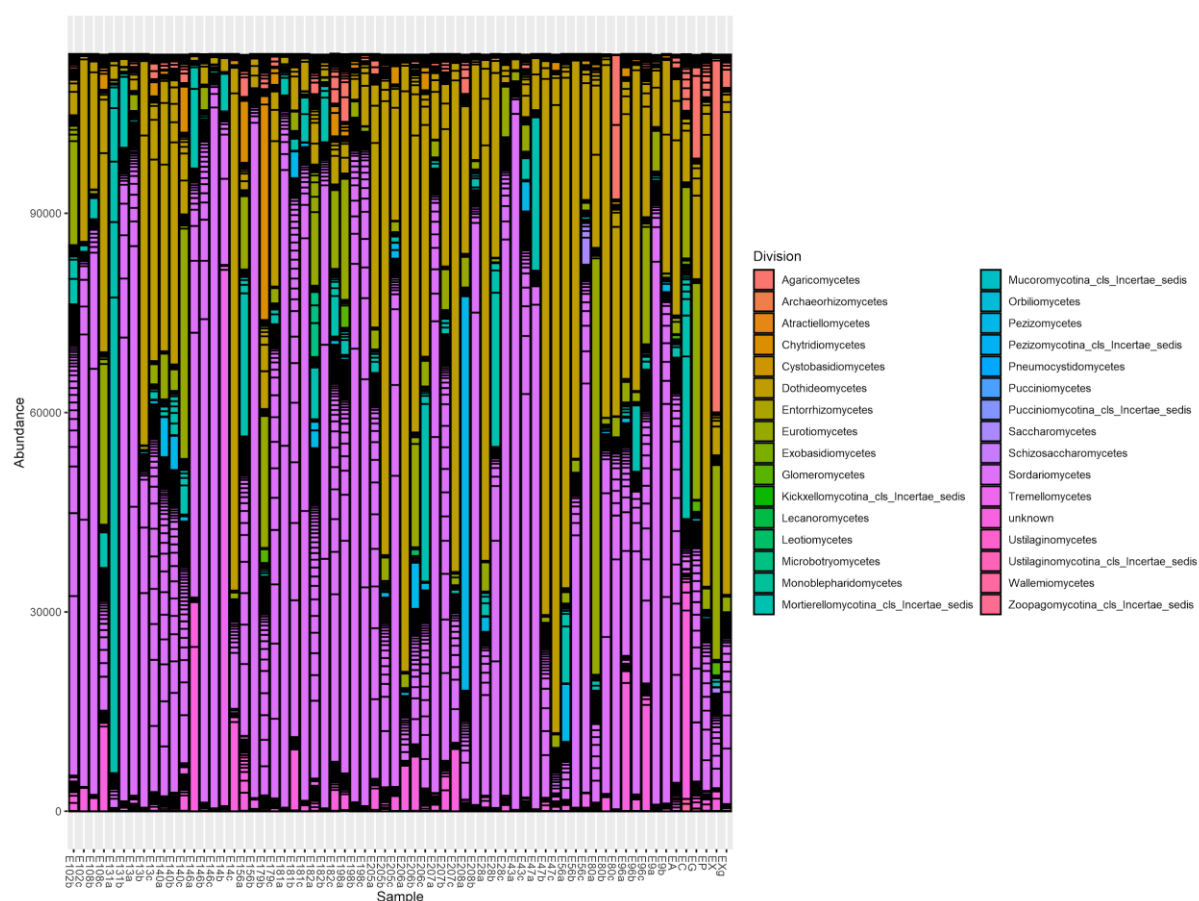


**Figure 4.7 Abundance of bacterial classes across all samples.** The number of reads per sample were normalised using median sequencing depth.

159

# 4.4.2.3 Avalon and Cadenza

Due to the challenge of extraction of high quality DNA from a large number of soil samples and the cost of sequencing, parental samples included three replicates of Avalon rhizosheath and two replicates of Cadenza rhizosheath in addition to one replicate of Avalon exudate and one replicate of Cadenza exudate. Due to few replicates, the power of statistical tests was too low for reliable statistical comparisons between the cultivars, Avalon and Cadenza. However, in the data presented, the Cadenza rhizosheath contained a greater abundance of all fungal phyla (Figure 4.8). For five out of seven phyla, all three Avalon replicates were of lower abundance than the two Cadenza replicates. The Chytridiomycota and Zygomycota had a small overlap in abundance.

Due to poor DNA extraction and sequencing results, only one replicate of each exudate sample could be examined. However, used as preliminary results, these samples suggest that soil supplemented with Cadenza exudate may contain a greater abundance of the Ascomycota, Basidiomycota, Cercozoa, Rozellomycota and Zygomycota than soil supplemented with Avalon exudate. The Chytridiomycota reads were of low abundance in these samples (lower than Avalon and Cadenza) and the Glomeromycota were more abundant in the sample containing Avalon exudate.

Examining the six most abundant bacterial phyla, there did not appear to be notable differences between Avalon and Cadenza except for the Bacteroidetes, Gemmatimonadetes and Proteobacteria (Figure 4.9). All Avalon rhizosheath samples contained a greater number of Bacteroidetes than Cadenza samples. In contrast, all Cadenza rhizosheath samples contained a greater number of Gemmatimonadetes and Proteobacteria than Avalon samples. As with the abundance of fungi, the trend in bacterial abundance in the exudate samples followed the genotype trend, with the exception of the Bacteroides.
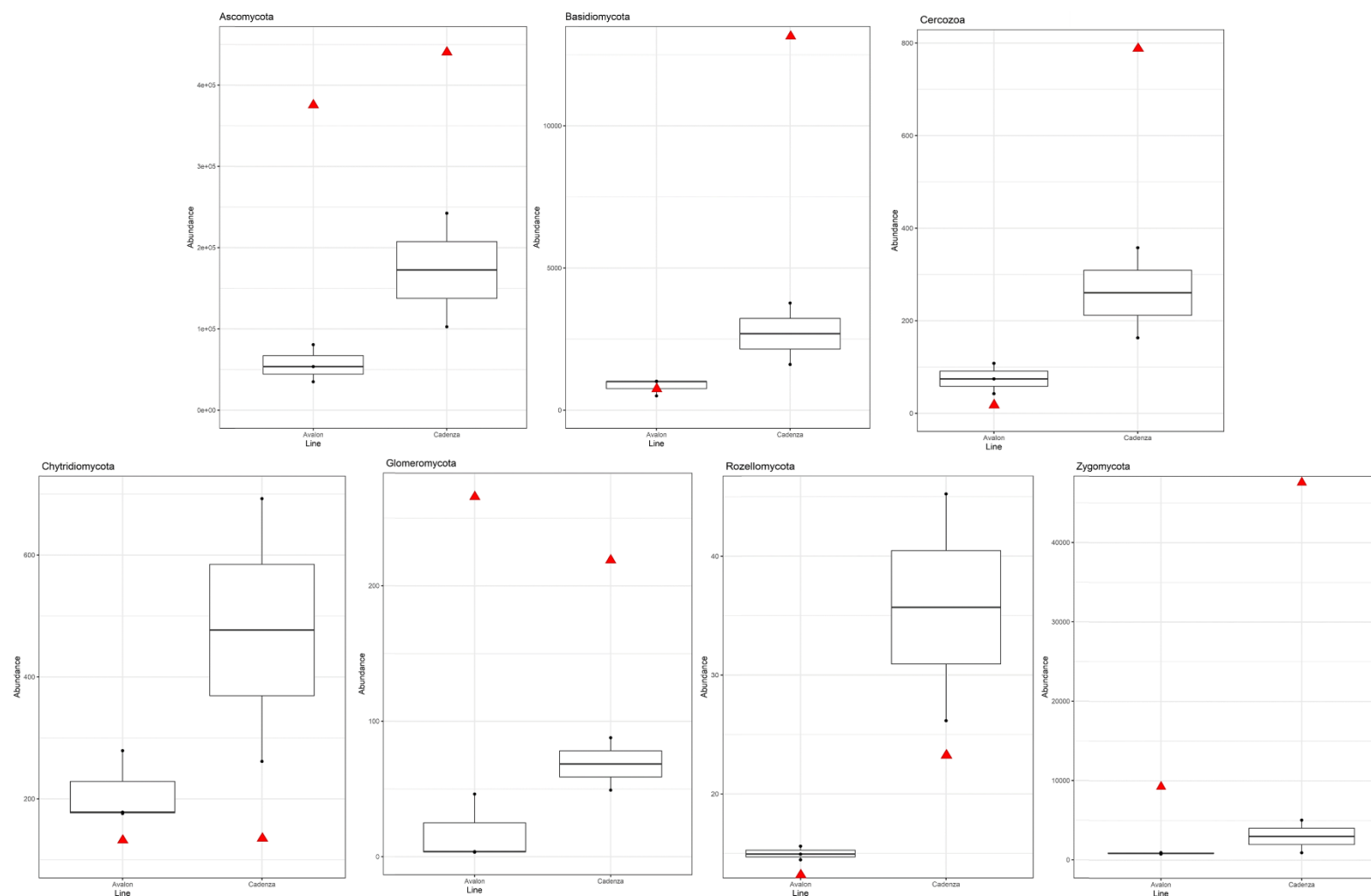
**Figure 4.8 The normalised abundance of fungal phyla in the rhizosheath of wheat varieties, Avalon and Cadenza**. Points denote biological replicates (Avalon 3, Cadenza 2). Red triangles denote the abundance of fungi detected in sterilised soil supplemented with exudates extracted from Avalon and Cadenza rhizosheaths. Reads were determined by ITS sequencing. A, Ascomycota; B, Basidiomycota; C, Cercozoa; D, Chytridiomycota; E, Glomeromycota; F, Rozellomycota; G, Zygomycota
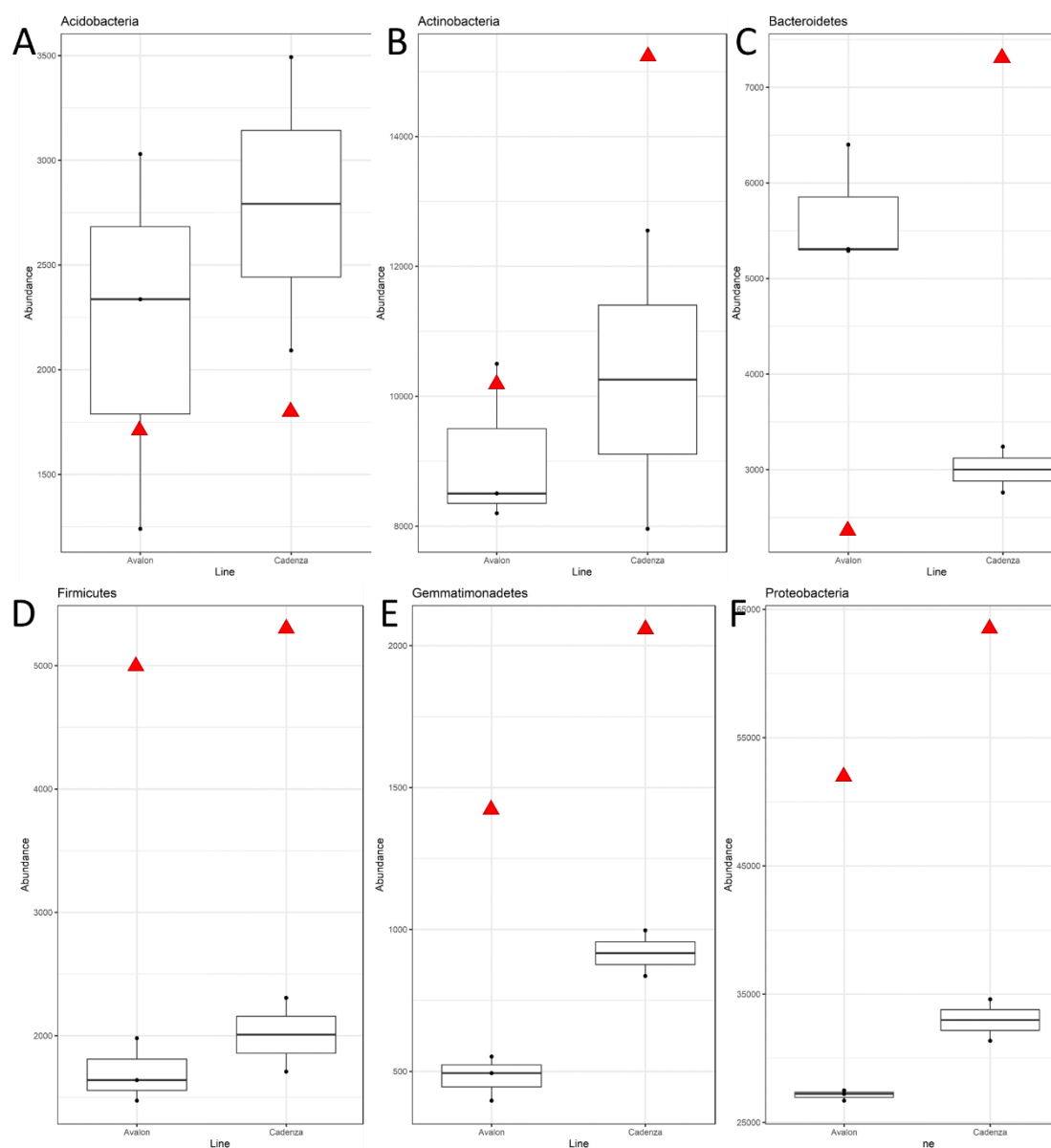
**Figure 4.9 The normalised abundance of the most common bacterial phyla in the rhizosheath of wheat varieties, Avalon and Cadenza.** Points denote biological replicates (Avalon 3, Cadenza 2). Red triangles denote the abundance of bacteria detected in sterilised soil supplemented with exudates extracted from Avalon and Cadenza rhizosheaths. Reads were determined by ITS sequencing. A, Acidobacteria; B, Actinobacteria; C, Bacteroidetes; D, Firmicutes; E, Gemmatimonadetes; F, Proteobacteria.

# 4.4.3 Alpha diversity of the AxC tails

The alpha diversity in each sample was calculated using Phyloseq and means per line are displayed in Tables 4.6 and 4.7. Average bacterial diversity was higher than fungal diversity. Bacterial diversity had an average Chao1 richness of 8441 (range 4829 - 17063); ACE 7395 (range 4829-8793); Shannon-Weaver index 6.5 (range 6.9-7.1); Simpson 0.98 (range 0.92-0.99). Across all samples, the average fungal Chao1 richness was 2091 (range 364 – 15,535); ACE 657 (range 364 - 857); Shannon-weaver index, 2.0 (range 1.24 – 3.39); and Simpson index of 1.0 (0.42 – 0.90).

**Table 4.6 Fungal diversity in rhizosheath samples of the AxC tails**. Displayed are the mean diversity indices of biological replicates and their standard deviation (sd). Standard deviation not applicable for samples with only one replicate.

| Sample | Chao1 | | ACE | | Shannon-Weaver | | Simpson | |
|---|---|---|---|---|---|---|---|---|
| | Mean | sd | Mean | sd | Mean | sd | Mean | sd |
| AxC9 | 720 | NA | 702 | NA | 1.8 | NA | 0.65 | NA |
| AxC13 | 740 | 17 | 744 | 0.67 | 2.4 | 0.90 | 0.79 | 0.16 |
| AxC14 | 547 | 110 | 577 | 97 | 1.4 | 0.76 | 0.51 | 0.097 |
| AxC28 | 7460 | 105 | 590 | 59 | 1.9 | 0.11 | 0.65 | 0.015 |
| AxC43 | 767 | 125 | 740 | 113 | 1.5 | 0.26 | 0.43 | 0.049 |
| AxC47 | 674 | 81 | 679 | 76 | 1.3 | 0.17 | 0.44 | 0.013 |
| AxC56 | 766 | 53 | 768 | 67 | 1.7 | 0.87 | 0.60 | 0.34 |
| AxC80 | 526 | 9724 | 509 | 157 | 2.0 | 2.0 | 0.73 | 0.51 |
| AxC96 | 675 | 244 | 666 | 240 | 2.6 | 0.051 | 0.82 | 0.030 |
| AxC102 | 560 | 38 | 560 | 44 | 3.4 | 0.90 | 0.90 | 0.15 |
| AxC108 | 527 | 119 | 539 | 98 | 2.2 | 1.2 | 0.75 | 0.11 |
| AxC131 | 555 | 109 | 539 | 103 | 1.6 | 0.63 | 0.59 | 0.13 |
| AxC140 | 832 | 36 | 834 | 39 | 3.4 | 0.51 | 0.89 | 0.14 |
| AxC146 | 540 | 4797 | 521 | 74 | 1.5 | 0.87 | 0.51 | 0.24 |
| AxC156 | 7468 | 142 | 710 | 151 | 2.1 | 0.84 | 0.57 | 0.18 |
| AxC179 | 702 | 98 | 699 | 106 | 3.2 | 0.46 | 0.90 | 0.098 |
| AxC181 | 647 | 5943 | 663 | 37 | 2.2 | 0.31 | 0.76 | 0.19 |
| AxC182 | 881 | 284 | 867 | 296 | 3.3 | 1.3 | 0.88 | 0.39 |
| AxC198 | 619 | 72 | 629 | 67 | 2.5 | 0.26 | 0.77 | 0.11 |
| AxC205 | 659 | 33 | 632 | 334 | 2.5 | 0.36 | 0.77 | 0.073 |
| AxC206 | 3519 | 69 | 707 | 50 | 2.3 | 0.27 | 0.69 | 0.070 |
| AxC207 | 684 | 192 | 674 | 194 | 2.5 | 0.44 | 0.75 | 0.24 |
| AxC208 | 841 | 146 | 785 | 141 | 1.8 | 0.75 | 0.62 | 0.10 |
| AvalonExudate | 757 | NA | 753 | NA | 3.1 | NA | 0.90 | NA |
| CadenzaExudate | 12229 | NA | 732 | NA | 3.0 | NA | 0.87 | NA |

**Table 4.7 Bacterial diversity in rhizosheath samples of the AxC tails**. Displayed are the mean diversity indices of biological replicates and their standard deviation (sd).

| Line | Chao1 | | ACE | | Shannon-Weaver | | Simpson | |
|---|---|---|---|---|---|---|---|---|
| | mean | sd | mean | sd | mean | sd | mean | sd |
| AxC 1 | 8847 | 3898 | 8399 | 3009 | 5.1 | 0.93 | 0.93 | 0.059 |
| AxC 102 | 7549 | 198 | 7825 | 231 | 6.8 | 0.43 | 0.99 | 0.0035 |
| AxC 108 | 7775 | 681 | 8215 | 261 | 6.7 | 0.15 | 0.99 | 0.0014 |
| AxC 13 | 10543 | 8167 | 6354 | 982 | 7.1 | 0.28 | 0.99 | 0.0018 |
| AxC 131 | 9441 | 3018 | 8541 | 1546 | 6.6 | 0.53 | 0.98 | 0.0084 |
| AxC 14 | 9772 | 7350 | 5988 | 789 | 5.6 | 2.0 | 0.92 | 0.12 |
| AxC 140 | 8151 | 314 | 8359 | 387 | 7.0 | 0.24 | 0.99 | 0.0021 |
| AxC 146 | 7466 | 607 | 7922 | 253 | 6.3 | 0.71 | 0.98 | 0.022 |
| AxC 156 | 8652 | 2469 | 8535 | 944 | 6.2 | 1.3 | 0.98 | 0.028 |
| AxC 179 | 7297 | 648 | 7690 | 127 | 6.5 | 0.12 | 0.99 | 0.0024 |
| AxC 181 | 7848 | 532 | 8190 | 336 | 6.6 | 0.38 | 0.99 | 0.0049 |
| AxC 182 | 8612 | 454 | 8793 | 416 | 7.0 | 0.57 | 0.99 | 0.0040 |
| AxC 198 | 8358 | 181 | 8465 | 283 | 6.7 | 0.19 | 0.99 | 0.0019 |
| AxC 205 | 11230 | 8142 | 7016 | 1968 | 6.8 | 0.092 | 0.99 | 0.0011 |
| AxC 206 | 7286 | 2224 | 7436 | 2356 | 7.0 | 0.16 | 0.99 | 0.0015 |

| | | | | | | | | |
|---|---|---|---|---|---|---|---|---|
| **AxC 207** | 8334 | 323 | 8417 | 520 | 7.0 | 0.049 | 0.99 | 0.00030 |
| **AxC 208** | 14731 | 12412 | 7006 | 1488 | 7.1 | 0.25 | 0.99 | 0.0019 |
| **AxC 28** | 12076 | 7570 | 7851 | 221 | 6.1 | 0.50 | 0.99 | 0.0075 |
| **AxC 43** | 8199 | 579 | 8310 | 807 | 7.0 | 0.26 | 0.99 | 0.0014 |
| **AxC 47** | 4829 | 344 | 4829 | 344 | 6.9 | 0.31 | 0.99 | 0.0041 |
| **AxC 5** | 8466 | 4299 | 7437 | 2952 | 5.5 | 1.6 | 0.94 | 0.084 |
| **AxC 56** | 7760 | 531 | 8002 | 706 | 6.6 | 0.46 | 0.99 | 0.0032 |
| **AxC 6** | 5137 | 1691 | 5419 | 1574 | 5.0 | 0.65 | 0.94 | 0.033 |
| **AxC 7** | 8442 | 4018 | 7694 | 2808 | 6.3 | 0.76 | 0.98 | 0.020 |
| **AxC 80** | 7494 | 348 | 7782 | 453 | 6.5 | 0.062 | 0.99 | 0.0025 |
| **AxC 9** | 7266 | 372 | 7391 | 369 | 6.0 | 0.26 | 0.98 | 0.0024 |
| **AxC 96** | 17063 | 7839 | 7805 | 362 | 6.9 | 0.14 | 0.99 | 0.00030 |
| **Avalon Exudate** | 14524 | 308 | 6409 | 355 | 6.6 | 0.69 | 0.99 | 0.0053 |
| **Cadenza Exudate** | 6116 | 32 | 6287 | 57 | 5.9 | 0.23 | 0.98 | 0.0057 |

# 4.4.3.1 Differences in alpha diversity between phenotypic groups

In order to test for the effect of genotype, RSA traits and the level of rhizosheath polysaccharide on alpha diversity, the samples were grouped by trait and tested with ANOVA and a pairwise Wilcox test.

# 4.4.3.1.1 Fungi

The one-way ANOVA on the alpha indices of all rhizosheath samples indicated that there was a significant genotype effect on ACE (Table 4.8). There was no significant genotypic effect on the Chao1, Shannon-Weaver and Simpson indices, although Chao1 and Shannon-Weaver approached significance (p<0.08). RSA had no effect on fungal alpha diversity (angle and length, p>0.1) and no significant variation was detected between lines secreting contrasting levels of most polysaccharides (p>0.1), with the exception of homogalacturonan.

On the other hand, differences were observed between lines known to secrete large or small amounts of homogalacturonan (Table 4.8). In particular, lines that secreted small amounts of homogalacturonan had a greater Chao1 and significantly greater ACE index than lines with high levels in their rhizosheath. There was no difference in Shannon-Weaver and Simpson indices. This suggests that a greater number of species were present in rhizosheaths containing low concentrations of homogalacturonan and that their distribution was as uniform as samples with high concentrations (Figure 4.10). Samples from plants known to exude high concentrations of xyloglucan displayed marginally greater Shannon-Weaver and Simpson diversity but this did not reach statistical significance (p = 0.1).

The parental lines, Cadenza and Avalon did not differ significantly for alpha diversity, probably owing to the small number of replicates (Figure 4.11).

**Table 4.8 p-values for differences in fungal alpha diversity indices between rhizosheath samples contrasting for specific traits**. ITS sequencing was undertaken on rhizosheath samples from lines of the Avalon x Cadenza (AxC) mapping population. Samples were grouped according to the concentration (high or low) of specific polysaccharides exuded by the AxC line, shoot mass and total root length in order to apply a pairwise Wilcox test. In parentheses are the antibodies used to detect polysaccharide levels in the rhizosheath.

| Sample Group | Chao1 | ACE | Shannon-Weaver | Simpson |
|---|---|---|---|---|
| Genotype | 0.069 | 0.023* | 0.074 | 0.14 |
| Parental lines | 0.27 | 0.44 | 0.35 | 0.43 |
| Xyloglucan (LM25) | 1 | 0.74 | 0.1 | 0.1 |
| Arabinogalactan protein (LM2) | 1 | 0.93 | 1 | 1 |
| Heteroxylan (LM27) | 0.94 | 1 | 1 | 1 |
| Extensin (LM1) | 0.64 | 0.78 | 0.59 | 0.57 |
| Xylan (LM11) | 1 | 1 | 1 | 1 |
| Homogalacturonan (LM19) | 0.077 | 0.02* | 0.26 | 0.71 |
| Shoot mass | 1 | 0.1 | 1 | 0.96 |
| Total root length | 0.16 | 0.39 | 0.77 | 0.49 |
| Rhizosheath size per cm of root | 1 | 0.56 | 0.53 | 0.85 |
| Root angle | 0.19 | 0.14 | 0.51 | 0.30 |
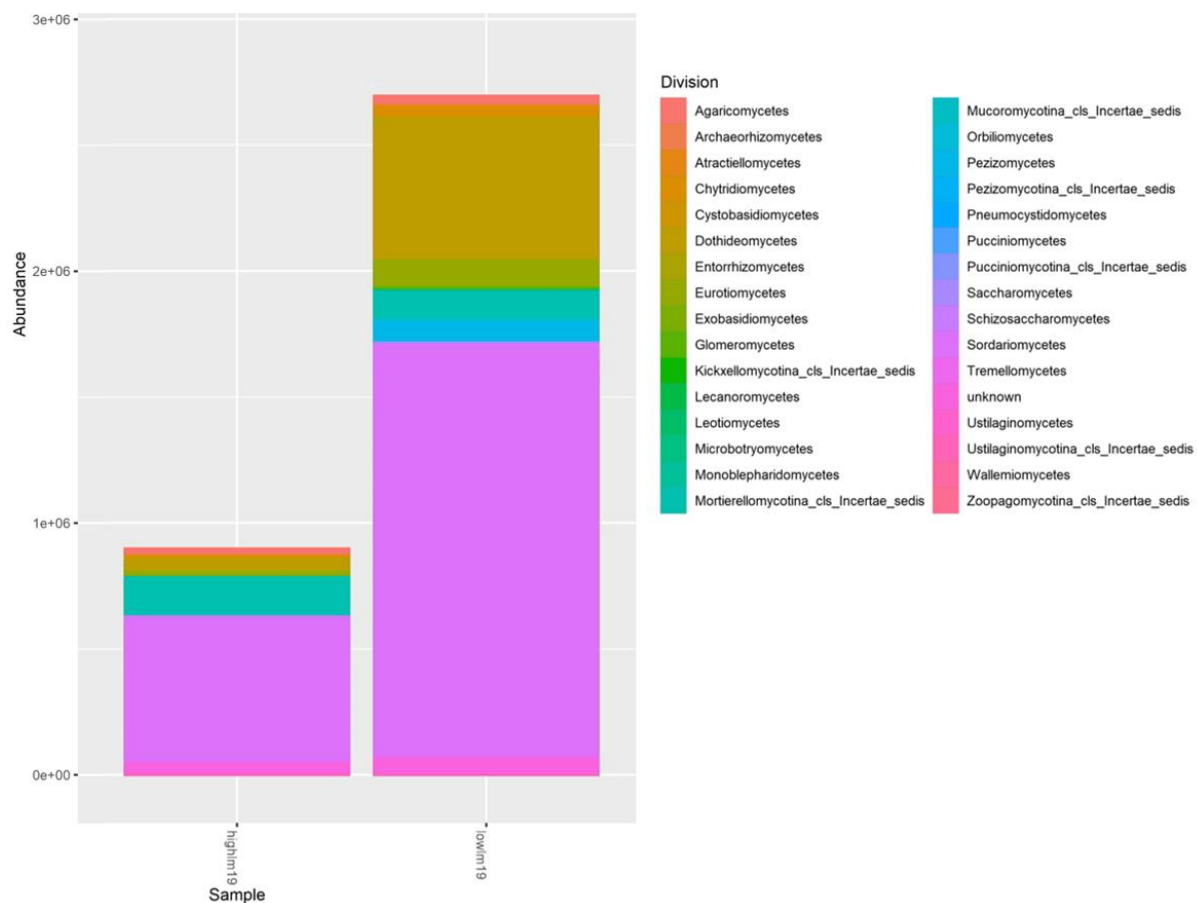
**Figure 4.10 Abundance of fungal phyla in samples derived from plants with high and low levels of LM19 in their rhizosheath.** Figure based on ten samples per group (high or low LM19).
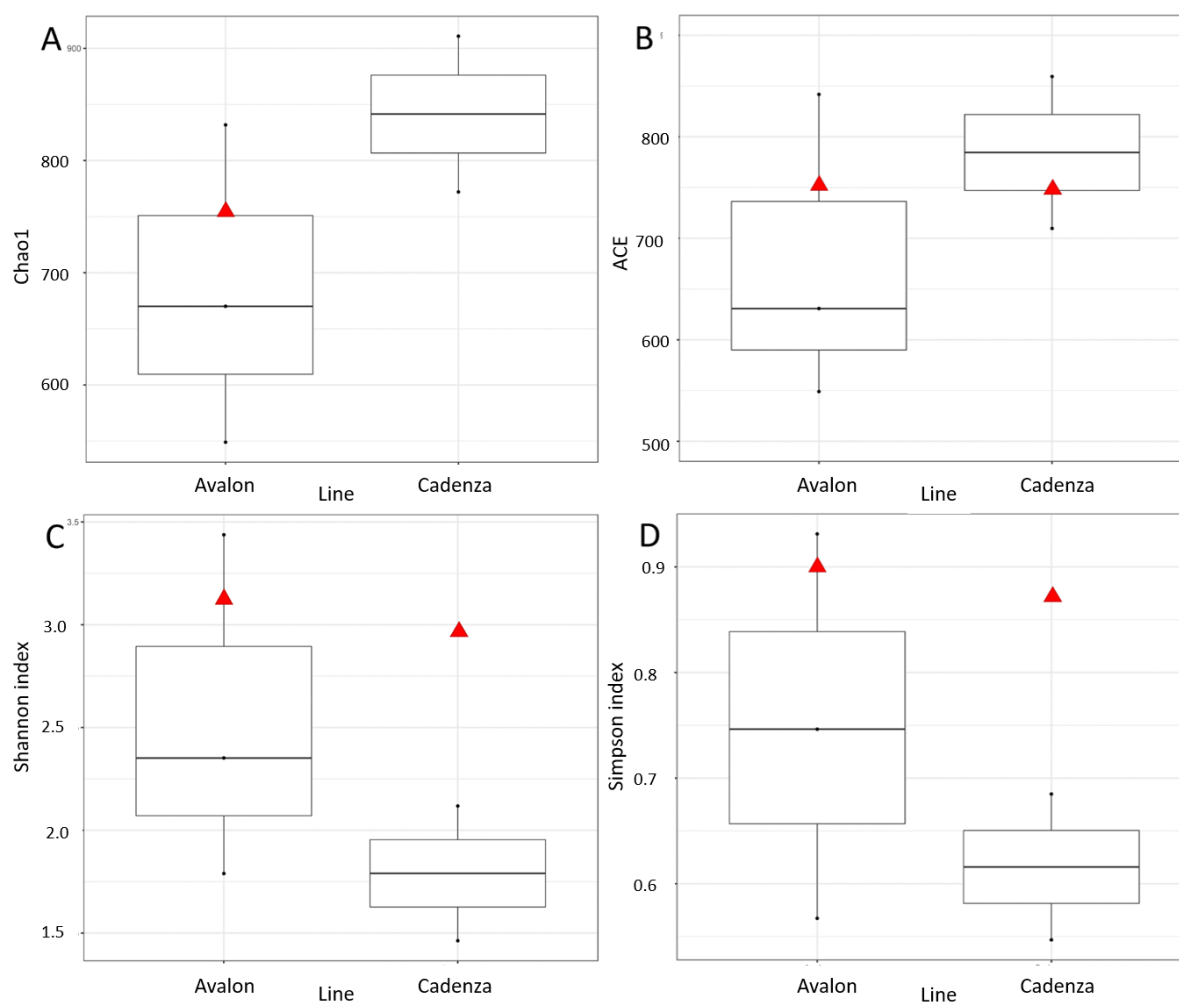
**Figure 4.11 Alpha indices of fungal diversity in rhizosheath samples of wheat cultivars, Avalon and Cadenza.** Red triangles indicate the diversity in soil supplemented with Avalon and Cadenza root exudate (n=1). Triangle not indicated for Cadenza in A due to being far above the scale. (A) Chao1 (B) ACE (C) Shannon-Weaver (D) Simpson.

## 4.4.3.1.2 Bacteria

Running a one-way ANOVA on the alpha indices of all the rhizosheath samples indicated that there was a significant genotypic effect on Shannon-Weaver diversity (p=0.007), a near significant effect on ACE (p=0.06), and no significant effect on Chao1 and Simpson (p > 0.1) (Table 4.9). Looking specifically at the parental lines, Cadenza and Avalon, no significant differences were identified (Figure 4.12). Samples were grouped by the size of the rhizosheath. Chao1 and Simpson indices did not differ significantly between groups (Table 4.9). To identify correlations

between bacterial diversity and the level of secretion of certain polysaccharides, samples were grouped according to the known level of secretion of the AxC line. Rhizosheaths of plants known to secrete high levels of xyloglucan (detected by antibody, LM25) contained significantly greater Shannon-Weaver and Simpson diversity but equivalent Chao1 and ACE richness (Table 4.9). No differences in alpha diversity were identified between rhizosheath samples derived from plants contrasting for levels of other polysaccharides, rhizosheath size or root length (Table 4.9).

**Table 4.9 p-values for differences in bacterial alpha diversity indices between rhizosheath samples contrasting for specific traits**. 16S sequencing was undertaken on rhizosheath samples from lines of the Avalon x Cadenza (AxC) mapping population. Samples were grouped according to the concentration (high or low) of specific polysaccharides exuded by the AxC line, shoot mass and total root length in order to apply ANOVA. See Table 4.8 Legend for explanation of carbohydrate epitopes (LMxx).

| Sample Group | Chao1 | ACE | Shannon-Weaver | Simpson |
|---|---|---|---|---|
| Genotype | 0.13 | 0.065 | 0.0069** | 0.23 |
| Parental Lines | 0.42 | 0.27 | 0.57 | 0.74 |
| LM25 | 0.27 | 0.11 | 0.0061** | 0.0084** |
| LM2 | 0.84 | 0.69 | 0.27 | 0.35 |
| LM27 | 0.77 | 0.73 | 0.27 | 0.25 |
| LM1 | 0.88 | 0.29 | 0.95 | 0.93 |
| LM11 | 0.84 | 0.51 | 0.58 | 0.73 |
| LM19 | 1 | 0.65 | 0.94 | 0.99 |
| Shoot mass | 1 | 0.52 | 0.3 | 0.41 |
| Total Root length | 0.13 | 0.07 | 0.43 | 0.25 |
| Rhizosheath size | 1 | 0.53 | 0.34 | 0.3 |
| Root Angle | 0.27 | 0.23 | 0.87 | 0.88 |
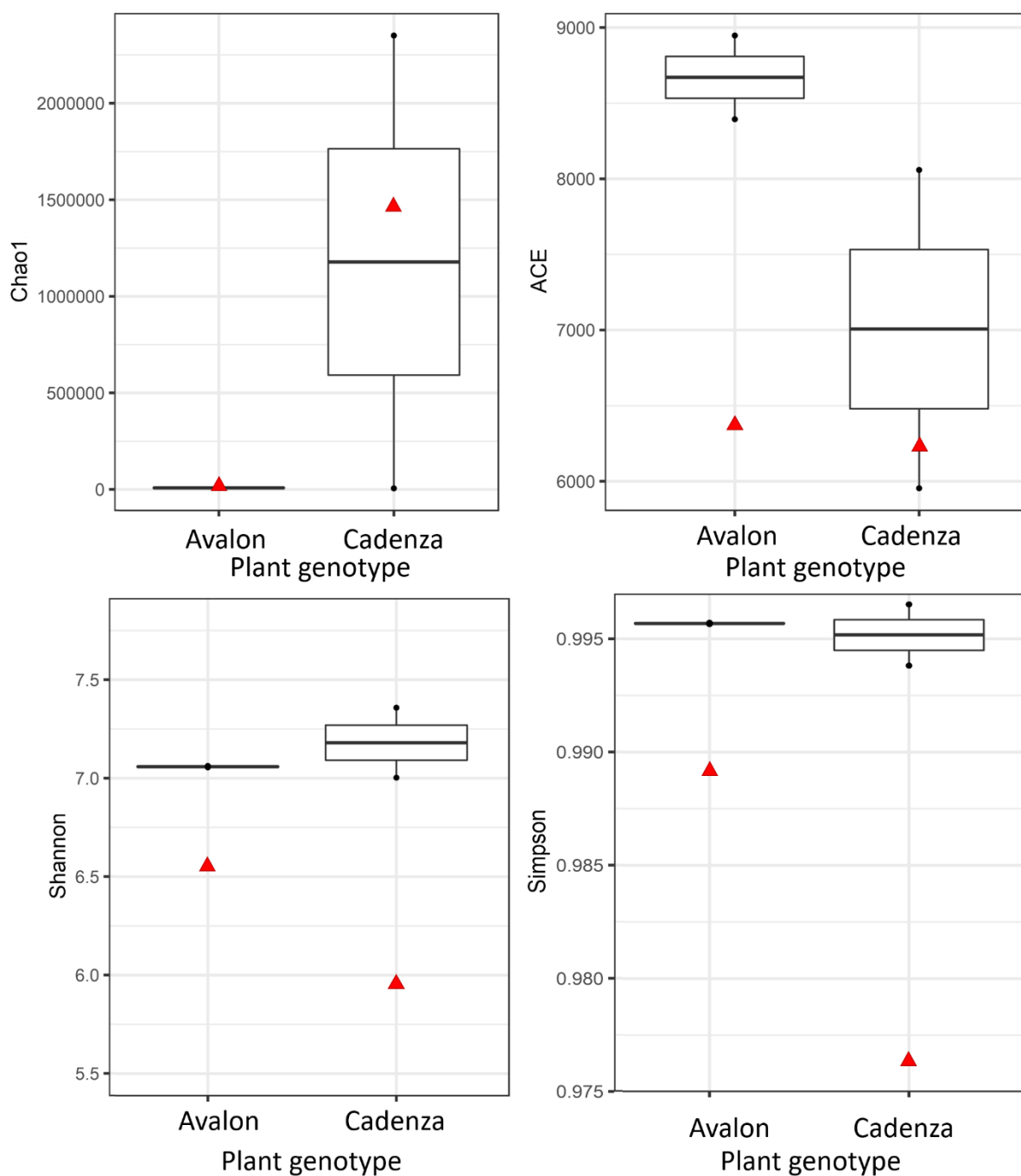
**Figure 4.12 Alpha indices of bacterial diversity in rhizosheath samples of wheat cultivars, Avalon and Cadenza.** Red triangles indicate the diversity in soil supplemented with Avalon and Cadenza root exudate (n=1). (A) Chao1 (B) ACE (C) Shannon-Weaver (D) Simpson.

# 4.4.4 Beta diversity of the AxC tails

Beta diversity refers to intra-group diversity and involves the comparison of different groups of samples based on the composition of their microbial communities (Whittaker, 1960; Baselga, 2007). A square matrix of distance was calculated to reflect the dissimilarity between samples based on weighted and unweighted UniFrac. UniFrac measures the phylogenetic distance between sets of taxa as the fraction of the branch length of a phylogenetic tree that leads to descendants from either one environment or the other, but not both (Lozupone and Knight, 2005). Here, tests were run on weighted UniFrac to take into account species abundance, and unweighted UniFrac to determine variation in the presence or absence of taxa.

A combination of PCA analysis and PERMANOVA was used to determine a correlation between beta diversity and the level of a factor (e.g. whether beta diversity correlated with the concentration of a particular polysaccharide in the root mucilage). Samples were grouped discretely according to the concentration (high or low) of specific polysaccharides exuded by the AxC line, seedling root angle (wide or narrow), seedling root length (long or short), rhizosheath size per cm root length, and final grain yield of the mature plants.

Further analysis into the specific taxa that varied between two conditions was undertaken via Wilcoxon tests (pairwise comparisons between group levels with corrections for multiple testing) and Wald tests (to test whether the log 2-fold change in abundance of specific taxa between the two conditions was equal to zero).

I uncovered factors that may be important for explaining differences in beta diversity, although without targeted experimental evidence, I cannot directly attribute changes in beta diversity to specific factors.

## 4.4.4.1 Certain plant phenotypes correlated with differences in fungal beta diversity

PERMANOVA results on fungal beta diversity based on unweighted UniFrac (Table 4.10) and weighted UniFrac (Table 4.11) are reported. PERMANOVA on unweighted UniFrac resulted in a greater number of significant differences in beta diversity in contrasting levels of plant

phenotypes. Five out of eleven phenotypes (seedling root angle, grain yield, and the concentrations of homogalacturonan, xyloglucan and heteroxylan) displayed a significant unweighted UniFrac difference in beta diversity between high and low levels, indicating a difference in the presence/absence of certain phyla (Table 4.10). The parents, cvs. Avalon and Cadenza, did not contrast for beta diversity, although the small number of replicates makes it challenging to draw substantial conclusions. There was no effect for root length, rhizosheath size, or concentration of xylan and AGP.

Only extensin levels were significantly correlated with weighted UniFrac (Table 4.11). However, plants with contrasting extensin levels did not differ in beta diversity based on unweighted UniFrac, suggesting that samples with differing levels of extensin had skewed species abundance but the same species present.

**Table 4.10 Permutational multivariate analysis of variance (PERMANOVA) of unweighted UniFrac distance of fungal diversity in the wheat rhizosphere.** Differences in beta diversity were tested for the rhizospheres of plants with contrasting phenotypes. Levels of significance are denoted by * (< 0.05); ** (< 0.01); *** (< 0.001).

| Plant phenotype | Df | Sum of Squares | Mean squares | F-model | p-value | Permutations |
|---|---|---|---|---|---|---|
| Seedling root angle | 1, 31 | 0.28 | 0.14 | 1.5 | 0.017* | 999 |
| Seedling root length | 2, 37 | 0.12 | 0.12 | 1.3 | 0.096 | 999 |
| Avalon vs Cadenza | 3, 3 | 0.28 | 0.094 | 1.1 | 0.10 | 999 |
| Extensin (LM1) | 1, 38 | 0.089 | 0.089 | 0.94 | 0.56 | 999 |
| Xylan (LM11) | 1, 33 | 0.089 | 0.089 | 0.91 | 0.64 | 999 |
| Homogalacturonan (LM19) | 1, 34 | 0.19 | 0.19 | 2.0 | 0.003** | 999 |
| Xyloglucan (LM25) | 1, 35 | 0.21 | 0.22 | 2.2 | 0.001*** | 999 |
| Arabinogalactan protein (LM2) | 1, 38 | 0.11 | 0.11 | 1.1 | 0.22 | 999 |
| Heteroxylan (LM27) | 1, 38 | 0.14 | 0.14 | 1.4 | 0.029* | 999 |
| Rhizosheath size | 1, 33 | 0.098 | 0.098 | 1.0 | 0.42 | 999 |
| Grain yield | 1, 21 | 0.13 | 0.13 | 1.4 | 0.040* | 999 |

**Table 4.11 Permutational multivariate analysis of variance (PERMANOVA) of weighted UniFrac distance of fungal diversity in the wheat rhizosphere.** Differences in beta diversity were tested for the rhizospheres of plants with contrasting phenotypes. Levels of significance are denoted by * (< 0.05); ** (< 0.01); *** (< 0.001).

| Plant phenotype | Df | Sum of Squares | Mean squares | F-model | p-value | Permutations |
|---|---|---|---|---|---|---|
| Seedling root angle | 1, 31 | 0.27 | 0.27 | 1.1 | 0.32 | 999 |
| Seedling root length | 1, 38 | 0.28 | 0.28 | 1.2 | 0.29 | 999 |
| Avalon vs Cadenza | 3, 3 | 0.60 | 0.20 | 1.1 | 0.38 | 999 |
| Extensin (LM1) | 1, 38 | 0.51 | 0.51 | 2.1 | 0.009** | 999 |
| Xylan (LM11) | 1, 33 | 0.31 | 0.31 | 1.5 | 0.12 | 999 |
| Homogalacturonan (LM19) | 1, 34 | 0.31 | 0.31 | 1.4 | 0.13 | 999 |
| Xyloglucan (LM25) | 1, 35 | 0.25 | 0.25 | 1.1 | 0.31 | 999 |
| Arabinogalactan protein (LM2) | 1,38 | 0.25 | 0.25 | 1.2 | 0.26 | 999 |
| Heteroxylan (LM27) | 1, 38 | 0.21 | 0.21 | 0.91 | 0.55 | 999 |
| Rhizosheath size | 1, 33 | 0.25 | 0.25 | 1.0 | 0.38 | 999 |
| Grain yield | 1, 21 | 0.28 | 0.28 | 1.3 | 0.19 | 999 |

PCA plots based on VST data did not display distinct clustering. The plot of xyloglucan showed the most distinct clusters, supporting the highly significant correlation between unweighted UniFrac distance and xyloglucan concentration (Figure 4.13). There was a small contribution from PC1 (12%) and PC2 (7%) towards explaining beta diversity. For the parental genotypes cv. Avalon samples clustered and appeared to have a greater contribution of PC2 than both cv. Cadenza samples (Figure 4.14). Cv. Cadenza rhizosheath samples did not cluster.

Although the other tested factors significantly correlated with unweighted UniFrac distance, their effect size was small, with a lack of distinct clustering and a low percentage contribution of PC1 and PC2.
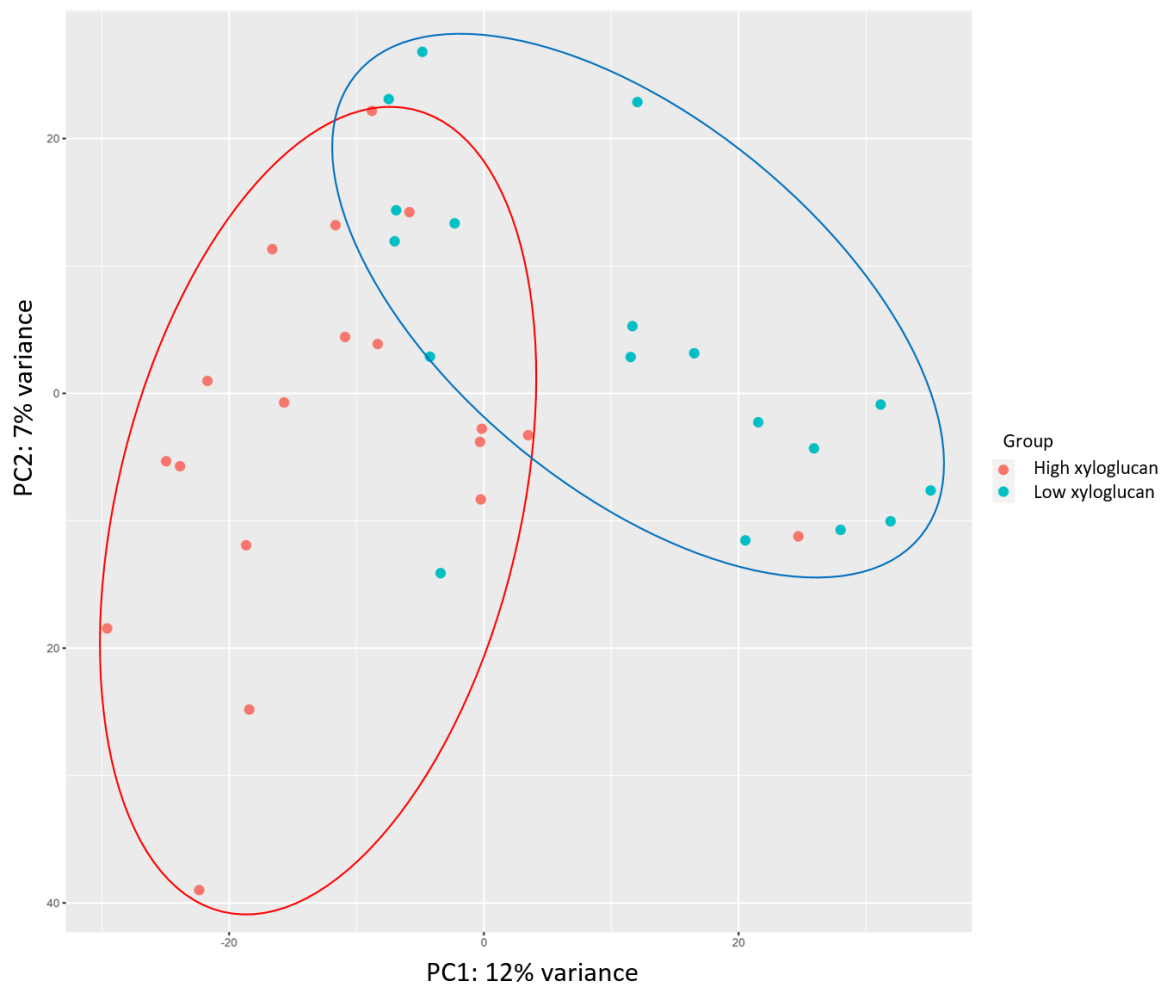
**Figure 4.13 Principal coordinate analysis (PCA) plot based on rhizosphere abundance of fungal OTUs for wheat cultivars with contrasting levels of rhizosheath xyloglucan.**
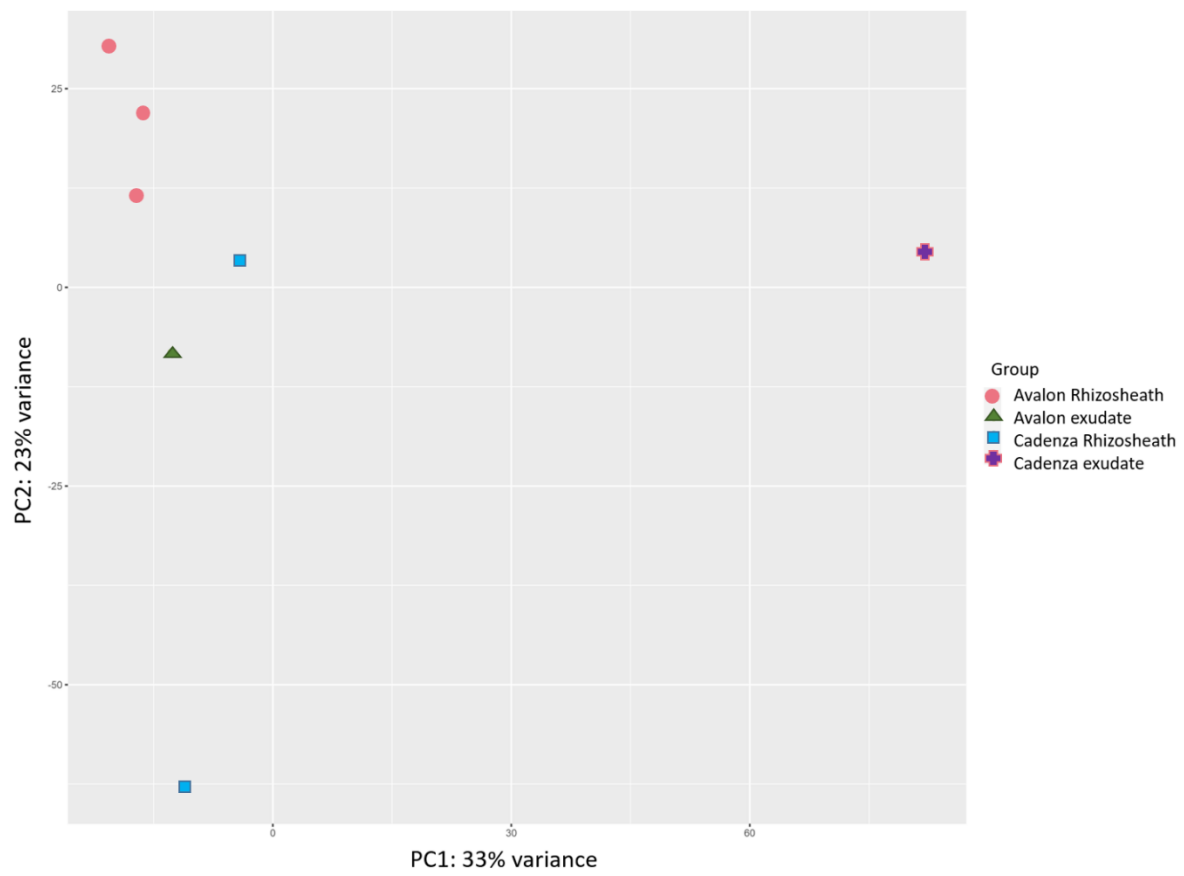
**Figure 4.14 Principal coordinate analysis (PCA) plot based on soil abundance of fungal OTUs.** Samples were taken from the rhizosheath of wheat cultivars, Avalon (pink circle) and Cadenza (blue square), or from soil supplemented with exudates isolated from Avalon (green triangle) and Cadenza (purple cross).

# 4.4.4.2 Differential abundance in fungal taxa between phenotypic groups

For closer investigation of which taxa differed significantly between the rhizosheaths of plants with contrasting phenotypes, the Wald test and Wilcoxon pairwise test were applied.

# 4.4.4.2.1 Extensin

Plants with differing levels of extensin had significant variation in fungal beta diversity. Taxa that differed belonged to the Ascomycota, Basidiomycota, Chytridiomycota and Zygomycota and were mainly saprophytic fungi (Figures 4.15 and 4.16). Higher levels of extensin were associated with higher abundance of the *Glomeraceae* family in the Basidiomycota division, known to have a symbiotic lifestyle (Smith and Read, 2010). Lower levels of extensin were correlated with higher abundance of species of the *Nectriaceae* family and Spizellomycetaceae order, which can be pathogenic (Cannon and Kirk, 2007).



**Figure 4.15 Heat tree of the relative abundance of fungal species between plants with contrasting levels of rhizosheath extensin.** The relative difference in abundance is expressed as log2FoldChange with positive values (bay colour) indicating that the relative abundance of specific OTUs is higher in greater levels extensin. Negative values (cyan colour) indicate that the relative abundance of specific OTUs is higher in lower levels extensin. The size of nodes represents the abundance of rhizosphere fungi at the specific taxonomic rank. The graph is drawn with the R package—Metacoder (Foster *et al.*, 2017).

**Figure 4.16 Heat map of the 50 most abundant fungal species between plants with contrasting levels of rhizosheath extensin.** Blocks represent species, labelled by the order to which the species belong.

## 4.4.4.2.2 Xyloglucan

Plants with a higher level of xyloglucan in the rhizosheath tended to have a significantly greater abundance of certain species of Chytridiomycota, Cercozoa and Glomeromycota than plants with lower levels of xyloglucan (Figures 4.17 and 4.18). Among the Ascomycota and Basidiomycota most species displaying significance were more abundant in plants with high levels of xyloglucan. However, certain taxa were more abundant in plants with low xyloglucan levels, notably the yeasts: the Saccharomycetales order and *Cryptococcus* genus.



**Figure 4.17 Heat tree of the relative abundance of fungal species between plants with contrasting levels of rhizosheath xyloglucan.** The relative difference in abundance is expressed as log2FoldChange with positive values (bay colour) indicating that the relative abundance of specific OTUs is higher in greater levels xyloglucan. Negative values (cyan colour) indicate that the relative abundance of specific OTUs is higher in lower levels xyloglucan. The size of nodes represents the abundance of rhizosphere fungi at the specific taxonomic rank. The graph is drawn with the R package—Metacoder (Foster *et al.*, 2017).

**Figure 4.18 Heat map of the 50 most abundant fungal species between plants with contrasting levels of rhizosheath xyloglucan.** Blocks represent species, labelled by the order to which the species belong.

# 4.4.4.2.3 Heteroxylan

Plants with higher levels of heteroxylan in their rhizosheath displayed greater abundance of certain species of Cercozoa, Chytridiomycota, Rozellomycota and Zygomycota (Figures 4.19 and 4.20) than plants with lower levels of heteroxylan. There was a mixture of differential abundance of Ascomycota and Basidiomycota species but no significant differences in the Glomeromycota.

Most identified Ascomycota and Basidiomycota species had saprotrophic lifestyles. The symbiotrophic Pezzizales (order) were more abundant in low levels of heteroxylan. The Chytridiomycota species identified did not have a lifestyle assignment in the FUNGuild database but their order is known to comprise pathotrophic and saprotrophic fungi. Similarly, the species in the Rozellomycota division that exhibited differential abundance belonged to an order containing pathotrophs, saprotrophs, and symbiotrophs. The Zygomycota identified were saprotroph-symbiotrophs.
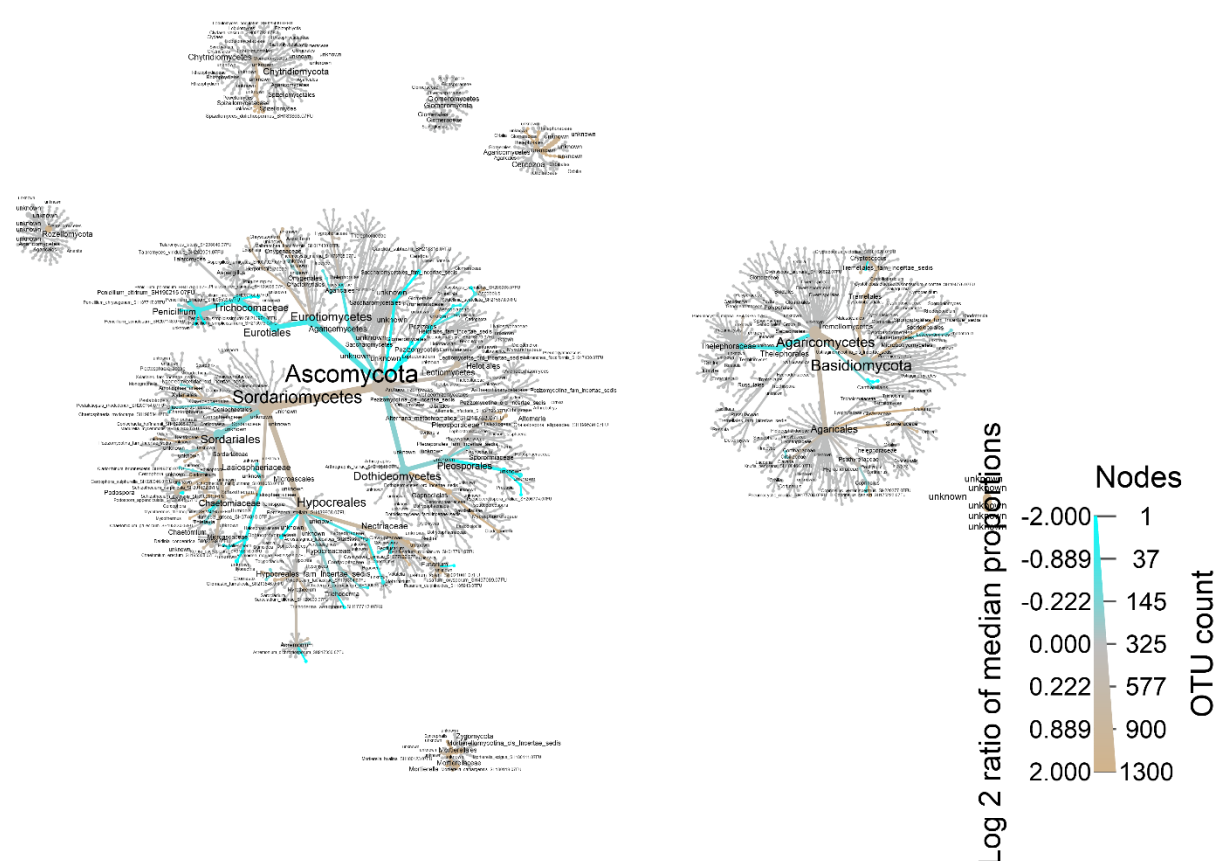
**Figure 4.19 Heat tree of the relative abundance of fungal species between plants with contrasting levels of rhizosheath heteroxylan.** The relative difference in abundance is expressed as log2FoldChange with positive values (bay colour) indicating that the relative abundance of specific OTUs is higher in greater levels heteroxylan. Negative values (cyan colour) indicate that the relative abundance of specific OTUs is higher in lower levels xyloglucan. The size of nodes represents the abundance of rhizosphere fungi at the specific taxonomic rank. The graph is drawn with the R package—Metacoder (Foster *et al.*, 2017).

**Figure 4.20 Heat map of the 50 most abundant fungal species between plants with contrasting levels of rhizosheath heteroxylan.** Blocks represent species, labelled by the order to which the species belong.

# 4.4.4.2.4 Homogalacturonan

Almost all species displaying significance were more numerous in the rhizosheaths of genotypes with low levels of homogalacturonan (Figures 4.21 and 4.22). The exceptions were saprotrophs, including the Basidiomycete, *Rhodosporidium*, and the Ascomycete, *Schizothecium.*
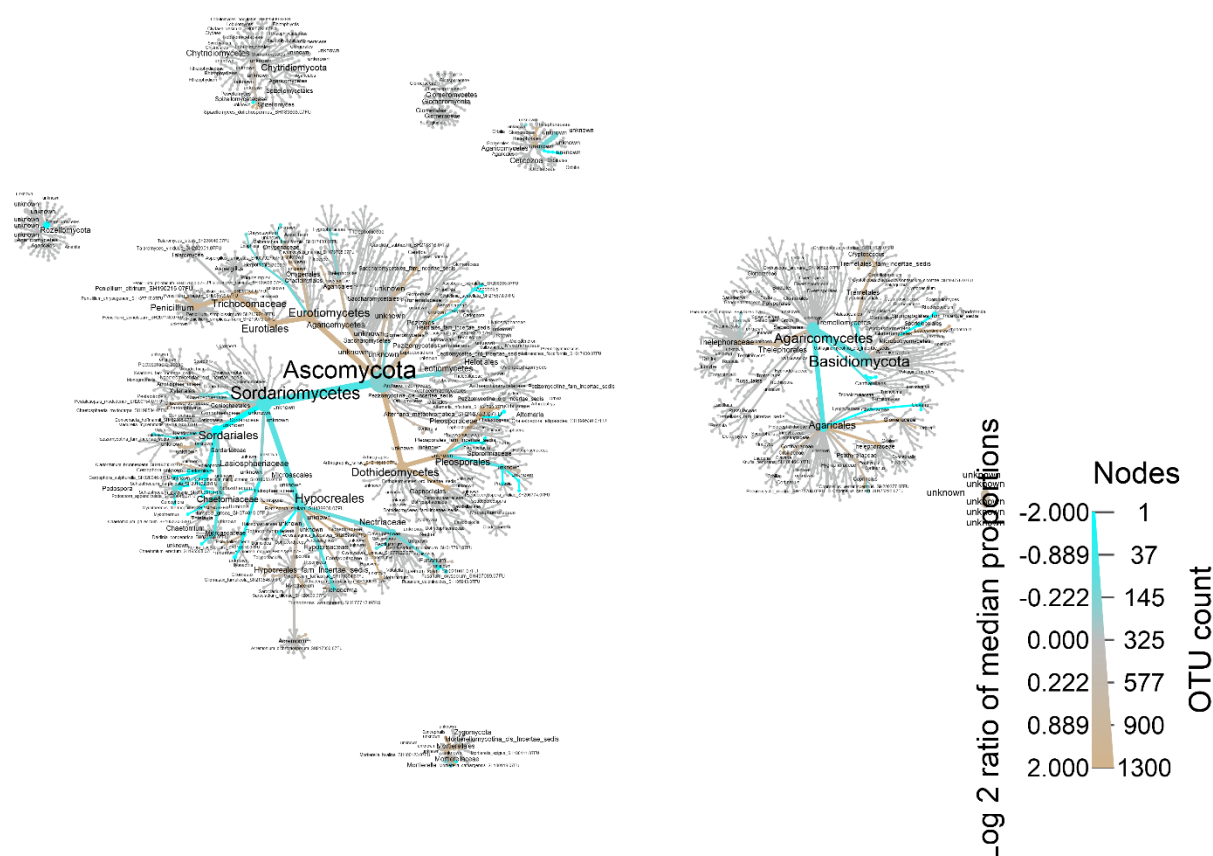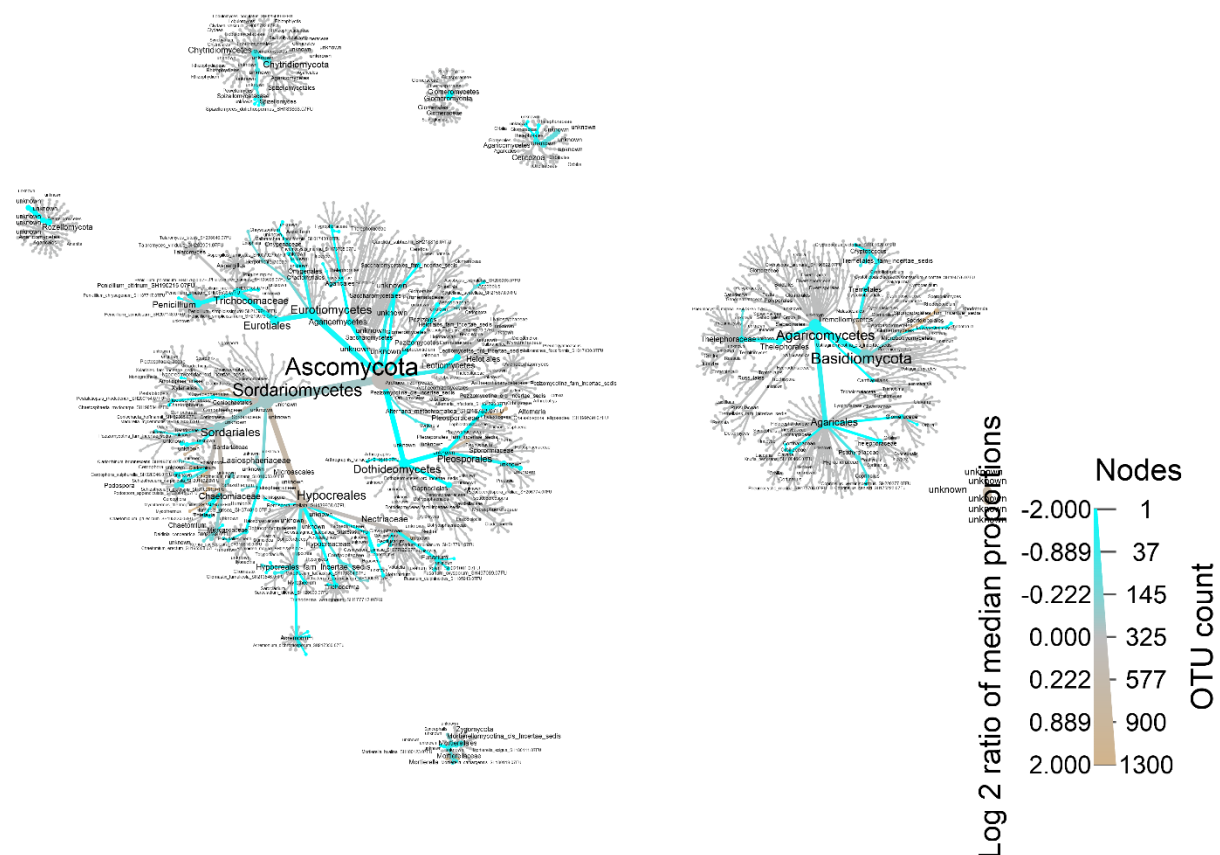


**Figure 4.21 Heat tree of the relative abundance of fungal species between plants with contrasting levels of rhizosheath homogalacturonan.** The relative difference in abundance is expressed as log2FoldChange with positive values (bay colour) indicating that the relative abundance of specific OTUs is higher in greater levels xyloglucan. Negative values (cyan colour) indicate that the relative abundance of specific OTUs is higher in lower levels xyloglucan. The size of nodes represents the abundance of rhizosphere fungi at the specific taxonomic rank. The graph is drawn with the R package—Metacoder (Foster *et al.*, 2017).
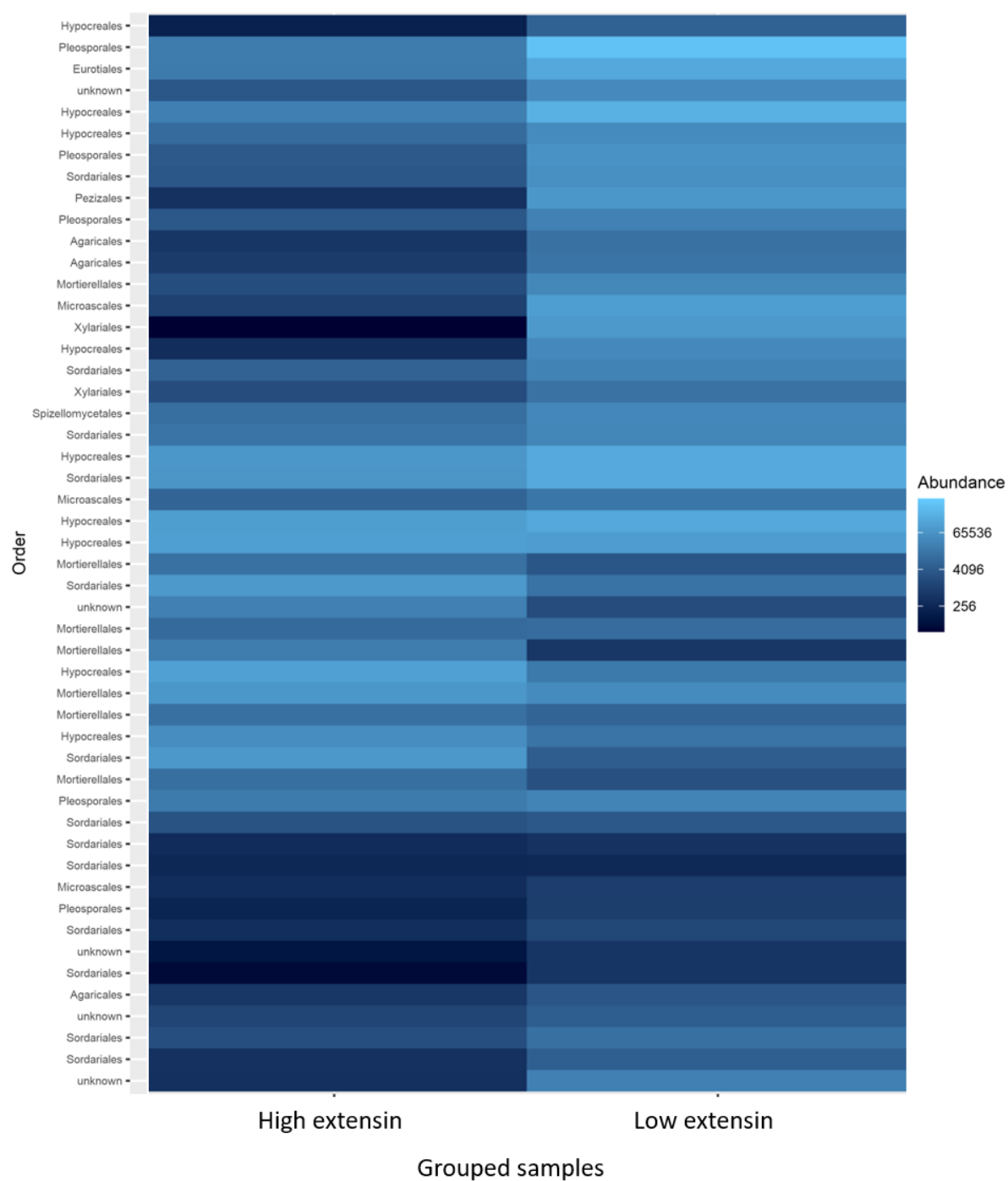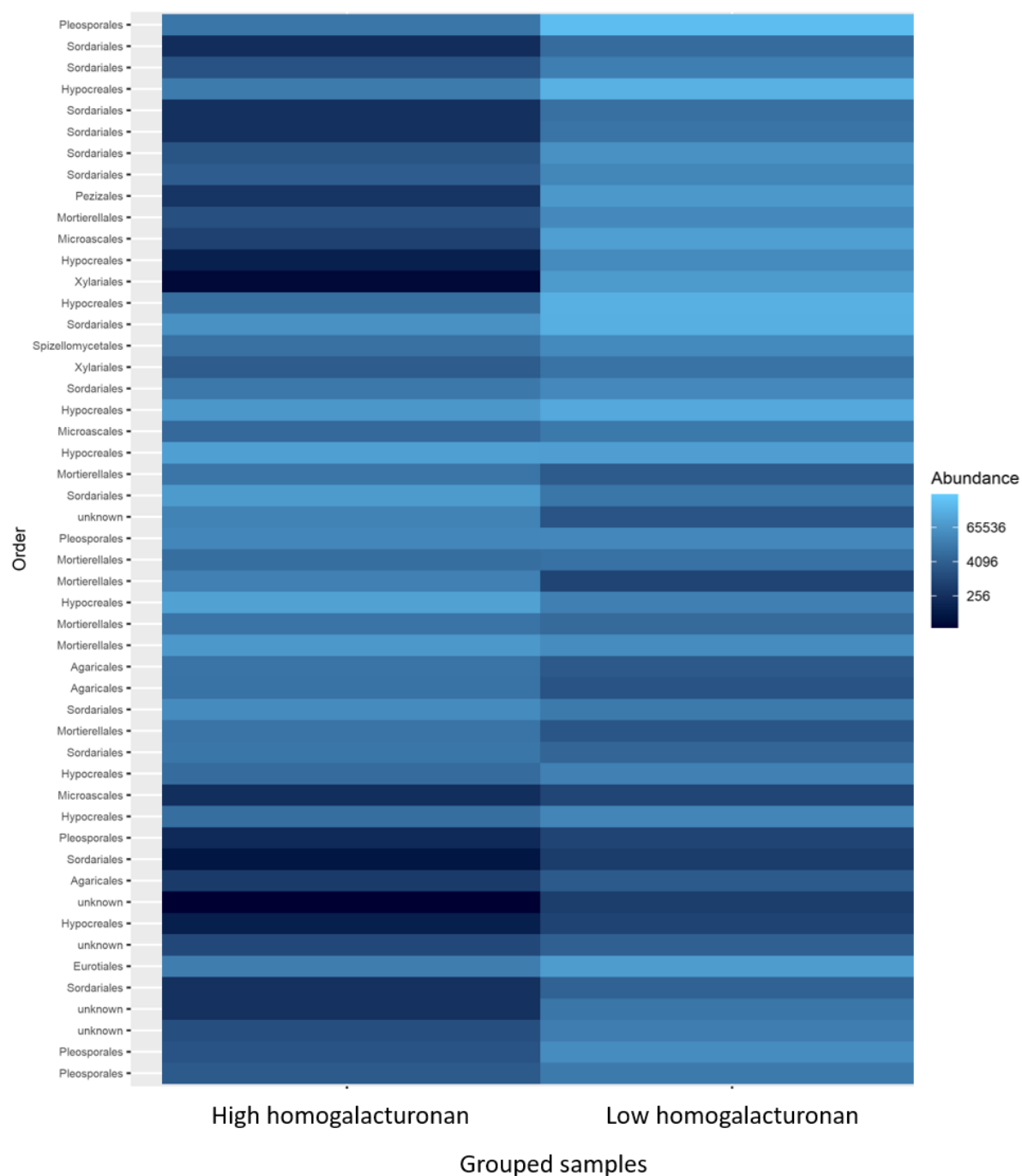
**Figure 4.22 Heat map of the 50 most abundant fungal species between plants with contrasting levels of rhizosheath homogalacturonan.** Blocks represent species, labelled by the order to which the species belong.

# 4.4.4.2.5 Seedling root angle

Fewer fungal species varied between genotypes with a narrow or wide root angle compared with the analyses run on genotype groups that differed in polysaccharide. Those that varied significantly in abundance were mainly from the Ascomycota and Basidiomycota phyla (Figures 4.23 and 4.24). Most Chytridiomycota tended to be more abundant in plants with wide angles. However one species, *Spizellomyces dolichospermus*, was more abundant in genotypes with narrow root angles. No information is available on the specific lifestyle of *S. dolichospermus* but species of this genus tend to be common in soil and occur as saprotrophs or parasites of mycorrhizal fungi (James *et al.*, 2006; Cannon and Kirk, 2007). Among the Basidiomycota, most of the significant taxa were more abundant in wide-angled plants. These included some saprophytic animal pathogens, namely *Cryptococcus aerius, C. terreus* and *Pneumocystis murina.* The exceptions were the saprophytic genera *Orbilia* and *Coprinellus,* which were more abundant in plants with narrow root angles. Among the Ascomycota, there was a similar distribution of fungal species with greater presence in wide-angled plants versus narrow-angled plants. They consisted of saprotrophs, possible symbiotrophs and animal pathogens. Of note, the well-known plant pathogen, *Fusarium oxysporum,* was more abundant in the rhizosheath of plants with wide root angles.
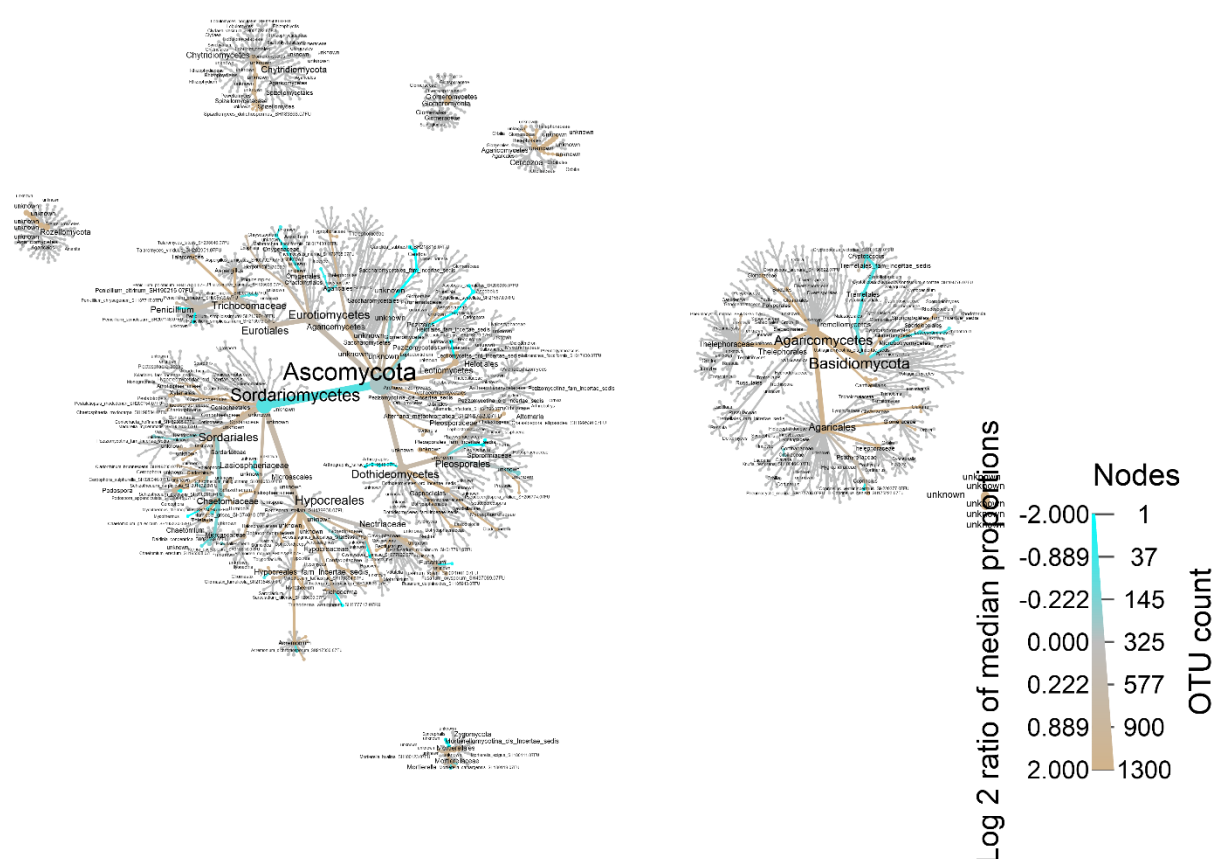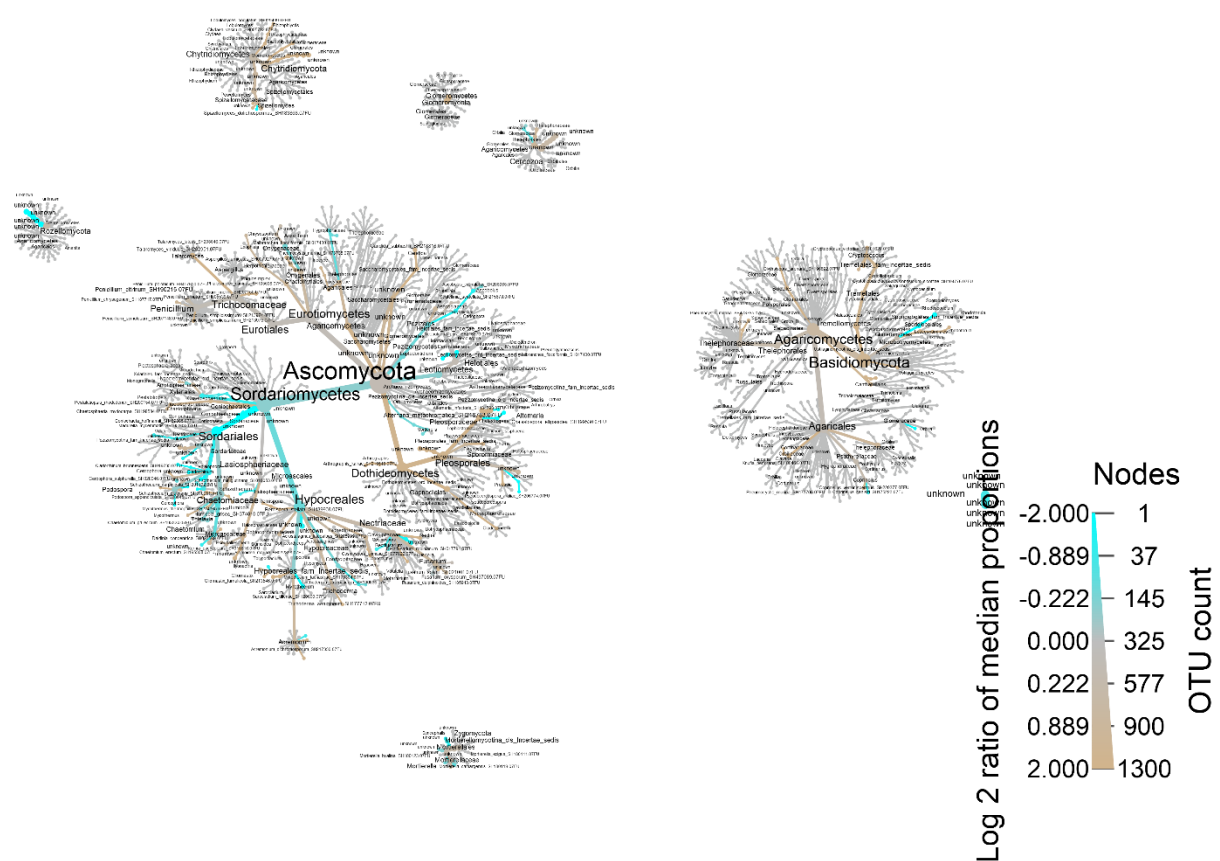
**Figure 4.23 Heat tree of the relative abundance of fungal species between plants with contrasting root angles.** The relative difference in abundance is expressed as log2FoldChange with positive values (bay colour) indicating that the relative abundance of specific OTUs is higher in plants with a wide root angle. Negative values (cyan colour) indicate that the relative abundance of specific OTUs is higher in plants with a narrow root angle. The size of nodes represents the abundance of rhizosphere fungi at the specific taxonomic rank. The graph is drawn with the R package—Metacoder (Foster *et al.*, 2017).
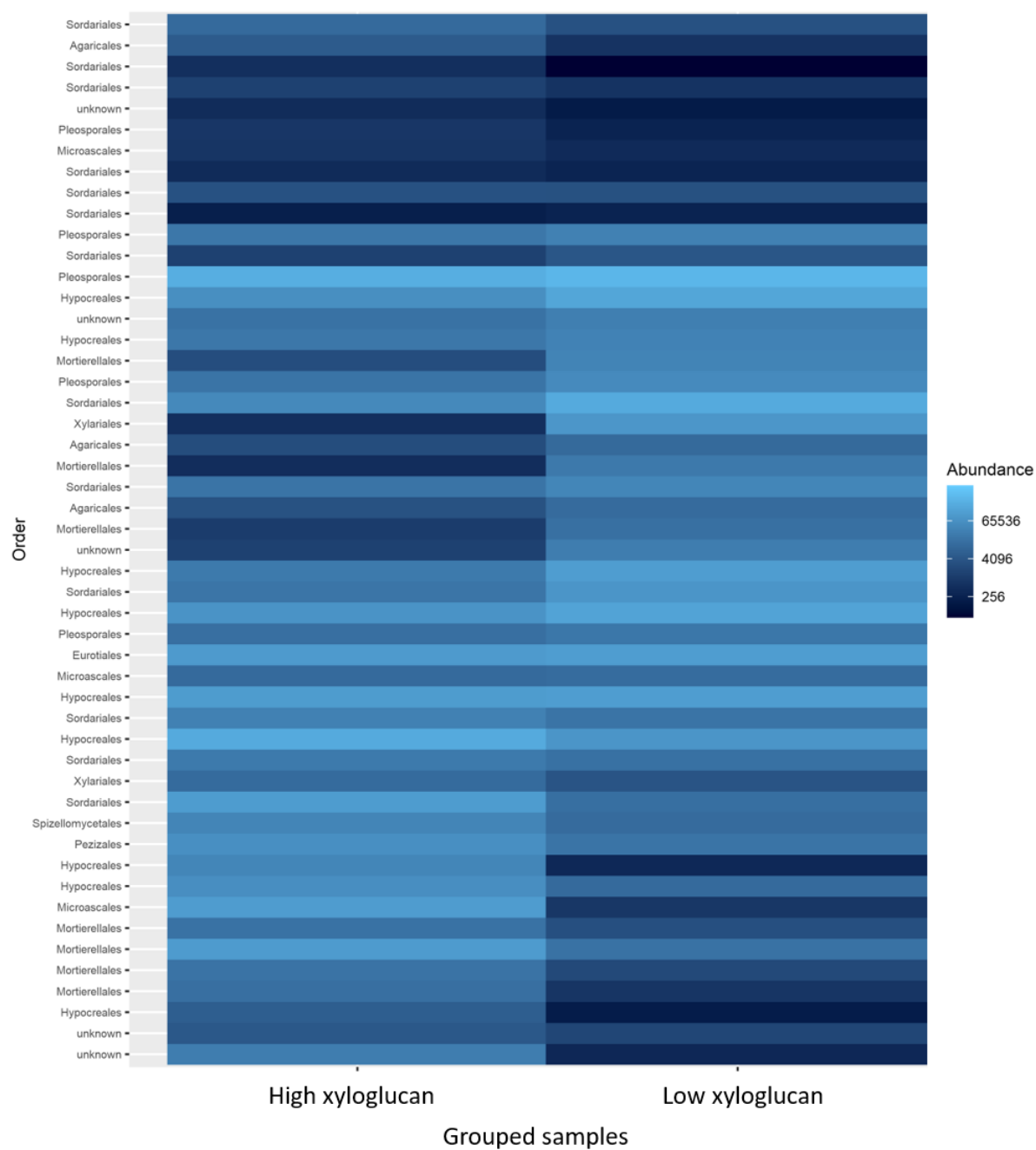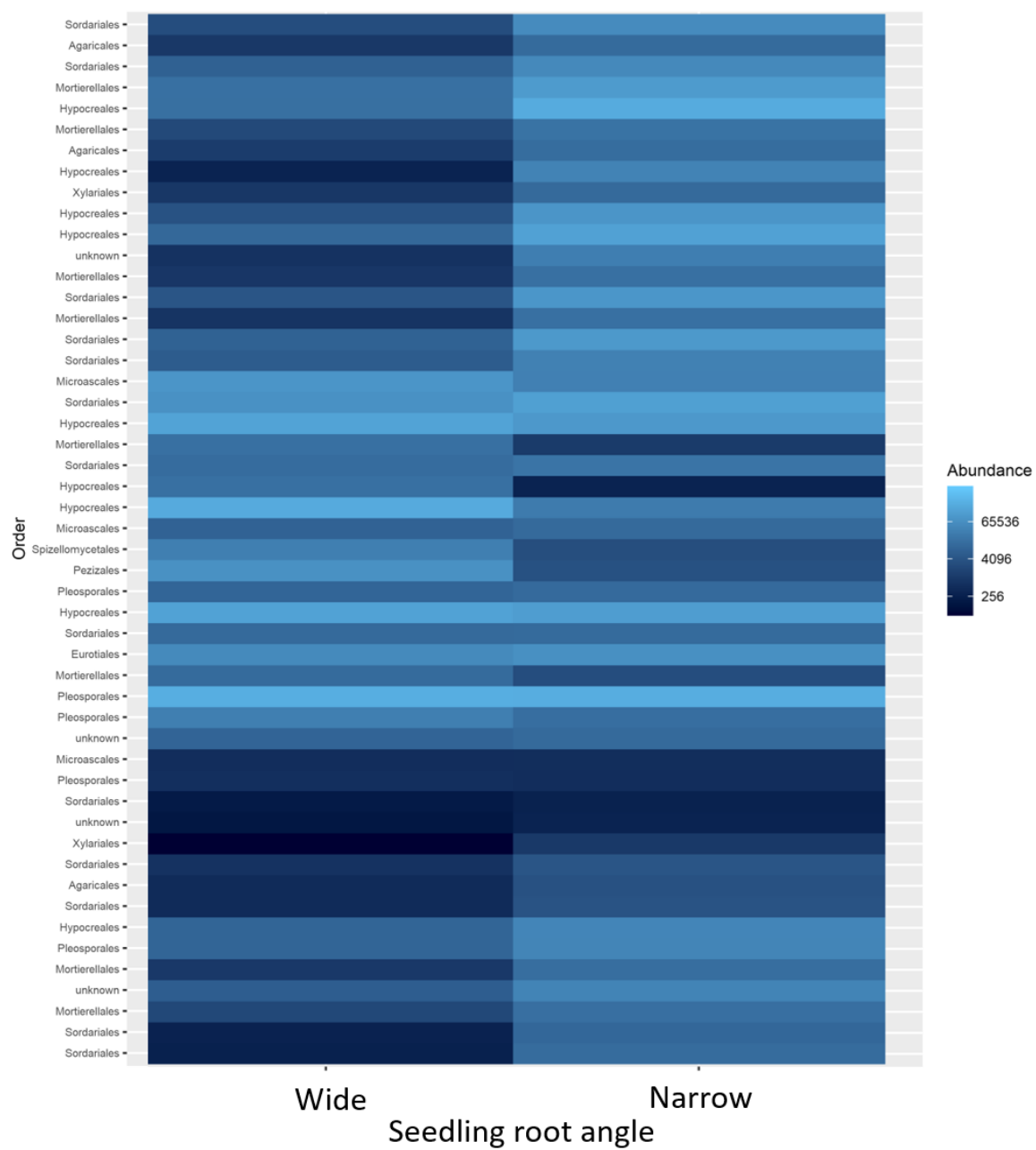
**Figure 4.24 Heat map of the 50 most abundant fungal species between plants with contrasting root angles.** Blocks represent species, labelled by the order to which the species belong.

# 4.4.4.2.6 Grain yield

High yielding genotypes had a greater abundance of Glomeromycota in the rhizosheath than lower yielding genotypes (Figures 2.25 and 2.26). Lower yielding genotypes had a greater abundance of certain Chytridiomycota, namely of the saprophytic *Spizellomyces* genus. There were significant differences among unknown species of the Cercozoa. There was a similar number of Zygomycota species (genus *Mortierella*, known saprophytes) with increased abundance in high yielding genotypes as there were in lower yielding genotypes. The same was true for the Ascomycota and Basidiomycota. In particular, low-yielding genotypes tended to have a greater abundance of the *Alternaria* species, *A. metachromatica*. While no record was available for this species, members of the same genus are known plant pathogens. In addition, species of the *Nectria* genus, which may be either saprophytes or pathogens, were more present in low-yielding genotypes. However, most identified taxa were assigned to the saprotrophic lifestyle by FUNGuild.
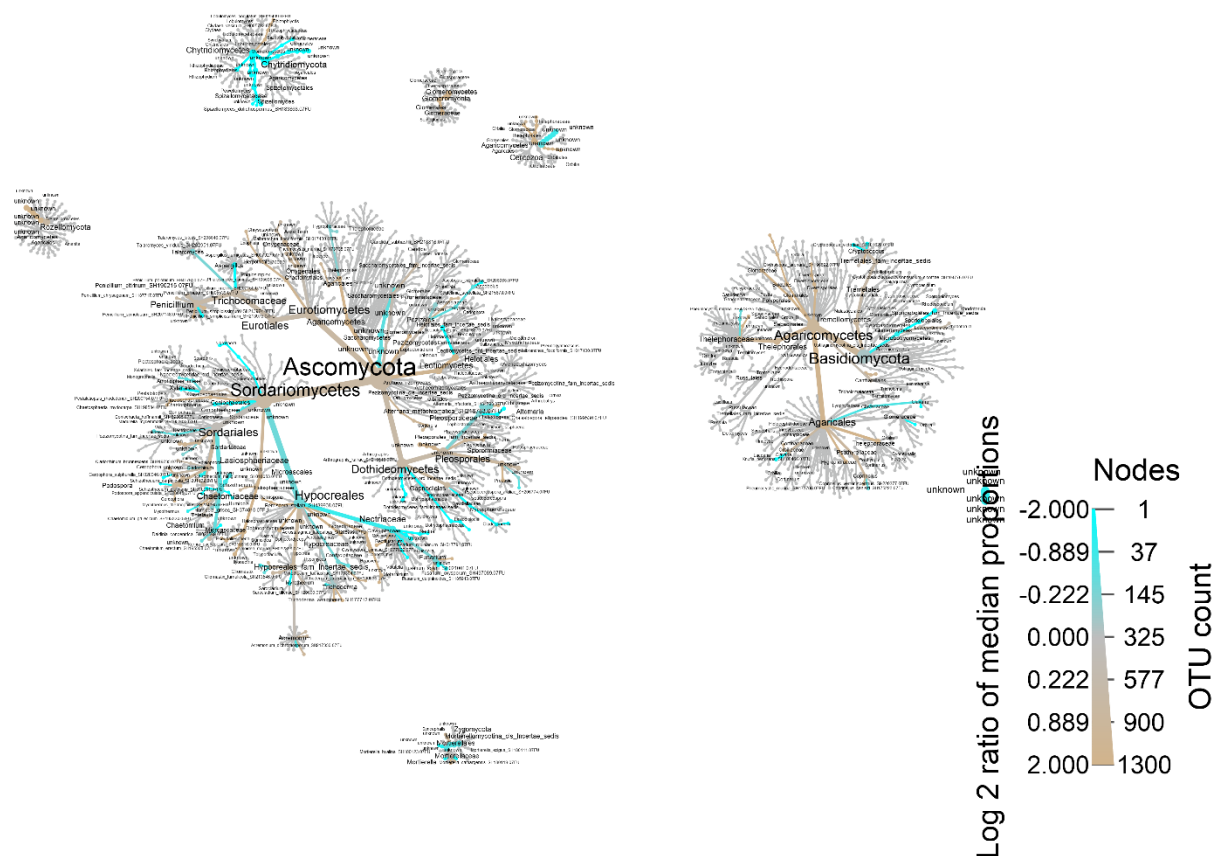
**Figure 2.25 Heat tree of the relative abundance of fungal species between wheat genotypes with contrasting grain yield.** The relative difference in abundance is expressed as log2FoldChange with positive values (bay colour) indicating that the relative abundance of specific OTUs is higher in plants with higher grain yield. Negative values (cyan colour) indicate that the relative abundance of specific OTUs is higher in plants with a lower grain yield. The size of nodes represents the abundance of rhizosphere fungi at the specific taxonomic rank. The graph is drawn with the R package–Metacoder (Foster *et al.*, 2017).
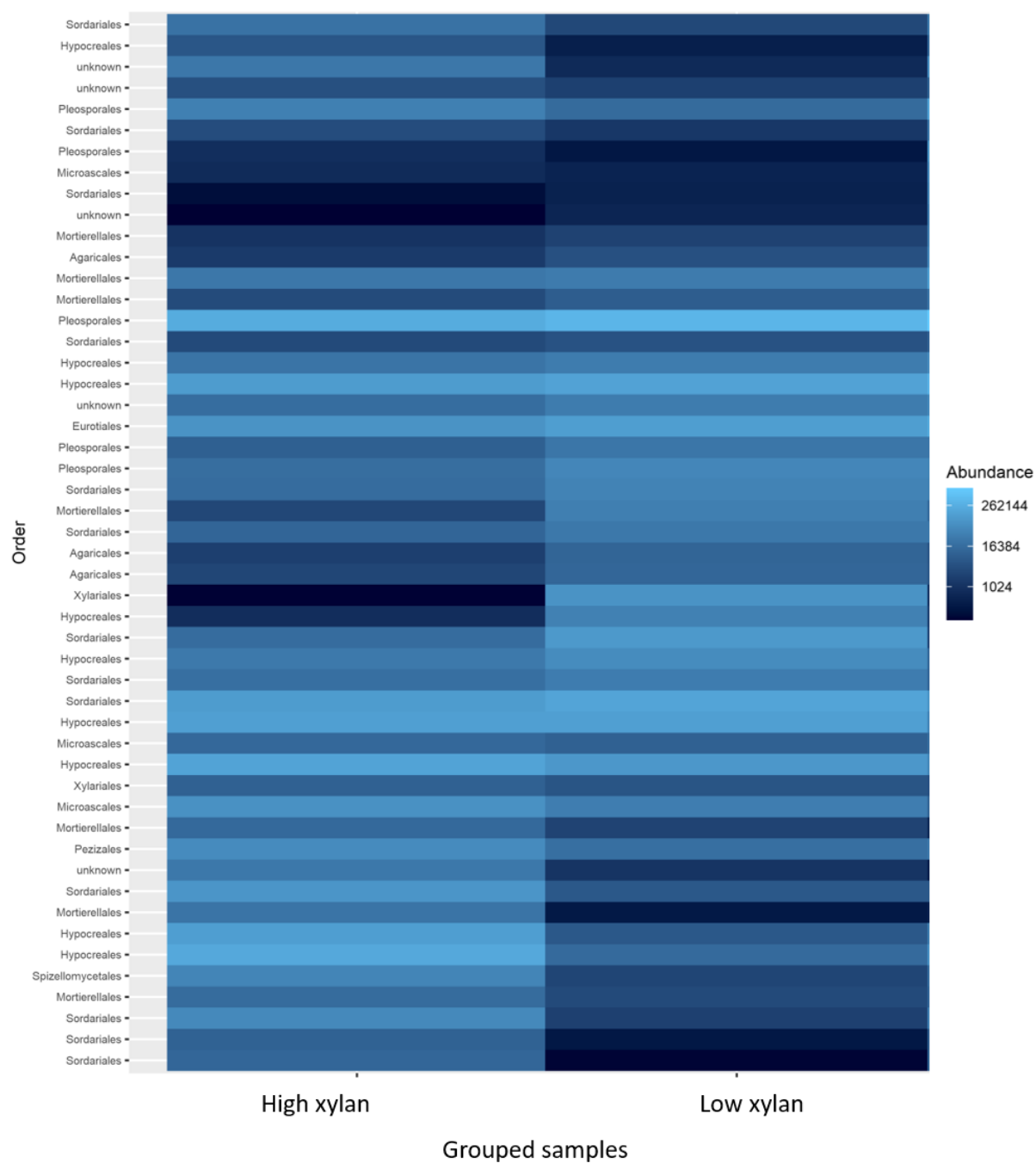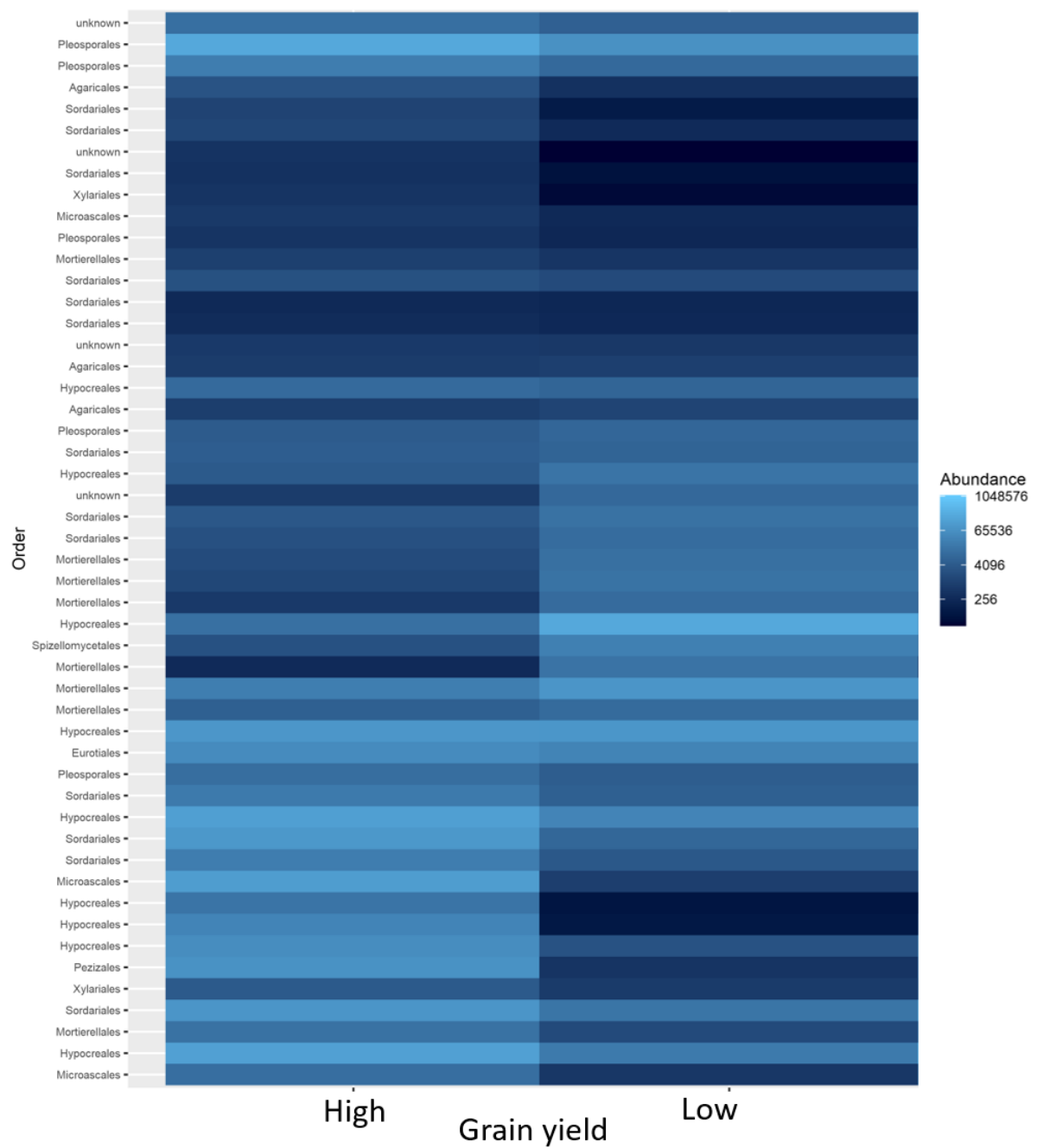
**Figure 2.26 Heat map of the 50 most abundant fungal species between plants with contrasting grain yield.** Blocks represent species, labelled by the order to which the species belong.

# 4.4.4.2.7 Soil with and without plants

The aim of soil supplementation was to test the effect of supplementing bulk soil with purified solutions of the specific polysaccharides, pectin, xylan, arabinogalactan protein, extensin and xyloglucan on the bacterial and fungal microbiome. As a control, soil samples with the same treatment were sterilised before supplementation. This could have indicated whether certain microbial taxa were particularly responsive to specific polysaccharides. The microbial profile of lines known to contain high or low levels of the polysaccharides in the rhizosheath would have provided additional support to the results of soil supplementation.

However, for a combination of reasons, including cost and repercussions from the covid-19 pandemic, sequencing results were not achieved for all of the samples, resulting in an incomplete dataset. As such, comparisons are not made here between the different polysaccharides.

# 4.4.4.3 Certain plant phenotypes correlated with differences in bacterial beta diversity

PERMANOVA results for bacterial beta diversity based on unweighted UniFrac (Table 4.12) and weighted UniFrac (Table 4.13) are reported. PERMANOVA on unweighted UniFrac resulted in a greater number of significant differences in beta diversity in contrasting levels of plant phenotypes.

Seven out of eleven phenotypes/conditions (seedling root angle, parental lines, and the concentrations of homogalacturonan, xyloglucan, AGP and heteroxylan) displayed a significant unweighted UniFrac difference in beta diversity between high and low levels, indicating a difference in the presence/absence of certain phyla (Table 4.12). There was no effect for root length, rhizosheath size, or concentration of xylan and extensin.

Testing weighted UniFrac distances revealed a significant difference in beta diversity between the parental lines, between the rhizosheath and supplemented soil, and between high and low levels of xyloglucan and AGP (Table 4.13). This suggests that samples with contrasting root angle, homogalacturonan and heteroxylan had differential presence of bacterial species but similar abundance of the present species.

**Table 4.12 Permutational multivariate analysis of variance (PERMANOVA) of unweighted UniFrac distance of bacterial diversity in the wheat rhizosphere.** Differences in beta diversity were tested for the rhizospheres of plants with contrasting phenotypes. Levels of significance are denoted by * (< 0.05); ** (< 0.01); *** (< 0.001).

| Plant phenotype | Df | Sum of Squares | Mean squares | F-model | p-value | Permutations |
|---|---|---|---|---|---|---|
| Seedling root angle | 2, 56 | 0.14 | 0.072 | 1.42 | 0.017* | 999 |
| Seedling root length | 1, 57 | 0.057 | 0.057 | 1.1 | 0.22 | 999 |
| Avalon vs Cadenza | 3, 3 | 0.21 | 0.069 | 2.2 | 0.0050** | 999 |
| Extensin (LM1) | 1, 54 | 0.067 | 0.067 | 1.2 | 0.091 | 999 |

| | | | | | | |
|---|---|---|---|---|---|---|
| Xylan (LM11) | 1, 49 | 0.065 | 0.065 | 1.2 | 0.15 | 999 |
| Homogalacturonan (LM19) | 1, 51 | 0.082 | 0.082 | 1.5 | 0.040* | 999 |
| Xyloglucan (LM25) | 1, 51 | 0.15 | 0.15 | 2.9 | 0.0020** | 999 |
| Arabinogalactan protein (LM2) | 1, 54 | 0.083 | 0.083 | 1.6 | 0.024* | 999 |
| Heteroxylan (LM27) | 1, 54 | 0.10 | 0.20 | 2.9 | 0.0040** | 999 |
| Rhizosheath size | 1, 48 | 0.052 | 0.052 | 0.96 | 0.48 | 999 |
| Grain yield | 1, 36 | 0.069 | 0.069 | 1.3 | 0.097 | 999 |

**Table 4.13 Permutational multivariate analysis of variance (PERMANOVA) of weighted UniFrac distance of bacterial diversity in the wheat rhizosphere.** Differences in beta diversity were tested for the rhizospheres of plants with contrasting phenotypes. Levels of significance are denoted by * (< 0.05); ** (< 0.01); *** (< 0.001).

| Plant phenotype | Df | Sum of Squares | Mean squares | F-model | p-value | Permutations |
|---|---|---|---|---|---|---|
| Plant phenotype | 2, 56 | 0.12 | 0.059 | 1.3 | 0.15 | 999 |
| Seedling root angle | 1, 57 | 0.057 | 0.057 | 1.1 | 0.20 | 999 |
| Seedling root length | 6, 3 | 0.31 | 0.051 | 3.4 | 0.005** | 999 |
| Avalon vs Cadenza | 3, 3 | 0.14 | 0.046 | 5.5 | 0.006** | 999 |
| Extensin (LM1) | 1, 54 | 0.04019 | 0.040189 | 1.2 | 0.22 | 999 |
| Xylan (LM11) | 1, 49 | 0.060 | 0.060 | 1.5 | 0.14 | 999 |
| Homogalacturonan (LM19) | 1, 51 | 0.058 | 0.058 | 1.6 | 0.1 | 999 |
| Xyloglucan (LM25) | 1, 51 | 0.11 | 0.11 | 3.1 | 0.004** | 999 |
| Arabinogalactan protein (LM2) | 1, 54 | 0.063 | 0.063 | 1.8 | 0.049* | 999 |
| Heteroxylan (LM27) | 1, 54 | 0.065 | 0.065 | 1.9 | 0.051 | 999 |
| Rhizosheath size | 1, 48 | 0.052 | 0.052 | 1.3 | 0.20 | 999 |
| Grain yield | 1, 36 | 0.035 | 0.035 | 0.80 | 0.58 | 999 |

PCA plots based on VST data displayed distinct clustering for certain conditions. For example, there were distinct clusters which separated along the x-axis for the parental genotypes, with PC1 explaining 66% variance (Figure 4.27 A). The soil supplemented with Avalon and Cadenza

exudates clustered together, suggesting that the difference between plants growing in the soil and no plants growing was larger than the effect of parental genotype on the exudate (Figure 4.27 A). The other conditions identified as significant by PERMANOVA did not display distinct clusters, as illustrated by Figures 4.27 B and 4.27 C.  For seedling root angle, genotypes with narrow angles generally had greater contribution of PC2 than genotypes with wide angles but did not separate clearly (Figure 4.27 B). Of all polysaccharides, xyloglucan displayed the most distinct separation between high and low levels and PC1 explained 27% of variation (Figure 4.27 C).
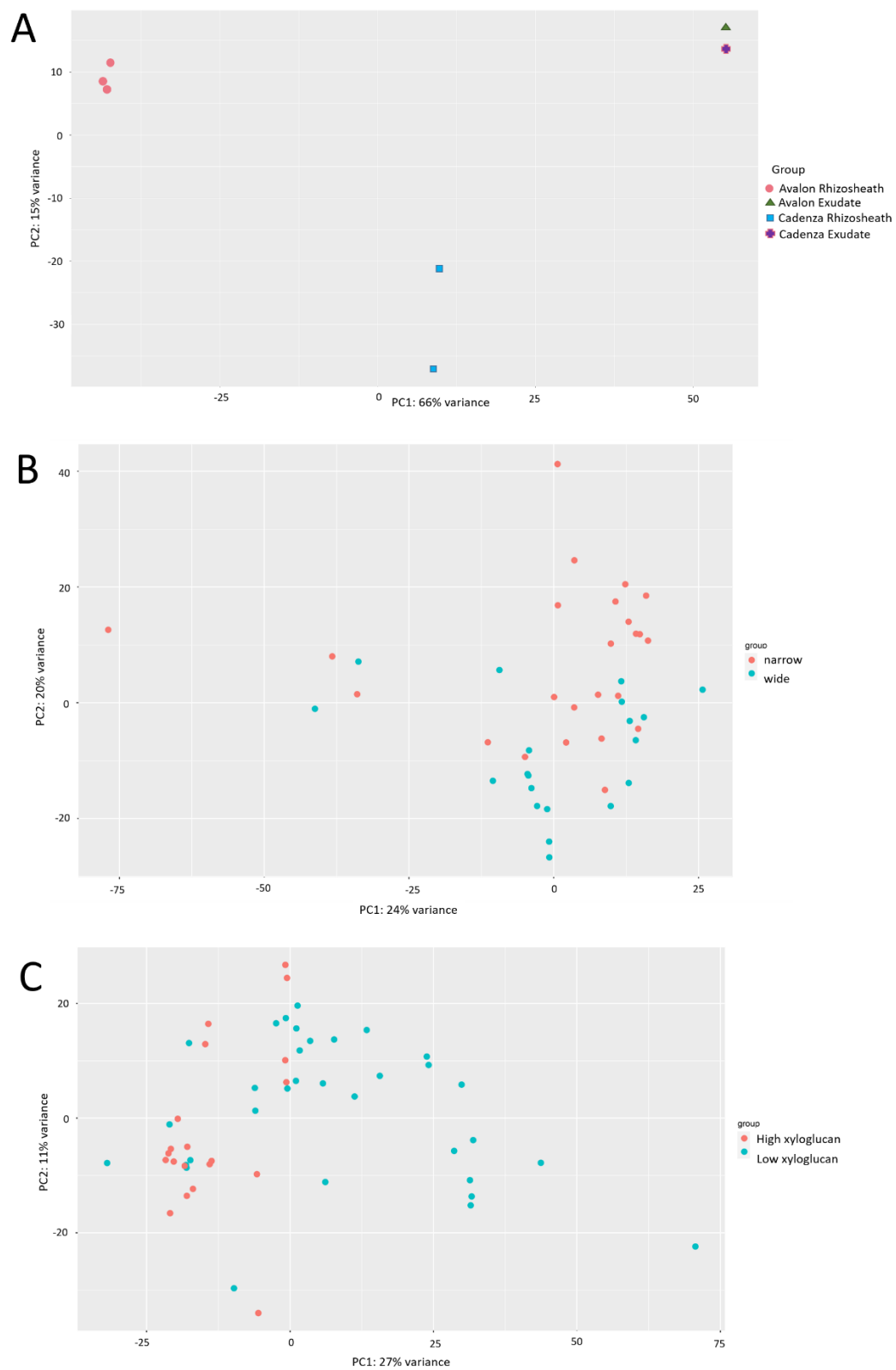
**Figure 4.27 Principal coordinate analysis (PCA) plot based on soil abundance of bacterial OTUs.** Samples were taken from the rhizosheath of wheat cultivars or from soil supplemented with polysaccharides. (A) parental genotypes (B) plants contrasting for root angle (C) plants contrasting for rhizosheath xyloglucan level.

# 4.4.4.4 Differential abundance of bacterial taxa between phenotypic groups

For closer investigation of which taxa differed significantly between the rhizosheaths of plants with contrasting phenotypes, the Wald test and Wilcoxon pairwise test were applied.

## 4.4.4.4.1 Xyloglucan

Plants with differing levels of xyloglucan had significant variation in bacterial beta diversity based on unweighted and weighted UniFrac distance (Tables 4.12 and 4.13). Most species showing differential abundance were of the Proteobacteria, Bacteroidetes, Firmicutes and Actinobacteria phyla (Figures 4.28 and 4.29). According to the Wald test, 2 Chlamydiae species, 1 Verrucomicrobia species and 2 Acidobacteria species were significantly more abundant the rhizosheath of plants with high levels of xyloglucan

Among the Actinobacteria, some species were more abundant in the rhizosheath of plants with high levels and some with low levels of xyloglucan. OTUs assigned to the *Propionibacteriaceae* and *Micrococcaceae* families were more abundant in low xyloglucan while *Nocardioidaceae* were more abundant in high xyloglucan.

Most of the Bacteriodetes showing differential abundance were of the *Flavobacteriaceae* family and were more abundant in the rhizosheath of plants with low levels of xyloglucan. Other Bacteroidetes families were more abundant in high levels of xyloglucan, including few species from the *Cytophagales*, *Chitinophagaceae* and *Sphingobacteriales*.

Most of the Firmicutes showing differential abundance were of the *Paenibacillus* genus and were more abundant in low levels. *Bacillus* and *Clostridium* genera were also more abundant in low levels while *Cohnella* species were more abundant in high levels.

The Proteobacteria comprised the largest phylum. Among Proteobacteria classes, the Alphaproteobacteria, Deltaproteobacteria and Rhizobiales primarily showed higher levels of abundance in high levels of xyloglucan, with the exception of the genera, *Syntrophobacter* and *Pelobacter*. Among the Betaproteobacteria, the dominating order was the Burkholderiales, which

showed variation in differential abundance at the genus level. Most significantly different Gammaproteobacteria were more abundant in the rhizosheath of plants with low levels of xyloglucan.



**Figure 4.28 Heat tree of the relative abundance of bacterial species between plants with contrasting levels of rhizosheath xyloglucan.** The relative difference in abundance is expressed as log2FoldChange with positive values (bay colour) indicating that the relative abundance of specific OTUs is higher in greater levels xyloglucan. Negative values (cyan colour) indicate that the relative abundance of specific OTUs is higher in lower levels xyloglucan. The size of nodes represents the abundance of rhizosphere fungi at the specific taxonomic rank. The graph is drawn with the R package—Metacoder (Foster *et al.*, 2017).

**Figure 4.29 Heat map of the 50 most abundant fungal species between plants with contrasting levels of rhizosheath xyloglucan.** Blocks represent species, labelled by the order to which the species belong.

## 4.4.4.4.2 Homogalacturonan

Plants with differing levels of homogalacturonan had significant variation in bacterial beta diversity based on unweighted UniFrac distance (Figures 4.30 and 4.31). Most species showing differential abundance were of the phyla, Bacteroidetes, Proteobacteria, Firmicutes and Actinobacteria, with a smaller number of species from the pyla, Chlamydiae, Acidobacteria and Ignavibacteriae. The overall pattern was for greater abundance of bacteria in the rhizosheath of plants with lower levels of homogalacturonan. The exception comprised the Clostridiales order in the Firmicutes phylum.
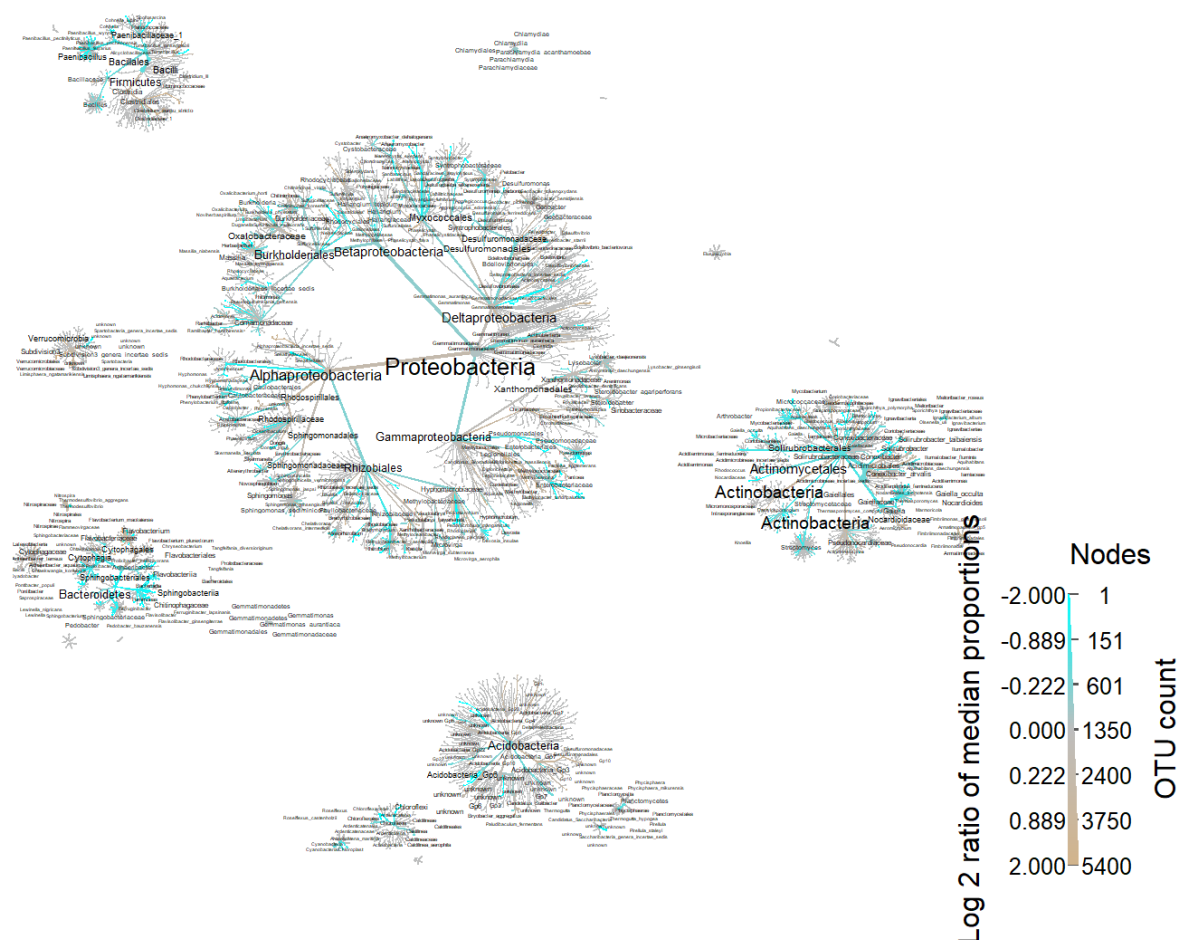


**Figure 4.30 Heat tree of the relative abundance of bacterial species between plants with contrasting levels of rhizosheath homogalacturonan.** The relative difference in abundance is expressed as log2FoldChange with positive values (bay colour) indicating that the relative abundance of specific OTUs is higher in greater levels homogalacturonan. Negative values (cyan colour) indicate that the relative abundance of specific OTUs is higher in lower levels homogalacturonan. The size of nodes represents the abundance of rhizosphere fungi at the specific taxonomic rank. The graph is drawn with the R package—Metacoder (Foster *et al.*, 2017).

**Figure 4.31 Heat map of the 50 most abundant fungal species between plants with contrasting levels of rhizosheath homogalacturonan.** Blocks represent species, labelled by the order to which the species belong.

# 4.4.4.4.3 Heteroxylan

Plants with differing levels of heteroxylan had significant variation in bacterial beta diversity based on unweighted UniFrac distance. Most species showing differential abundance were from the phyla, Proteobacteria, Bacteroidetes, Firmicutes and Actinobacteria, with a smaller number of species from the phyla, Chlamydiae, Verrucomicrobia, Acidobacteria and Ignavibacteriae (Figures 4.32 and 4.33).

Plants with high levels of heteroxylan were enriched in OTUs assigned to the Actinobacteria (notably the *Arthrobacter* genus), the Acidobacteria (namely the Desulfovibrionaceae order) and the Chlamydia phyla.

For the Bacteroidetes, the *Flavobacterium* genus dominated the significantly enriched species and was of greater abundance in low levels of heteroxylan. However, the *Chitinophagaceae* and *Cytophagaceae* families were more enriched in the rhizosheath of plants with high levels of heteroxylan.

The *Paenibacillus* genus dominated the differentially abundant OTUs assigned to the Firmicutes. While *Paenibacillus* and *Clostridium* species were more abundant in lower heteroxylan levels, *Saccharibacillus* species were more abundant in high levels.

There were mixed responses among the Proteobacteria. For example, the *Pseudomonas* genus was enriched in rhizosheaths containing high levels of heteroxylan, while for the Rhizobiales order, certain species were enriched in high levels and some in low levels of heteroxylan. The Enterobacteriales order was mostly enriched in low levels with a few exceptions. The Betaproteobacteria (dominated by the Burkholderiales order), Deltaproteobacteria (dominated by Bdellovibrionales) and Gammaproteobacteria (dominated by Pantoea) were mainly enriched rhizosheaths with low levels of heteroxylan.

Of the Verrucomicrobia, 2 were enriched in low levels and 1 in high levels of heteroxylan.
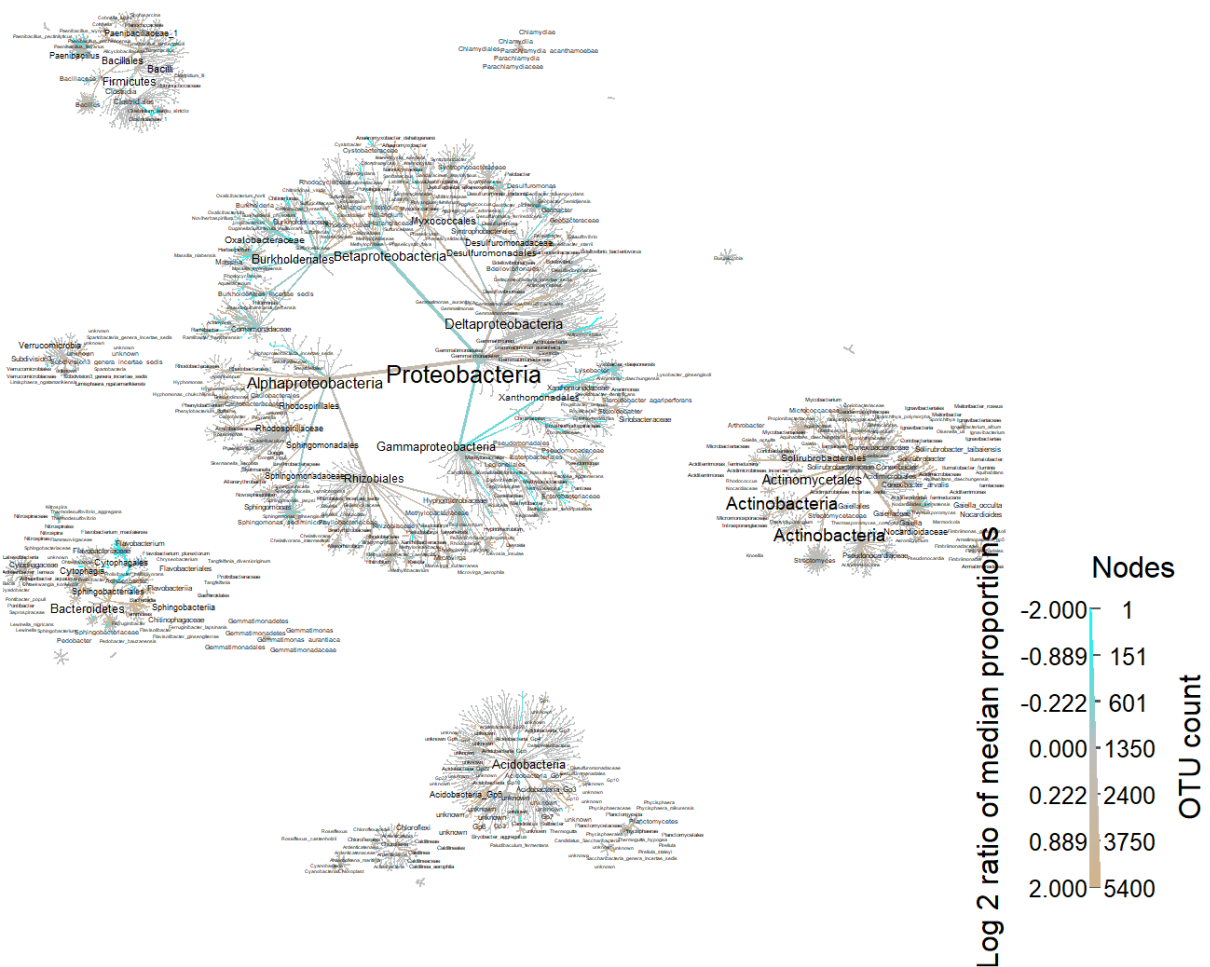
**Figure 4.32 Heat tree of the relative abundance of bacterial species between plants with contrasting levels of rhizosheath heteroxylan.** The relative difference in abundance is expressed as log2FoldChange with positive values (bay colour) indicating that the relative abundance of specific OTUs is higher in greater levels heteroxylan. Negative values (cyan colour) indicate that the relative abundance of specific OTUs is higher in lower levels heteroxylan. The size of nodes represents the abundance of rhizosphere fungi at the specific taxonomic rank. The graph is drawn with the R package—Metacoder (Foster *et al.*, 2017).

**Figure 4.33 Heat map of the 50 most abundant fungal species between plants with contrasting levels of rhizosheath heteroxylan.** Blocks represent species, labelled by the order to which the species belong.

# 4.4.4.4.4 Arabinogalactan protein

As plant genotypes displayed similar patterns of heteroxylan and AGP in their rhizosheath, the differential abundance of bacteria was similar between the two polysaccharides (Figures 4.34 and 4.35). However, plants with differing levels of AGP had significant variation in bacterial beta diversity based on both weighted and unweighted UniFrac distance, and five additional OTUs were found to vary significantly compared with heteroxylan.
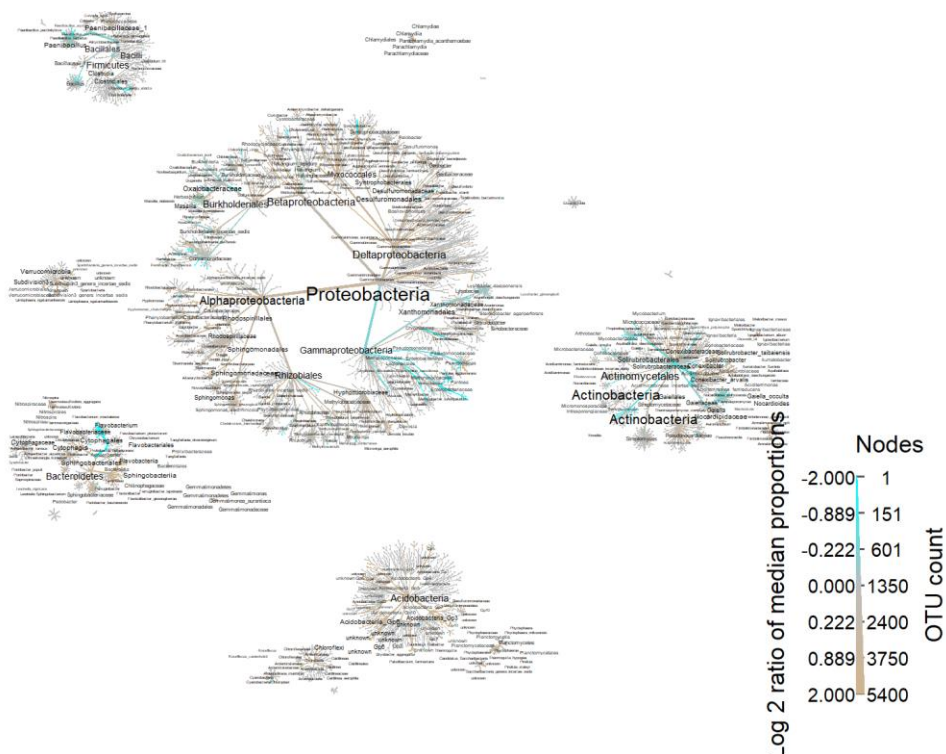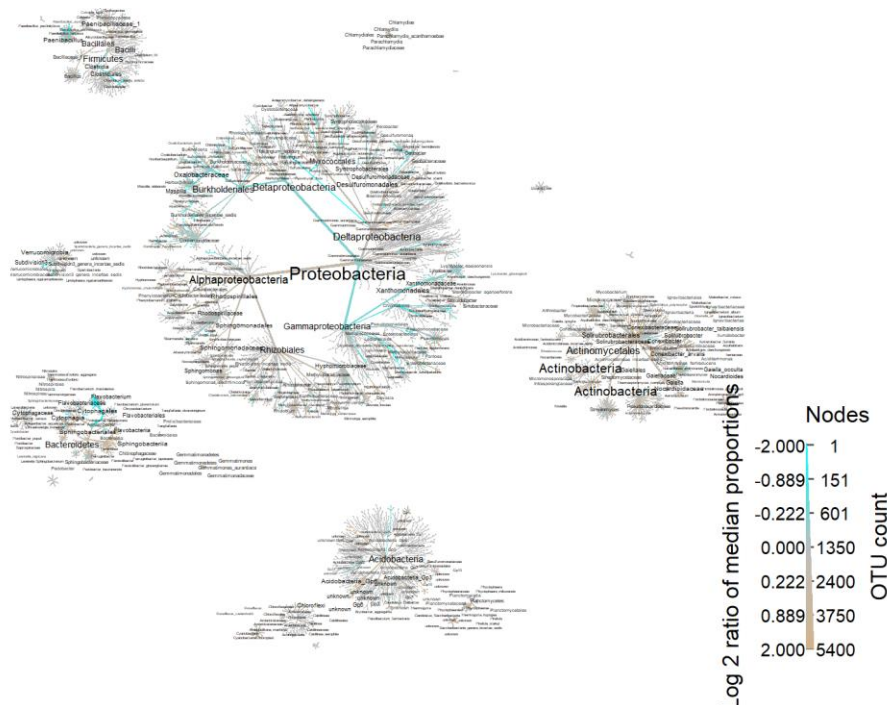


**Figure 4.34 Heat tree of the relative abundance of bacterial species between plants with contrasting levels of rhizosheath arabinogalactan protein.** The relative difference in abundance is expressed as log2FoldChange with positive values (bay colour) indicating that the relative abundance of specific OTUs is higher in greater levels AGP. Negative values (cyan colour) indicate that the relative abundance of specific OTUs is higher in lower levels AGP. The size of nodes represents the abundance of rhizosphere fungi at the specific taxonomic rank. The graph is drawn with the R package–Metacoder (Foster *et al.*, 2017).
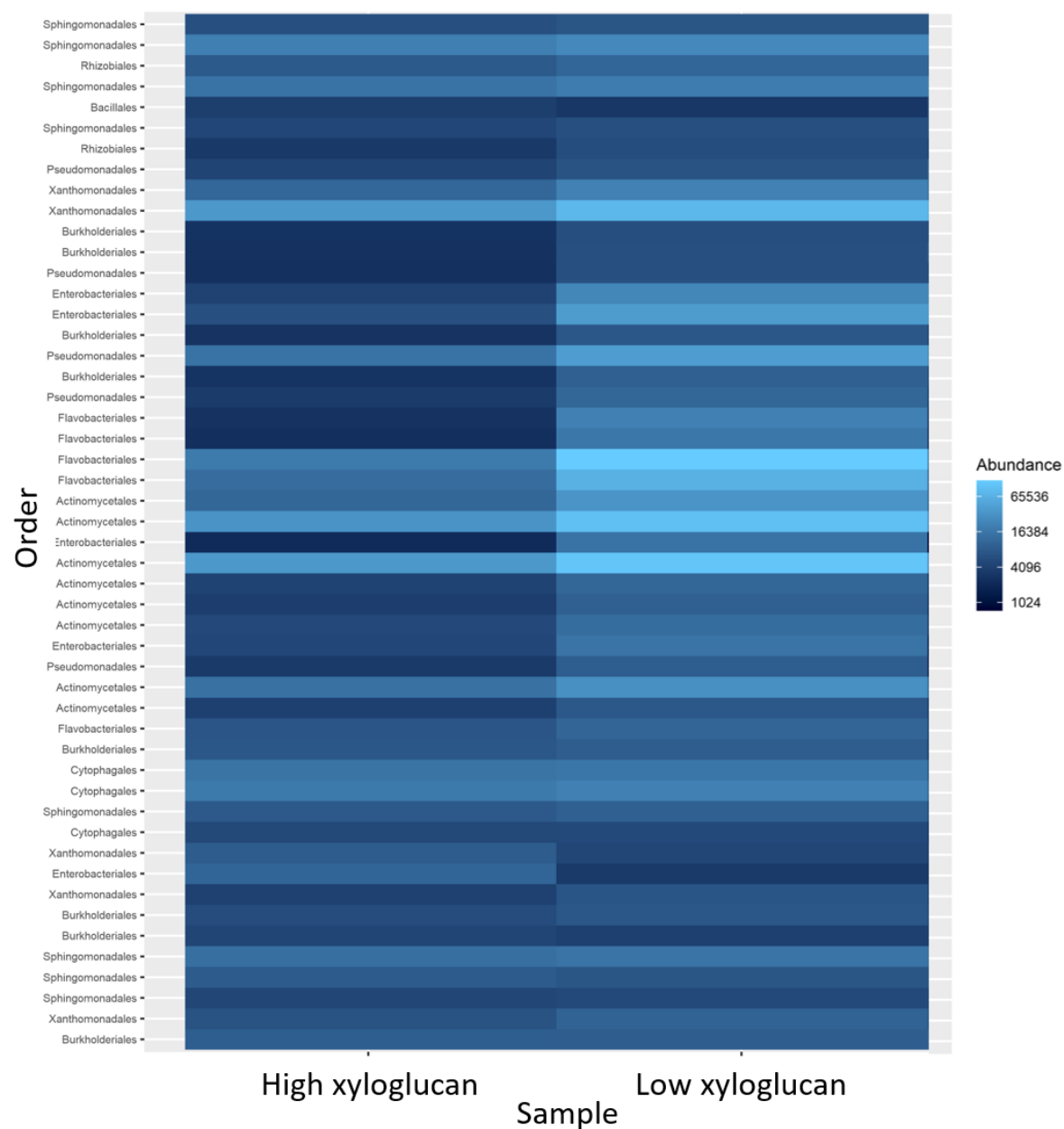
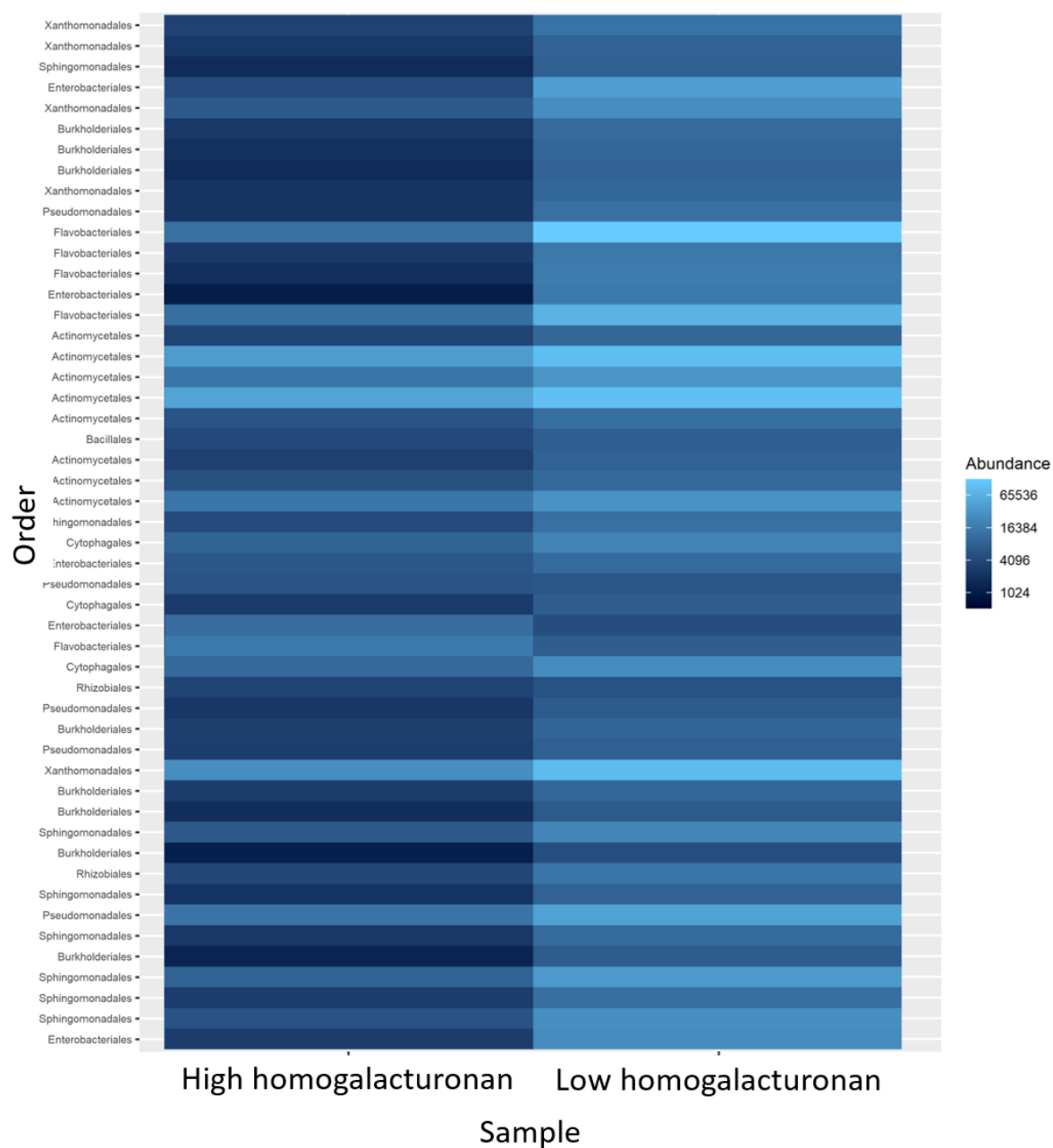**Figure 4.35 Heat map of the 50 most abundant fungal species between plants with contrasting levels of rhizosheath Arabinogalactan protein.** Blocks represent species, labelled by the order to which the species belong.

# 4.4.4.4.5 Parental lines

Cultivars, Avalon and Cadenza, showed significant variation in bacterial beta diversity based on weighted and unweighted UniFrac distance (Figures 4.36 and 4.37). Most of the OTUs that displayed differential abundance between the parents, Avalon and Cadenza, belonged to the Proteobacteria. Similar numbers of the less abundant phyla showed differential abundance, and a greater number of phyla were represented than when comparing groups of the AxC tails differing for a specific phenotype. Phyla with OTUs showing differential expression between cvs. Avalon and Cadenza included the Actinobacteria, Bacteroidetes, Acidobacteria, Firmicutes, Elusimicrobia, Gemmatimonadetes, Nitrospirae, Planctomycetes, Poribacteria and Verrucamicrobia.

Overall Actinobacteria were more abundant in Avalon but specific species were more abundant in Cadenza, such as certain species of the genera, Streptomyces and Nocardia.

A similar number of Acidobacteria species were favoured in Avalon rhizosheaths as Cadenza rhizosheaths.

Among the Bacteroidetes, the Cytophagales, Flavobacteriales and Sphingobacteriales were overall more abundant in Avalon, although certain genera such as *Pedobacter* were more abundant in Cadenza. Globally less common phyla, the Elusimicrobia, Gemmatimonadetes and Plancomycetes, were more abundant in Cadenza. Among the Firmicutes, the Wald test detected differential abundance in the Bacillales order, which were more abundant in Cadenza. Some Proteobacteria species were more abundant in Avalon while others were more abundant in Cadenza. This was the case across all classes of Proteobacteria. However, there was noticeable consistency in all *Oxalobacteraceae* species, which were more abundant in Avalon, and all *Rhodospirillaceae*, which were more abundant in Cadenza.
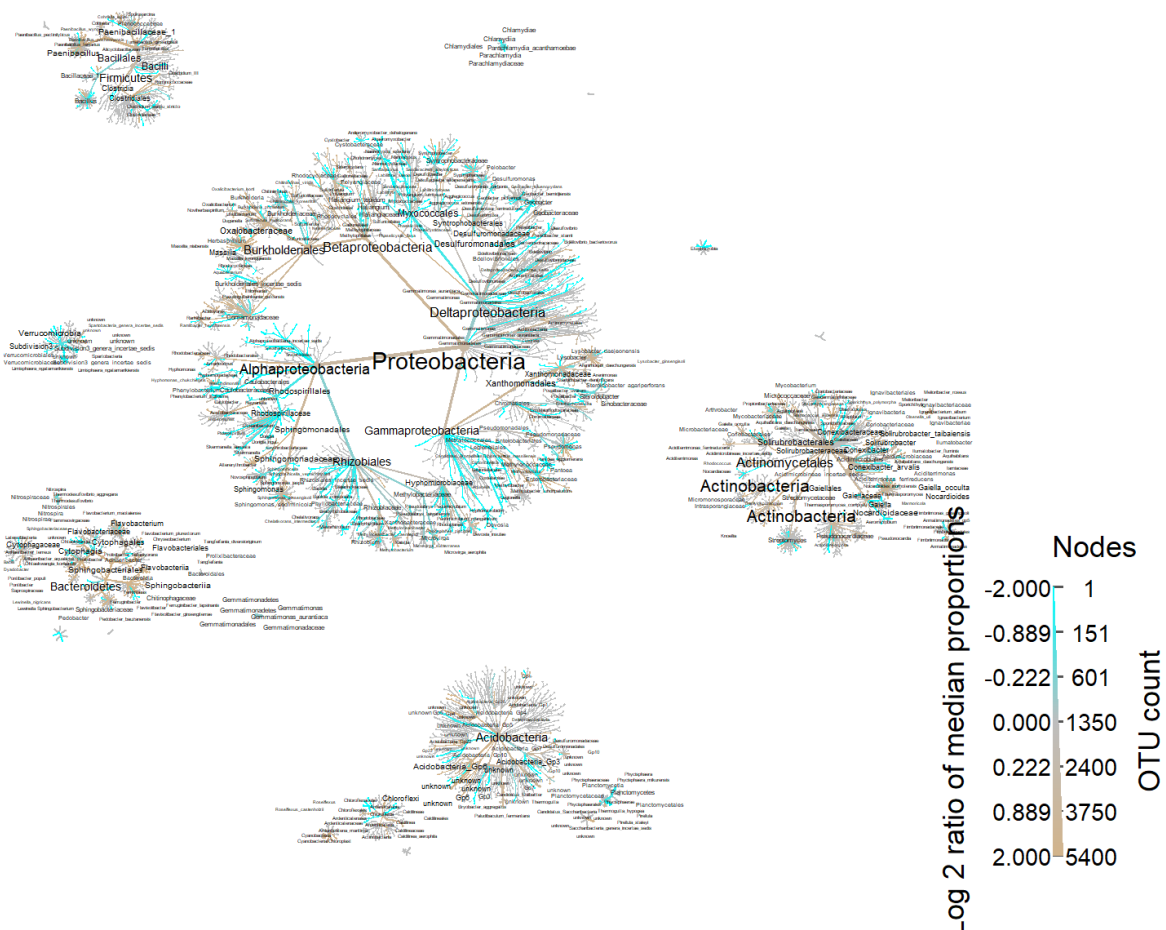
**Figure 4.36. Heat tree of the relative abundance of bacterial species between wheat varieties, Avalon and Cadenza.** The relative difference in abundance is expressed as log2FoldChange with positive values (bay colour) indicating that the relative abundance of specific OTUs is higher in Cadenza. Negative values (cyan colour) indicate that the relative abundance of specific OTUs is higher in Avalon. The size of nodes represents the abundance of rhizosphere fungi at the specific taxonomic rank. The graph is drawn with the R package–Metacoder (Foster *et al.*, 2017).
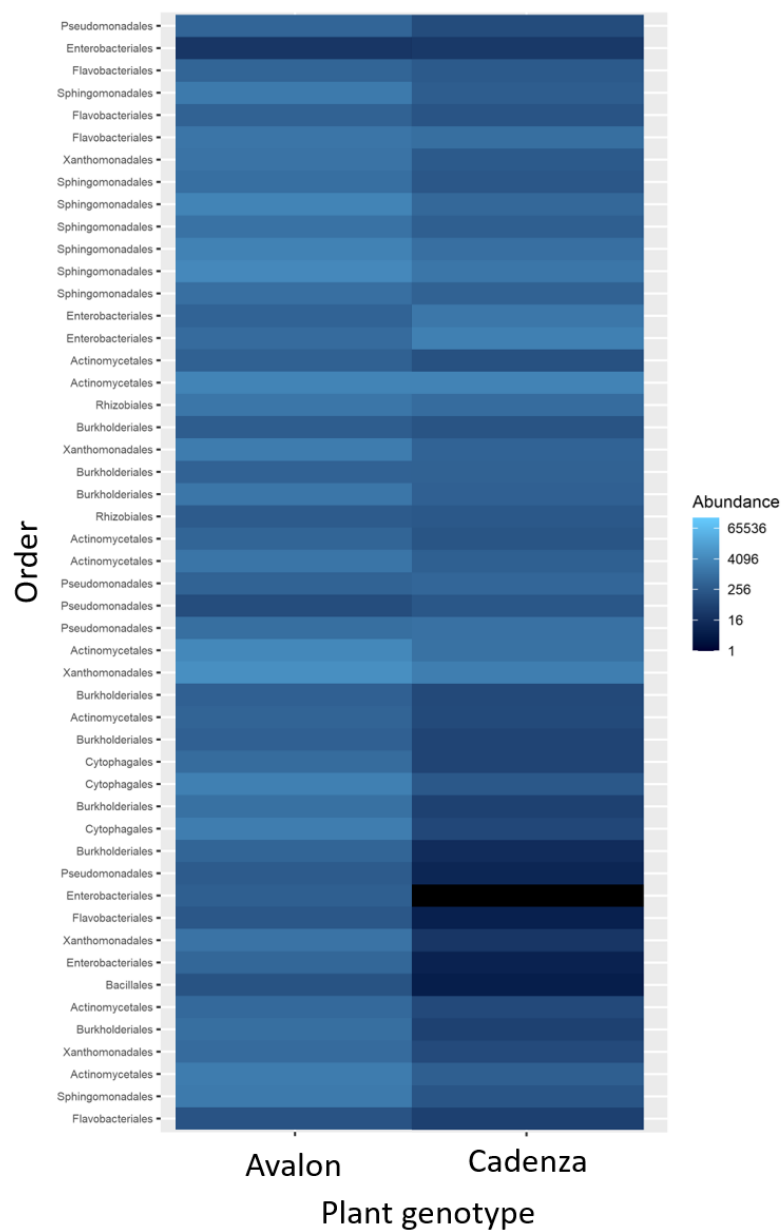
**Figure 4.37 Heat map of the 50 most abundant fungal species in wheat varieties, Avalon and Cadenza.** Blocks represent species, labelled by the order to which the species belong.

# 4.4.4.4.6 Root angle

Most bacterial species showing differential abundance between plants with wide and narrow seedling root angles were from the Protebacteria, followed by the Actinobacteria, Bacteroidetes, Firmicutes and Acidobacteria (Figures 4.38 and 4.39). Other taxa included the Verrucomycetes, Chloroflexi, Planctomycetes and Gemmatimonadetes. The Actinomycetales were broadly more abundant in plants with wide angles, although specific species were more abundant in plants with narrow angles. The Acidobacteria contained both species of greater abundance in plants with wide angles and narrow angles. The Bacteroidetes were mainly more abundant in plants with narrow angles, with the exception of a few species including Sphingobacteriia. Chlamydiae and Verrucomicrobia were more abundant in plants with wide angles. The Bacilli arm of the Firmicutes were more abundant in plants with narrow angles while the Clostridia were more abundant in plants with wide angles. Overall, most Proteobacteria which showed differential abundance were enriched in the rhizosheath of plants with narrow angles. These included in particular, the Betaproteobacteria.
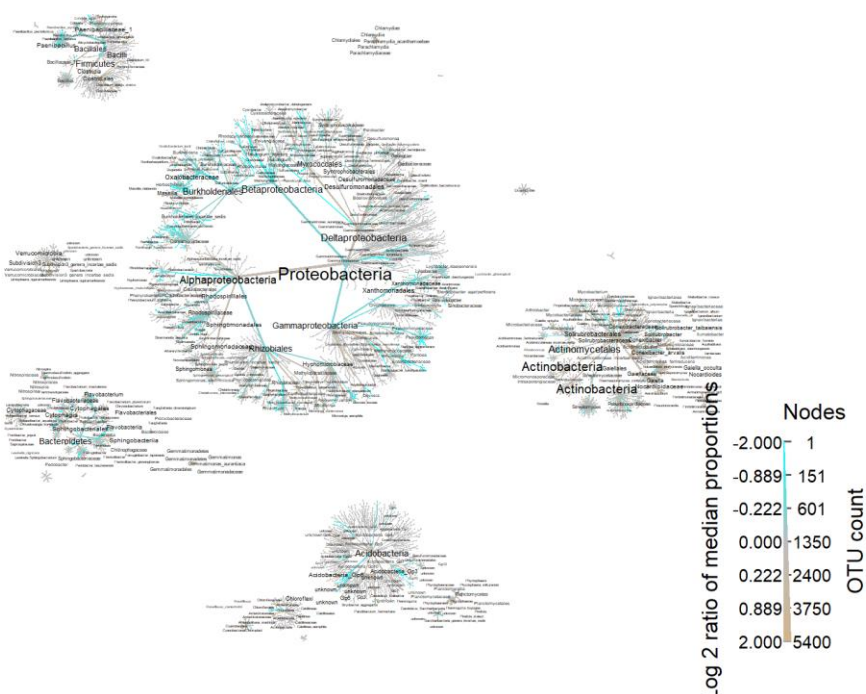


**Figure 4.38 Heat tree of the relative abundance of bacterial species between wheat lines contrasting for seedling root angle.** The relative difference in abundance is expressed as log2FoldChange with positive values (bay colour) indicating that the relative abundance of specific OTUs is higher in plants from the Avalon x Cadenza population with a wide angle. Negative values (cyan colour) indicate that the relative abundance of specific OTUs is higher in

plants with a narrow angle. The size of nodes represents the abundance of rhizosphere fungi at the specific taxonomic rank. The graph is drawn with the R package—Metacoder (Foster *et al.*, 2017).
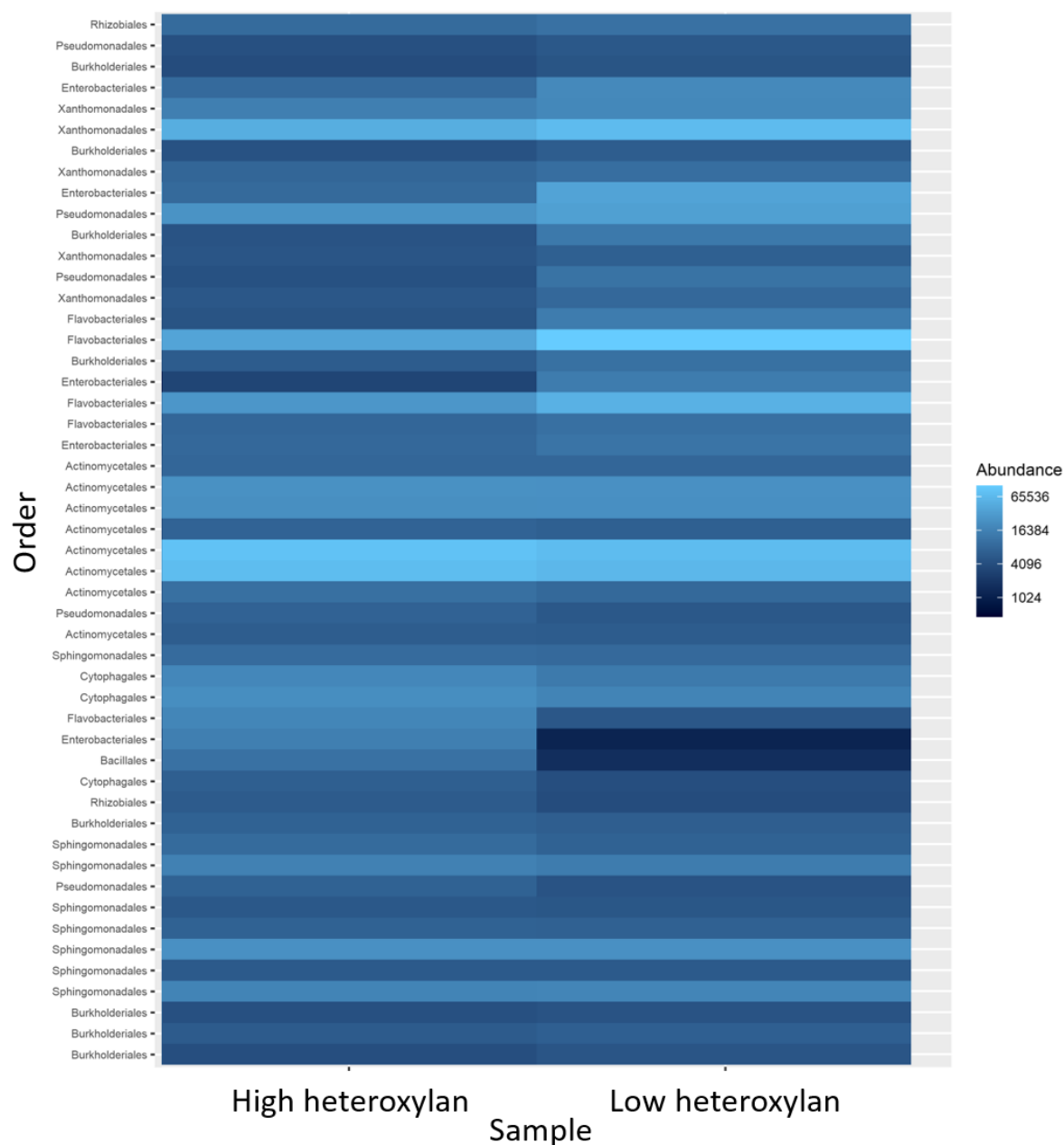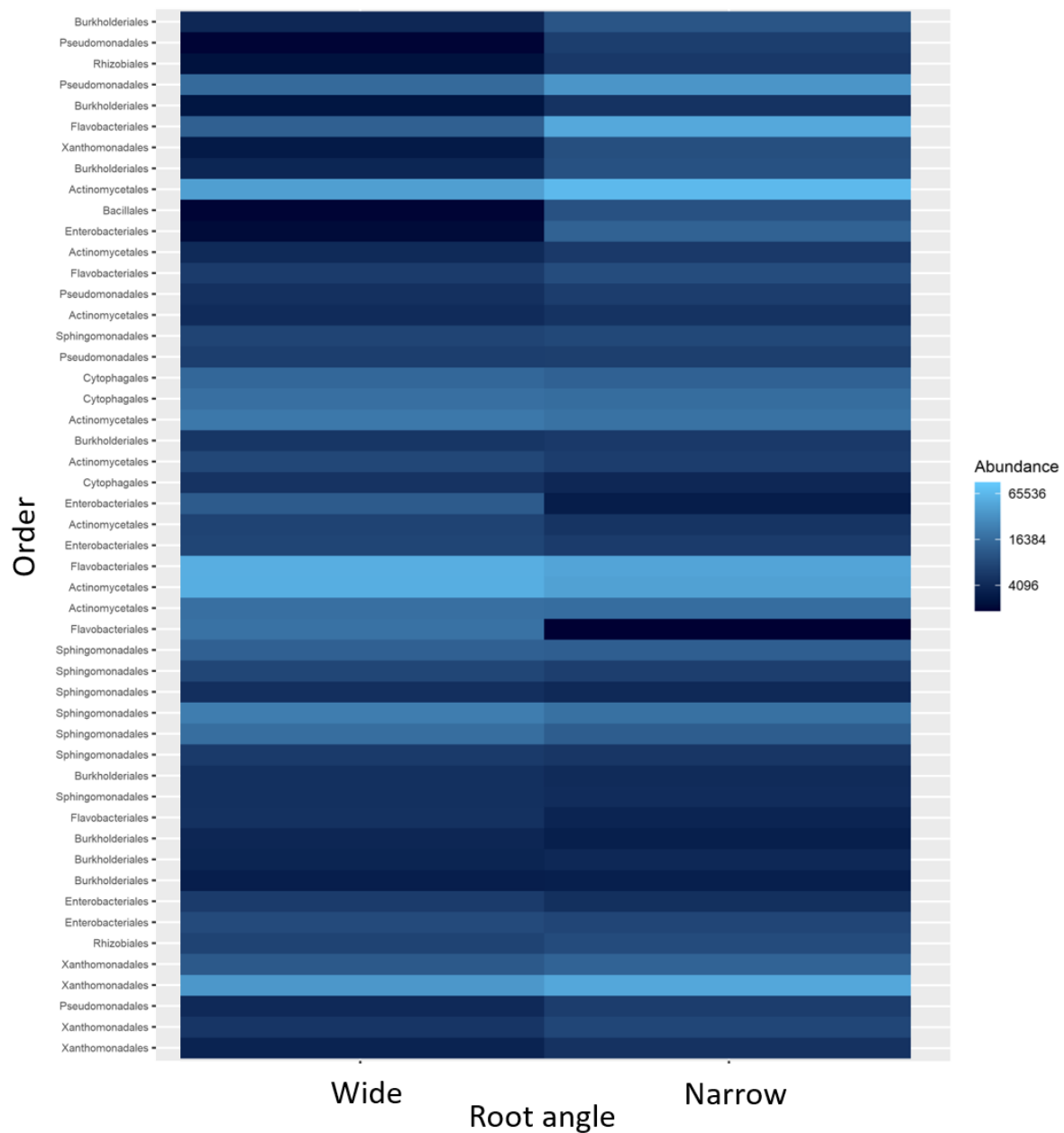


**Figure 4.39. Heat map of the 50 most abundant fungal species in wheat lines of the Avalon x Cadenza population contrasting for seedling seminal root angle.** Blocks represent species, labelled by the order to which the species belong.

# 4.4.4.4.7 Soil supplementation

In addition to testing plant rhizosheaths, bulk soil was supplemented with purified solutions of the specific polysaccharides, pectin, xylan, arabinogalactan protein, extensin and xyloglucan in order to test their effect on the bacterial and fungal microbiome. As a control, soil samples with the same treatment were sterilised before supplementation. This could have indicated whether certain microbial taxa were particularly responsive to specific polysaccharides. The microbial profile of lines known to contain high or low levels of the polysaccharides in the rhizosheath would have provided additional support to the results of soil supplementation. However, for a combination of reasons including cost and pandemic-induced constraints, sequencing results were not achieved for all of the samples, resulting in an incomplete dataset. As such, comparisons are not made here between the different polysaccharides. It would be highly interesting to carry out this experiment to test the effect of specific polysaccharides on soil bacteria and fungi.

# 4.5 Discussion

## 4.5.1 General sequencing results

Rarefaction assesses species richness from the sampling results and initially the curve grows rapidly as common species are recorded, but reaches a plateau as rarer species are found or remain to be sampled. Here, the curve did not reach a plateau, indicating species richness did not reach full potential. This may be due to the growth of the plants in an artificial environment as opposed to in the field. The ITS rarefaction curve was nearer to reaching an asymptote than the 16S curve, indicating a greater portion of fungal richness was surveyed than bacterial richness.

Out of a total of 16 identified bacterial phyla, the Proteobacteria, Actinobacteria, Bacteroidetes and Firmicutes were the most abundant, collectively accounting for 96.6% of the bacterial microbiome (Figure 4.9, Table 4.5). The next most abundant phyla were Acidobacteria and Gemmatimonadetes, coinciding with previous reports of the six most abundant phyla in rhizosphere soil (Hirsch and Mauchline, 2012; Turner *et al.*, 2013; Roesch *et al.*, 2007; Kavamura *et al.*, 2020). Fewer studies have looked at the abundance of fungi in soil, and specifically the rhizosphere. It is accepted that the Ascomycota dominate most soil environments (van der Walt *et al.*, 2016; Marasco *et al.*, 2018). Here I found that Ascomycota accounted for 85% of reads, of which most were Sordariomycetes and Dothideomycetes (Figure 4.4, Table 4.4). Following in order of abundance were the Zygomycota, Basidiomycota, Chytridiomycota, Cercozoa, Rozellomycota and Glomeromycota. Both fungal and bacterial phyla tended to be dominated by one to three classes. This was more apparent among fungi, as reflected by the higher bacterial alpha diversity indices (e.g. a mean Shannon-Weaver index of 6.5 for bacteria compared with 2.0 for fungi).

Alpha diversity was measured by species richness (Chao1 and ACE) and by community diversity, taking into account both richness and evenness (Shannon-Weaver and Simpson). The Beta diversity metric was used to examine intra-group diversity by comparing different groups of samples based on the composition of their microbial communities (Baselga, 2007).

Average alpha bacterial diversity was higher than fungal diversity, reflecting the larger number of bacterial species and the greater uniformity of bacterial communities relative to fungi. Among fungi, a small number of taxa dominated more than was seen in bacterial communities. Some of the few studies comparing bacterial and fungal diversity, also found soil fungal communities to be less even than bacterial communities, for example in bulk soil in a field planted with potato (*Solanum tuberosum* L.) (Fierer *et al.,* 2007) and in apple rhizosphere (*Malus pumila*) (Tilston *et al.,* 2019). Overall, there was limited variation in alpha diversity indices for bacteria and fungi but more variation in beta diversity, indicating that variation in species composition was more striking than variation in microbial abundance and uniformity. However, there was a genotypic effect on alpha diversity, notably ACE species diversity.

## 4.5.2 Wheat cultivars harbour distinct microbiomes

Various studies have found microbial differences between the rhizosphere of different plant species growing in the same soil, including wheat and potato (Viebahn *et al.,* 2005), strawberry and oilseed rape (Berg *et al.,* 2006), and *Zea mays* L. (maize), oat, *Hordeum vulgare* L. (barley) and commercial grass mix (Garbeva *et al.,* 2008). A study in Arabidopsis also found that genotypes of the same species can develop distinct microbial communities (Micallef *et al.,* 2009). Wheat breeding has inadvertently shaped the rhizosphere microbiome, as seen by the microbiome differences between tall and semi-dwarf wheat cultivars (Kavamura *et al.,* 2020). Furthermore, the diversity of rhizosphere bacteria was higher in ancient land races compared to cultivars that are more recent, but this difference was not statistically significant (Germida *et al.,* 2001). Both Avalon and Cadenza cultivars have been subject to the pressures of modern breeding and may have experienced the same pressures on the rhizosphere microbiome. However, they possess distinct above-ground characteristics, such as ear glaucosity, straw thickness, lower glume etc., and evidence presented in other chapters supports differences in below-ground characteristics too.

Here, I report results that may indicate a greater abundance of all fungal phyla as well as the bacterial Proteobacteria, Gemmatimonadetes, Elusimicrobia and Plancomycetes in the Cadenza rhizosheath compared with that of Avalon. The Avalon rhizosheath samples in this experiment contained a greater number of OTUs assigned to the Bacteroidetes than that of Cadenza. Due to a combination of cost and pandemic-induced constraints, the small number of replicates (3

for Avalon and 2 for Cadenza) meant that there was little power with so few replicates to distinguish statistically significant differences. However, these results support the hypothesis that different genotypes harbour distinct microbial communities. Indeed, one study looking at nutrient exchange between wheat cultivars and arbuscular mycorrhizal fungi found that Cadenza contained more P (both fungal- and plant-acquired) than Avalon (Thirkell *et al.*, 2020), suggesting that Cadenza capitalised on the fungi in the rhizosphere. This could coincide with a greater abundance of fungi in the Cadenza rhizosheath, as suggested by our results.

The fact that alpha diversity in Avalon and Cadenza rhizosheaths did not appear to differ could suggest that while community diversity of the two cultivars does not vary, the specific microbial composition (particularly bacterial) does. The PCA plot of UniFrac distances showed distinct clusters for the bacterial composition of Avalon and Cadenza rhizosheaths. Although only a preliminary result, the greater abundance of five fungal phyla in soil supplemented with Cadenza exudate than Avalon exudate coincided with the greater abundance of these phyla in the rhizosheath of the cultivars. This could suggest that the composition of Cadenza exudate favours fungal abundance.

# 4.5.3 Microbial diversity varies between plant phenotypic groups

For the interpretation of results, I would like to remind the reader that the grouping of genotypes based on polysaccharide concentration, RSA and yield arose from separate experiments to determine the patterns of secretion of specific AxC genotypes. The correlation between the rhizosheath microbial profile and the concentration of certain polysaccharides may arise from the effect of mucilage components on bacterial and fungal species diversity. However, it is also known that microbes can trigger an increase in mucilage production and may influence the type of polysaccharides present in the rhizosheath (Driouich *et al.*, 2013). For example, border cells in maize and pea respond to the presence of bacteria and fungal spores by increasing mucilage production (Hawes *et al.*, 2020). Polysaccharide production may be upregulated as an immune response. The polysaccharide may be of microbial origin and increase due to a greater abundance of microbes. Thus, the correlation between polysaccharide levels and microbial diversity may have multiple causes and interactions.

# 4.5.3.1 Seedling root angle

Selection of dwarf and semi-dwarf wheat cultivars, and breeding for yield have altered RSA, including root length and diameter (Kavamura *et al.*, 2020). While it is difficult to make a direct link between root angle and the microbiome, it is possible that factors co-regulating RSA and plant-microbial interactions could lead to observed differences between plants with contrasting root angle. For example, auxin is responsible for regulating many processes in plant development, and its distribution in relation to root angle regulation could also influence processes relating to root secretion and govern microbial species selection (Kamilova *et al.*, 2005). Control may equally happen in the opposite direction, as microbes are known to produce plant growth promoting factors, which may influence RSA (Kamilova *et al.*, 2005; Korenblum *et al.*, 2020). For example, many Rhizobacteria convert tryptophan from root exudates into auxin, which can result in enhanced plant growth (Frankenberger and Arshad 1995). Moreover, the seedling stage of a plant is most sensitive to plant growth stimulation by auxin (Kamilova *et al.*, 2005). Presumably the microbe-derived auxin can modulate RSA. In addition, a study on *Bacillus amyloliquefaciens* and *Triticum aestivum* found that applied exogenous auxin triggers increased C exudation by *Triticum aestivum* roots (Talboys *et al.*, 2014). This highlights the feedback that occurs between plant and microbial activity and the influence that each has over the other. When looking at interlinked entities and processes, it becomes understandable that genotypes with differences in RSA could have different microbiomes. A systems biology approach could help to predict and elucidate the effects of complex interactions, in conjunction with a reductionist approach looking at the effect of single factors at one time.

In an experiment comparing the rhizosphere of tall and semi-dwarf cultivars, Kavamura *et al.* (2020) found that semi-dwarf cultivars are enriched in members belonging to the phyla Acidobacteria and Verrucomicrobia, which are typically more associated with bulk soil rather than the wheat rhizosphere. On the other hand, tall cultivars showed a higher percentage of Bacteroidetes, Actinobacteria and Gemmatimonadetes. The authors discuss the involvement of gibberellin in shaping the microbiome and how the shift in the rhizosphere bacterial community could be a side-effect of increased endogenous gibberellin levels in semi-dwarf plants. Another study found that the diversity of rhizosphere bacteria was higher in ancient land races compared

to recent cultivars, although the difference was not statistically significant (Germida and Siciliano, 2001).

It is known that some microbes, such as *Bacillus* produce auxin (Lopez-Bucio *et al.*, 2007; Ahmed *et al.*, 2010; Ambreetha *et al.*, 2018), and in the present study I found these bacteria to be more abundant in the rhizosheath of plants with narrow angles. Altered auxin gradients in these plants may lead to a steeper gravitropic set point. Auxin concentration in the rhizosheath could affect both RSA and plant-microbe communication in the root environment.

More broadly, most Proteobacteria and Bacteroidetes that showed differential abundance were enriched in the rhizosheath of plants with narrow root angles. Conversely, the rhizosheath of plants with wide angles was enriched in Chlamydiae and Verrucomicrobia, the Clostridia class, and the Actinomycetales, although specific species were more abundant in plants with narrow angles. Further study could investigate the potential of different bacteria to modify RSA.

Fungi that varied significantly in abundance were mainly from the Ascomycota and Basidiomycota phyla. Most Basidiomycota and Chytridiomycota tended to be more abundant in plants with wide angles, with the exception of some saprophytic genera. The Ascomycota comprised a fairly even distribution of genera that were more abundant in wide-angled plants and genera that were more abundant in narrow-angled plants. Of note, *Fusarium oxysporum*, known for its pathogenic strains, was more abundant in the rhizosheath of plants with wide root angles.

Overall, these results suggest that plants with narrow seminal root angles have a more beneficial root microbiome, enriched in plant growth-promoting bacteria (PGPB).

Another avenue for thought is the change of microbial communities between different soil layers. For example, soil organic matter decreases with depth and tillage practices that alter soil properties at different depths also seem to affect microbial mass with depth and degree of tillage (Berner *et al.*, 2008). Narrow root angles are indicative of deeper root systems while wider root angles indicate a shallow root system (Lynch, 2013). It is therefore likely that plants with deep root systems have access to different microbial communities than plants restricted to the shallower soil strata. Differences in root depth are not relevant in this experiment as rhizosheath samples were taken from seedling roots, which were limited to surface soil layers.

# 4.5.3.2 Extensin

Extensin is found in all plant tissues. Specifically, the *ext1* gene which is involved in extensin synthesis is primarily expressed in roots, and multiple studies link extensin to root functioning (Plancot *et al.*, 2013; Sujkowska-Rybkowska and Borucki, 2014).

Here, we found that extensin levels were significantly correlated with weighted UniFrac (Table 4.11), indicating that plants with high levels of extensin in the rhizosheath have a different fungal composition to those with low levels. Samples mainly differed in abundance of saprotrophic fungi. However, two taxa implicated in parasitism, the *Nectriaceae* family and Spizellomycetaceae order, also correlated with extensin levels. Plants with low levels of extensin in the rhizosheath had a greater abundance of species from these orders. The *Nectriaceae* contain known plant parasites, namely the white rot fungi, although these can also have a saprophytic lifestyle (Cannon and Kirk, 2007). The Spizellomycetaceae are also probable parasites (Cannon and Kirk, 2007).

Extensin has previously been implicated in root-microbial associations: the presence of LM1 epitopes has been found in pea root nodules infected with *Rhizobium*, leading to the suggestion that extensins may be involved in the attachment of *Rhizobium* to nodules (Sujkowska-Rybkowska and Borucki, 2014). The *ext1* gene, primarily expressed in roots, is upregulated during pathogen infection. For example, LM1 epitopes are more abundant in the mucilage of potato (*Solanum tuberosum*) plants treated with pathogen elicitors suggesting that production is triggered as an immune response (Koroney *et al.*, 2016). Its involvement in plant defence is thought to be through increasing extensin production for strengthening cell walls. It is possible that extensin is also indirectly implicated in pathogen defence as a component of root border-like cell walls (Plancot *et al.*, 2013; Baetz and Martinoia, 2014). As root border-like cells are sloughed off during root growth, they join the extracellular trap along with other elements of mucilage (Hawes *et al.*, 2002; Vicré *et al.*, 2005; Driouich *et al.*, 2010). The lower abundance of *Nectriaceae* and Spizellomycetaceae in the rhizosheath of genotypes known to secrete high levels of extensin could suggest that these genotypes are well equipped to combat these pathogens. There were also higher levels of *Penicillium* in the roots of plants containing large amounts of extensin. Although not pathogenic, *Penicillium* species have been shown to induce systemic resistance in melon, cotton,

grapevine, onion and tomato (Singh, 2016). This wide cross-species response means *Penicillium* may well induce the same response in wheat.

# 4.5.3.3 Arabinogalactan protein

Plants with differing levels of rhizosheath AGP varied significantly for beta diversity among bacteria but not fungi. Species of the common bacterial phyla, Proteobacteria, Bacteroidetes, Firmicutes and Actinobacteria, showed differential abundance. Y*et also* a small number of species of the rarer phyla, Chlamydiae, Verrucomicrobia, Acidobacteria and Ignavibacteriae, showed differential abundance. These rarer phyla were enriched in high-AGP rhizosheaths with the exception of two Verrucomicrobia species. Plants with high levels of AGP were enriched in bacteria known as PGPB, including those of the *Arthrobacter*, *Pseudomonas* and *Streptomyces* genera. However, other genera of PGPB were more abundant in the rhizosheath of plants with low levels of AGP, such as *Burkholderia* and *Paenibacillus* genera. Furthermore, certain species of *Rhizobium*, notably *R. sphaerophysae*, *R. vignae*, and *R. soli*, were more abundant in the rhizosheath of plants containing higher levels of AGP. However, there were also some Rhizobiales that were more abundant in low levels of AGP.

AGP is abundantly secreted by roots and is widely reported to be involved in positive and negative plant-microbe interactions (Nguema-Ona *et al.*, 2013). Besides providing an adhesive structure for microbes to attach to, AGP is a food source. Many soil microbes, including but not limited to *Trichoderma viride*, *Streptomyces avermitilis* and the pathogenic fungus *Fusarium oxysporum*, produce AGP glycan-degrading enzymes (Nguema-Ona *et al.*, 2013).

Several studies in Arabidopsis and pea have shown that AGP is involved in recognition of host roots by beneficial microbes and contributes to successful root colonisation by symbiotic bacteria (Nguema-Ona *et al.*, 2013). AGP has also been abundantly detected in cells containing arbuscular mycorrhizae, namely fungi of the *Glomus* genus, in *Medicago truncatula* (Van Buuren *et al.*, 1999; Schultz *et al.*, 2008). AGPs have been found in the "extracellular trap" that the mucilage forms as part of a defence mechanism. Moreover, increased release of AGP may be induced by the presence of pathogens, as seen by the increase in AGP in response to bacterial pathogens in potato exudate (Koroney *et al.*, 2016). It is unclear how AGP could discriminate between promoting beneficial microbes and suppressing pathogens. However, it is possible that the

presence of AGP allows plants to select for beneficial microbes, while protecting the root from pathogenesis.

Pea, known for a rich microbiome, could provide insight into enriching the wheat microbiome. A study using liquid chromatography gel filtration found that pea root mucilage is greatly enriched compared with wheat, rice and maize in a material that is similar to arabinogalactan protein (Knee *et al.*, 2001). Furthermore, several cultivated rhizosphere bacteria were found to use pea mucilage as their sole carbon source. If this is true for other legumes as well, this suggests that legume-based cover crops that precede a cereal in the arable rotation could provide this benefit.

The results presented here suggest contrasting correlations between AGP and different genera known to promote plant growth. PGPB genera that were more abundant in genotypes secreting higher levels of AGP included *Arthrobacter, Pseudomonas, Rhizobium* and *Streptomyces*. The lack of significance in fungal beta diversity could suggest that AGP plays less of a role in shaping the fungal microbiome, or that fungi are less implicated in triggering AGP release into the rhizosphere.

# 4.5.3.4 Xyloglucan

A growing body of evidence indicates that xyloglucan is a common feature of root mucilage and it has been documented in the exudates of many species including wheat, barley, maize, tomato, and Arabidopsis (Galloway *et al.*, 2017). Its role has primarily been reported in relation to structure, promoting cohesion of soil particles for rhizosheath formation and linking sloughed border cells to each other (Akhtar *et al.*, 2018; Galloway *et al.*, 2018; Ropitaux *et al.*, 2019). Less research exists on the relationship of microorganisms with xyloglucan, although many microorganisms possess enzymes to degrade xyloglucan (Chen *et al.*, 2020). For example, xyloglucan hydrolases are characteristic of rhizosphere bacterial taxa (Nuccio *et al.*, 2020). As a carbon source, xyloglucan indubitably has involvement in supporting and potentially modulating the rhizosphere microbiome. Besides their well-established role as substrates for microbial metabolism, high molecular weight polysaccharides such as xyloglucan may facilitate the diffusion of low-molecular-weight exudates (Dennis *et al.*, 2010; Holz *et al.*, 2018; Zhalnina *et al.*, 2018).

Of all the polysaccharides tested here, xyloglucan was perhaps one of the most interesting. In addition to its established prominence in the rhizosphere, the results presented here show that it correlates to some extent with both bacterial and fungal diversity: plants with high levels of xyloglucan in the rhizosheath had significantly higher bacterial diversity (Shannon-Weaver and Simpson) than plants with lower levels. While significance was not attained when comparing fungal alpha diversity, plants with higher levels of xyloglucan tended towards greater Shannon-Weaver and Simpson indices (p=0.1). The higher Shannon-Weaver and Simpson diversity in plants with high levels of xyloglucan in the rhizosheath could indicate that rarer species are enriched in these plants, whereas plants with lower levels of xyloglucan are enriched in a subset of dominant phyla. Furthermore, both bacterial and fungal beta diversity varied significantly between plants with high and low levels of rhizosheath xyloglucan. Overall, plants with a higher level of xyloglucan had a significantly greater abundance of most species of fungi. Few species, notably yeasts (Saccharomycetales and *Cryptococcus*) were more abundant in plants with lower levels of xyloglucan. Rhizosheaths with high levels of xyloglucan were enriched in most species of the common bacterial phyla (Proteobacteria, Bacteroidetes, Firmicutes and Actinobacteria), as well as less common phyla including the Chlamydiae, Verrucomicrobia and Acidobacteria. However, there was variation at lower taxonomic ranks, with certain families and classes displaying enrichment in lower xyloglucan levels. Some bacterial taxa known to contain PGPB were more abundant in the rhizosheath of genotypes enriched in xyloglucan (e.g. Rhizobiales, *Clostridium, Cohnella*) while others were more abundant in low xyloglucan (e.g. *Flavobacteriaceae, Paenibacillus, Bacillus*).

Very little research has been done on the effect of xyloglucan on microorganisms. Here I show the correlation between microbial diversity and xyloglucan concentration in the rhizosheath. It is known that xyloglucan is pivotal for rhizosheath formation through its structural properties, such as adhering soil particles and increasing the size of water-stable soil aggregates (Galloway *et al.*, 2019). It may also recruit microorganisms that are important for promoting rhizosheath formation, as well as drought tolerance. Future study should investigate responses of microbial communities to this polysaccharide.

# 4.5.3.5 Homogalacturonan

Overall, homogalacturonan appeared to reduce the presence of both fungi and bacteria. Plants with lower levels of homogalacturonan in the rhizosheath had significantly greater fungal species richness than plants with higher levels. There was no difference in Shannon-Weaver and Simpson indices. This suggests that a greater number of species were present in rhizosheaths containing low concentrations of homogalacturonan and that their distribution was as uniform as samples with high concentrations. Regarding species composition, almost all species displaying significant differential abundance were more numerous in the rhizosheaths of genotypes with low levels of homogalacturonan. The exceptions were saprotrophs, including the Basidiomycete genus, *Rhodosporidium*, and the Ascomycete genus, *Schizothecium*.

Bacterial alpha diversity did not vary significantly but species composition did and the taxa which displayed differential abundance tended to be more abundant in rhizosheaths containing low levels of homogalacturonan.

Homogalacturonan, a well-known pectic polysaccharide found in dicot plant cell walls, contributes to cell extension, cell-to-cell adhesion and wall porosity. However, it has a less well-defined role in the rhizosphere, particularly that of cereals. Furthermore, it is generally secreted in low concentrations by wheat roots (Galloway *et al.*, 2019). It is known that homogalacturonan is crucial in the organisation of root border cells in Arabidopsis. Furthermore, in Arabidopsis, homogalacturonans are broken down to oligogalacturonans to activate plant defence mechanisms in response to pathogenic microbes (Vorwerk *et al.*, 2004). Homogalacturonan appears to promote the secretion of mucilage, rich in xylogalacturonan and AGP, which contributes to the "extracellular trap" (Durand *et al.*, 2009). It is not known whether the same is true for wheat or indeed other cereals. However, it is possible that the reduction of microbial diversity in the rhizosheath of plants rich in homogalacturonan could be due to the antimicrobial properties of homogalacturonan. Furthermore, the homogalacturonan measured in the present study was a de-esterified homogalacturonan detected by the LM19 antibody. Previous studies have indicated that de-esterified pectins that are involved in the defence strategy of a plant (Basińska-Barczak *et al.*, 2020). Alternatively, high levels of homogalacturonan may give an advantage to a particular species or group of microbes (e.g. as a species-specific carbon source),

which out-compete others and gain dominance in the community. The results of this differential abundance analysis are interesting as homogalacturonan was unique among tested polysaccharide in being negatively correlated with the abundance of most microorganisms. Further study should investigate potential trade-offs between plant defence and enhanced nutrient uptake in cultivars with low levels of esterified and de-esterified homogalacturonan.

# 4.5.3.6 Heteroxylan

There is a dearth of knowledge on the influence of heteroxylans on microbes, particularly in the rhizosphere. Xylan is known for its structural role, with strong evidence of it forming polysaccharide complexes with xyloglucan and AGP in wheat root exudates (Galloway *et al.*, 2020), linkages with pectin in potato tuber cell walls (Cornuault *et al.*, 2015), and linkages AGP in oat grain cell walls (Cornuault *et al.*, 2015).

Here, we report variation in differential abundance across bacterial and fungal phyla, particularly at lower taxonomic levels, indicating a range of relationships between heteroxylan and microorganisms. Both common (Proteobacteria, Bacteroidetes, Firmicutes, Actinobacteria) and rare (Chlamydiae, Verrucomicrobia, Acidobacteria, Ignavibacteriae) bacterial phyla exhibited differential abundance. Most of the differentially abundant taxa from the rarer phyla were enriched in high-heteroxylan rhizosheaths. Similarly for the fungi, species from the rarer Cercozoa, Chytridiomycota, Rozellomycota and Zygomycota were more abundant in high-heteroxylan rhizosheaths, while the Ascomycota and Basidiomycota varied in response.

The variation in differential abundance between taxa could reflect the ability of microbes to degrade heteroxylans. For example, certain microbes contain xylanases which allow them to metabolise xylans. These xylanases are specific to the structure of specific heteroxylans (McCartney *et al.*, 2006). Most endohydrolases that have been identified belong to saprophytic bacteria and fungi (Simpson *et al.*, 2003). It would be interesting to examine the gene content of the rhizosphere and the genetic profile of the differentially abundant microbes to test whether xylanase-expressing microbes were enriched in genotypes with xylan-rich rhizosheaths. The heteroxylan levels determined in this study were for an LM27-epitope, which is a xylan of unknown structure. The other tested xylan, an LM11-epitope, did not correlate with microbial beta diversity, indicating the significance of structural specificities. The biological significance of

structural diversity among xylans is unclear (McCartney *et al.*, 2006). However, it is possible for example that the LM11 epitope has more recalcitrance in the soil through resistance to degradation. Structural diversity both provides enhanced potential for physiological roles within the plant (e.g. primary and secondary cell walls) and potential for a greater diversity of microorganisms in the soil as species specialise for a particular xylan and experience less competition for food sources.

# 4.5.3.7 Grain yield

There was a significant difference in fungal beta diversity between higher- and lower-yielding AxC genotypes. Conversely, bacteria did not display significant differential abundance in the rhizosheath of seedlings of genotypes contrasting for yield. The importance of the soil microbiome for crop yield has been demonstrated from the perspective of increased nutrient availability and disease suppression (Mendes *et al.*, 2011; Seymour *et al.*, 2012; Turner *et al.*, 2013). Crop rotations including legumes enhance the yield of wheat thanks to improved microbial richness and diversity in the soil and a resulting increase in available N (Seymour *et al.*, 2012). Another well-known phenomenon is that of disease-suppressive soils (Haas *et al.*, 2005). Through antibiosis, competition, parasitism and predation, consortia of microorganisms prevent the establishment and persistence of pathogens (Mendes *et al.*, 2011; Chandrashekara *et al.*, 2012). Arrays of bacteria have been found to be involved in disease suppression such as the synergistic action of members of the *Pseudomonadaceae* family, *Burkholderiaceae* family, Xanthomonadales order, and Actinobacteria in a study by Mendes *et al.* (2011).

The greater abundance of Glomeromycota in the rhizosheath of higher-yielding genotypes is most interesting from a nutritional point of view as species from this phylum form arbuscular mycorrhizae. Studies have shown the benefit of Glomeromycota on crop performance. For example, inoculating maize with Glomeromycota fungi reduced the need for phosphorus fertilization by up to 33% without compromising grain yield in a study in Venezuela (Cabrales *et al.*, 2019). Studies in wheat indicate the benefits of arbuscular mycorrhizal fungi for grain yield, as well as other traits (Pellegrino *et al.* 2015; Zhu *et al.*, 2018).

Evidence to support the basis of the relationship between yield and fungal symbionts comes from a study on nutrient exchange between wheat cultivars and arbuscular mycorrhizal fungi (Thirkell

*et al.*, 2020). It found that Cadenza contained more P (both fungal- and plant-acquired) than Avalon (Thirkell *et al.*, 2020), suggesting that Cadenza benefited more from fungi in the rhizosphere. Cadenza also has higher yield than Avalon (Chapter 2).

Here, lower-yielding genotypes tended to have a greater abundance of the *Alternaria* species, *A. metachromatica*, in their rhizosheath. *Alternaria* species are implicated in disease and the host of *A. metachromatica* has previously been identified as *Triticum* (Andersen *et al.*, 2009). Here we see that seedling plants of specific genotypes already contain a greater abundance of this pathogen in an experiment that is independent of that determining grain yield. This would suggest that lower-yielding cultivars are genetically prone to harbouring a less favourable microbiome. The same can be said for other observations in the microbiome. For example, higher-yielding genotypes had a greater abundance of Glomeromycota in the rhizosheath than lower yielding genotypes. If these observations are made in an experiment that is independent of the field experiment determining yield, it means that lower-yielding genotypes may not be capable of recruiting as favourable a microbiome as higher-yielding genotypes as early as the seedling stage. This is a critical observation which should be followed up with work to experimentally demonstrate the effect of the seedling microbiome on later developmental stages. Such work was being undertaken in the field in collaboration with the researchers at the Natural History Museum (H. Van Schalkwyk and M. Clark) but was interrupted by the covid-19 pandemic: landrace and modern wheat grown in different N treatments were sampled at multiple growth stages for rhizosheath, bulk soil and the root endosphere to test the effect of high input fertilisation on the microbiome of old and new wheat varieties in a range of nutrient levels. If the seedling microbiome has a significant effect on later stages, such as grain yield, drought tolerance, nutrient uptake, it could be an early selection tool for breeding. For example, a specific sentinel species could be used a biomarker for positive rhizosphere interactions, without the expense of sequencing the entire microbiome.

# 4.5.4 Concluding Remarks

Growing awareness of the depletion of soils in abiotic and biotic factors has led to increased research into restoring and maintaining soil richness (Stockdale *et al.*, 2013). Microorganisms are key to sustaining soil processes. Of particular relevance to food security, the presence of microbes

on agricultural land can have large impacts on crop health, yield and quality. Due to the enormous complexity of microbial communities, their interactions with each other, the environment and the crop, our understanding of the rhizosphere microbiome presents vast gaps. However, it is widely acknowledged that many microorganisms provide benefits to plants for mineral uptake (Bais *et al.*, 2006), drought tolerance (Kim *et al.*, 2012), heat tolerance (Castiglioni *et al.*, 2008), salt tolerance (Zhang *et al.*, 2008; Fatima *et al.*, 2019) and protection from pathogens (Berendsen *et al.*, 2012).

The studies here were undertaken in seedlings but the microbiome experiences successional changes as plants age (Christian *et al.*, 2015). In the present study, the sampling of the rhizosheath at the seedling stage had a two-fold advantage: (i) the seedling stage is instrumental in setting the performance of a plant at later growth stages (ii) it enabled sampling over a short time scale of a week after sowing, using a small amount of space. This is an important factor for scaling up to larger scale experiments or screening for breeding programmes. Moreover, one of the most striking observations here was that the beta diversity of the rhizosheath microbiome of seedlings differed significantly between genotypes known to have high yields and those known to have low yields in field studies. The rhizosheath microbiome recruited early on in plant development could be critical for later stages. The genotypic differences between lines of a same species lead to the ability to foster different rhizosphere environments. This coincides with variations in the rhizosphere microbiome in terms of species richness and microbial composition. To add to the growing understanding of the role of xyloglucan in the formation of the rhizosheath, I found that xyloglucan plays an important role in the microbial composition of the rhizosheath. It was implicated in both bacterial and fungal community composition. Variation in the levels of extensin, AGP, homogalacturonan and heteroxylan in different genotypes was also linked to microbial community composition. Contrary to the other tested polysaccharides, homogalacturonan appeared to correlate negatively with the abundance of most microbial taxa. Interestingly, there was a difference in both fungal and bacterial beta diversity in the rhizosheath of plants contrasting for root angle. Links to plant- and microbe-derived phytohormones such as auxin could be involved in the interaction between RSA and microbial communities.

Cultivars with a particular secretion profile can cultivate more beneficial microbial communities. Insights into the effect of specific polysaccharides can inform more sustainable agricultural

practices and varieties could be bred to help engineer the rhizosphere in ways that promote yield and climate resiliency.

# 5
# Conclusion

This research project has accomplished what few in the root research community have done: it has taken a genetically and phenotypically characterised set of lines in an important crop species, and tested performance at multiple developmental stages in the glasshouse and in the field, looking at roots, shoots, and grain yield. In addition to this, the project has characterised the degree and molecular composition of secretion of polysaccharides from the roots of the same lines and dissected the bacterial and fungal populations occurring in the rhizosheath of the lines. The use of the Avalon x Cadenza (AxC) doubled haploid population for all these studies enabled direct comparison of the same lines for a range of agronomically important plant characters. Moreover, the use of AxC tails with phenotypes at the extremes of the population distribution enabled the screening of fewer lines without compromising on the ability to identify genetic correlations.

## 5.1 Methodology

The study of the wheat root system has several challenges that must be considered when designing experiments. These include but are not limited to: a large number of replicates is required; wheat is a hexaploid; wheat has a long life-cycle (relative to the speed of research in Arabidopsis); the mature root system is extensive, fragile if improperly handled and buried underground.

The study of root system architecture requires a large number of replicates because of the plasticity of the root system. Phenotypic variation between individual plants comes from a combination of (i) genetics: root traits are polygenic and are determined by epistatic and additive effects of multiple genes; (ii) the environment: roots respond to small changes in a range of environmental cues and these can occur very locally within field soils, which are often heterogeneous; (iii) gene x environment (GxE) interactions: the genetic makeup of a plant determines how it will respond to a particular environmental cue. As a consequence, a large number of replicates are required to reliably assess whether phenotypic differences are due to the genetic makeup of individuals.

The need for a large number of replicates and the large number of AxC lines (201) meant that high throughput was paramount. Therefore, innovative methods were conceived to balance high throughput with the acquisition of sufficient, meaningful measures (e.g. construction of a large-scale Falcon tube rack for rhizosheath metagenomics and mucilage analysis).

A researcher may need to choose between minimising "noise" arising from environmental variation and maintaining realistic conditions, which could enable the translation of results into agricultural scenarios. Often the choice of experimental conditions depends on the goal of the study. Here it was appropriate to begin experiments in controlled glasshouse conditions, which allowed for increased sensitivity for identifying QTLs. Progression to field evaluation was important for testing hypotheses in real-world conditions and the power of statistics allowed me to account for environmental variation. Trial and experimental design benefited from robust randomisation strategies. In the clear pot screen, it would have been advisable to be more rigorous about soil moisture and temperature. Moisture probes could guide the degree of watering to maintain uniform soil moisture across all pots and temperature probes could inform the researcher about temperature variation to consider during statistical analyses. Similarly, soil in Falcon tubes was prone to drying out quickly and required close monitoring. It would have also been advisable to pre-germinate and select seeds that were at the same stage of development for sowing, though the small number of seed available did not provide the luxury of discarding seed that germinated early or later than the median. To circumvent potential differences in root length arising from different germination times, root growth rate was measured as an indicator of early seedling vigour.

As a hexaploid with a large complex genome (AABBDD, 2n = 6x = 42, ~17 G), bread wheat is challenging to study genetically and molecularly. Difficulty in genetic transformation has also hampered molecular and genetic studies (Wang *et al.*, 2018). Thanks to its associated resources, the Avalon x Cadenza (AxC) doubled haploid mapping population provided a good platform for study. For example, there has been continuous improvement of a high-density genetic map (Allen *et al.* 2011; Wang *et al.* 2014; Downie *et al.*, unpublished). A population of near-isogenic lines (NILs) derived from cvs. Avalon and Cadenza has been developed (Germplasm Resource Unit, John Innes Centre). Multiple studies have used the AxC population, providing a body of literature to refer to (Bai *et al.*, 2013; Ma *et al.*, 2015; Atkinson *et al.*, 2015), although the only study of root traits was conducted in a non-soil system by Bai *et al.* (2013). Future work should benefit from the full genome sequences of both parental varieties as the Avalon genome is expected to be released soon while the Cadenza genome is already available (Grassroots Genomics, Earlham Institute, UK). Sequence alignment of the Avalon and Cadenza sequences could enable researchers to identify allelic differences that could be responsible for phenotypic differences. A limitation of the AxC population is that Avalon is relatively old (released in 1980) and may be less physiologically and genetically relevant to the modern higher-yielding varieties currently cultivated. The eight-parent and sixteen-parent Multiparent Advanced Generation Intercross (MAGIC) mapping populations could have provided finer resolution thanks to higher-density genetic maps and greater allelic diversity (Mackay and Powell, 2007; Gardner *et al.*, 2016). However, a minimum of ~300 lines of the whole population are required in experiments to make best use of the MAGIC resources (J. Cockram, pers. comm), and as I was doing new analyses with new methods, results from smaller scale pilot experiments would be prudent before the heavy commitment of resources to such a large-scale mapping endeavour.

The use of deletion lines for wheat research continues to reach milestones. For example, the Chinese Spring deletion lines were developed over twenty years ago, yet have not been accurately and fully genetically characterised (Endo and Gill, 1996). Using skim sequence data, this project is the first to accurately determine the location of deletions to a 2Kb resolution. The use of Chinese Spring as the wheat reference genome facilitated the genetic characterisation of the deletion lines. The lines have limitations as the large deletions of several hundred megabases affect vast numbers of genes and can have extensive phenotypic effects. The more recently developed Paragon gamma deletion lines benefit from smaller aberrations, which allow

characterisation to a finer resolution (R. Ramirez-Gonzalez, personal communication). Their drawback is the gaps in tiling of deletions, meaning that the genome is not exhaustively covered. Furthermore, aberrations were not limited to the QTL region and deletions elsewhere in the genome may have resulted in particular phenotypes. Overall, deletion lines can complement and validate results from other techniques. Here, it so happened that they did not support the tested hypotheses, nor support results from the QTL analysis. For the validation of QTLs, time may have been better invested in developing near-isogenic lines (NILs) as NILs containing a single introgression in a uniform genetic background would be a strong validation of a QTL. NIL development to refine introgressions to a finer scale would have taken multiple generations and would be facilitated by speed-breeding strategies, although the vernalisation requirement of cv. Avalon makes speed-breeding less effective (Watson *et al.*, 2018).

# 5.2 Characterisation of root system architecture

Many members of the root research community do not have access to field facilities, and can therefore only speculate on how results of their laboratory experiments relate to crops in the field. The path followed here from laboratory to field is an example for future root studies and will lead to results that have real-world meaning. It is unfortunate that insufficient field data were obtained to draw strong conclusions (the 2020 field season took place amidst a pandemic) but the information derived from the data provided promising insights. The reasonably high heritability of seedling root angle (especially compared with root length and growth rate) identified in the clear pot screens indicated that there would be a large response to selection and high transmissibility to the next generation. This could be useful for accelerating breeding by selecting at the seedling stage. The benefit of selecting narrow seminal root angles in seedlings may not be translated into the yield of mature plants growing in the field, yet I found correlations that could inform decisions for selection. In general, the narrower the seedling seminal root angle, the greater the rate of green canopy gain early in the season, the greater the maximum NDVI value, the greater the number of roots per tiller observed at maturity and the wider the crown root angle.

This means that following further refinement, the root angle QTLs identified here could be used for marker-assisted selection. Two QTLs for root angle, *QRa.niab.4D-1* and *QRa.niab.3A-1*, were mapped to the long arm of chromosome 4D and the long arm of chromosome 3A respectively, and each contributed a proportion of phenotypic variance (PVE) of around 7%. A large number of QTLs have been identified for RSA in crop species (Sanguineti *et al.* 2007; Landjeva *et al.* 2008; Sharma *et al.* 2011; Hamada *et al.* 2012; Bai *et al.* 2013; Zhang *et al.* 2014; Christopher *et al.* 2013; Canè *et al.* 2014; Kabir *et al.* 2015; Petrarulo *et al.* 2015), but few are validated or fine mapped. In this study, QTLs were verified across multiple independent experiments. However, validation in other genetic materials proved unsuccessful. NILs were screened for root angle to test the hypothesis that the QTL would confer the root angle phenotype of the donor parent. They displayed root angle phenotypes that were more similar to the parent contributing to the genetic background, indicating that the introgressed region had negligible effect on phenotype. More extensive backcrossing may be needed to refine the introgression region to the size of the identified QTLs as the NILs used had introgressions in locations other than the QTL region. Deletion lines did not bring conclusive evidence on the location of the QTL. This further highlights the complexity of RSA, and particularly root angle, regulation. Although seedling root length and growth rate were not very heritable traits, they were predictors of field traits: the greater the seedling root growth rate and length, the faster the gain and loss of canopy density, the greater the maximum NDVI value and the later the peak in NDVI value. Overall, some strong correlations were observed between seedling root traits and the root traits of mature plants and these could inform breeding strategies.

# 5.3 Root mucilage and the rhizosheath

Studies on the composition of rhizosheath mucilage have not previously been conducted on such a large scale. Here, the AxC tails were evaluated for the concentration of xylan, heteroxylan, arabinogalactan protein, extensin and xyloglucan in their rhizosheath at the seedling stage. There was significant genotypic variation among the AxC tails for rhizosheath size, root length, shoot length and the concentration of polysaccharides in the rhizosheath. The decreasing order of abundance of polysaccharides detected in the rhizosheath across the lines was heteroxylan, homogalacturonan, AGP, xyloglucan, extensin and xylan. As the order of abundance detected here in soil differs from studies in different growth systems such as hydroponics, it is clear that

different environments have an impact on root secretion. This is an important consideration for applying results to breeding strategies. In order to help deliver increased food security while reducing environmental impacts, a rhizosphere that contains optimal proportions of polysaccharides could provide the specific sources of C required for the proliferation of a microbiome that increases plant growth, nutrient uptake, and suppresses pathogens. For this, accurate determination of polysaccharide concentration in a field scenario is needed. I have demonstrated that polysaccharide concentrations in a soil-based assessment vary from those detected in a hydroponic system. The principal limitation of the soil-based screen is the possible adsorption of compounds onto soil particles and further testing would be required to ensure this was not a confounding factor.

There were significant positive correlations between levels of AGP and heteroxylan, and between xylan, extensin and homogalacturonan, indicating that these polysaccharides may be linked in a polysaccharide matrix in proportional concentrations. Rhizosheath size per unit root length displayed a significant positive correlation with heteroxylan and AGP. The correlation indicates that rhizosheath formation may be enhanced by the secretion of these polysaccharides. Selecting for cultivars that have heteroxylan- and AGP-rich mucilage could promote rhizosheath formation and resilience to abiotic stress. However, the relative benefit of an enhanced rhizosphere on crop shoot growth and yield should be further examined: there was a negative correlation between shoot length/mass and the concentrations of xylan, AGP and extensin, perhaps due to the cost of directing photosynthate towards root secretions. There was significant genotypic variation in root hair density, meaning that there is potential for selection of this trait. There was no relationship between the root hair density measured on germination paper and the size of the rhizosheath of the same genotypes grown in soil. Assuming that root hair density is positively correlated with rhizosheath size (Moreno-Espinola *et al.*, 2007; Shane *et al.*, 2011; Delhaize *et al.*, 2012; George *et al.*, 2014 Brown *et al.*, 2017), this demonstrates the importance of phenotyping for root hairs in a growth environment as close as possible to natural conditions.

# 5.4 The root microbiome

To my knowledge, this is the first study to conduct metagenomics analysis on a plant mapping population. Moreover, the choice of conducting metagenomics on the well-characterised AxC population has allowed me to add to the current knowledge on the phenotypes and genetics of AxC lines. This study found that bacterial and fungal communities were dominated by a small number of phyla, each of which was dominated by a small number of classes. AxC lines did not vary in the diversity of their rhizosheath microbiome but they did vary in the species composition of their microbiome. This indicates that specific plant genotypes exhibit differential selection of the microbial inhabitants of the rhizosheath. One of the selective pressures exerted by plant roots on microorganisms is the secretion of high molecular weight polysaccharides. This is important because in order to design an effective rhizosphere microbiome, it is necessary to know the effect of major mucilage components on the microbial community and how the production of these are controlled by the host plant genetics. There were differences in microbial beta diversity between lines known to contrast for the level of AGP, extensin, homogalacturonan, heteroxylan and xyloglucan in the rhizosheath. The fungal beta diversity of higher-yielding AxC lines differed significantly from lower-yielding lines. This was not the case for bacterial beta diversity. Higher yields could arise from enhanced nutrient acquisition thanks to a more beneficial population of fungi. Elements of root system architecture, namely seedling root angle, were associated with fungal and bacterial diversity. Plants with narrow seminal root angles appeared to have a more beneficial root microbiome, based on the known lifestyle of constituent microbes. To tie in with the fitness landscape of the root system, narrower seedling seminal root angles were found (as mentioned in Chapter 2) to correlate with greater rates of early green canopy gain, a greater peak in NDVI, a greater number of roots per tiller observed at maturity and a wider crown root angle. I can only speculate on underlying mechanisms but the evidence from this project suggests a link between root angle, microbial populations and crop biomass gain.

There has not yet been a concerted effort among academics, industry researchers and farmers to develop a crop management system that takes into account plant genotype x environment x microbiome x management interactions. Here, the use of a genetically characterised panel of AxC lines for the study of bacterial and fungal communities could encourage the development

of larger scale endeavours in crop rhizosphere microbiology, using host plant genetics as a tool to achieve this.

# 5.5 Future work

Crop management practices such as tillage and crop rotation have a crucial impact on agricultural output but are often neglected when studying the rhizosphere microbiome (Zhou *et al.*, 2020). My data suggest that the choice of variety, too, could be an important management tool to optimise rhizosphere dynamics for different farming systems. This is particularly true for our understanding of the establishment of the rhizosphere microbial communities at the seedling stage. A recent paper demonstrates that early rhizosphere communities are defined by the detritusphere: the soil surrounding the decaying root from the previous crop (Zhou *et al.*, 2020). Future work could examine microbial succession in the field at specific developmental stages in the panel of AxC tails, taking samples of bulk soil, rhizosheath soil and roots. The same samples could be tested for polysaccharides in order to test the hypothesis that the change in root secretion during plant development drives a change in microbial communities. The trial would also test the hypothesis that the microbial community at the seedling stage helps to determine crop performance at later stages, including grain yield. Other measurements at multiple developmental stages could include leaf canopy cover and root crown phenotypes. In order to test the effect of specific polysaccharides on microbial diversity in a controlled setting without confounding environmental factors, further work should include a metagenomics analysis of soil samples supplemented with purified solutions of polysaccharide at concentrations equivalent those found in the rhizosheath. With added labour, scaling up to the entire AxC population would allow QTL analysis on these traits. Further investigation of heteroxylan, AGP, homogalacturonan and xyloglucan could utilise a candidate gene approach using exome capture data. To take the root angle QTLs forward, the development of NILs by backcrossing to reduce the introgression size and eliminate other introgressions could be undertaken. The development of sub-NILs could further allow fine-mapping. There is still uncertainty over the location of mucilage secretion and whether different polysaccharides are secreted from different root zones. Further work could use the probing of nitrocellulose sheets with antibodies on which roots of a growing plant had been placed.

Based at the National Institute of Agricultural Botany (NIAB), this PhD has used cutting-edge genomic, molecular and phenotyping approaches highly relevant to the crop research and development sector, providing a unique interface between crop research and translation.

# BIBLIOGRAPHY

**Adamski NM, Borrill P, Brinton J, Harrington SA, Marchal C, Bentley AR, Bovill WD, Cattivelli L, Cockram J, Contreras-Moreira B**. 2020. A roadmap for gene functional characterisation in crops with large genomes: Lessons from polyploid wheat. Elife **9**, e55646.

**AHDB**. 2018. Wheat Growth Guide.

**Ahmed A, Hasnain S**. 2010. Auxin-producing Bacillus sp.: auxin quantification and effect on the growth of Solanum tuberosum. Pure and Applied Chemistry **82**, 313-319.

**Ahmed MA, Zarebanadkouki M, Meunier F, Javaux M, Kaestner A, Carminati A**. 2018. Root type matters: measurement of water uptake by seminal, crown, and lateral roots in maize. Journal of experimental botany **69**, 1199-1206.

**Ahmed MA, Kroener E, Benard P, Zarebanadkouki M, Kaestner A, Carminati A**. 2016. Drying of mucilage causes water repellency in the rhizosphere of maize: measurements and modelling. Plant and Soil **407**, 161-171.

**Aira M, Gómez-Brandón M, Lazcano C, Bååth E, Domínguez J**. 2010. Plant genotype strongly modifies the structure and growth of maize rhizosphere microbial communities. Soil biology and biochemistry **42**, 2276-2281.

**Akhtar J, Galloway AF, Nikolopoulos G, Field KJ, Knox P**. 2018. A quantitative method for the high throughput screening for the soil adhesion properties of plant and microbial polysaccharides and exudates. Plant and Soil **428**, 57-65.

**Alahmad S, El Hassouni K, Bassi FM, Dinglasan E, Youssef C, Quarry G, Aksoy A, Mazzucotelli E, Juhász A, Able JA**. 2019. A major root architecture QTL responding to water limitation in durum wheat. Frontiers in Plant Science **10**, 436.

**Alaux M, Rogers J, Letellier T, Flores R, Alfama F, Pommier C, Mohellibi N, Durand S, Kimmel E, Michotey C**. 2018. Linking the International Wheat Genome Sequencing Consortium bread wheat reference genome sequence to wheat genetic and phenomic data. Genome biology **19**, 111.

**Albersheim P, Darvill A, Roberts K, Sederoff R, Staehelin A**. 2010. Biochemistry of the cell wall molecules. *Plant cell walls*: Garland Science, 85-136.

**Albersheim P, Darvill A, Roberts K, Sederoff R, Staehelin A**. 2010. *Plant cell walls*: Garland Science.

**Aleklett K, Hart M, Shade A**. 2014. The microbial ecology of flowers: an emerging frontier in phyllosphere research. Botany **92**, 253-266.

**Ali B, Sabri A, Ljung K, Hasnain S**. 2009. Auxin production by plant associated bacteria: impact on endogenous IAA content and growth of Triticum aestivum L. Letters in applied microbiology **48**, 542-547.

**Ali SZ, Sandhya V, Grover M, Kishore N, Rao LV, Venkateswarlu B**. 2009. Pseudomonas sp. strain AKM-P6 enhances tolerance of sorghum seedlings to elevated temperatures. Biology and Fertility of Soils **46**, 45-55.

**Allen AM, Winfield MO, Burridge AJ, Downie RC, Benbow HR, Barker GL, Wilkinson PA, Coghill J, Waterfall C, Davassi A**. 2017. Characterization of a Wheat Breeders' Array suitable for high-throughput SNP genotyping of global accessions of hexaploid bread wheat (Triticum aestivum). Plant biotechnology journal **15**, 390-401.

**Alonso-Blanco C, Koornneef M**. 2000. Naturally occurring variation in Arabidopsis: an underexploited resource for plant genetics. Trends in plant science **5**, 22-29.

**Ambreetha S, Chinnadurai C, Marimuthu P, Balachandar D**. 2018. Plant-associated Bacillus modulates the expression of auxin-responsive genes of rice and modifies the root architecture. Rhizosphere **5**, 57-66.

**Anders S, Huber W**. 2010. Differential expression analysis for sequence count data. Nature Precedings, 1-1.

**Anderson MJ, Crist TO, Chase JM, Vellend M, Inouye BD, Freestone AL, Sanders NJ, Cornell HV, Comita LS, Andersen B, Sørensen JL, Nielsen KF, van den Ende BG, de Hoog**

S. 2009. A polyphasic approach to the taxonomy of the Alternaria infectoria species–group. Fungal Genetics and Biology **46**, 642-656.

**Anderson MJ, Crist TO, Chase JM, Vellend M, Inouye BD, Freestone AL, Sanders NJ, Cornell HV, Comita LS, Davies KF**. 2011. Navigating the multiple meanings of β diversity: a roadmap for the practicing ecologist. Ecology letters **14**, 19-28.

**Araus JL, Slafer GA, Royo C, Serret MD**. 2008. Breeding for yield potential and stress adaptation in cereals. Critical Reviews in Plant Science **27**, 377-412.

**Archambault DJ, Zhang G, Taylor GJ**. 1996. Accumulation of Al in root mucilage of an Al-resistant and an Al-sensitive cultivar of wheat. Plant physiology **112**, 1471-1478.

**Arshad M, Shaharoona B, Mahmood T**. 2008. Inoculation with Pseudomonas spp. containing ACC-deaminase partially eliminates the effects of drought stress on growth, yield, and ripening of pea (Pisum sativum L.). Pedosphere **18**, 611-620.

**Atkinson JA, Wingen LU, Griffiths M, Pound MP, Gaju O, Foulkes MJ, Le Gouis J, Griffiths S, Bennett MJ, King J**. 2015. Phenotyping pipeline reveals major seedling root growth QTL in hexaploid wheat. Journal of experimental botany **66**, 2283-2292.

**Awata LA, Beyene Y, Gowda M, LM S, Jumbo MB, Tongoona P, Danquah E, Ifie BE, Marchelo-Dragga PW, Olsen M**. 2020. Genetic analysis of QTL for resistance to maize lethal necrosis in multiple mapping populations. Genes **11**, 32.

**Bacic A, Moody SF, Clarke AE**. 1986. Structural analysis of secreted root slime from maize (Zea mays L.). Plant Physiology **80**, 771-777.

**Badr A, Rabey HE, Effgen S, Ibrahim H, Pozzi C, Rohde W, Salamini F**. 2000. On the origin and domestication history of barley (Hordeum vulgare). Molecular biology and evolution **17**, 499-510.

**Badri DV, Vivanco JM**. 2009. Regulation and function of root exudates. Plant, cell & environment **32**, 666-681.

**Baetz U, Martinoia E**. 2014. Root exudates: the hidden part of plant defense. Trends in plant science **19**, 90-98.

**Bai C, Liang Y, Hawkesford MJ**. 2013. Identification of QTLs associated with seedling root traits and their correlation with plant height in wheat. Journal of experimental botany **64**, 1745-1753.

**Bai C, Ge Y, Ashton R, Evans J, Milne A, Hawkesford M, Whalley W, Parry M, Melichar J, Feuerhelm D**. 2019. The relationships between seedling root screens, root growth in the field and grain yield for wheat. Plant and Soil **440**, 311-326.

**Bais HP, Weir TL, Perry LG, Gilroy S, Vivanco JM**. 2006. The role of root exudates in rhizosphere interactions with plants and other organisms. Annu. Rev. Plant Biol. **57**, 233-266.

**Bakker MG, Manter DK, Sheflin AM, Weir TL, Vivanco JM**. 2012. Harnessing the rhizosphere microbiome through plant breeding and agricultural management. Plant and Soil **360**, 1-13.

**Bakker P, Berendsen R, Doornbos R, Wintermans P, Pieterse C**. 2013. The rhizosphere revisited: root microbiomics. Frontiers in Plant Science **4**.

**Balmford A, Amano T, Bartlett H, Chadwick D, Collins A, Edwards D, Field R, Garnsworthy P, Green R, Smith P**. 2018. The environmental costs and benefits of high-yield farming. Nature Sustainability **1**, 477-485.

**Barka EA, Nowak J, Clément C**. 2006. Enhancement of chilling resistance of inoculated grapevine plantlets with a plant growth-promoting rhizobacterium, Burkholderia phytofirmans strain PsJN. Applied and environmental microbiology **72**, 7246-7252.

**Barker GL, Edwards KJ**. 2009. A genome-wide analysis of single nucleotide polymorphism diversity in the world's major cereal crops. Plant Biotechnology Journal **7**, 318-325.

**Baselga A, JIMÉNEZ-VALVERDE AL.** 2007. Environmental and geographical determinants of beta diversity of leaf beetles (Coleoptera: Chrysomelidae) in the Iberian Peninsula. Ecological Entomology. **32**, 312-8.

**Bashiardes S, Zilberman-Schapira G, Elinav E**. 2016. Use of metatranscriptomics in microbiome research. Bioinformatics and biology insights **10**, BBI. S34610.

**Basińska-Barczak A, Błaszczyk L, Szentner K**. 2020. Plant Cell Wall Changes in Common Wheat Roots as a Result of Their Interaction with Beneficial Fungi of Trichoderma. Cells **9**, 2319.

**Bates D, Mächler M, Bolker B, Walker S**. 2014. Fitting linear mixed-effects models using lme4. arXiv preprint arXiv:1406.5823.

**Bateson P**. 2002. William Bateson: a biologist ahead of his time. Journal of Genetics **81**, 49-58.

**Bateson P**. 2014. Sudden Changes in Ontogeny 10 and Phylogeny. *Behavioral Evolution and Integrative Levels: The Tc Schneirla Conferences Series, Volume 1*: Psychology Press, 155.

**Bekkering CS, Huang J, Tian L**. 2020. Image-Based, Organ-Level Plant Phenotyping for Wheat Improvement. Agronomy **10**, 1287.

**Benjamini Y, Speed TP**. 2012. Summarizing and correcting the GC content bias in high-throughput sequencing. Nucleic acids research **40**, e72-e72.

**Bentley DR, Balasubramanian S, Swerdlow HP, Smith GP, Milton J, Brown CG, Hall KP, Evers DJ, Barnes CL, Berg G, Opelt K, Zachow C, Lottmann J, Götz M, Costa R, Smalla K**. 2006. The rhizosphere effect on bacteria antagonistic towards the pathogenic fungus Verticillium differs depending on plant species and site. FEMS microbiology ecology **56**, 250-261.

**Berner A, Hildermann I, Fliessbach A, Pfiffner L, Niggli U, Mäder P**. 2008. Crop yield and soil fertility response to reduced tillage under organic management. Soil and Tillage Research **101**, 89-96.

**Bignell HR**. 2008. Accurate whole human genome sequencing using reversible terminator chemistry. Nature **456**, 53-59.

**Beckers B, Op De Beeck M, Thijs S, Truyens S, Weyens N, Boerjan W, Vangronsveld J**. 2016. Performance of 16s rDNA Primer Pairs in the Study of Rhizosphere and Endosphere Bacterial Microbiomes in Metabarcoding Studies. Frontiers in Microbiology **7**.

**Berendsen RL, Pieterse CM, Bakker PA**. 2012. The rhizosphere microbiome and plant health. Trends in plant science **17**, 478-486.

**Berry P, Sylvester-Bradley R, Berry S**. 2007. Ideotype design for lodging-resistant wheat. Euphytica **154**, 165-179.

**Bertin C, Yang X, Weston LA**. 2003. The role of root exudates and allelochemicals in the rhizosphere. Plant and soil **256**, 67-83.

**Bittel P, Robatzek S**. 2007. Microbe-associated molecular patterns (MAMPs) probe plant immunity. Current opinion in plant biology **10**, 335-341.

**Blum A, Shpiler L, Golan G, Mayer J**. 1989. Yield stability and canopy temperature of wheat genotypes under drought-stress. Field Crops Research **22**, 289-296.

**Bogard M, Allard V, Brancourt-Hulmel M, Heumez E, Machet J-M, Jeuffroy M-H, Gate P, Martre P, Le Gouis J**. 2010. Deviation from the grain protein concentration–grain yield negative relationship is highly correlated to post-anthesis N uptake in winter wheat. Journal of experimental botany **61**, 4303-4312.

**Bokulich NA, Mills DA**. 2013. Improved selection of internal transcribed spacer-specific primers enables quantitative, ultra-high-throughput profiling of fungal communities. Applied and environmental microbiology **79**, 2519-2526.

**Bolot S, Abrouk M, Masood-Quraishi U, Stein N, Messing J, Feuillet C, Salse J**. 2009. The 'inner circle'of the cereal genomes. Current opinion in plant biology **12**, 119-125.

**Bonfante P, Genre A**. 2010. Mechanisms underlying beneficial plant–fungus interactions in mycorrhizal symbiosis. Nature communications **1**, 1-11.

**Bonkowski M**. 2004. Protozoa and plant growth: the microbial loop in soil revisited. New Phytologist **162**, 617-631.

**Börner A, Plaschke J, Korzun V, Worland A**. 1996. The relationships between the dwarfing genes of wheat and rye. Euphytica **89**, 69-75.

**Bouffaud ML, Kyselková M, Gouesnard B, Grundmann G, Muller D, MOËNNE-LOCCOZ Y**. 2012. Is diversification history of maize influencing selection of soil bacteria by roots? Molecular ecology **21**, 195-206.

**Bouranis DL, Chorianopoulou SN, Kollias C, Maniou P, Protonotarios VE, Siyiannis VF, Hawkesford MJ**. 2006. Dynamics of aerenchyma distribution in the cortex of sulfate-deprived adventitious roots of maize. Annals of Botany **97**, 695-704.

**Boyer JS**. 2009. Evans Review: Cell wall biosynthesis and the molecular mechanism of plant enlargement. Functional plant biology **36**, 383-394.

**Brinker P, Fontaine MC, Beukeboom LW, Salles JF**. 2019. Host, symbionts, and the microbiome: the missing tripartite interaction. Trends in microbiology **27**, 480-488.

**Britschgi TB**. 1990. An analysis of Sargasso Sea bacterioplankton diversity using 16S ribosomal RNA.

**Brouwer D, Clair DS**. 2004. Fine mapping of three quantitative trait loci for late blight resistance in tomato using near isogenic lines (NILs) and sub-NILs. Theoretical and Applied Genetics **108**, 628-638.

**Brown L, George T, Thompson J, Wright G, Lyon J, Dupuy L, Hubbard S, White P**. 2012. What are the implications of variation in root hair length on tolerance to phosphorus deficiency in combination with water stress in barley (Hordeum vulgare)? Annals of Botany **110**, 319-328.

**Brown L, George T, Dupuy L, White P**. 2013. A conceptual model of root hair ideotypes for future agricultural environments: what combination of traits should be targeted to cope with limited P availability? Annals of Botany **112**, 317-330.

**Brown LK, George TS, Neugebauer K, White PJ**. 2017. The rhizosheath–a potential trait for future agricultural sustainability occurs in orders throughout the angiosperms. Plant and Soil **418**, 115-128.

**Bruce WB, Edmeades GO, Barker TC**. 2002. Molecular and physiological approaches to maize improvement for drought tolerance. Journal of experimental botany **53**, 13-25.

**Bulgarelli D, Rott M, Schlaeppi K, van Themaat EVL, Ahmadinejad N, Assenza F, Rauf P, Huettel B, Reinhardt R, Schmelzer E**. 2012. Revealing structure and assembly cues for Arabidopsis root-inhabiting bacterial microbiota. Nature **488**, 91-95.

**Burton RA, Gidley MJ, Fincher GB**. 2010. Heterogeneity in the chemistry, structure and function of plant cell walls. Nature chemical biology **6**, 724-732.

**Busby PE, Soman C, Wagner MR, Friesen ML, Kremer J, Bennett A, Morsy M, Eisen JA, Leach JE, Dangl JL**. 2017. Research priorities for harnessing plant microbiomes in sustainable agriculture. PLoS biology **15**, e2001793.

**Buyer JS, Roberts DP, Russek-Cohen E**. 1999. Microbial community structure and function in the spermosphere as affected by soil and seed type. Canadian Journal of Microbiology **45**, 138-144.

**Byrt CS, Zhao M, Kourghi M, Bose J, Henderson SW, Qiu J, Gilliham M, Schultz C, Schwarz M, Ramesh SA**. 2017. Non-selective cation channel activity of aquaporin AtPIP2; 1 regulated by Ca2+ and pH. Plant, Cell & Environment **40**, 802-815.

**Cabrales E, Lopez-Hernández D, Toro M**. 2019. Effect of Inoculation with Glomeromycota Fungi and Fertilization on Maize Yield in Acid Soils. *Microbial Probiotics for Agricultural Systems*: Springer, 205-212.

**Cane MA, Maccaferri M, Nazemi G, Salvi S, Francia R, Colalongo C, Tuberosa R**. 2014. Association mapping for root architectural traits in durum wheat seedlings as related to agronomic performance. Molecular Breeding **34**, 1629-1645.

**Cannesan MA, Durand C, Burel C, Gangneux C, Lerouge P, Ishii T, Laval K, Follet-Gueye M-L, Driouich A, Vicré-Gibouin M**. 2012. Effect of arabinogalactan proteins from the root caps of pea and Brassica napus on Aphanomyces euteiches zoospore chemotaxis and germination. Plant Physiology **159**, 1658-1670.

**Cannesan MA, Gangneux C, Lanoue A, Giron D, Laval K, Hawes M, Driouich A, Vicré-Gibouin M**. 2011. Association between border cell responses and localized root infection by pathogenic Aphanomyces euteiches. Annals of Botany **108**, 459-469.

**Cannon PF, Kirk PM**. 2007. *Fungal families of the world*: Cabi.

**Cannon MC, Terneus K, Hall Q, Tan L, Wang Y, Wegenhart BL, Chen L, Lamport DT, Chen Y, Kieliszewski MJ**. 2008. Self-assembly of the plant cell wall requires an extensin scaffold. Proceedings of the National Academy of Sciences **105**, 2226-2231.

**Carminati A**. 2013. Rhizosphere wettability decreases with root age: a problem or a strategy to increase water uptake of young roots? Frontiers in Plant Science **4**.

**Carminati A, Vetterlein D**. 2013. Plasticity of rhizosphere hydraulic properties as a key for efficient utilization of scarce resources. Annals of botany **112**, 277-290.

**Carpita NC, Gibeaut DM**. 1993. Structural models of primary cell walls in flowering plants: consistency of molecular structure with the physical properties of the walls during growth. The Plant Journal **3**, 1-30.

**Case RJ, Boucher Y, Dahllöf I, Holmström C, Doolittle WF, Kjelleberg S**. 2007. Use of 16S rRNA and rpoB genes as molecular markers for microbial ecology studies. Applied and environmental microbiology **73**, 278-288.

**Castiglioni P, Warner D, Bensen RJ, Anstrom DC, Harrison J, Stoecker M, Abad M, Kumar G, Salvador S, D'Ordine R**. 2008. Bacterial RNA chaperones confer abiotic stress tolerance in plants and improved grain yield in maize under water-limited conditions. Plant physiology **147**, 446-455.

**Castilleux R, Plancot B, Ropitaux M, Carreras A, Leprince J, Boulogne I, Follet-Gueye M-L, Popper ZA, Driouich A, Vicré M**. 2018. Cell wall extensins in root–microbe interactions and root secretions. Journal of experimental botany **69**, 4235-4247.

**Ceauşu S, Hofmann M, Navarro LM, Carver S, Verburg PH, Pereira HM**. 2015. Mapping opportunities and challenges for rewilding in Europe. Conservation Biology **29**, 1017-1027.

**Chandrashekara C, Bhatt J, Kumar R, Chandrashekara K**. 2012. Supressive soils in plant disease management. Eco-Friendly Innovative Approaches in Plant Disease Management, ed. A. Singh (New Delhi: International Book Distributors), 241-256.

**Chao A**. 1984. Nonparametric estimation of the number of classes in a population. Scandinavian Journal of statistics, 265-270.

**Chao A, Bunge J**. 2002. Estimating the number of species in a stochastic abundance model. Biometrics **58**, 531-539.

**Chao A, Chazdon RL, Colwell RK, Shen TJ**. 2006. Abundance-based similarity indices and their estimation when there are unseen species in samples. Biometrics **62**, 361-371.

**Chao A, Lee S-M**. 1992. Estimating the number of classes via sample coverage. Journal of the American statistical Association **87**, 210-217.

**Chao A, Yang MC**. 1993. Stopping rules and estimation for recapture debugging with unequal failure rates. Biometrika **80**, 193-201.

**Chen S, Waghmode TR, Sun R, Kuramae EE, Hu C, Liu B**. 2019. Root-associated microbiomes of wheat under the combined effect of plant development and nitrogen fertilization. Microbiome **7**, 136.

**Chen H, Jiang X, Li S, Qin W, Huang Z, Luo Y, Li H, Wu D, Zhang Q, Zhao Y**. 2020. Possible beneficial effects of xyloglucan from its degradation by gut microbiota. Trends in Food Science & Technology **97**, 65-75.

**Chen C-G, Mau S-L, Du H, Gane AM, Bacic A, Clarke AE**. 1998. Plant arabinogalactan protein (AGP) genes. Google Patents.

**Cheng T, Xu C, Lei L, Li C, Zhang Y, Zhou S**. 2016. Barcoding the kingdom Plantae: new PCR primers for ITS regions of plants with improved universality and specificity. Molecular Ecology Resources **16**, 138-149.

**Chew P, Meade K, Hayes A, Harjes C, Bao Y, Beattie AD, Puddephat I, Gusmini G, Tanksley SD**. 2016. A study on the genetic relationships of Avena taxa and the origins of hexaploid oat. Theoretical and Applied Genetics **129**, 1405-1415.

**Cholick FA, Welsh JR, Cole CV**. 1977. Rooting Patterns of Semi-dwarf and Tall Winter Wheat Cultivars under Dryland Field Conditions 1. Crop Science **17**, 637-639.

**Chormova D, Fry SC**. 2016. Boron bridging of rhamnogalacturonan-II is promoted in vitro by cationic chaperones, including polyhistidine and wall glycoproteins. New Phytologist **209**, 241-251.

**Christian N, Whitaker BK, Clay K**. 2015. Microbiomes: unifying animal and plant systems through the lens of community ecology theory. Frontiers in Microbiology **6**, 869.

**Christopher J, Christopher M, Jennings R, Jones S, Fletcher S, Borrell A, Manschadi AM, Jordan D, Mace E, Hammer G**. 2013. QTL for root angle and number in a population developed from bread wheats (Triticum aestivum) with contrasting adaptation to water-limited environments. Theoretical and Applied Genetics **126**, 1563-1574.

**Chu C-G, Xu S, Friesen T, Faris J**. 2008. Whole genome mapping in a wheat doubled haploid population using SSRs and TRAPs and the identification of QTL for agronomic traits. Molecular Breeding **22**, 251-266.

**Churchill GA, Doerge RW**. 1994. Empirical threshold values for quantitative trait mapping. Genetics **138**, 963-971.

**Clausen MH, Willats WG, Knox JP**. 2003. Synthetic methyl hexagalacturonate hapten inhibitors of anti-homogalacturonan monoclonal antibodies LM7, JIM5 and JIM7. Carbohydrate research **338**, 1797-1800.

**Cole JR, Wang Q, Fish JA, Chai B, McGarrell DM, Sun Y, Brown CT, Porras-Alfaro A, Kuske CR, Tiedje JM**. 2014. Ribosomal Database Project: data and tools for high throughput rRNA analysis. Nucleic acids research **42**, D633-D642.

**Collard BC, Jahufer M, Brouwer J, Pang E**. 2005. An introduction to markers, quantitative trait loci (QTL) mapping and marker-assisted selection for crop improvement: the basic concepts. Euphytica **142**, 169-196.

**Collins HM, Burton RA, Topping DL, Liao ML, Bacic A, Fincher GB**. 2010. Variability in fine structures of noncellulosic cell wall polysaccharides from cereal grains: potential importance in human health and nutrition. Cereal Chemistry **87**, 272-282.

**Condon A, Richards R**. 1992. Broad sense heritability and genotype× environment interaction for carbon isotope discrimination in field-grown wheat. Australian Journal of Agricultural Research **43**, 921-934.

**Cordell D, Drangert J-O, White S**. 2009. The story of phosphorus: global food security and food for thought. Global environmental change **19**, 292-305.

**Cornuault V, Buffetto F, Rydahl MG, Marcus SE, Torode TA, Xue J, Crépeau M-J, Faria-Blanc N, Willats WG, Cosgrove DJ**. 2014. Re-constructing our models of cellulose and primary cell wall assembly. Current Opinion in Plant Biology **22**, 122-131.

**Costa R, Götz M, Mrotzek N, Lottmann J, Berg G, Smalla K**. 2006. Effects of site and plant species on rhizosphere community structure as revealed by molecular analysis of microbial guilds. FEMS microbiology ecology **56**, 236-249.

**Dalmastri C, Chiarini L, Cantale C, Bevivino A, Tabacchioni S**. 1999. Soil type and maize cultivar affect the genetic diversity of maize root–associated Burkholderia cepacia populations. Microbial Ecology **38**, 273-284.

**Datta S, Jankowicz-Cieslak J, Nielen S, Ingelbrecht I, Till BJ**. 2018. Induction and recovery of copy number variation in banana through gamma irradiation and low-coverage whole-genome sequencing. Plant biotechnology journal **16**, 1644-1653.

**David LA, Maurice CF, Carmody RN, Gootenberg DB, Button JE, Wolfe BE, Ling AV, Devlin AS, Varma Y, Fischbach MA**. 2014. Diet rapidly and reproducibly alters the human gut microbiome. Nature **505**, 559-563.

**de Ridder-Duine AS, Kowalchuk GA, Gunnewiek PJK, Smant W, van Veen JA, de Boer W**. 2005. Rhizosphere bacterial community composition in natural stands of Carex arenaria (sand sedge) is determined by bulk soil community composition. Soil Biology and Biochemistry **37**, 349-357.

**Deakin G, Tilston EL, Bennett J, Passey T, Harrison N, Fernández-Fernández F, Xu X**. 2018. Spatial structuring of soil microbial communities in commercial apple orchards. Applied Soil Ecology **130**, 1-12.

**Delhaize E, Rathjen TM, Cavanagh CR**. 2015. The genetics of rhizosheath size in a multiparent mapping population of wheat. Journal of Experimental Botany **66**, 4527-4536.

**Delmont TO, Robe P, Cecillon S, Clark IM, Constancias F, Simonet P, Hirsch PR, Vogel TM**. 2011. Accessing the soil metagenome for studies of microbial diversity. Applied and environmental microbiology **77**, 1315-1324.

**Dennis PG, Miller AJ, Hirsch PR**. 2010. Are root exudates more important than other sources of rhizodeposits in structuring rhizosphere bacterial communities? FEMS microbiology ecology **72**, 313-327.

**Dixon P**. 2003. VEGAN, a package of R functions for community ecology. Journal of Vegetation Science **14**, 927-930.

**Dupree P**. 2015. Monoclonal antibodies indicate low-abundance links between heteroxylan and other glycans of plant cell walls. Planta **242**, 1321-1334.

**Curlango-Rivera G, Hawes MC**. 2011. Root tips moving through soil: an intrinsic vulnerability. Plant signaling & behavior **6**, 726-727.

**de Dorlodot S, Forster B, Pagès L, Price A, Tuberosa R, Draye X**. 2007. Root system architecture: opportunities and constraints for genetic improvement of crops. Trends in plant science **12**, 474-481.

**Deepak S, Shailasree S, Kini RK, Muck A, Mithöfer A, Shetty SH**. 2010. Hydroxyproline-rich glycoproteins and plant defence. Journal of Phytopathology **158**, 585-593.

**Delhaize E, James RA, Ryan PR**. 2012. Aluminium tolerance of root hairs underlies genotypic differences in rhizosheath size of wheat (Triticum aestivum) grown on acid soil. New phytologist **195**, 609-619.

**Dias ACF, Hoogwout EF, e Silva MdCP, Salles JF, van Overbeek LS, van Elsas JD**. 2012. Potato cultivar type affects the structure of ammonia oxidizer communities in field soil under potato beyond the rhizosphere. Soil biology and biochemistry **50**, 85-95.

**Dinka SJ, Campbell MA, Demers T, Raizada MN**. 2007. Predicting the size of the progeny mapping population required to positionally clone a gene. Genetics **176**, 2035-2054.

**Dippold MA, Boesel S, Gunina A, Kuzyakov Y, Glaser B.** 2014. Improved $\delta$13C analysis of amino sugars in soil by ion chromatography–oxidation–isotope ratio mass spectrometry. Rapid Communications in Mass Spectrometry. **6**, 569-76.

**Dittrich-Reed DR, Fitzpatrick BM**. 2013. Transgressive hybrids as hopeful monsters. Evolutionary biology **40**, 310-315.

**Dobzhansky T**. 1936. Studies on hybrid sterility. II. Localization of sterility factors in Drosophila pseudoobscura hybrids. Genetics **21**, 113.

**Dodd IC, Belimov A, Sobeih W, Safronova V, Grierson D, Davies W**. 2004. Will modifying plant ethylene status improve plant productivity in water-limited environments. *Handbook and abstracts for the 4th International Science Congress', Brisbane, Australia*, 134.

**Donn S, Kirkegaard JA, Perera G, Richardson AE, Watt M**. 2015. Evolution of bacterial communities in the wheat crop rhizosphere. Environmental microbiology **17**, 610-621.

**Doré C, Varoquaux F**. 2006. *Histoire et amélioration de cinquante plantes cultivées*: Editions Quae.

**Drew M, Jackson M, Giffard S**. 1979. Ethylene-promoted adventitious rooting and development of cortical air spaces (aerenchyma) in roots may be adaptive responses to flooding in Zea mays L. Planta **147**, 83-88.

**Driouich A, Durand C, Cannesan M-A, Percoco G, Vicré-Gibouin M**. 2010. Border cells versus border-like cells: are they alike? Journal of experimental botany **61**, 3827-3831.

**Driouich A, Follet-Gueye M-L, Vicré-Gibouin M, Hawes M**. 2013. Root border cells and secretions as critical elements in plant host defense. Current Opinion in Plant Biology **16**, 489-495.

**Driouich A, Smith C, Ropitaux M, Chambard M, Boulogne I, Bernard S, Follet-Gueye ML, Vicré M, Moore J**. 2019. Root extracellular traps versus neutrophil extracellular traps in host defence, a case of functional convergence? Biological Reviews **94**, 1685-1700.

**Dubcovsky J, Dvorak J**. 2007. Genome plasticity a key factor in the success of polyploid wheat under domestication. Science **316**, 1862-1866.

**Durand C, Vicré-Gibouin M, Follet-Gueye ML, Duponchel L, Moreau M, Lerouge P, Driouich A**. 2009. The organization pattern of root border-like cells of Arabidopsis is dependent on cell wall homogalacturonan. Plant physiology **150**, 1411-1421.

**Edgar RC**. 2013. UPARSE: highly accurate OTU sequences from microbial amplicon reads. Nature methods **10**, 996-998.

**Edgar RC, Flyvbjerg H**. 2015. Error filtering, pair assembly and error correction for next-generation sequencing reads. Bioinformatics **31**, 3476-3482.

**Egamberdieva D, Kamilova F, Validov S, Gafurova L, Kucharova Z, Lugtenberg B**. 2008. High incidence of plant growth-stimulating bacteria associated with the rhizosphere of wheat grown on salinated soil in Uzbekistan. Environmental microbiology **10**, 1-9.

**Ehdaie B, Layne AP, Waines JG**. 2012. Root system plasticity to drought influences grain yield in bread wheat. Euphytica **186**, 219-232.

**Eid MH**. 2009. Estimation of heritability and genetic advance of yield traits in wheat (Triticum aestivum L.) under drought condition. International Journal of Genetics and Molecular Biology **1**, 115-120.

**El Baidouri M, Murat F, Veyssiere M, Molinier M, Flores R, Burlot L, Alaux M, Quesneville H, Pont C, Salse J**. 2017. Reconciling the evolutionary origin of bread wheat (Triticum aestivum). New phytologist **213**, 1477-1486.

**Elliott AJ, Daniell TJ, Cameron DD, Field KJ**. 2020. A commercial arbuscular mycorrhizal inoculum increases root colonization across wheat cultivars but does not increase assimilation of mycorrhiza-acquired nutrients. Plants, People, Planet.

**Ellis M, Egelund J, Schultz CJ, Bacic A**. 2010. Arabinogalactan-proteins: key regulators at the cell surface? Plant Physiology **153**, 403-419.

**Ellis M, Egelund J, Schultz CJ, Bacic A**. 2010. Arabinogalactan-proteins: key regulators at the cell surface? Plant Physiology **153**, 403-419.

**Elwell AL, Gronwall DS, Miller ND, Spalding EP, DURHAM BROOKS TL**. 2011. Separating parental environment from seed size effects on next generation growth and development in Arabidopsis. Plant, cell & environment **34**, 291-301.

**Endo T**. 1988. Induction of chromosomal structural changes by a chromosome of Aegilops cylindrica L. in common wheat. Journal of Heredity **79**, 366-370.

**Endo T, Gill B**. 1996. The deletion stocks of common wheat. Journal of Heredity **87**, 295-307.

**Endo TR, Tsunewaki K**. 1975. Sterility of common wheat with Aegilops triuncialis cytoplasm. Journal of Heredity **66**, 13-18.

**Ewers RM, Scharlemann JP, Balmford A, Green RE**. 2009. Do increases in agricultural yield spare land for nature? Global change biology **15**, 1716-1726.

**Fageria N, Baligar V**. 2005. Enhancing nitrogen use efficiency in crop plants. Advances in agronomy **88**, 97-185.

**Fan M, Zhu J, Richards C, Brown KM, Lynch JP**. 2003. Physiological roles for aerenchyma in phosphorus-stressed roots. Functional Plant Biology **30**, 493-506.

**Fan K, Cardona C, Li Y, Shi Y, Xiang X, Shen C, Wang H, Gilbert JA, Chu H**. 2017. Rhizosphere-associated bacterial network structure and spatial distribution differ significantly from bulk soil in wheat crop fields. Soil biology and biochemistry **113**, 275-284.

**Fatima T, Arora NK**. 2019. Plant Growth-Promoting Rhizospheric Microbes for Remediation of Saline Soils. *Phyto and Rhizo Remediation*: Springer, 121-146.

**Fierer N, Breitbart M, Nulton J, Salamon P, Lozupone C, Jones R, Robeson M, Edwards RA, Felts B, Rayhawk S**. 2007. Metagenomic and small-subunit rRNA analyses reveal the genetic diversity of bacteria, archaea, fungi, and viruses in soil. Applied and environmental microbiology **73**, 7059-7066.

**Fierer N, Leff JW, Adams BJ, Nielsen UN, Bates ST, Lauber CL, Owens S, Gilbert JA, Wall DH, Caporaso JG**. 2012. Cross-biome metagenomic analyses of soil microbial communities and their functional attributes. Proceedings of the National Academy of Sciences **109**, 21390-21395.

**Figueroa-Bustos V, Palta JA, Chen Y, Stefanova K, Siddique KH**. 2020. Wheat Cultivars With Contrasting Root System Size Responded Differently to Terminal Drought. Frontiers in plant science **11**, 1285.

**Fischer SE, Jofré EC, Cordero PV, Manero FJ, Mori GB.** 2010. Survival of native Pseudomonas in soil and wheat rhizosphere and antagonist activity against plant pathogenic fungi. Antonie Van Leeuwenhoek. **97**, 241-51**.**

**Fitzgerald G**. 2010. Characterizing vegetation indices derived from active and passive sensors. International Journal of Remote Sensing **31**, 4335-4348.

**Fitzpatrick CR, Copeland J, Wang PW, Guttman DS, Kotanen PM, Johnson MT**. 2018. Assembly and ecological function of the root microbiome across angiosperm plant species. Proceedings of the National Academy of Sciences **115**, E1157-E1165.

**Foster ZS, Sharpton TJ, Grünwald NJ**. 2017. Metacoder: an R package for visualization and manipulation of community taxonomic diversity data. PLoS computational biology **13**, e1005404.

**Fradgley N, Evans G, Biernaskie JM, Cockram JS, Marr EC, Oliver AG, Ober E, Jones H**. 2020. Effects of breeding history and crop management on the root architecture of wheat. BioRxiv.

**Furbank RT, Tester M**. 2011. Phenomics–technologies to relieve the phenotyping bottleneck. Trends in plant science **16**, 635-644.

**Galbally IE, Kirstine W**. 2002. The production of methanol by flowering plants and the global cycle of methanol. Journal of Atmospheric Chemistry **43**, 195-229.

**Gale MD, Marshall GA**. 1973. Insensitivity to gibberellin in dwarf wheats. Annals of Botany **37**, 729-735.

**Galloway AF, Akhtar J, Marcus SE, Fletcher N, Field K, Knox P**. 2020. Cereal root exudates contain highly structurally complex polysaccharides with soil-binding properties. The Plant Journal.

**Galloway AF, Knox P, Krause K**. 2020. Sticky mucilages and exudates of plants: putative microenvironmental design elements with biotechnological value. New Phytologist **225**, 1461-1469.

**Galloway AF, Pedersen MJ, Merry B, Marcus SE, Blacker J, Benning LG, Field KJ, Knox JP**. 2018. Xyloglucan is released by plants and promotes soil particle aggregation. New Phytologist **217**, 1128-1136.

**Gao Y, Lynch JP**. 2016. Reduced crown root number improves water acquisition under water deficit stress in maize (Zea mays L.). Journal of Experimental Botany **67**, 4545-4557.

**Gao W, Blaser SR, Schlüter S, Shen J, Vetterlein D**. 2019. Effect of localised phosphorus application on root growth and soil nutrient dynamics in situ–comparison of maize (Zea mays) and faba bean (Vicia faba) at the seedling stage. Plant and Soil **441**, 469-483.

**Garbeva P, Van Elsas J, Van Veen J**. 2008. Rhizosphere microbial community and its response to plant species and soil history. Plant and Soil **302**, 19-32.

**Garnett T, Appleby MC, Balmford A, Bateman IJ, Benton TG, Bloomer P, Burlingame B, Dawkins M, Dolan L, Fraser D**. 2013. Sustainable intensification in agriculture: premises and policies. Science **341**, 33-34.

**Gaspar YM, Nam J, Schultz CJ, Lee L-Y, Gilson PR, Gelvin SB, Bacic A**. 2004. Characterization of the Arabidopsis lysine-rich arabinogalactan-protein AtAGP17 mutant (rat1) that results in a decreased efficiency of Agrobacterium transformation. Plant Physiology **135**, 2162-2171.

**Ge Z, Rubio G, Lynch JP**. 2000. The importance of root gravitropism for inter-root competition and phosphorus acquisition efficiency: results from a geometric simulation model. Plant and Soil **218**, 159-171.

**George TS, Brown LK, Ramsay L, White PJ, Newton AC, Bengough AG, Russell J, Thomas WT**. 2014. Understanding the genetic control and physiological traits associated with rhizosheath production by barley (H ordeum vulgare). New phytologist **203**, 195-205.

**Germida J, Siciliano S**. 2001. Taxonomic diversity of bacteria associated with the roots of modern, recent and ancient wheat cultivars. Biology and Fertility of Soils **33**, 410-415.

**Gilbert JA, Meyer F, Jansson J, Gordon J, Pace N, Tiedje J, Ley R, Fierer N, Field D, Kyrpides N**. 2010. The earth microbiome project: meeting report of the "1 st EMP meeting on sample selection and acquisition" at Argonne National Laboratory October 6 th 2010. Standards in genomic sciences **3**, 249-253.

**Gilbert N**. 2012. One-third of our greenhouse gas emissions come from agriculture. Nature **31**, 10-12.

**Golan G, Hendel E, Méndez Espitia GE, Schwartz N, Peleg Z**. 2018. Activation of seminal root primordia during wheat domestication reveals underlying mechanisms of plant resilience. Plant, cell & environment **41**, 755-766.

**Goldberg N, Hawes M, Stanghellini M**. 1989. Specific attraction to and infection of cotton root cap cells by zoospores of Pythium dissotocum. Canadian Journal of Botany **67**, 1760-1767.

**Gomes N, Heuer H, Schönfeld J, Costa R, Mendonca-Hagler L, Smalla K**. 2001. Bacterial diversity of the rhizosphere of maize (Zea mays) grown in tropical soil studied by temperature gradient gel electrophoresis. Plant and Soil **232**, 167-180.

**Gomes NCM, Fagbola O, Costa R, Rumjanek NG, Buchner A, Mendona-Hagler L, Smalla K**. 2003. Dynamics of fungal communities in bulk and maize rhizosphere soil in the tropics. Applied and environmental microbiology **69**, 3758-3766.

**Goron TL, Watts S, Shearer C, Raizada MN**. 2015. Growth in Turface® clay permits root hair phenotyping along the entire crown root in cereal crops and demonstrates that root hair growth can extend well beyond the root hair zone. BMC Research Notes **8**, 143.

**Gregory P, McGowan M, Biscoe P, Hunter B**. 1978. Water relations of winter wheat: 1. Growth of the root system. The Journal of Agricultural Science **91**, 91-102.

**Gregory PJ, Hutchison D, Read DB, Jenneson PM, Gilboy WB, Morton EJ**. 2003. Non-invasive imaging of roots with high resolution X-ray micro-tomography. *Roots: the dynamic interface between plants and the Earth*: Springer, 351-359.

**Grierson CS, Parker JS, Kemp AC**. 2001. Arabidopsis genes with roles in root hair development. Journal of Plant Nutrition and Soil Science **164**, 131-140.

**Guinel F, McCully M**. 1986. Some water-related physical properties of maize root-cap mucilage. Plant, Cell & Environment **9**, 657-666.

**Gunina A, Kuzyakov Y**. 2015. Sugars in soil: Review of sources, contents, fate and functions. EGUGA, 1311.

**Gupta A, SM V**. 1973. Note on the rooting pattern of three-gene-dwarf wheats.

**Guseman JM, Webb K, Srinivasan C, Dardick C**. 2017. DRO 1 influences root system architecture in Arabidopsis and Prunus species. The Plant Journal **89**, 1093-1105.

**Haas D, Défago G**. 2005. Biological control of soil-borne pathogens by fluorescent pseudomonads. Nature reviews microbiology **3**, 307-319.

**Haichar F, Marol C, Berge O, Rangel-Castro J, Prosser J, Balesdent J, Heulin T, Achouak W**. 2008. Plant host habitat and root exudates shape soil bacterial community structure. The ISME Journal 2: 1221-1230. https. doi. org/10.1038/ismej.

**Hales B, Steed A, Giovannelli V, Burt C, Lemmens M, Molnár-Láng M, Nicholson P**. 2020. Type II Fusarium head blight susceptibility conferred by a region on wheat chromosome 4D. Journal of experimental botany **71**, 4703-4714.

**Haling RE, Richardson AE, Culvenor RA, Lambers H, Simpson RJ**. 2010. Root morphology, root-hair development and rhizosheath formation on perennial grass seedlings is influenced by soil acidity. Plant and Soil **335**, 457-468.

**Haling RE, Brown LK, Bengough AG, Valentine TA, White PJ, Young IM, George TS**. 2014. Root hair length and rhizosheath mass depend on soil porosity, strength and water content in barley genotypes. Planta **239**, 643-651.

**Hall Q, Cannon MC**. 2002. The cell wall hydroxyproline-rich glycoprotein RSH is essential for normal embryo development in Arabidopsis. The Plant Cell **14**, 1161-1172.

**Hamada A, Nitta M, Nasuda S, Kato K, Fujita M, Matsunaka H, Okumoto Y**. 2012. Novel QTLs for growth angle of seminal roots in wheat (Triticum aestivum L.). Plant and Soil **354**, 395-405.

**Hamblin A, Tennant D**. 1987. Root length density and water uptake in cereals and grain legumes: how well are they correlated. Australian Journal of Agricultural Research **38**, 513-527.

**Hao Z, Mohnen D**. 2014. A review of xylan and lignin biosynthesis: foundation for studying Arabidopsis irregular xylem mutants with pleiotropic phenotypes. Critical reviews in biochemistry and molecular biology **49**, 212-241.

**Hartmann A, Lemanceau P, Prosser JI**. 2008. Multitrophic interactions in the rhizosphere Rhizosphere microbiology: at the interface of many disciplines and expertises. FEMS Microbiol Ecol **65**, 179.

**Hartmann A, Rothballer M, Schmid M**. 2008. Lorenz Hiltner, a pioneer in rhizosphere microbial ecology and soil bacteriology research. Plant and Soil **312**, 7-14.

**Hartnett DC, WILSON GW, Ott JP, Setshogo M**. 2013. Variation in root system traits among African semi-arid savanna grasses: Implications for drought tolerance. Austral Ecology **38**, 383-392.

**Hawes MC, Gunawardena U, Miyasaka S, Zhao X**. 2000. The role of root border cells in plant defense. Trends in plant science **5**, 128-133.

**Hawes MC, Bengough G, Cassab G, Ponce G**. 2002. Root caps and rhizosphere. Journal of plant growth regulation **21**, 352-367.

**Hawes MC, Gunawardena U, Miyasaka S, Zhao X**. 2000. The role of root border cells in plant defense. Trends in plant science **5**, 128-133.

**Hayashi T**. 1989. Xyloglucans in the primary cell wall. Annual review of plant biology **40**, 139-168.

**Hayashi T**. 2006. *The Science and Lore of the Plant Cell Wall: Biosynthesis, Structure and Function*: Universal-Publishers.

**Hertenberger G, Zampach P, Bachmann G**. 2002. Plant species affect the concentration of free sugars and free amino acids in different types of soil. Journal of Plant Nutrition and Soil Science **165**, 557-565.

**Hiltner L**. 1904. Uber neuere Erfahrungen und Probleme auf dem Gebiete der Bodenbakteriologie unter besonderden berucksichtigung und Brache. Arb. Dtsch. Landwirtsch. Gesellschaft **98**, 59-78.

**Hirsch PR, Mauchline TH**. 2012. Who's who in the plant root microbiome? Nature biotechnology **30**, 961.

**Ho MD, Rosas JC, Brown KM, Lynch JP**. 2005. Root architectural tradeoffs for water and phosphorus acquisition. Functional plant biology **32**, 737-748.

**Hoad S, Russell G, Lucas M, Bingham I**. 2001. The management of wheat, barley, and oat root systems.

**Holz M, Leue M, Ahmed MA, Benard P, Gerke HH, Carminati A**. 2018. Spatial Distribution of Mucilage in the Rhizosphere Measured With Infrared Spectroscopy. Frontiers in Environmental Science **6**.

**Huang S, Sirikhachornkit A, Su X, Faris J, Gill B, Haselkorn R, Gornicki P**. 2002. Genes encoding plastid acetyl-CoA carboxylase and 3-phosphoglycerate kinase of the Triticum/Aegilops complex and the evolutionary history of polyploid wheat. Proceedings of the National Academy of Sciences **99**, 8133-8138.

**Huang Y, Kuang Z, Wang W, Cao L**. 2016. Exploring potential bacterial and fungal biocontrol agents transmitted from seeds to sprouts of wheat. Biological Control **98**, 27-33.

**Hunt J, Lilley JM, Trevaskis B, Peake A, Fletcher A, Flohr BM, Zwart AB, Gobbett D, Kirkegaard J**. 2017. Early Sowing Systems Can Adapt Australian Wheat Production to Rainfall Decline. *ASA, CSSA and SSSA International Annual Meetings*: ASA-CSSA-SSSA.

**Iijima M, Higuchi T, Barlow PW**. 2004. Contribution of root cap mucilage and presence of an intact root cap in maize (Zea mays) to the reduction of soil mechanical impedance. Annals of botany **94**, 473-477.

**Iijima M, Morita S, Barlow PW**. 2008. Structure and function of the root cap. Plant production science **11**, 17-27.

**İnceoğlu Ö, Al-Soud WA, Salles JF, Semenov AV, van Elsas JD**. 2011. Comparative analysis of bacterial communities in a potato field as determined by pyrosequencing. PloS one **6**, e23321.

**İnceoğlu Ö, Al-Soud WA, Salles JF, Semenov AV, van Elsas JD**. 2011. Comparative analysis of bacterial communities in a potato field as determined by pyrosequencing. PloS one **6**, e23321.

**İnceoğlu Ö, Salles JF, van Overbeek L, van Elsas JD**. 2010. Effects of plant genotype and growth stage on the betaproteobacterial communities associated with different potato cultivars in two fields. Applied and environmental microbiology **76**, 3675-3684.

**International V**. 2017. Genstat for Windows 19th Edition. VSN International, Hemel Hempstead, UK. Web page: Genstat.co.uk.

**James RA, Weligama C, Verbyla K, Ryan PR, Rebetzke GJ, Rattey A, Richardson AE, Delhaize E**. 2016. Rhizosheaths on wheat grown in acid soils: phosphorus acquisition efficiency and genetic control. Journal of Experimental Botany **67**, 3709-3718.

**James TY, Kauff F, Schoch CL, Matheny PB, Hofstetter V, Cox CJ, Celio G, Gueidan C, Fraker E, Miadlikowska J**. 2006. Reconstructing the early evolution of Fungi using a six-gene phylogeny. Nature **443**, 818-822.

**Jones D, Kemmitt S, Wright D, Cuttle S, Bol R, Edwards A**. 2005. Rapid intrinsic rates of amino acid biodegradation in soils are unaffected by agricultural management strategy. Soil biology and biochemistry **37**, 1267-1275.

**Kamilova F, Validov S, Azarova T, Mulders I, Lugtenberg B**. 2005. Enrichment for enhanced competitive plant root tip colonizers selects for a new class of biocontrol bacteria. Environmental Microbiology **7**, 1809-1817.

**Kasha K, Maluszynski M**. 2003. Production of doubled haploids in crop plants. An introduction. *Doubled haploid production in crop plants*: Springer, 1-4.

**Kashtan N, Roggensack SE, Rodrigue S, Thompson JW, Biller SJ, Coe A, Ding H, Marttinen P, Malmstrom RR, Stocker R**. 2014. Single-cell genomics reveals hundreds of coexisting subpopulations in wild Prochlorococcus. Science **344**, 416-420.

**Kavamura VN, Rifat Hayat, Ian M. Clark, Maike Rossmann, Rodrigo Mendes, Penny R. Hirsch, and Tim H. Mauchline**. 2018. Inorganic nitrogen application affects both taxonomical and predicted functional structure of wheat rhizosphere bacterial communities. Frontiers in Microbiology **9**, 1074.

**Kavamura VN, Robinson RJ, Hughes D, Clark I, Rossmann M, de Melo IS, Hirsch PR, Mendes R, Mauchline TH**. 2020. Wheat dwarfing influences selection of the rhizosphere microbiome. Scientific reports **10**, 1-11.

**Keegstra K, Talmadge KW, Bauer W, Albersheim P**. 1973. The structure of plant cell walls: III. A model of the walls of suspension-cultured sycamore cells based on the interconnections of the macromolecular components. Plant physiology **51**, 188-197.

**Kieliszewski MJ**. 2001. The latest hype on Hyp-O-glycosylation codes. Phytochemistry **57**, 319-323.

**Kim Y-C, Glick BR, Bashan Y, Ryu C-M**. 2012. Enhancement of Plant Drought Tolerance by Microbes. In: Aroca R, ed. *Plant Responses to Drought Stress: From Morphological to Molecular Features*. Berlin, Heidelberg: Springer Berlin Heidelberg, 383-413.

**Kim B-R, Shin J, Guevarra RB, Lee JH, Kim DW, Seol K-H, Lee J-H, Kim HB, Isaacson RE**. 2017. Deciphering diversity indices for a better understanding of microbial communities. Journal of Microbiology and Biotechnology **27**, 2089-2093.

**Kirkegaard J, Lilley J, Howe G, Graham J**. 2007. Impact of subsoil water use on wheat yield. Australian Journal of Agricultural Research **58**, 303-315.

**Klepper B, Belford R, Rickman R**. 1984. Root and Shoot Development in Winter Wheat 1. Agronomy journal **76**, 117-122.

**Knee EM, Gong F-C, Gao M, Teplitski M, Jones AR, Foxworthy A, Mort AJ, Bauer WD**. 2001. Root mucilage from pea and its utilization by rhizosphere bacteria as a sole carbon source. Molecular Plant-Microbe Interactions **14**, 775-784.

**Knief C, Delmotte N, Chaffron S, Stark M, Innerebner G, Wassmann R, Von Mering C, Vorholt JA**. 2012. Metaproteogenomic analysis of microbial communities in the phyllosphere and rhizosphere of rice. The ISME journal **6**, 1378-1390.

**Knox JP, Linstead PJ, King J, Cooper C, Roberts K**. 1990. Pectin esterification is spatially regulated both within cell walls and between developing tissues of root apices. Planta **181**, 512-521.

**Knudson L**. 1920. The secretion of invertase by plant roots. American Journal of Botany **7**, 371-379.

**Kõljalg U, Nilsson RH, Abarenkov K, Tedersoo L, Taylor AF, Bahram M, Bates ST, Bruns TD, Bengtsson-Palme J, Callaghan TM**. 2013. Towards a unified paradigm for sequence-based identification of fungi. Molecular ecology **22**, 5271-5277.

**Korenblum E, Dong Y, Szymanski J, Panda S, Jozwiak A, Massalha H, Meir S, Rogachev I, Aharoni A**. 2020. Rhizosphere microbiome mediates systemic root metabolite exudation by root-to-root signaling. Proceedings of the National Academy of Sciences **117**, 3874-3883.

**Koroney AS, Plasson C, Pawlak B, Sidikou R, Driouich A, Menu-Bouaouiche L, Vicré-Gibouin M**. 2016. Root exudate of Solanum tuberosum is enriched in galactose-containing molecules and impacts the growth of Pectobacterium atrosepticum. Annals of Botany **118**, 797-808.

**Kowalchuk GA, Stienstra AW, Stephen JR, Woldendorp JW**. 2000. Changes in the community structure of ammonia-oxidizing bacteria during secondary succession of calcareous grasslands. Environmental Microbiology **2**, 99-110.

**Kowalchuk GA, Buma DS, de Boer W, Klinkhamer PG, van Veen JA**. 2002. Effects of above-ground plant species composition and diversity on the diversity of soil-borne microorganisms. Antonie Van Leeuwenhoek **81**, 509.

**Kreuger M, van Holst G-J**. 1993. Arabinogalactan proteins are essential in somatic embryogenesis of Daucus carota L. Planta **189**, 243-248.

**Kuzyakov Y, Razavi BS**. 2019. Rhizosphere size and shape: Temporal dynamics and spatial stationarity. Soil biology and biochemistry **135**, 343-360.

**Lamport DT, Kieliszewski MJ, Chen Y, Cannon MC**. 2011. Role of the extensin superfamily in primary cell wall architecture. Plant Physiology **156**, 11-19.

**Landi P, Sanguineti M, Liu C, Li Y, Wang T, Giuliani S, Bellotti M, Salvi S, Tuberosa R**. 2007. Root-ABA1 QTL affects root lodging, grain yield, and other agronomic traits in maize grown under well-watered and water-stressed conditions. Journal of Experimental Botany **58**, 319-326.

**Larbi A, Mekliche A**. 2004. Relative water content (RWC) and leaf senescence as screening tools for drought tolerance in wheat. Options Méditerranéennes. Série A, Séminaires Méditerranéens **60**, 193-196.

**Lee KJ, Marcus SE, Knox JP**. 2011. Cell wall biology: perspectives from cell wall imaging. Molecular plant **4**, 212-219.

**Leff B, Ramankutty N, Foley JA**. 2004. Geographic distribution of major crops across the world. Global biogeochemical cycles **18**.

**Le Gouis J, Béghin D, Heumez E, Pluchard P**. 2000. Genetic differences for nitrogen uptake and nitrogen utilisation efficiencies in winter wheat. European Journal of Agronomy **12**, 163-173.

**Lehnert H, Serfling A, Friedt W, Ordon F**. 2018. Genome-wide association studies reveal genomic regions associated with the response of wheat (Triticum aestivum L.) to mycorrhizae under drought stress conditions. Frontiers in Plant Science **9**, 1728.

**Lemos LN, Fulthorpe RR, Triplett EW, Roesch LF.** 2011. Rethinking microbial diversity analysis in the high throughput sequencing era. Journal of microbiological methods. **1**, 42-51.

**Leng L, Nobu MK, Narihiro T, Yang P, Tan G-YA, Lee P-H**. 2019. Shaping microbial consortia in coupling glycerol fermentation and carboxylate chain elongation for co-production of 1, 3-propanediol and caproate: pathways and mechanisms. Water research **148**, 281-291.

**Liao M, Palta JA, Fillery IR**. 2006. Root characteristics of vigorous wheat improve early nitrogen uptake. Australian Journal of Agricultural Research **57**, 1097-1107.

**Li P, Chen J, Wu P, Zhang J, Chu C, See D, Brown-Guedira G, Zemetra R, Souza E**. 2011. Quantitative Trait Loci Analysis for the Effect of Rht-B1 Dwarfing Gene on Coleoptile Length and Seedling Root Length and Number of Bread Wheat. Crop Science **51**, 2561-2568.

**Li H**. 2013. Aligning sequence reads, clone sequences and assembly contigs with BWA-MEM. arXiv preprint arXiv:1303.3997.

**Liu Y, Chen L, Fu D, Lou Q, Mei H, Xiong L, Li M, Xu X, Mei X, Luo L**. 2014. Dissection of additive, epistatic effect and QTL× environment interaction of quantitative trait loci for sheath blight resistance in rice. Hereditas **151**, 28-37.

**Lopes MS, Reynolds MP**. 2010. Partitioning of assimilates to deeper roots is associated with cooler canopies and increased yield under drought in wheat. Functional plant biology **37**, 147-156.

**López-Bucio J, Campos-Cuevas JC, Hernández-Calderón E, Velásquez-Becerra C, Farías-Rodríguez R, Macías-Rodríguez LI, Valencia-Cantero E**. 2007. Bacillus megaterium rhizobacteria promote growth and alter root-system architecture through an auxin-and ethylene-independent signaling mechanism in Arabidopsis thaliana. Molecular Plant-Microbe Interactions **20**, 207-217.

**Love MI, Huber W, Anders S**. 2014. Moderated estimation of fold change and dispersion for RNA-seq data with DESeq2. Genome biology **15**, 550.

**Lozupone C, Knight R**. 2005. UniFrac: a new phylogenetic method for comparing microbial communities. Applied and environmental microbiology **71**, 8228-8235.

**Lu Y, Rosencrantz D, Liesack W, Conrad R**. 2006. Structure and activity of bacterial community inhabiting rice roots and the rhizosphere. Environmental Microbiology **8**, 1351-1360.

**Lucas M, Hoad S, Russell G, Bingham I**. 2000. Management of cereal root systems. Management of cereal root systems.

**Lucas García JA, Barbas C, Probanza A, Barrientos ML, Gutierrez Mañero FJ.** 2001. Low molecular weight organic acids and fatty acids in root exudates of two Lupinus cultivars at flowering and fruiting stages. Phytochemical Analysis: An International Journal of Plant Chemical and Biochemical Techniques. **5,** 305-11.

**Lundberg DS, Lebeis SL, Paredes SH, Yourstone S, Gehring J, Malfatti S, Tremblay J, Engelbrektson A, Kunin V, Del Rio TG**. 2012. Defining the core Arabidopsis thaliana root microbiome. Nature **488**, 86-90.

**Lynch JP**. 2007. Roots of the second green revolution. Australian Journal of Botany **55**, 493-512.

**Lynch JP**. 2013. Steep, cheap and deep: an ideotype to optimize water and N acquisition by maize root systems. Annals of botany **112**, 347-357.

**Lyon TL, Wilson JK.** 1921. Liberation of organic matter by roots of growing plants. Cornell University

**Mac Key ., Sears ER and Sears LMS. 1973.** The Wheat Root. Proceedings 4th International Wheat Genetics Symposium, Columbia, Missouri, USA, 827-842.

**Mackay I, Powell W**. 2007. Methods for linkage disequilibrium mapping in crops. Trends in plant science **12**, 57-63.

**MacMillan K, Emrich K, Piepho H-P, Mullins C, Price A**. 2006. Assessing the importance of genotype× environment interaction for root traits in rice using a mapping population II: conventional QTL analysis. Theoretical and Applied Genetics **113**, 953-964.

**Magurran AE. Measuring biological diversity.** 2004. Malden, Ma: Blackwell Pub. viii.

**Mahoney AK, Yin C, Hulbert SH**. 2017. Community structure, species variation, and potential functions of rhizosphere-associated bacteria of different winter wheat (Triticum aestivum) cultivars. Frontiers in Plant Science **8**, 132.

**Mai CD, Phung NT, To HT, Gonin M, Hoang GT, Nguyen KL, Do VN, Courtois B, Gantet P**. 2014. Genes controlling root development in rice. Rice **7**, 30.

**Manschadi AM, Christopher J, deVoil P, Hammer GL**. 2006. The role of root architectural traits in adaptation of wheat to water-limited environments. Functional plant biology **33**, 823-837.

**Manschadi AM, Hammer GL, Christopher JT, Devoil P**. 2008. Genotypic variation in seedling root architectural traits and implications for drought adaptation in wheat (Triticum aestivum L.). Plant and Soil **303**, 115-129.

**Manschadi A, Manske G, Vlek P**. 2013. Root architecture and resource acquisition: wheat as a model plant. Plant roots: The hidden half, 1-22.

**Manske GG, Vlek PL**. 2002. Root architecture–wheat as a model plant. Plant roots: The hidden half **3**, 249-259.

 **Marasco R, Rolli E, Fusi M, Michoud G, Daffonchio D**. 2018. Grapevine rootstocks shape underground bacterial microbiome and networking but not potential functionality. Microbiome **6**, 3.

**Marcel TC, Aghnoum R, Durand J, Varshney RK, Niks RE**. 2007. Dissection of the barley 2L1. 0 region carrying the 'Laevigatum'quantitative resistance gene to leaf rust using near-isogenic lines (NIL) and subNIL. Molecular Plant-Microbe Interactions **20**, 1604-1615.

**Margulies M, Egholm M, Altman WE, Attiya S, Bader JS, Bemben LA, Berka J, Braverman MS, Chen Y-J, Chen Z**. 2005. Genome sequencing in microfabricated high-density picolitre reactors. Nature **437**, 376-380.

**Marschner P, Yang C-H, Lieberei R, Crowley DE**. 2001. Soil and plant specific effects on bacterial community composition in the rhizosphere. Soil biology and biochemistry **33**, 1437-1445.

**Marschner P, Neumann G, Kania A, Weiskopf L, Lieberei R**. 2002. Spatial and temporal dynamics of the microbial community structure in the rhizosphere of cluster roots of white lupin (Lupinus albus L.). Plant and Soil **246**, 167-174.

**Mauchline T, Chedom-Fotso D, Chandra G, Samuels T, Greenaway N, Backhaus A, McMillan V, Canning G, Powers S, Hammond-Kosack K**. 2015. An analysis of P seudomonas genomic diversity in take-all infected wheat fields reveals the lasting impact of wheat cultivars on the soil microbiota. Environmental microbiology **17**, 4764-4778.

**Mauchline TH, Nessner Kavamura V, Robinson R, Hayat R, Clark IM, Hughes D, Rossmann M, Hirsch P,**

**Mavrodi DV, Mavrodi OV, Elbourne LD, Tetu S, Bonsall RF, Parejko J, Yang M, Paulsen IT, Weller DM, Thomashow LS**. 2018. Long-term irrigation affects the dynamics and activity of the wheat rhizosphere microbiome. Frontiers in Plant Science **9**, 345.

**Mayak S, Tirosh T, Glick BR**. 2004. Plant growth-promoting bacteria confer resistance in tomato plants to salt stress. Plant Physiology and Biochemistry **42**, 565-572.

**McCann MC, Roberts K**. 1994. Changes in cell wall architecture during cell elongation. Journal of Experimental Botany, 1683-1691.

**McCartney L, Marcus SE, Knox JP**. 2005. Monoclonal antibodies to plant cell wall xylans and arabinoxylans. Journal of Histochemistry & Cytochemistry **53**, 543-546.

**McCully ME**. 1999. Roots in soil: unearthing the complexities of roots and their rhizospheres. Annual review of plant biology **50**, 695-718.

**McCully ME, Sealey LJ.** 1996. The expansion of maize root-cap mucilage during hydration. 2. Observations on soil-grown roots by cryo-scanning electron microscopy. Physiologia Plantarum. **3,** 454-62.

**McDougall BM, Rovira A**. 1970. Sites of exudation of 14C-labelled compounds from wheat roots. New Phytologist **69**, 999-1003.

**McElgunn J, Harrison C**. 1969. Formation, Elongation, and Longevity of Barley Root Hairs 1. Agronomy Journal **61**, 79-81.

**McGrail RK, Van Sanford DA, McNear DH**. 2020. Trait-Based Root Phenotyping as a Necessary Tool for Crop Selection and Improvement. Agronomy **10**, 1328.

**McMurdie PJ, Holmes S**. 2013. phyloseq: an R package for reproducible interactive analysis and graphics of microbiome census data. PloS one **8**, e61217.

**Medzhitov R, Janeway CA**. 1997. Innate immunity: the virtues of a nonclonal system of recognition. Cell **91**, 295-298.

**Mendes R**. 2019. Land management and microbial seed load effect on rhizosphere and endosphere bacterial community assembly in wheat. Frontiers in Microbiology **10**, 2625.

**Mendes R, Kruijt M, De Bruijn I, Dekkers E, van der Voort M, Schneider JH, Piceno YM, DeSantis TZ, Andersen GL, Bakker PA**. 2011. Deciphering the rhizosphere microbiome for disease-suppressive bacteria. Science **332**, 1097-1100.

**Merkouropoulos G, Shirsat AH**. 2003. The unusual Arabidopsis extensin gene atExt1 is expressed throughout plant development and is induced by a variety of biotic and abiotic stresses. Planta **217**, 356-366.

**Messina CD, Sinclair TR, Hammer GL, Curan D, Thompson J, Oler Z, Gho C, Cooper M**. 2015. Limited-transpiration trait may increase maize drought tolerance in the US Corn Belt. Agronomy Journal **107**, 1978-1986.

**Met Office** (2019). Available Online at: https://www.metoffice.gov.uk/research/approach/collaboration/ukcp/index

**Micallef SA, Shiaris MP, Colón-Carmona A**. 2009. Influence of Arabidopsis thaliana accessions on rhizobacterial communities and natural variation in root exudates. Journal of experimental botany **60**, 1729-1742.

**Michael G**. 2001. The control of root hair formation: suggested mechanisms. Journal of Plant Nutrition and Soil Science **164**, 111-119.

**Mohnen D**. 2008. Pectin structure and biosynthesis. Current opinion in plant biology **11**, 266-277.

**Mohsin T, Khan N, Naqvi FN**. 2009. Heritability, phenotypic correlation and path coefficient studies for some agronomic characters in synthetic elite lines of wheat. Journal of Food Agriculture and Environment **7**, 278-282.

**Moody SF, Clarke AE, Bacic A**. 1988. Structural analysis of secreted slime from wheat and cowpea roots. Phytochemistry **27**, 2857-2861.

**Morel J, Mench M, Guckert A**. 1986. Measurement of Pb 2+, Cu 2+ and Cd 2+ binding with mucilage exudates from maize (Zea mays L.) roots. Biology and Fertility of Soils **2**, 29-34.

**Moreno-Espíndola IP, Rivera-Becerril F, de Jesús Ferrara-Guerrero M, De León-González F**. 2007. Role of root-hairs and hyphae in adhesion of sand particles. Soil biology and biochemistry **39**, 2520-2526.

**Morgan JL, Darling AE, Eisen JA**. 2010. Metagenomic sequencing of an in vitro-simulated microbial community. PloS one **5**, e10209.

**Mounier E, Hallet S, Chèneby D, Benizri E, Gruet Y, Nguyen C, Piutti S, Robin C, Slezack-Deschaumes S, Martin-Laurent F, Germon JC**. 2004. Influence of maize mucilage on the diversity and activity of the denitrifying community. Environmental Microbiology. **3,** 301-12.

**Muller HJ**. 1939. REVERSIBILITY IN EVOLUTION CONSIDERED FROM THE STANDPOINT OF GENETICS 1. Biological Reviews **14**, 261-280.

 **Nagel KA, Putz A, Gilmer F, Heinz K, Fischbach A, Pfeifer J, Faget M, Blossfeld S, Ernst M, Dimaki C**. 2012. GROWSCREEN-Rhizo is a novel phenotyping robot enabling simultaneous measurements of root and shoot growth for plants grown in soil-filled rhizotrons. Functional plant biology **39**, 891-904.

**Narasimhan K, Basheer C, Bajic VB, Swarup S.** 2003. Enhancement of plant-microbe interactions using a rhizosphere metabolomics-driven approach and its application in the removal of polychlorinated biphenyls. Plant Physiology. **1,** 146-53.

**Navarro LM, Pereira HM**. 2015. Rewilding abandoned landscapes in Europe. *Rewilding European Landscapes*: Springer, Cham, 3-23.

**Naveed M, Mitter B, Reichenauer TG, Wieczorek K, Sessitsch A**. 2014. Increased drought stress resilience of maize through endophytic colonization by Burkholderia phytofirmans PsJN and Enterobacter sp. FD17. Environmental and Experimental Botany **97**, 30-39.

**Neumann G, Römheld V.** 1999. Root excretion of carboxylic acids and protons in phosphorus-deficient plants. Plant and Soil. **211**, 121-30.

**Newman E**. 1985. The rhizosphere: carbon sources and microbial populations. Ecological interactions in soil: plants, microbes and animals, 107-121.

**Newman M-A, Sundelin T, Nielsen JT, Erbs G**. 2013. MAMP (microbe-associated molecular pattern) triggered immunity in plants. Frontiers in Plant Science **4**, 139.

**Nguema-Ona E, Vicré-Gibouin M, Cannesan M-A, Driouich A**. 2013. Arabinogalactan proteins in root–microbe interactions. Trends in plant science **18**, 440-449.

**Nguyen C.** 2003. Rhizodeposition of organic C by plants: mechanisms and controls.

**Nguyen NH, Song Z, Bates ST, Branco S, Tedersoo L, Menke J, Schilling JS, Kennedy PG**. 2016. FUNGuild: an open annotation tool for parsing fungal community datasets by ecological guild. Fungal Ecology **20**, 241-248.

**North GB, Nobel PS**. 1997. Drought-induced changes in soil contact and hydraulic conductivity for roots of Opuntia ficus-indica with and without rhizosheaths. Plant and Soil **191**, 249-258.

**Nuccio EE, Starr E, Karaoz U, Brodie EL, Zhou J, Tringe SG, Malmstrom RR, Woyke T, Banfield JF, Firestone MK**. 2020. Niche differentiation is spatially and temporally regulated in the rhizosphere. The ISME journal **14**, 999-1014.

**Oburger E, Dell'mour M, Hann S, Wieshammer G, Puschenreiter M, Wenzel WW**. 2013. Evaluation of a novel tool for sampling root exudates from soil-grown plants compared to conventional techniques. Environmental and experimental botany **87**, 235-247.

**Ortiz R, Wagoire W, Hill J, Chandra S, Madsen S, Stølen O**. 2001. Heritability of and correlations among genotype-by-environment stability statistics for grain yield in bread wheat. Theoretical and Applied Genetics **103**, 469-474.

**Osborn HM, Lochey F, Mosley L, Read D.** 1999. Analysis of polysaccharides and monosaccharides in the root mucilage of maize (Zea mays L.) by gas chromatography. Journal of Chromatography A. **2**, 267-76.

**Palta JA, Chen X, Milroy SP, Rebetzke GJ, Dreccer MF, Watt M**. 2011. Large root systems: are they useful in adapting wheat to dry environments? Functional Plant Biology **38**, 347-354.

**Parker JS, Cavell AC, Dolan L, Roberts K, Grierson CS**. 2000. Genetic interactions during root hair morphogenesis in Arabidopsis. The Plant Cell **12**, 1961-1974.

**Paterson AH, DeVerna JW, Lanini B, Tanksley SD**. 1990. Fine mapping of quantitative trait loci using selected overlapping recombinant chromosomes, in an interspecies cross of tomato. Genetics **124**, 735-742.

**Pattathil S, Avci U, Miller JS, Hahn MG**. 2012. Immunological approaches to plant cell wall and biomass characterization: glycome profiling. *Biomass Conversion*: Springer, 61-72.

**Pausch J, Loeppmann S, Kühnel A, Forbush K, Kuzyakov Y, Cheng W**. 2016. Rhizosphere priming of barley with and without root hairs. Soil biology and biochemistry **100**, 74-82.

**Pearce S, Saville R, Vaughan SP, Chandler PM, Wilhelm EP, Sparks CA, Al-Kaff N, Korolev A, Boulton MI, Pearson R, Parkinson D**. 1960. The sites of excretion of ninhydrin-positive substances by broad bean seedlings. Plant and Soil **13**, 391-396.

**Pedersen HL, Fangel JU, McCleary B, Ruzanski C, Rydahl MG, Ralet M-C, Farkas V, von Schantz L, Marcus SE, Andersen MC**. 2012. Versatile high resolution oligosaccharide microarrays for plant glycobiology and cell wall research. Journal of Biological Chemistry **287**, 39429-39438.

**Pedersen HL, Fangel JU, McCleary B, Ruzanski C, Rydahl MG, Ralet M-C, Farkas V, von Schantz L, Marcus SE, Andersen MC**. 2012. Versatile high resolution oligosaccharide

microarrays for plant glycobiology and cell wall research. Journal of Biological Chemistry **287**, 39429-39438.

**Peiffer JA, Spor A, Koren O, Jin Z, Tringe SG, Dangl JL, Buckler ES, Ley RE**. 2013. Diversity and heritability of the maize rhizosphere microbiome under field conditions. Proceedings of the National Academy of Sciences **110**, 6548-6553.

**Pellegrino E, Öpik M, Bonari E, Ercoli L**. 2015. Responses of wheat to arbuscular mycorrhizal fungi: a meta-analysis of field studies from 1975 to 2013. Soil biology and biochemistry **84**, 210-217.

**Pena MJ, Darvill AG, Eberhard S, York WS, O'Neill MA**. 2008. Moss and liverwort xyloglucans contain galacturonic acid and are structurally distinct from the xyloglucans synthesized by hornworts and vascular plants. Glycobiology **18**, 891-904.

**Pereira CS, Ribeiro JM, Vatulescu AD, Findlay K, MacDougall AJ, Jackson PA**. 2011. Extensin network formation in Vitis vinifera callus cells is an essential and causal event in rapid and $H_2O_2$-induced reduction in primary cell wall hydration. BMC Plant Biology **11**, 106.

**Pervaiz ZH, Contreras J, Hupp BM, Lindenberger JH, Chen D, Zhang Q, Wang C, Twigg P, Saleem M**. 2020. Root microbiome changes with root branching order and root chemistry in peach rhizosphere soil. Rhizosphere **16**, 100249.

**Pettolino FA, Walsh C, Fincher GB, Bacic A**. 2012. Determining the polysaccharide composition of plant cell walls. Nature protocols **7**, 1590-1607.

**Phillips AL**. 2011. Molecular characterization of Rht-1 dwarfing genes in hexaploid wheat. Plant physiology **157**, 1820-1831.

**Piqué N, Gómez-Guillén MDC, Montero MP**. 2018. Xyloglucan, a plant polymer with barrier protective properties over the mucous membranes: an overview. International journal of molecular sciences **19**, 673.

**Plancot B, Santaella C, Jaber R, Kiefer-Meyer MC, Follet-Gueye M-L, Leprince J, Gattin I, Souc C, Driouich A, Vicré-Gibouin M**. 2013. Deciphering the responses of root border-like cells of Arabidopsis and flax to pathogen-derived elicitors. Plant physiology **163**, 1584-1597.

**Plaut Z, Butow B, Blumenthal C, Wrigley C**. 2004. Transport of dry matter into developing wheat kernels and its contribution to grain yield under post-anthesis water deficit and elevated temperature. Field Crops Research **86**, 185-198.

**Pollard DA**. 2012. Design and construction of recombinant inbred lines. *Quantitative Trait Loci (QTL)*: Springer, 31-39.

**Postma JA, Lynch JP**. 2012. Complementarity in root architecture for nutrient uptake in ancient maize/bean and maize/bean/squash polycultures. Annals of Botany **110**, 521-534.

**Ray TC, Callow JA, Kennedy JF.** 1988. Composition of root mucilage polysaccharides from Lepidium sativum. Journal of Experimental Botany. **9**, 1249-61.

**Price SR.** 1911. The roots of some North African desert-grasses. New phytologist. 10, 328–329.

**Price AH, Tomos A**. 1997. Genetic dissection of root growth in rice (Oryza sativa L.). II: mapping quantitative trait loci using molecular markers. Theoretical and Applied Genetics **95**, 143-152.

**Rashid A**. 2016. Defense responses of plant cell wall non-catalytic proteins against pathogens. Physiological and Molecular Plant Pathology **94**, 38-46.

**Read D, Gregory P**. 1997. Surface tension and viscosity of axenic maize and lupin root mucilages. The New Phytologist **137**, 623-628.

**Read D, Bengough AG, Gregory PJ, Crawford JW, Robinson D, Scrimgeour C, Young IM, Zhang K, Zhang X**. 2003. Plant roots release phospholipid surfactants that modify the physical and chemical properties of soil. New phytologist **157**, 315-326.

**Rebetzke G, Ellis M, Bonnett D, Mickelson B, Condon A, Richards R**. 2012. Height reduction and agronomic performance for selected gibberellin-responsive dwarfing genes in bread wheat (Triticum aestivum L.). Field Crops Research **126**, 87-96.

**Rebetzke G, Richards R, Holland J**. 2017. Population extremes for assessing trait value and correlated response of genetically complex traits. Field Crops Research **201**, 122-132.

**Reyes A, Haynes M, Hanson N, Angly FE, Heath AC, Rohwer F, Gordon JI**. 2010. Viruses in the faecal microbiota of monozygotic twins and their mothers. Nature **466**, 334-338.

**Rich SM, Christopher J, Richards R, Watt M**. 2020. Root phenotypes of young wheat plants grown in controlled environments show inconsistent correlation with mature root traits in the field. Journal of experimental botany.

**Richard CA, Hickey LT, Fletcher S, Jennings R, Chenu K, Christopher JT**. 2015. High-throughput phenotyping of seminal root traits in wheat. Plant Methods **11**, 1-11.

**Ridley BL, O'Neill MA, Mohnen D**. 2001. Pectins: structure, biosynthesis, and oligogalacturonide-related signaling. Phytochemistry **57**, 929-967.

**Ringli C**. 2010. The hydroxyproline-rich glycoprotein domain of the Arabidopsis LRX1 requires Tyr for function but not for insolubilization in the cell wall. The Plant Journal **63**, 662-669.

**Roesch LF, Fulthorpe RR, Riva A, Casella G, Hadwin AK, Kent AD, Daroub SH, Camargo FA, Farmerie WG, Triplett EW**. 2007. Pyrosequencing enumerates and contrasts soil microbial diversity. The ISME journal **1**, 283-290.

**Ropitaux M, Bernard S, Follet-Gueye M-L, Vicré M, Boulogne I, Driouich A**. 2019. Xyloglucan and cellulose form molecular cross-bridges connecting root border cells in pea (Pisum sativum). Plant Physiology and Biochemistry **139**, 191-196.

**Rosquete MR, Von Wangenheim D, Marhavý P, Barbez E, Stelzer EH, Benková E, Maizel A, Kleine-Vehn J**. 2013. An auxin transport mechanism restricts positive orthogravitropism in lateral roots. Current Biology **23**, 817-822.

**Ross-Ibarra J, Morrell PL, Gaut BS**. 2007. Plant domestication, a unique opportunity to identify the genetic basis of adaptation. Proceedings of the National Academy of Sciences **104**, 8641-8648.

**Rousk J, Bååth E, Brookes PC, Lauber CL, Lozupone C, Caporaso JG, Knight R, Fierer N**. 2010. Soil bacterial and fungal communities across a pH gradient in an arable soil. The ISME journal **4**, 1340-1351.

**Rovira AD**. 1969. Plant root exudates. The botanical review **35**, 35-57.

**Roychoudhry S, Del Bianco M, Kieffer M, Kepinski S**. 2013. Auxin controls gravitropic setpoint angle in higher plant lateral branches. Current Biology **23**, 1497-1504.

**Rubio G, Walk T, Ge Z, Yan X, Liao H, Lynch JP**. 2001. Root gravitropism and below-ground competition among neighbouring plants: a modelling approach. Annals of Botany **88**, 929-940.

**Sandhu D, Gill KS**. 2002. Gene-containing regions of wheat and the other grass genomes. Plant physiology **128**, 803-811.

**Sanguineti M, Li S, Maccaferri M, Corneti S, Rotondo F, Chiari T, Tuberosa R**. 2007. Genetic dissection of seminal root architecture in elite durum wheat germplasm. Annals of Applied Biology **151**, 291-305.

**Saville R, Gosman N, Burt C, Makepeace J, Steed A, Corbitt M, Chandler E, Brown J, Boulton M, Nicholson P**. 2012. The 'Green Revolution'dwarfing genes play a role in disease resistance in Triticum aestivum and Hordeum vulgare. Journal of experimental botany **63**, 1271-1283.

**Schloss PD, Handelsman J**. 2006. Introducing SONS, a tool for operational taxonomic unit-based comparisons of microbial community memberships and structures. Applied and environmental microbiology **72**, 6773-6779.

**Schloss PD, Westcott SL, Ryabin T, Hall JR, Hartmann M, Hollister EB, Lesniewski RA, Oakley BB, Parks DH, Robinson CJ**. 2009. Introducing mothur: open-source, platform-independent, community-supported software for describing and comparing microbial communities. Applied and environmental microbiology **75**, 7537-7541.

**Schmidt P, Hartung J, Bennewitz J, Piepho H-P**. 2019. Heritability in plant breeding on a genotype-difference basis. Genetics **212**, 991-1008.

**Schneider CA, Rasband WS, Eliceiri KW**. 2012. NIH Image to ImageJ: 25 years of image analysis. Nature methods **9**, 671-675.

**Schneider HM, Lynch JP**. 2020. Should root plasticity be a crop breeding target? Frontiers in Plant Science **11**.

**Schultz CJ, Harrison MJ**. 2008. Novel plant and fungal AGP-like proteins in the Medicago truncatula–Glomus intraradices arbuscular mycorrhizal symbiosis. Mycorrhiza **18**, 403-412.

**Schüßler A, Walker C**. 2011. 7 Evolution of the 'Plant-Symbiotic' Fungal Phylum, Glomeromycota. *Evolution of fungi and fungal-like organisms*: Springer, 163-185.

**Semenov A, Van Bruggen A, Zelenev V**. 1999. Moving waves of bacterial populations and total organic carbon along roots of wheat. Microbial Ecology **37**, 116-128.

**Seymour M, Kirkegaard JA, Peoples MB, White PF, French RJ**. 2012. Break-crop benefits to wheat in Western Australia–insights from over three decades of research. Crop and Pasture Science **63**, 1-16.

**Shane MW, McCully ME, Canny MJ, Pate JS, Lambers H**. 2011. Development and persistence of sandsheaths of Lyginia barbata (Restionaceae): relation to root structural development and longevity. Annals of Botany **108**, 1307-1322.

**Shi S, Nuccio EE, Shi ZJ, He Z, Zhou J, Firestone MK**. 2016. The interconnected rhizosphere: high network complexity dominates rhizosphere assemblages. Ecology letters **19**, 926-936.

**Shimizu A, Yanagihara S, Kawasaki S, Ikehashi H**. 2004. Phosphorus deficiency-induced root elongation and its QTL in rice (Oryza sativa L.). Theoretical and Applied Genetics **109**, 1361-1368.

**Simmons TJ, Mortimer JC, Bernardinelli OD, Pöppler A-C, Brown SP, Deazevedo ER, Dupree R, Dupree P**. 2016. Folding of xylan onto cellulose fibrils in plant cell walls revealed by solid-state NMR. Nature communications **7**, 1-9.

**Simpson EH.** 1949.Measurement of diversity. Nature. **4148**, 688

**Simpson DJ, Fincher GB, Huang AH, Cameron-Mills V**. 2003. Structure and function of cereal and related higher plant (1→ 4)-β-xylan endohydrolases. Journal of Cereal Science **37**, 111-127.

**Singh S**. 2016. Role of nonpathogenic fungi in inducing systemic resistance in crop plants against phytopathogens. *Microbial Inoculants in Sustainable Agricultural Productivity*: Springer, 69-83.

**Singh BK, Trivedi P**. 2017. Microbiome and the future for food and nutrient security. Microbial biotechnology **10**, 50.

**Sivasithamparam K, Parker C, Edwards C**. 1979. Rhizosphere micro-organisms of seminal and nodal roots of wheat grown in pots. Soil biology and biochemistry **11**, 155-160.

**Smalla K, Wieland G, Buchner A, Zock A, Parzy J, Kaiser S, Roskot N, Heuer H, Berg G**. 2001. Bulk and rhizosphere soil bacterial communities studied by denaturing gradient gel electrophoresis: plant-dependent enrichment and seasonal shifts revealed. Appl. Environ. Microbiol. **67**, 4742-4751.

**Smallwood M, Martin H, Knox JP**. 1995. An epitope of rice threonine-and hydroxyproline-rich glycoprotein is common to cell wall and hydrophobic plasma-membrane glycoproteins. Planta **196**, 510-522.

**Smallwood M, Yates EA, Willats WG, Martin H, Knox JP**. 1996. Immunochemical comparison of membrane-associated and secreted arabinogalactan-proteins in rice and carrot. Planta **198**, 452-459.

**Smith SE, Read DJ**. 2010. *Mycorrhizal symbiosis*: Academic press.

**Smith S, De Smet I**. 2012. Root system architecture: insights from Arabidopsis and cereal crops. The Royal Society.

**Sprent JI**. 1975. Adherence of sand particles to soybean roots under water stress. New phytologist **74**, 461-463.

**Steele K, Price AH, Shashidhar H, Witcombe J**. 2006. Marker-assisted selection to introgress rice QTLs controlling root traits into an Indian upland rice variety. Theoretical and Applied Genetics **112**, 208-221.

**Steele K, Virk D, Kumar R, Prasad S, Witcombe J**. 2007. Field evaluation of upland rice lines selected for QTLs controlling root traits. Field Crops Research **101**, 180-186.

**Stockdale E, Shepherd M, Fortune S, Cuttle SP**. 2002. Soil fertility in organic farming systems–fundamentally different? Soil use and management **18**, 301-308.

**Sturtevant AH**. 1913. A third group of linked genes in Drosophila ampelophila. Science **37**, 990-992.

**Subbiah B, Katyal J, Narasimham R, Dakshinamurti C**. 1968. Preliminary investigations on root distribution of high yielding wheat varieties. The International Journal of Applied Radiation and Isotopes **19**, 385-390.

**Sujkowska-Rybkowska M, Borucki W**. 2015. Pectins esterification in the apoplast of aluminum-treated pea root nodules. Journal of plant physiology **184**, 1-7.

**Sultan SE**. 2000. Phenotypic plasticity for plant development, function and life history. Trends in plant science **5**, 537-542.

**Talboys PJ, Owen DW, Healey JR, Withers PJ, Jones DL**. 2014. Auxin secretion by Bacillus amyloliquefaciens FZB42 both stimulates root exudation and limits phosphorus uptake in Triticum aestivum. BMC plant biology **14**, 51.

**Tang X, Li J, Ma Y, Hao X, Li X**. 2008. Phosphorus efficiency in long-term (15 years) wheat–maize cropping systems with various soil and climate conditions. Field Crops Research **108**, 231-237.

**Tardieu F, Cabrera-Bosquet L, Pridmore T, Bennett M**. 2017. Plant phenomics, from sensors to knowledge. Current Biology **27**, R770-R783.

**Teixeira LC, Peixoto RS, Cury JC, Sul WJ, Pellizari VH, Tiedje J, Rosado AS**. 2010. Bacterial diversity in rhizosphere soil from Antarctic vascular plants of Admiralty Bay, maritime Antarctica. The ISME journal **4**, 989-1001.

**Thirkell TJ, Pastok D, Field KJ**. 2020. Carbon for nutrient exchange between arbuscular mycorrhizal fungi and wheat varies according to cultivar and changes in atmospheric carbon dioxide concentration. Global change biology **26**, 1725-1738.

**Tilston EL, Deakin G, Bennett J, Passey T, Harrison N, O'Brien F, Fernández-Fernández F, Xu X**. 2018. Candidate causal organisms for apple replant disease in the United Kingdom. Phytobiomes Journal **2**, 261-274.

**Tranquilli G, Dubcovsky J**. 2000. Epistatic interaction between vernalization genes Vrn-Am1 and Vrn-Am2 in diploid wheat. Journal of Heredity **91**, 304-306.

**Trachsel S, Kaeppler SM, Brown KM, Lynch JP**. 2011. Shovelomics: high throughput phenotyping of maize (Zea mays L.) root architecture in the field. Plant and soil **341**, 75-87.

**Tringe SG, Von Mering C, Kobayashi A, Salamov AA, Chen K, Chang HW, Podar M, Short JM, Mathur EJ, Detter JC**. 2005. Comparative metagenomics of microbial communities. Science **308**, 554-557.

**Tuberosa R, Salvi S, Sanguineti MC, Landi P, Maccaferri M, Conti S**. 2002. Mapping QTLs regulating morpho-physiological traits and yield: Case studies, shortcomings and perspectives in drought-stressed maize. Annals of Botany **89**, 941-963.

**Turnbaugh PJ, Ley RE, Hamady M, Fraser-Liggett CM, Knight R, Gordon JI**. 2007. The human microbiome project. Nature **449**, 804-810.

**Turner TR, James EK, Poole PS**. 2013. The plant microbiome. Genome biology **14**, 1-10.

**Uga Y, Okuno K, Yano M**. 2011. Dro1, a major QTL involved in deep rooting of rice under upland field conditions. Journal of Experimental Botany **62**, 2485-2494.

**Uga Y, Sugimoto K, Ogawa S, Rane J, Ishitani M, Hara N, Kitomi Y, Inukai Y, Ono K, Kanno N**. 2013. Control of root system architecture by DEEPER ROOTING 1 increases rice yield under drought conditions. Nature genetics **45**, 1097-1102.

**Uga Y, Yamamoto E, Kanno N, Kawai S, Mizubayashi T, Fukuoka S**. 2013. A major QTL controlling deep rooting on rice chromosome 4. Scientific reports **3**, 3040.

**Ulrich DE, Sevanto S, Ryan M, Albright MB, Johansen RB, Dunbar JM**. 2019. Plant-microbe interactions before drought influence plant physiological responses to subsequent severe drought. Scientific reports **9**, 1-10.

**Unno Y, Okubo K, Wasaki J, Shinano T, Osaki M**. 2005. Plant growth promotion abilities and microscale bacterial dynamics in the rhizosphere of Lupin analysed by phytate utilization ability. Environmental microbiology **7**, 396-404.

**USDA (2020).** Available Online at:
https://usda.library.cornell.edu/concern/publications/5q47rn72z?locale=en

**Usyk M, Zolnik CP, Patel H, Levi MH, Burk RD**. 2017. Novel ITS1 fungal primers for characterization of the mycobiome. MSphere **2**.

**Vadez V**. 2014. Root hydraulics: the forgotten side of roots in drought adaptation. Field Crops Research **165**, 15-24.

**Van Buuren ML, Maldonado-Mendoza IE, Trieu AT, Blaylock LA, Harrison MJ**. 1999. Novel genes induced during an arbuscular mycorrhizal (AM) symbiosis formed between Medicago truncatula and Glomus versiforme. Molecular Plant-Microbe Interactions **12**, 171-181.

**Van der Ent S, Van Wees SC, Pieterse CM**. 2009. Jasmonate signaling in plant interactions with resistance-inducing beneficial microbes. Phytochemistry **70**, 1581-1588.

**Van der Walt AJ, Johnson RM, Cowan DA, Seely M, Ramond J-B**. 2016. Unique microbial phylotypes in Namib Desert dune and gravel plain Fairy Circle soils. Applied and environmental microbiology **82**, 4592-4601.

**Vassilev N, Vassileva M, Nikolaeva I**. 2006. Simultaneous P-solubilizing and biocontrol activity of microorganisms: potentials and future trends. Applied microbiology and biotechnology **71**, 137-144.

**Velasquez SM, Ricardi MM, Dorosz JG, Fernandez PV, Nadra AD, Pol-Fachin L, Egelund J, Gille S, Harholt J, Ciancia M**. 2011. O-glycosylated cell wall proteins are essential in root hair growth. Science **332**, 1401-1403.

**Velasquez SM, Ricardi MM, Poulsen CP, Oikawa A, Dilokpimol A, Halim A, Mangano S, Juarez SPD, Marzol E, Salter JDS**. 2015. Complex regulation of prolyl-4-hydroxylases impacts root hair expansion. Molecular plant **8**, 734-746.

**Verhertbruggen Y, Marcus SE, Haeger A, Ordaz-Ortiz JJ, Knox JP**. 2009. An extended set of monoclonal antibodies to pectic homogalacturonan. Carbohydrate research **344**, 1858-1862.

**Vicré M, Santaella C, Blanchet S, Gateau A, Driouich A**. 2005. Root border-like cells of Arabidopsis. Microscopical characterization and role in the interaction with rhizobacteria. Plant physiology **138**, 998-1008.

**Viebahn M, Veenman C, Wernars K, van Loon LC, Smit E, Bakker PA**. 2005. Assessment of differences in ascomycete communities in the rhizosphere of field-grown wheat and potato. FEMS microbiology ecology **53**, 245-253.

**Virmani S**. 1971. Rooting patterns of dwarf wheats. Indian journal of agronomy.

**Vogel J**. 2008. Unique aspects of the grass cell wall. Current opinion in plant biology **11**, 301-307.

**Volder A, van Iersel M**. 2019. Root Growth, Physiology, and Potential Impact of Soilless Culture on Their Functioning. *Soilless Culture*: Elsevier, 15-32.

**Vorholt J**. 2012. Microbial life in the phyllosphere. Nat Publ Gr 10: 828–840.

**Vorwerk S, Somerville S, Somerville C**. 2004. The role of plant cell wall polysaccharide composition in disease resistance. Trends in plant science **9**, 203-209.

**Voss-Fels KP, Robinson H, Mudge SR, Richard C, Newman S, Wittkop B, Stahl A, Friedt W, Frisch M, Gabur I**. 2018. VERNALIZATION1 modulates root system architecture in wheat and barley. Molecular plant **11**, 226-229.

**Waines JG, Ehdaie B**. 2007. Domestication and crop physiology: roots of green-revolution wheat. Annals of Botany **100**, 991-998.

**Walkowiak S, Gao L, Monat C, Haberer G, Kassa MT, Brinton J, Ramirez-Gonzalez RH, Kolodziej MC, Delorean E, Thambugala D**. 2020. Multiple wheat genomes reveal global variation in modern breeding. Nature, 1-7.

**Walter A, Silk WK, Schurr U**. 2009. Environmental effects on spatial and temporal patterns of leaf and root growth. Annual review of plant biology **60**, 279-304.

**Wardle D**. 1992. A comparative assessment of factors which influence microbial biomass carbon and nitrogen levels in soil. Biological reviews **67**, 321-358.

**Wasson A, Bischof L, Zwart A, Watt M**. 2016. A portable fluorescence spectroscopy imaging system for automated root phenotyping in soil cores in the field. Journal of experimental botany **67**, 1033-1043.

**Watt M, McCully ME, Canny MJ**. 1994. Formation and stabilization of rhizosheaths of Zea mays L.(Effect of soil water content). Plant physiology **106**, 179-186.

**Watt M, Magee LJ, McCully ME**. 2008. Types, structure and potential for axial water flow in the deepest roots of field-grown cereals. New Phytologist **178**, 135-146.

**Watt M, Moosavi S, Cunningham SC, Kirkegaard J, Rebetzke G, Richards R**. 2013. A rapid, controlled-environment seedling root screen for wheat correlates well with rooting depths at vegetative, but not reproductive, stages at two field sites. Annals of Botany **112**, 447-455.

**Weaver JE, Bruner WE**. 1926. Root development of field crops.

**Weese DJ, Heath KD, Dentinger BT, Lau JA**. 2015. Long-term nitrogen addition causes the evolution of less-cooperative mutualists. Evolution **69**, 631-642.

**Werker E, Kislev M**. 1978. Mucilage on the root surface and root hairs of Sorghum: heterogeneity in structure, manner of production and site of accumulation. Annals of botany **42**, 809-816.

**Whalley WR, Binley A, Watts C, Shanahan P, Dodd IC, Ober E, Ashton R, Webster C, White R, Hawkesford MJ**. 2017. Methods to estimate changes in soil water for phenotyping root activity in the field. Plant and Soil **415**, 407-422.

**Whipps J, Lynch J**. 1983. Substrate flow and utilization in the rhizosphere of cereals. New phytologist **95**, 605-623.

**Whipps J**. 1984. Environmental factors affecting the loss of carbon from the roots of wheat and barley seedlings. Journal of experimental botany **35**, 767-773.

**Whipps J**. 1987. Carbon loss from the roots of tomato and pea seedlings grown in soil. Plant and Soil **103**, 95-100.

**White TJ, Bruns T, Lee S, Taylor J**. 1990. Amplification and direct sequencing of fungal ribosomal RNA genes for phylogenetics. PCR protocols: a guide to methods and applications **18**, 315-322.

**Wickham H**. 2011. ggplot2. Wiley Interdisciplinary Reviews: Computational Statistics **3**, 180-185.

**Willats WG, Limberg G, Buchholt HC, van Alebeek G-J, Benen J, Christensen TM, Visser J, Voragen A, Mikkelsen JD, Knox JP**. 2000. Analysis of pectic epitopes recognised by hybridoma and phage display monoclonal antibodies using defined oligosaccharides, polysaccharides, and enzymatic degradation. Carbohydrate Research **327**, 309-320.

**Willats WG, McCartney L, Mackie W, Knox JP**. 2001. Pectin: cell biology and prospects for functional analysis. Plant Mol Biol **47**, 9-27.

**Wolf S, Mouille G, Pelloux J**. 2009. Homogalacturonan methyl-esterification and plant development. Molecular plant **2**, 851-860.

**Wooley JC, Ye Y**. 2010. Metagenomics: facts and artifacts, and computational challenges. Journal of computer science and technology **25**, 71-81.

**Wu Y, Cosgrove DJ**. 2000. Adaptation of roots to low water potentials by changes in cell wall extensibility and cell wall proteins. Journal of experimental botany **51**, 1543-1553.

**Yang CH, Crowley DE**. 2000. Rhizosphere microbial community structure in relation to root location and plant iron nutritional status. Applied and environmental microbiology. **66**, 345-51.

**Yang D-L, Jing R-L, Chang X-P, Li W**. 2007. Identification of quantitative trait loci and environmental interactions for accumulation and remobilization of water-soluble carbohydrates in wheat (Triticum aestivum L.) stems. Genetics **176**, 571-584.

**Yang J, Zhang J**. 2006. Grain filling of cereals under soil drying. New phytologist **169**, 223-236.

**Yang H, Zhou J, Weih M, Li Y, Zhai S, Zhang Q, Chen W, Liu J, Liu L, Hu S**. 2020. Mycorrhizal nitrogen uptake of wheat is increased by earthworm activity only under no-till and straw removal conditions. Applied Soil Ecology **155**, 103672.

 **Yates EA, Valdor J-F, Haslam SM, Morris HR, Dell A, Mackie W, Knox JP**. 1996. Characterization of carbohydrate structural features recognized by anti-arabinogalactan-protein monoclonal antibodies. Glycobiology **6**, 131-139.

**York WS, Kolli VK, Orlando R, Albersheim P, Darvill AG**. 1996. The structures of arabinoxyloglucans produced by solanaceous plants. Carbohydrate Research **285**, 99-128.

**Young IM**. 1995. Variation in moisture contents between bulk soil and the rhizosheath of wheat (Triticum aestivum L. cv. Wembley). New Phytologist. **130**, 135-9.

**Young JPW, Crossman LC, Johnston AW, Thomson NR, Ghazoui ZF, Hull KH, Wexler M, Curson AR, Todd JD, Poole PS**. 2006. The genome of Rhizobium leguminosarum has recognizable core and accessory components. Genome biology **7**, R34.

**Zhalnina K, Louie KB, Hao Z, Mansoori N, da Rocha UN, Shi S, Cho H, Karaoz U, Loqué D, Bowen BP**. 2018. Dynamic root exudate chemistry and microbial substrate preferences drive patterns in rhizosphere microbial community assembly. Nature microbiology **3**, 470-480.

**Zhang H, Kim M-S, Sun Y, Dowd SE, Shi H, Paré PW**. 2008. Soil bacteria confer plant salt tolerance by tissue-specific regulation of the sodium transporter HKT1. Molecular Plant-Microbe Interactions **21**, 737-744.

**Zhang Y, Du H, Xu F, Ding Y, Gui Y, Zhang J, Xu W**. 2020. Root-Bacteria Associations Boost Rhizosheath Formation in Moderately Dry Soil through Ethylene Responses. Plant physiology **183**, 780-792.

**Zhang X, Ren Y, Zhao J**. 2008. Roles of extensins in cotyledon primordium formation and shoot apical meristem activity in Nicotiana tabacum. Journal of experimental botany **59**, 4045-4058.

**Zhu J, Brown KM, Lynch JP**. 2010. Root cortical aerenchyma improves the drought tolerance of maize (Zea mays L.). Plant, cell & environment **33**, 740-749.

**Zhu C, Tian G, Luo G, Kong Y, Guo J, Wang M, Guo S, Ling N, Shen Q**. 2018. N-fertilizer-driven association between the arbuscular mycorrhizal fungal community and diazotrophic community impacts wheat yield. Agriculture, Ecosystems & Environment **254**, 191-201.

**Zickenrott IM, Woche SK, Bachmann J, Ahmed MA, Vetterlein D**. 2016. An efficient method for the collection of root mucilage from different plant species—a case study on the effect of mucilage on soil water repellency. Journal of Plant Nutrition and Soil Science **179**, 294-302.

**Zobel R, Waisel Y**. 2010. A plant root system architectural taxonomy: a framework for root nomenclature. Plant Biosystems **144**, 507-512.

**Zykwinska A, Thibault J-F, Ralet M-C**. 2007. Organization of pectic arabinan and galactan side chains in association with cellulose microfibrils in primary cell walls and related models envisaged. Journal of Experimental Botany **58**, 1795-1802.
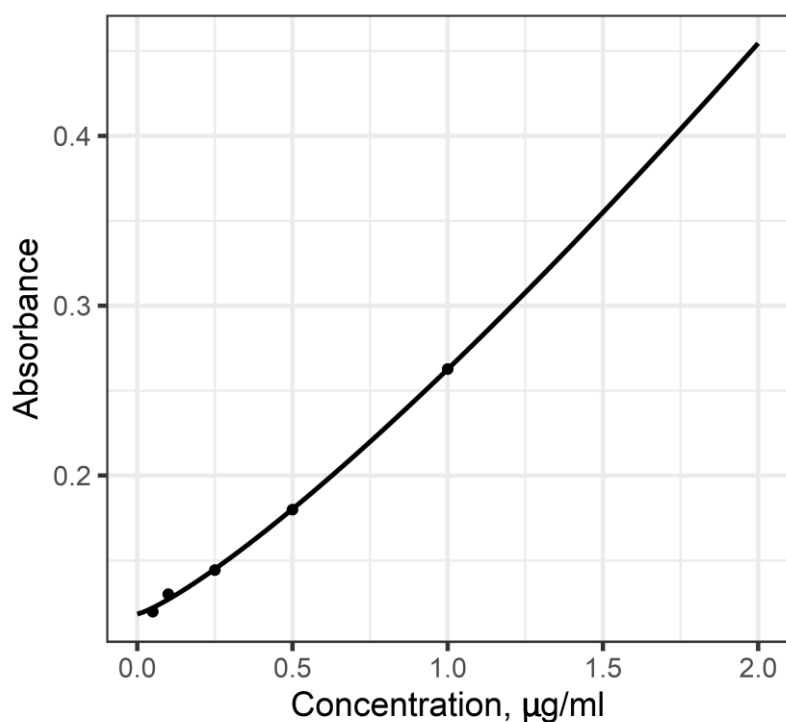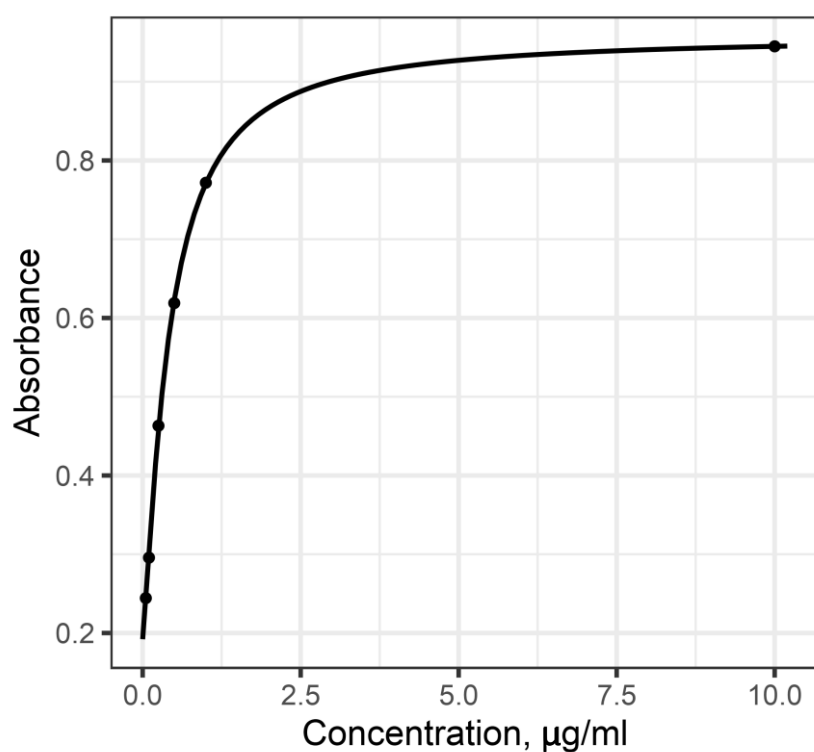
# Appendix 1
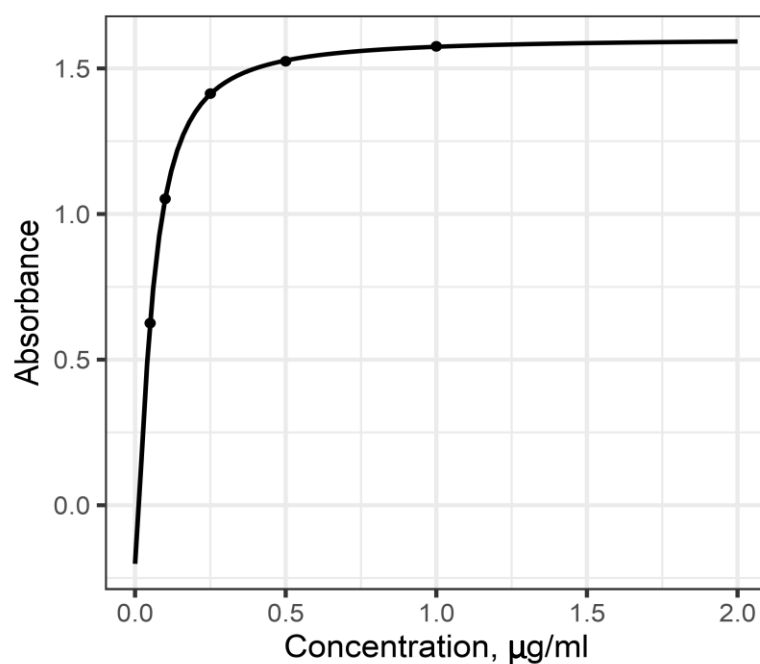


**Supplementary Figure 1.1 ELISA calibration curve for the xylan epitope specific to antibody LM11.** The equation was fit to experimentally determined data points with a goodness of fit of $r^2 = 0.99$. $y = 1.603 + (-0.201 - 1.603)/(1 + (x/0.0563)^{1.429}$
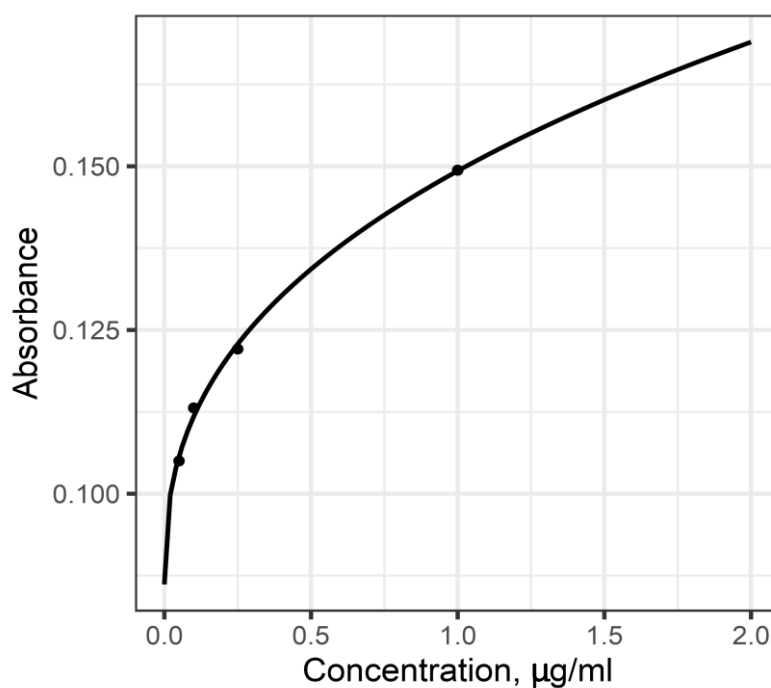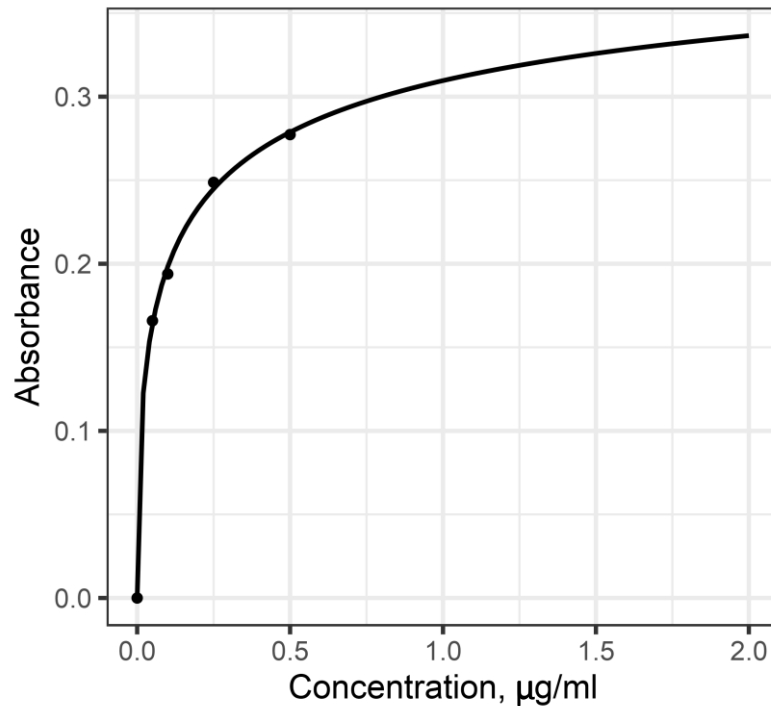


**Supplementary Figure 1.2 ELISA calibration curve for the heteroxylan epitope specific to antibody LM27.** The equation was fit to experimentally determined data points with a goodness of fit of $r^2 = 0.99$. $y = 45.145 + (0.08615 - 45.145)/(1 + (x/1899)^{0.392}$
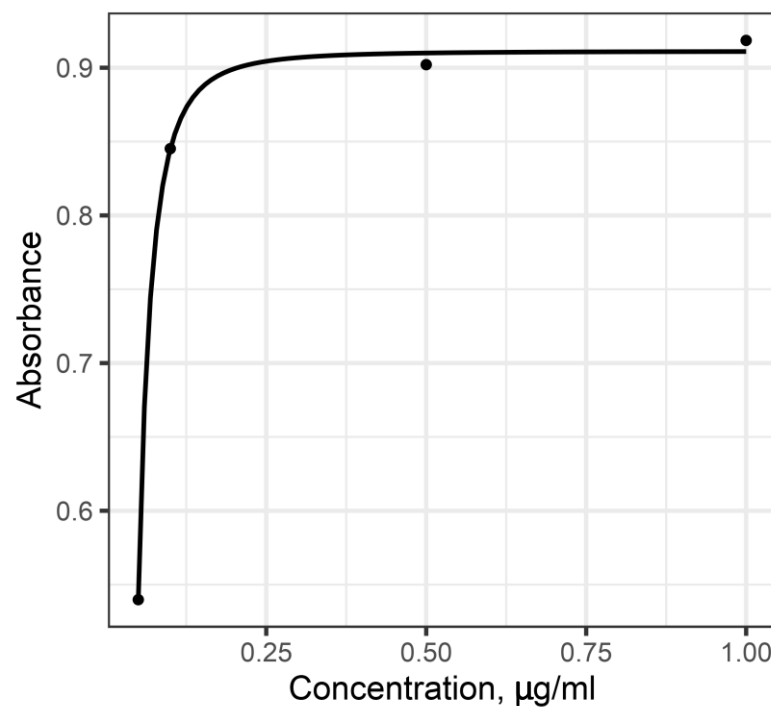
**Supplementary Figure 1.3 ELISA calibration curve for the arabinogalactan protein epitope specific to antibody LM2.** The equation was fit to experimentally determined data points with a goodness of fit of $r^2 = 0.99$. $y = 62504.73 + (0.1184 - 62504.73)/(1 + (x/41407)^{1.2209}$



**Supplementary Figure 1.4 ELISA calibration curve for the extensin epitope specific to antibody LM1.** The equation was fit to experimentally determined data points with a goodness of fit of $r^2 = 0.99$. $y = 0.958 + (0.192 - 0.958)/(1 + (x/0.411)^{1.27}$

**Supplementary Figure 1.5 ELISA calibration curve for the homogalacturonan epitope specific to antibody LM19.** The equation was fit to experimentally determined data points with a goodness of fit of $r^2$ = 0.99. y = 0.4342 + (0.00003502 - 0.4342)/(1 + (x/0.1448)$^{0.4709}$



**Supplementary Figure 1.6 ELISA calibration curve for the xyloglucan epitope specific to antibody LM25.** The equation was fit to experimentally determined data points with a goodness of fit of $r^2$ = 0.99. y = 0.9112 + (-205536.6 - 0.9112)/(1 + (x/0.000244)$^{2.484}$

# Appendix 2

**Appendix Table 2.1 BLUPs for lines of the Avalon x Cadenza tails.** Measurements were taken in a series of soil-based experiments, save the root hairs per unit root length, which were taken from a paper-based experiment. Data from two independent experiments were used to derive the BLUPs. XY, xylan; HX, heteroxylan; AGP, arabinogalactan protein; EX, extensin; HG, homogalacturonan; XG, xyloglucan.

| Line | Concentration of epitope per unit root length, µg mL$^{-1}$ cm$^{-1}$ | | | | | | Physical root and shoot traits | | | | |
|---|---|---|---|---|---|---|---|---|---|---|---|
| | XY (LM11) | HX (LM27) | AGP (LM2) | EX (LM1) | HG (LM19) | XG (LM25) | Rhizosheath (mg) per cm root length | Total root length, cm | Shoot mass, mg | Shoot length, cm | Root hairs per cm root |
| AxC 1 | 0.0087 | 0.78 | 0.085 | 0.0061 | 0.116 | 0.062 | 0.26 | 38.9 | 0.046 | 12.7 | 4.9 |
| AxC 5 | 0.0090 | 0.84 | 0.056 | 0.0047 | 0.106 | 0.102 | 0.23 | 29.8 | 0.035 | 8.4 | 3.7 |
| AxC 6 | 0.0129 | 0.83 | 0.107 | 0.0075 | 0.143 | 0.084 | 0.25 | 27.9 | 0.032 | 9.0 | 5.7 |
| AxC 7 | 0.0145 | 3.35 | 0.159 | 0.0195 | 0.136 | 0.088 | 0.30 | 24.9 | 0.035 | 9.4 | 2.5 |
| AxC 9 | 0.0035 | 0.97 | 0.099 | 0.0026 | 0.131 | 0.046 | 0.23 | 37.5 | 0.036 | 11.3 | 2.0 |
| AxC 28 | 0.0063 | 1.08 | 0.070 | 0.0092 | 0.156 | 0.048 | 0.22 | 29.9 | 0.036 | 8.9 | 1.9 |
| AxC 43 | 0.0130 | 1.08 | 0.056 | 0.0072 | 0.143 | 0.050 | 0.26 | 29.4 | 0.035 | 10.9 | 3.0 |
| AxC 56 | 0.0072 | 1.12 | 0.113 | 0.0055 | 0.164 | 0.071 | 0.22 | 33.5 | 0.049 | 11.7 | 4.1 |
| AxC 80 | 0.0060 | 0.95 | 0.080 | 0.0055 | 0.238 | 0.053 | 0.27 | 34.8 | 0.055 | 10.8 | 2.9 |
| AxC 102 | 0.0058 | 1.59 | 0.155 | 0.0091 | 0.266 | 0.097 | 0.26 | 31.2 | 0.046 | 12.2 | 5.1 |
| AxC 108 | 0.0088 | 1.70 | 0.149 | 0.0043 | 0.198 | 0.120 | 0.25 | 30.3 | 0.034 | 11.1 | 4.9 |
| AxC 131 | 0.0136 | 1.23 | 0.112 | 0.0177 | 0.834 | 0.103 | 0.22 | 28.8 | 0.027 | 9.7 | 2.5 |
| AxC 146 | 0.0087 | 1.49 | 0.135 | 0.0212 | 0.354 | 0.020 | 0.22 | 23.7 | 0.044 | 8.0 | 3.7 |
| AxC 156 | 0.0279 | 1.81 | 0.154 | 0.0339 | 0.571 | 0.069 | 0.28 | 15.3 | 0.031 | 7.8 | 4.2 |
| AxC 179 | 0.0094 | 1.39 | 0.144 | 0.0091 | 0.149 | 0.132 | 0.27 | 31.8 | 0.048 | 11.5 | 5.4 |
| AxC 181 | 0.0048 | 1.36 | 0.167 | 0.0101 | 0.140 | 0.085 | 0.22 | 47.1 | 0.054 | 10.8 | 1.3 |
| AxC 182 | 0.0035 | 1.04 | 0.095 | 0.0093 | 0.083 | 0.089 | 0.26 | 42.7 | 0.053 | 11.2 | 2.2 |
| AxC 198 | 0.0090 | 1.20 | 0.084 | 0.0164 | 0.223 | 0.092 | 0.25 | 27.8 | 0.040 | 8.8 | 1.6 |
| Avalon | 0.0064 | 2.30 | 0.208 | 0.0078 | 0.153 | 0.092 | 0.33 | 37.7 | 0.050 | 11.2 | 1.1 |
| Cadenza | 0.0033 | 2.02 | 0.165 | 0.0081 | 0.179 | 0.101 | 0.28 | 36.1 | 0.030 | 10.3 | 2.3 |

# Appendix 3
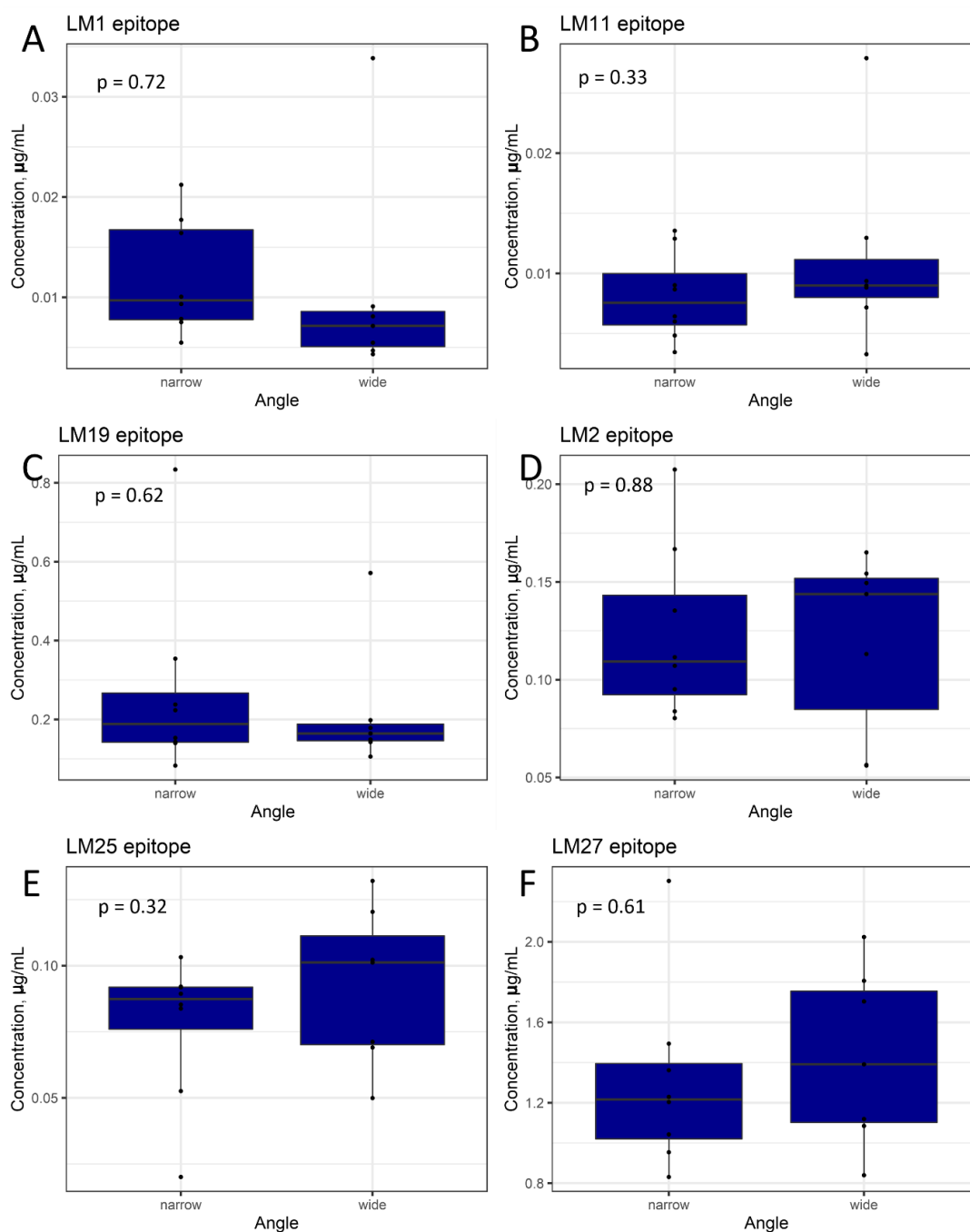


**Supplementary figure 3.1 Concentration of epitopes detected in the rhizosheath of wheat lines displaying wide or narrow seminal root angles.** Points represent BLUPs calculated for individual genotypes of Avalon x Cadenza doubled haploid lines. (A) LM1, extensin (B) LM11, xylan (C) LM19, homogalacturonan (D) LM2, arabinogalactan protein (E) LM25, xyloglucan (F) LM27, heteroxylan
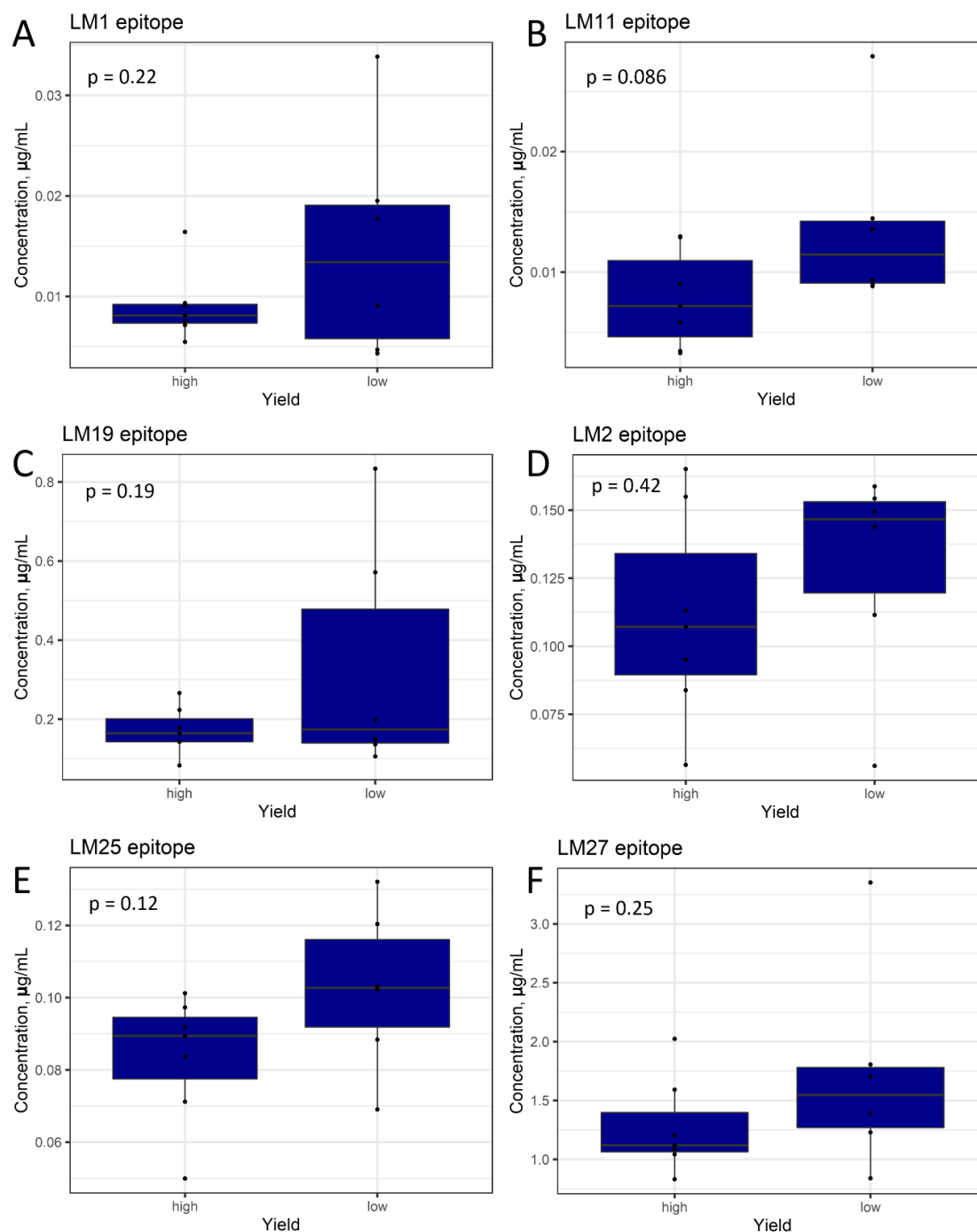
**Supplementary figure 3.2 Concentration of epitopes detected in the rhizosheath of wheat lines displaying high or low grain yield.** Points represent BLUPs calculated for individual genotypes of Avalon x Cadenza doubled haploid lines. (A) LM1, extensin (B) LM11, xylan (C) LM19, homogalacturonan (D) LM2, arabinogalactan protein (E) LM25, xyloglucan (F) LM27, heteroxylan. Lines were grouped according to yield data (measured in separate experiments to the rhizosheath experiments), based on means across two field seasons.